Systems Level Analysis of Immune Cell Subsets and Intercellular Communication Networks in Human Breast Cancer

Floriane Noël

université PARIS-SACLAY

NNT : 2018SACLS418

Thèse de doctorat

UNIVERSITE PARIS SUD
Comprendre le monde, construire l'avenir

Systems level analysis of immune cell subsets and intercellular communication networks in human breast cancer

Thèse de doctorat de l'Université Paris-Saclay
Préparée à l'Institut Curie

École doctorale n°582 Cancérologie : biologie – médecine – santé (CBMS)
Spécialité de doctorat: Aspects moléculaires et cellulaires de la biologie

Thèse présentée et soutenue à Paris, le 29 Octobre 2018, par

Floriane NOËL

Composition du Jury :

Fabrice ANDRÉ PUPH, Institut Gustave Roussy (– UMR 981)	Président
Jenny VALLADEAU-GUILEMOND Chargée de Recherche, Cancer Research Center Lyon (– UMR INSERM 1052)	Rapporteur
Antonio RAUSELL Chargé de Recherche, Institut Imagine (– Clinical Bioinformatics lab)	Rapporteur
Ioannis XENARIOS Professor, Swiss Institute of Bioinformatics	Examinateur
Alexandre ESCARGUEIL PU, Sorbonne Université	Examinateur
Vassili SOUMELIS MCUPH1, Institut Curie (– U932 Immunité et Cancer)	Directeur de thèse

"Adaptation is the key to survival."

The Citadel [3.18], Star Wars: The Clone Wars - George Lucas and Matt Michnovetz

Acknowledgements

Dans un premier temps, je tiens à remercier les membres de mon jury de thèse : mes deux rapporteurs Dr Jenny Valladeau-Guilemond et Dr Antonio Rausell, ainsi que mes examinateurs Pr Fabrice André, Pr Ioannis Xenarios et Pr Alexandre Escargueil, pour avoir accepter d'évaluer ces trois années de travail. Je remercie également la faculté Paris Saclay ainsi que le ministère de la Recherche et l'Ecole Doctorale CBMS pour m'avoir donné l'opportunité d'effectuer cette thèse.

Je tiens à remercier mon directeur de thèse, Pr Vassili Soumelis, pour m'avoir accueillie au sein de son équipe, pour m'avoir guidée, conseillée et fait confiance sur ce projet. J'ai pu apprendre à son contact la rigueur et l'intégrité scientifique, l'autonomie et la persévérance, des compétences qui me seront utiles dans ma vie de chercheuse mais également personnelle.

Je remercie bien entendu Paula qui ma permis d'en apprendre tant sur les DCs. Elle a été mon mentor sur ce projet, elle m'a fait découvrir limmunologie et m'a guidée tout au long du projet DC et Cancer. Nous avons formé un super duo et ce fut une collaboration tellement enrichissante, mille merci !!!

Un très grand merci à Maude pour sa bienveillance au quotidien, pour nos discussions scientifiques (ou pas ;)), mais également pour son soutien et son aide si précieuse.

Je souhaite évidemment remercier tous les membres de l'équipe, anciens et nou-

veaux : Philémon, Lilith, Caroline, Charlotte, Camille, Coline, Sarantis, Arturo, Léa, Élise, Ève, Max, Solana, Lucia, Alix, Ares, Marie, Carolina, Marine, Omar, Antonio, Rabie, Salvatore, FX, Clémence. Merci à tous pour ces fantastiques années avec vous, à partager votre expertise, votre bonne humeur, à raconter des blagues ou les anecdotes du labo, merci pour tous ces délicieuses recettes partagées (et oui! Nous avons quelques chefs pâtissiers incognito dans l'équipe ;)).

Je tiens à remercier Christel, sans qui je ne serai peut-être pas arrivée dans l'U932, ainsi que tous les bioinfos de l'unité. Merci pour votre aide, vos précieux conseils, votre soutien et pour le partage de votre expérience.

Je remercie également Dr Sebastian Amigorena et tous les membres de l'unité U932. L'environnement que représente l'U932 est scientifiquement et humainement tellement enrichissant, ce fut pour moi un bonheur de partager mon quotidien de doctorante avec chacun d'entre vous.

Je remercie les personnes avec qui j'ai collaboré notamment Nolwenn Lucas et Joël LeMaoult.

Merci à Alexandre de Brevern, pour ses mails humoristiques, pour son amitié précieuse, et ses conseils avisés.

Spéciale dédicace à la team BTS, Adeline, Garance, Camille, Frédo et Romain avec qui j'ai découvert la vie de labo et la recherche.

A tous les amis du badminton, merci de m'avoir supportée et encouragée. On forme une équipe, une famille, vive le LVLM. J'ai une attention particulière pour Virginie, Sam, Alex, Caro, Félix, “les Cuistôts”, promis je n'apporterai plus mon ordinateur pour travailler lors de nos soirées ;).

Et enfin, je remercie infiniment ma famille: mes parents, Chloé, Arnaud, ma belle-

famille. Ils ont été un soutien inébranlable. Ils ont toujours cru en moi, et m'ont appris à ne jamais abandoner. Je suis heureuse et fière de leur présenter ce travail.

Contents

Synthèse

Les systèmes vivants sont des systèmes ouverts qui échangent constamment des informations et de l'énergie-matière avec leur environnement. La communication, qui peut être définie comme un échange d'informations entre deux systèmes ou sous-systèmes, est donc un élément essentiel de la vie. Il permet la coordination efficace des processus homéostatiques et l'adaptation à un environnement en constante évolution, y compris la réponse aux menaces internes ou externes ou les processus autocuratifs. Les organismes multicellulaires sont structurés de manière hiérarchique, les cellules étant souvent considérées comme des unités fondamentales : les cellules s'organisent pour former des tissus, un ensemble de tissus forme des organes, qui forment eux-mêmes des organismes. Par conséquent, la communication intercellulaire est à la base de l'organisation d'ordre supérieur observée dans les tissus, les organes et les organismes. Il est essentiel de coordonner la fonction de divers types cellulaires impliqués dans des processus biologiques complexes, tels que l'embryogenèse, la formation et le renouvellement des tissus, la régulation hormonale, la réponse au stress, une réaction immunitaire efficace aux agents pathogènes microbiens et le remodelage tissulaire au cours d'une inflammation et de la cicatrisation. La dérégulation dans la communication intercellulaire peut entraîner une pathologie due à l'échec des processus homéostatiques et/ou à une adaptation défectueuse face aux menaces environnementales. Comment les cellules s'adaptent-elles à un microenvironnement spécifique en fonction de la communication intercellulaire ? Est-ce qu'elles gardent leur identité ou adoptent un comportement spécifique ? Ces questions sont particulièrement pertinentes quand on étudie le système immunitaire dans le contexte de l'inflammation et du cancer. Les interactions entre les cellules cancéreuses et le microenvironnement tumoral (TME) jouent un rôle crucial dans le développement

et la progression de la tumeur. Le TME est un système hétérogène constitué de nombreuses protéines et cellules de types différents qui interagissent au sein d'un réseau complexe. En particulier, de nombreux types de cellules immunitaires sont recrutés et participent à la réponse anti-tumorale, mais également à l'inflammation et à l'immunosuppression favorisant la tumeur. Il a été démontré que les cellules dendritiques (DCs) dans le TME étaient liées à la fois à la progression de la tumeur et à la prévention. Les DCs jouent un rôle essentiel dans le déclenchement des réponses immunitaires adaptatives. Chez l'homme, différentes sous-populations de DCs ont été identifiées. Des études antérieures ont montré que les DCs infiltrent des tumeurs solides, notamment le cancer du sein. Cependant, l'impact du TME sur le comportement des sous-ensembles de DCs infiltrant des tumeurs humaines est mal connu.

Dans le premier chapitre de la thèse, j'ai présenté les concepts généraux de la communication et du micro-environnement, puis j'ai décrit le cancer du sein et son microenvironnement, qui représentent un réseau complexe de cellules qui interagissent dans un contexte inflammatoire. Par la suite, j'ai présenté l'hétérogénéité des cellules présentatrices d'antigènes (APCs) qui infiltrent le TME du sein et leurs communications dans ce contexte. Enfin, je me suis concentrée sur les défis techniques et méthodologiques liés à l'étude de la communication cellulaire et sur les outils bioinformatiques que nous pouvons utiliser pour surveiller les communications intercellulaires.

Le deuxième chapitre de la thèse pose les hypothèses et objectifs de mon travail. Ce projet part de l'hypothèse que le microenvironnement tumoral module les réseaux de communication intra et intercellulaires formés par les APCs. Ces modifications auraient des conséquences sur l'interaction entre la tumeur et le système immunitaire de l'hôte et *a fortiori* sur sur le développement de la tumeur. Malheureusement, dans la littérature, il existe plusieurs limites concernant l'étude de APCs qui sont des cellules rares dans un contexte tissulaire. Les sous-populations d'APCs ont été caractérisées dans différents tissus (*e.g.* le sang, la rate, la peau), des maladies (*e.g.* cancers, maladies auto-immunes), des organismes (*e.g.* souris, humains). Cependant, dans le cancer du sein, seuls les macrophages et les cDC2 ont

été étudiés [Ojalvo, Whittaker, et al. 2010; Wargo et al. 2016] et aucune comparaison n'a été faite entre le tissu tumoral (T) et le tissu non malin appelé juxtatumoral (J), ni entre différents sous-types de cancer du sein. L'objectif général de ma thèse est de comprendre l'impact du microenvironnement tumoral sur les sous-populations de DCs par une analyse systémique. Dans la première partie de mon travail de thèse, je cherchais à identifier les sous-populations de DCs dans le microenvironnement de la tumeur du sein. Plus précisément, le projet s'est concentré sur l'identification et la caractérisation des fonctions biologiques de sous-populations de DCs isolées de tumeurs du sein de deux sous-types différents: Luminal (LBC) et Triple-Négatif (TNBC), dont le pronostic est le plus sombre. Les APCs étant des cellules rares dans le TME du sein, nous avons voulu définir les sous-ensembles de APCs infiltrant les tumeurs à une résolution supérieure à celle décrite dans la littérature. En utilisant la technologie de séquençage ARN, nous avons généré le profil moléculaire de ces cellules et avons voulu en déduire les fonctions biologiques. Dans un premier temps, l'objectif de cette étude était de décrypter comment le TME modulait le profil de transcription des sous-populations dAPCs, en comparant les profils de transcription des APCs dans les tumeurs et les juxtatumeurs et en liant la variation de l'expression des gènes aux fonctions biologiques. Dans un deuxième temps, nous avons évalué l'impact de l'hétérogénéité de la tumeur mammaire sur les DCs et les monocytes/macrophages (Monomacs). Pour ce faire, nous avons comparé le profil de transcription des sous-types d'APCs, isolés de deux types de cancer du sein, LBC et TNBC. Enfin, comme nous avions étudié le microenvironnement de la tumeur du sein et son impact potentiel sur le réseau de communication des sous-populations d'APCs, nous nous sommes demandé quel était le lien entre la caractérisation de chaque population spécifique d'APCs et le résultat clinique. Existe-t-il des différences au niveau de la population entre les résultats cliniques et les différents TME, en fonction du sous-type de cancer du sein ? À partir de l'extraction de listes de gènes spécifiques caractérisant chaque population dAPCs identifiée dans le TME du sein, nous avons cherché à relier les signatures des sous-types cellulaires dans les différents contextes au pronostic des patients. Dans une seconde partie, nous avons étudié les communications cellulaires afin de comprendre comment les

cellules intègrent les signaux provenant de leur environnement. Pour ce faire, nous avons cherché à créer un score de communication simple basé sur des profils transcriptomiques de cellules. Ce score pourrait être appliqué aux données de puces à ADN ainsi qu'aux données de séquençage ARN. Il fera partie d'un outil comprenant une base de données sur les interactions des ligands et des récepteurs organisée et triée manuellement et un ensemble de profils de transcription des cellules primaires accessibles au public dans BioGPS [cite mabbott$_{e}xpression_{2}$013].

Dans le troisième chapitre, les résultats de ma thèse sont présentés en deux parties. Dans une première partie, je présente les résultats publiés en montrant que les APCs s'adaptent au TME du sein dune manière spécifique selon la sous-population. Dans une seconde partie, je présente le manuscrit en préparation décrivant le développement et l'application d'un score de communication basé sur les profils transcriptomiques. Le TME est composé d'une grande variété de types de cellules qui influencent la progression de la tumeur et l'évasion immunitaire. Les DCs sont des APCs qui peuvent s'infiltrer dans la plupart des types de cancer. Ils peuvent jouer un rôle protecteur dans l'immunité antitumorale mais, inversement, ils peuvent également favoriser l'immunosuppression [DeNardo, Barreto, et al. 2009; Faget et al. 2012; Ghirelli et al. 2015]. L'influence du TME sur la diversité et la plasticité de ces APCs reste peu explorée. Dans le cadre de ma thèse, j'ai analysé les profils de séquençage à grande échelle des APCs infiltrant des tumeurs dans 8 échantillons de cancer du sein luminal (LBC) et 4 triples-négatifs (TNBC), en étroite collaboration avec Paula Michea, chercheuse post-doctorante au laboratoire. Sur la base d'analyses précédemment effectuées au sein du laboratoire et d'études publiées sur des sous-types de DCs humaines sur d'autres tissus, tels que le sang périphérique ou la peau, nous avons étudié quatre sous-populations de DCs et les macrophages au niveau phénotypique et transciptomique dans le cancer du sein. En comparant les transcriptomes de ces APCs provenant d'échantillons tumoraux et de tissus non cancéreux (juxtatumoraux) des mêmes patients, nous avons identifié des signatures géniques spécifiques à la tumeur pour chaque sous-population d'APCs, liées à des fonctions biologiques distinctes telles que la migration cellulaire chez les pDC. De plus, nous avons observé des différences substantielles entre les profils des

APCs infiltrant les TNBC et les LBC, révélant ldu microenvironnement tumoral et pas seulement l'empreinte tissulaire ou l'ontogenèse sur le comportement des APC. Il est intéressant de noter que la signature pDC était liée à une meilleure survie sans maladie dans les patients LBC, mais pas chez les patients TNBC, ce qui implique que le résultat associé à la signature pDC dépend du contexte. En conclusion, nous avons constaté que la reprogrammation transcriptionnelle d'APC infiltrant une tumeur est spécifique à un sous-type, ce qui suggère une interaction complexe entre l'ontogénie et l'empreinte tissulaire dans le conditionnement de la diversité des DCs dans le TME. Les signatures que nous avons générées sont particulièrement pertinentes pour l'identification de l'activation de voies biologiques et de nouveaux biomarqueurs dans les sous-types d'APCs.

Les résultats de la seconde partie de mon étude sont présentés sous la forme d'un manuscrit qui sera bientôt finalisé pour soumission. Il est intitulé “ńICELLNET: Reconstruction des réseaux de communication intercellulaires à l'aide de profils transcriptomiquesż”. Pour ce travail collaboratif, j'ai été impliqué dans le développement d'une approche systémique basée sur la transcriptomique pour reconstruire des réseaux de communications intercellulaires. En effet, la communication intercellulaire est essentielle pour transférer des informations entre des cellules dotées de fonctions et de capacités de détection différentes. La communication intercellulaire coordonne les activités de divers types de cellules nécessaires aux processus complexes tels que l'embryogenèse, le remodelage tissulaire au cours de l'inflammation et la cicatrisation des plaies, ainsi que les réponses immunitaires. Actuellement, il n'existe pas de méthode systématique pour reconstruire la communication intercellulaire de manière qualitative et quantitative. Dans cette étude, nous avons développé ICELLNET, un outil intégrant des informations sur les interactions ligand/récepteur, ainsi que des données d’expression génique spécifiques à une cellule et représentant des aspects quantitatifs et qualitatifs de la communication cellule à cellule sous forme de cartes de connectivité. ICELLNET peut être automatiquement appliqué à n'importe quel profil transcriptomique au niveau de la population cellulaire afin d'estimer et de quantifier sa communication avec plus de 12 autres types de cellules. Nous avons appliqué cette méthode aux cellules tumorales, aux

cellules immunitaires innées et adaptatives (*e.g.*, DC, cellules T, cellules B, NK), aux cellules épithéliales et stromales. En analysant un ensemble de données original de cellules dendritiques humaines générées de novo, nous avons identifié et validé expérimentalement l'IL-10 en tant que régulateur majeur de la connectivité intercellulaire des DCs au niveau systémique. Notre approche visant à évaluer la connectivité cellulaire peut constituer un outil précieux pour évaluer l'impact d'un contexte spécifique sur la communication entre cellules, en particulier dans un microenvironnement inflammatoire tel que le cancer. Dans les perspectives futures, les applications d'ICELLNET pourraient apporter des informations biologiques importantes et aider à orienter les manipulations pharmacologiques.

Dans la section discussion générale, je confronte mes résultats aux connaissances actuelles et expose les perspectives futures de ce travail. Dans un premier temps, j'ai discuté de la pertinence de caractériser les sous-populations d'APCs dans le cancer du sein et du positionnement de ce travail par rapport à la littérature. J'ai examiné l'impact de l 'hétérogénéité du cancer sur les communications cellulaires. En ce qui concerne les résultats biologiques que j'ai obtenus, j'ai discuté de la signature interféron trouvée dans les TNBC. De plus, j'ai souhaité examiner la pertinence d'utiliser des données transcriptomiques pour étudier la communication intercellulaire et l'impact du microenvironnement sur le comportement cellulaire. J'ai inclu des perspectives futures sur l'intérêt d'utiliser, dans ce domaine, une nouvelle technologie basée sur le séquençage d'ARN en cellule unique. Enfin, j'ai discuté de l'intérêt et de la complexité de la compréhension de la communication intercellulaire et des futurs développements pouvant être réalisés pour améliorer l'outil ICELLNET.

Enfin, en annexe, j'ai inclu deux manuscrits en préparation pour lesquels j'ai collaboré. Le premier décrit des îlots de DCs plasmacytoïdes dans la leucémie myélomonocytaire chronique. Le second est une étude de l'inhibition d'une population de lymphocytes T CD8+ cytotoxiques par le point de contrôle immunitaire HLA-G.

List of abbreviations

TME: Tumor Microenvironment

DC: Dendritic Cell

APC: Antigen Presenting Cell

MHC: Major Histocompatibility Complex

Th: T helper

IL: Interleukin

IFN: Interferon

BC: Breast Cancer

LBC: Luminal Breast Cancer

TNBC: Triple-Negative Breast Cancer

T: Tumor tissue

J: Juxtatumor tissue

HR: Hormone Receptors

ER: Estrogen Receptor

PR: Progesterone Receptor

HER2: Human Epidermal Growth Factor 2

NK: Natural Killer

CSC: Cancer Stem Cell

ECM: Extracellular Matrix

MDSCs: Myeloid Derived Suppressor Cells

PD-L1: Programmed Cell Death 1 Ligand

PD-1: Programmed Cell Death 1

pDC: plasmacytoid Dendritic Cell

cDC: classical Dendritic Cell

Monomacs: Monocytes/macrophages

TLR: Toll-like Receptor

PAMP: Pathogen-Associated Molecular Pattern

PRR: Pattern Recognition Receptor

CLR: C-type Lectin Receptor

TAM: Tumor-Associated Macrophage

DNA: Desoxyribonucleic Acid

mRNA: messenger Ribonucleic Acid

cDNA: complementary DNA

RNA-seq: RNA sequencing

scRNA-seq: single-cell RNA sequencing

DEG: Differentially Expressed Gene

TGF-β: transforming growth factor-β

NF-ϰB: nuclear factor βB

Preamble

Living systems are open systems constantly exchanging information and energy-matter with their environment. Communication, which can be defined as an information exchange between two systems or subsystems, is thus an essential part of life. It allows the efficient coordination of homeostatic processes, and the adaptation to an ever-changing environment including internal or external threat response or self-curative processes.

Multicellular organisms are structured in a hierarchical manner, with cells often being viewed as fundamental units: cells get organized to form tissues, multiple tissues form organs, which themselves form organisms. Hence, cell-cell communication is at the basis of the higher-order organisation observed in tissues, organs, and organisms. It is critical to coordinate the function of diverse cell types involved in complex biological processes, such as embryogenesis, tissue formation and renewal, hormonal regulation, response to stress, efficient immune reaction to microbial pathogens, and tissue remodelling during inflammation and wound healing. Dysregulation in cell-to-cell communication can lead to pathology through the failure of homeostatic processes, and/or the defective adaptation to environmental threats.

How cells adapt to a specific microenvironment depending on cell-to-cell communication? Do they keep their identity or adopt a specific behavior? These questions are particularly relevant when studying the immune system in the context of inflammation and cancer. Interactions between cancer cells and the tumor microenvironment (TME) play a critical role in tumor development and progression. The TME is a heterogeneous system, which consists of numerous proteins and cells of different type interacting within a complex network. In particular, many immune cell types are recruited and participate in anti-tumor response, but also in tumor-promoting

inflammation and immunosuppression. It has been shown that dendritic cells (DCs) within the TME were related to both tumor progression and prevention. DCs play a critical role in triggering adaptive immune responses. In human, different subsets of DCs have been identified. Previous studies reported that DCs infiltrate solid tumors, and particularly breast cancer. However, little is known about the impact of the TME on the behavior of DC subsets infiltrating human tumors.

As a framework of my study, I will introduce the general concepts of communication and microenvironment, then I will focus on breast cancer and its microenvironment which represent a complex network of cells that interact in an inflammatory context. Subsequently, I will introduce the heterogeneity of Antigen Presenting Cells (APCs) that infiltrate breast TME, and their communications in this context. Finally, I will focus on the technical and methodological challenges of studying cellular communication and the bioinformatic tools we can use to monitor cell-to-cell communications.

The results will be presented in two sections. In a first part, I will present our published results showing that APCs adjust to the breast TME in a subset-specific manner. In a second part, I will present a manuscript in preparation on the development and application of a communication score based on cell transcriptomic profiles.

In the general discussion section, I will confront my results to the current knowledge and expose future perspectives of this work.

Finally, in the appendix, I will include two manuscripts in preparation for which I collaborated. The first one describe plasmacytoid DC islands in chronic myelomonocytic leukemia. The second one is a study of the inhibition of a cytotoxic population of $CD8^+$ T cells by the immune checkpoint HLA-G.

List of Figures

Chapter 1

Introduction

1.1 Communication

1.1.1 What does communication refer to?

1.1.1.1 A General definition of communication

Communication is an important concept at the level of human being and it is simply defined by the transmission of a message or an information between entities or groups. The players of communication are represented by a transmitter of the message and a recipient. They can be two individuals, groups of individuals, entities or societies. A government communicating information to the population is one illustration of communication between two entities. Communication is also defined as a process by which information is exchanged between individuals through a common system of symbols, signs, or behavior. In this definition, the emphasis is put on the use of the same system of symbols. Two individuals can discuss and exchange information using the same language. In order for the receiving individual to understand and interpret the information, he has to be able to decode it (Figure 1.1). Coding and decoding processes of symbol systems can make communication more complex. In cryptology, a lot of methods and algorithms to encrypt data or messages coexist. A key to decode the message is required, in order to be understandable by the entity receiving the information. Coding and decoding messages are used to create a specific communication between two entities. One example of tools used to decipher crucial communications during World War II was the ancestor of computer created by Pr. Alan Turing, a british mathematician. His device enabled to decode messages encrypted by Nazis from the enigma machine and is considered as the ancestor of computer science. The methods to communicate between human beings are numerous and have evolved through time, from cave painting to the internet nowadays. Major forms of communication use writing (*e.g.* books, letters) or speaking (*e.g.* direct speaking, phone, radio). Another interesting form of communication implies representation, images as painting, sculpture or even sign language. Evolution of technologies and science helped to develop different ways of communication. In particular, the comprehension and use of waves allowed us to convey messages by sonar,

radio, television and phone.

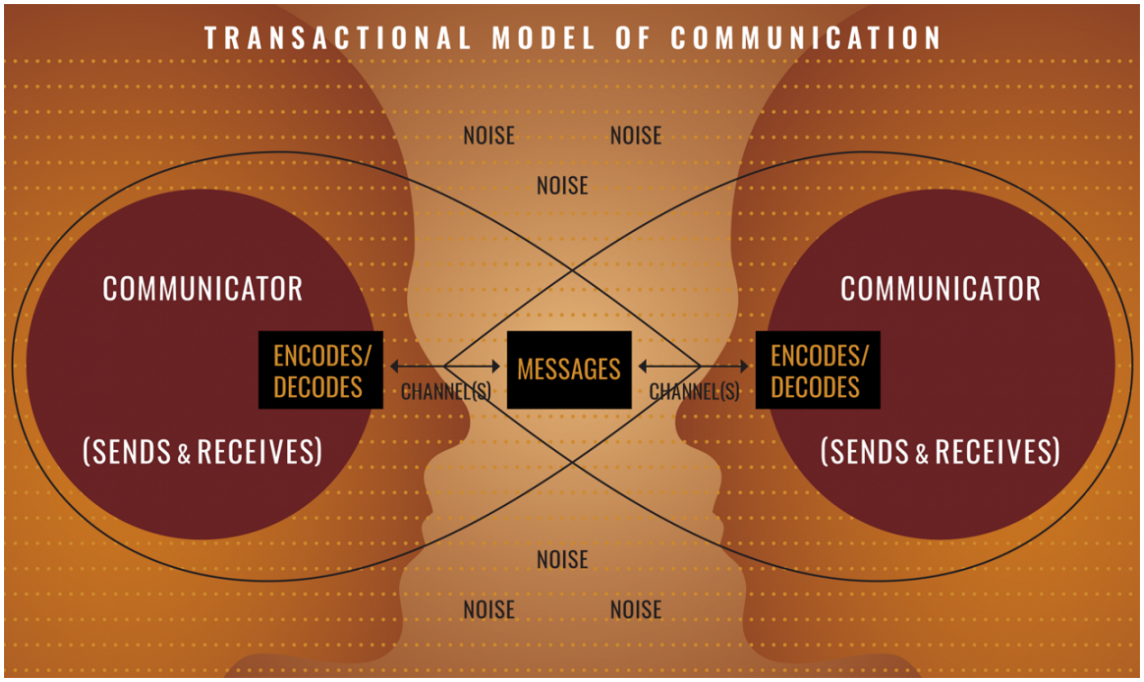

Figure 1.1: Schema representing a communication model. From National Communication Association (www.natcom.org).

At the level of the cell, we observe the same phenomenon of communication. One cell can communicate with an another by sending chemicals signals that will be sensed and processed by a receiving cell to trigger a specific response or mechanism (Figure 1.2). Cells can sense a great diversity of signals from the extracellular environment, such as growth factors, cytokines, danger signals, cell-to-cell contact and extracellular vesicles [Niel, D'Angelo, and Raposo 2018]. This signals are hundreds of distinct molecules, the majority being proteins and forming the words of the cell communication language. In cell biology, different types of signaling are described depending on the distance between the sending and the receiving cells. Paracrine signaling for short distance signaling, endocrine signaling for long distance signaling, autocrine signaling, and direct signaling across gap junctions are the four types of signaling used by cells in multicellular organisms. To sense and process the information, cells require decoding mechanisms. To detect the chemical signals, the receiving cell express specific receptors localized at their membrane or inside the cytoplasm or the nucleus. Once the ligand is attached to the receptor, the message

is transduced following complex signaling pathways inside the cell (Figure 1.2).

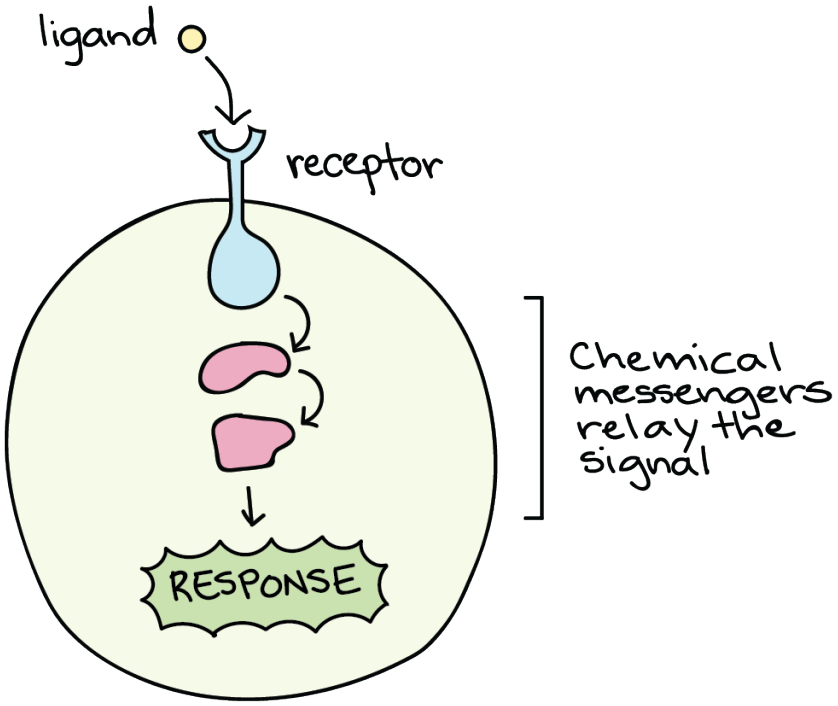

Figure 1.2: Message transduction at the cellular level, interaction between ligand and receptor. From Introduction to cell signaling, https://www.khanacademy.org.

1.1.1.2 Interest of communication

Communication is essential to human life in many ways. First of all, the use of communication can derive from a need for interacting and coordinating peoples actions in order to survive and grow. As Aristotle said, "Man is, by nature, a social animal" [Aristotle 2018]. Following this concept, humans are born to live in cities, and better exploit their potential *via* social interactions. Communities thrive around communication of a diversity of information between people, enabling to organize groups of individuals with rights and rules. Communication promotes social interactions which are key to human evolution. Social interactions and cooperation enhance the development of intelligence not only in humans but also in other species [McNally, Brown, and Jackson 2012]. Communication plays a role in the enhancement and expansion of societies, especially via education. Communication of emotions via art or entertainment is important for the psychological development of humans helping to

avoid stress and anxiety and improve productivity and stability. In Africa, a study showed that communication between members of a community promotes active citizen participation and initiatives to the development of the communities [Adedokun, Adeyemo, and Olorunsola 2010]. Throughout time, communication methods have evolved to improve the efficiency to convey information. We witness a fast evolution of communication technologies, and nowadays, thanks to the new digital technologies, the world is interconnected [E. Williams 2011]. This evolution of communication gave an easier and faster access to information, knowledge, and a faster transmission of information between individuals. More people are connected even if they are far away from each other thanks to the phone, internet, and social media replacing mailing post and telegraphy. Fast access to information and connection between individuals with different culture, origin, and experience enhance sharing and improvement of the world's knowledge that can be then applied in various disciplines such as agro-industries, politics, entertainment, economy or justice. In science, one of the most important parts of the work is to communicate about the research and results to spread knowledge and information by means of conferences, publications, and posters.

In cell biology, communication is essential to development, growth, survival, maintenance, and defense of the individual cell but also for the development of multicellular organisms [Niklas and S. A. Newman 2013]. Depending on the sensed signal, different responses are initiated by the receiving cells and impact their fate. Cell-to-cell interactions are crucial in the coordination of organism development and several signaling pathways are involved in and are responsible for most of the animal development: Hedgehog (Hh), wingless-related (Wnt), transforming growth factor-β (TGF-β), receptor tyrosine kinase (RTK), Notch, Janus kinase (JAK), signal transducer and activator of transcription (STAT) and nuclear hormone pathways [Barolo and Posakony 2002]. In the developed organism, intercellular communication coordinates the activities of multiple cell types required for complex processes such as immune response, growth, and homeostasis. When cells are damaged, they are also able to sense intracellular signals such as DNA in the cytosol and trigger mechanisms of cell death (*e.g.* apoptosis, autophagy). Another interest of communication be-

tween cells is the complex signaling network to enable cell migrations which are critical for immune cell trafficking, wound healing, and stem cell homing, among other processes. Immune cell crosstalks play a role in establishing central tolerance and preventing autoimmunity. Indeed, in the thymus, when $CD4^+CD8^+$T cells recognize the complex formed by an external peptide and the major histocompatibility complex (MHC) molecule presented on cortex thymic epithelial cells, they receive critical survival signals and differentiate into $CD4^+$ and $CD8^+$ T cells. Then, they undergo a step of negative selection in the medulla where the autoreactive T cells which recognize self-antigens presented by DCs are eliminated [Takaba and Takayanagi 2017]. Cell-to-cell communication is essential to trigger an immune response and depends on the stimuli that activate immune cells. An impair in cell-to-cell communication can lead to the development of severe pathology. For instance, a lack of a specific receptor such as interferon-gamma receptor (IFNGR) in macrophages cause a rupture of communication. Cells do not receive the immune defense signals anymore which induce an increase sensibility to mycobacteria infection [Newport et al. 1996].

1.1.2 Factors impacting communication

Considering the diversity of communication methods, messages and responses, it becomes evident that independent factors impact interactions between individuals. In sociology, different theories point out the cultural context as a major factor influencing communication and the efficacy of the message transmission. The theory introduced by anthropologist Edward T. Hall exposed that two types of culture, "low" and "high" contexts, are opposed and play a role in communication [Hall 1976]. "Low context" is defined by an explicit communication whereas "high context" is characterized by implicit communication, with the use of ambiguity where facial expression and the way of speaking can change the meaning of words. Therefore, low-context individuals, who are not used to read between lines, are less able to fully understand the messages transmitted by high-context individuals. This can be nefast for social interactions and *a fortiori* for the development of the society especially in diplomatic exchanges. A second interesting hypothesis by Sapir and Whorf shows that culture significantly affects how people think and communicate.

More precisely, the language which is one of the bases of a culture and brings together people strongly affects the way of thinking. Ciaccio and Bormann studied the influence of color terms on the behavior of Italian and German speakers [Ciaccio and Bormann 2013]. They demonstrated that the judgments of colors boundaries was influenced by the language which validate the hypothesis of Sapir and Whorf. Environmental factors (*e.g.* pollution) or physical factors (*e.g.* the intensity of a signal, the speed of the transmission) can affect the effectiveness of communication or alter the signal ending in a communication break. The clarity of the message is important for the comprehension between individuals. A study has revealed the nefaste impact of traffic noise on communication between frogs. The noises were masking the perception of acoustic communication signals preventing male frogs from communicating efficiently with female and it leads to a decrease of reproduction [Bee and Swanson 2007]. Personal history and previous communications can drive the way of thinking and interpreting information facilitating or complexifying coding and decoding processes. Internet and social media increase communication between people by simplifying interactions, increasing speed of connection between people all around the world and allowing the spread of all kind of information. But it raises questions on the quality of communication: is the information trustable since it is easy to spread any kind of information? Due to the multiplicity of connections and exchanges, are the communication effective? This questions highlight the complexity of communication networks which are impacted by several factors in a positive or negative manner.

Looking at the cellular level, cell signaling can be impaired by factors acting directly on cells, altering the transmission or the reception of messages. Therapeutic agents can be used as receptor blockade mechanisms mimicking the ligand but without carrying the message that would have induced a response from the sensing cell. Communication can also be altered by genetic mutation destabilizing gene expression and response to stimuli. Stimuli such as Ultraviolet radiation (UV) provoke genetic mutation that can alter the expression of key genes, inducing skin cancer [Seebode, Lehmann, and Emmert 2016]. Mutated cells use a communication system different from normal cells, notably they release new signals to proliferate

and survive. Cells can communicate and answer to stimuli differently according to their type and origin. If cells exhibit a plastic phenotype, they can sense external stimuli such as communication signals and adapt their future communication within the cellular environment (*e.g.* stress, UV, cigarette smoke, diet, culture medium). Given different stimuli and environments, a cell can differentiate into several states. A stimulus or a combination of stimuli sensed by one cell type can impact its communication with other cell types inducing various responses. For example, DCs have been identified as the main drivers of T helper (Th) polarization in 1999 [Rissoan et al. 1999]. However Th cells integrate numerous signals to specify their phenotypes [Zygmunt and Veldhoen 2011]. A large number of Th subsets have be defined based on the diversity cytokines patterns produced by Th cells [Raphael et al. 2015]. These results reveal the intrinsic complexity of the Th differentiation process as a central communication system integrating multiple signals coming from DCs and producing a large diversity of Th responses [Grandclaudon et al. n.d.]. The environment is a major factor impacting the signaling. Inflammation is triggered when innate immune cells detect infection or tissue injury. Changes occur in the inflamed environment such as the presence of cytokines impacting communication and behavior of non-immune cells. This peculiar microenvironment will be further described in section 1.4.2.

1.1.3 Network representation of communication

The organization of multiple entities through communication is a complex system that researchers try to understand. To study complex system such as cell-to-cell communication, networks are powerful tools to use [M. E. J. Newman 2003]. In mathematics, a network or graph is a set of nodes that are connected together by connections called edges or links. Two types of networks are distinguishable: directed and undirected. The first one is characterized by links indicating the direction in which the information circulates. If all edges are bidirectional, or undirected, the network is an undirected network. Representation of networks is often used in different fields of application. As examples we can cite connections between individuals on social media, the internet, financial networks or biological networks.

In the case of a communication network, nodes describe entities communicating and edges monitor the transmission of messages. Putting communication into the perspective of a network enables to organize knowledge on cell interactions into a systemic view. Cell-to-cell communication networks comprise both intra- and intercellular processes. Several studies focusing on intracellular communication networks are found in the literature and describe metabolic networks [Jeong et al. 2000], gene-regulatory networks [Thompson, Regev, and Roy 2015], or networks of protein-protein interactions [Hooda and Kim 2012]. These networks can model the signal transduction processes inside the cell and the response induced by the message. Intercellular networks model the interactions between different cell types. However, compared with intracellular signal transduction networks, the functions and engineering principles of cell-to-cell communication networks are less understood. Many studies have addressed cross-talks between a given pair of cell types [Ferlazzo and Morandi 2014; Haan, Arens, and Zelm 2014; Hivroz et al. 2012]. Most of the time, communication process is considered a linear signaling cascade, such as immune cascades [Ghirelli et al. 2015; Y.-J. Liu et al. 2007] involving the exchange of one information signal at each step. Some studies have focused their purpose on specific cases of communication such as the cytokines interleukin-2 (IL-2) [Fuhrmann et al. 2018], interferon-gamma (IFNγ) [Helmstetter et al. 2015], or tumor necrosis factor alpha((TNF-α) [Paszek et al. 2010; Tay et al. 2010]. This view has several limitations: 1) it does not consider the possibility that one given cell type could communicate with multiple cell types concomitantly within the same microenvironment [Bindea et al. 2013; C. Q. F. Wang et al. 2013], 2) it does not consider the multiplicity of information signals possibly sent by one cell to another, 3) it does not integrate the complex and constant rewiring and cell state modifications in the system following exchange of information, 4) it provides limited mechanistic insight into the complexity of multicellular pathophysiological processes, 5) as a consequence, it is very limited in predicting the effects of physiological or pharmacological perturbations in higher order multicellular systems.

To study cell-to-cell communication network, it is important to define and characterize the microenvironment of cells to model their interaction and behavior. In-

deed, the microenvironment impacts cell communication as culture impacts human communication.

1.1.4 A model of network: cellular microenvironment

1.1.4.1 Diversity of cellular microenvironments at the physiological state: role of the tissue type

Within an organism, each cell exists in the context of a complex extracellular microenvironment. Different types of tissues across the human body have been defined such as nervous tissue, muscle tissue, epithelial tissue and connective tissue. Within a given tissue, microenvironmental factors and extracellular matrix proteins cooperate to provide both the biochemical signals and structural constraints that are required to influence intracellular programs of gene expression and further the cellular behaviors in the tissue in question. Various cell populations are described having tissue-dependent functions creating a specific cellular environment. This is the case for certain populations of immune cells. Studies have shown that T-cell primed by tissue-specific dendritic cells (DCs) can change their specific functions if they are re-primed by other tissue-specific DCs [Mora and Andrian 2006]. Natural killer cells (NKs) are a type of lymphocyte that identify infected or transformed cells through a complex range of activating and inhibitory receptors that regulate direct and indirect killing mechanisms. They migrate from peripheral blood to peripheral organs through cytokines-mediated signals. However, studies have highlighted the existence of tissue-specific subpopulations of NKs [Shi et al. 2011]. Tissue-specific NK cells are found in different tissues across the body. Studies suggest that subpopulations of tissue-specific NK cells may undergo phenotypic changes under inuence of the microenvironment, but also differentiate *in situ* from tissue-resident hematopoietic progenitor cells [Lysakova-Devine and O'Farrelly 2014]. Macrophages are immune cells present in most tissues in vertebrates. They are best known for their phagocytic role in immunity, but they can also function as an important source of growth factors for other cell types within tissues. Tissue-resident macrophages are heterogeneous populations in terms of phenotype and function. According to the location they re-

side, tissue-resident macrophages display specific functions which are important for normal tissue homeostasis [Ginhoux and Guilliams 2016; Gosselin et al. 2014; Okabe and Medzhitov 2016]. Similarly, signaling factors derived from tissue environments play key roles in promoting the ontology and phenotype of the residing macrophage populations [Okabe and Medzhitov 2016].

1.1.4.2 Physiology versus pathology

In addition to the specificity of tissue microenvironment, one key factor to think of when studying cellular environment is the physiological or pathological context. Steady state and inflammation have a different impact on communication between cells creating a specific microenvironment. Inflammation is a state of the microenvironment due to the establishment of an adaptive immune response after pathogen infection, external injuries or an effect of chemicals or radiations. Inflammation reflects a complicated, multifactorial, and multidimensional process, in which acute and chronic inflammation are differentiated. Acute inflammation is a short-term process occurring in response to tissue injury appearing within minutes or hours. It is characterized by five main signs: pain, redness, loss of function, swelling and heat. Inflammation follows several steps independently of the stimulus initiating the immune response. First, cell surface pattern receptors recognize detrimental stimuli that lead to activation of inflammatory pathways such as NFκB or MAPK pathways. Then, inflammatory markers, inflammatory cytokines, proteins, or enzymes, are released and inflammatory cells are recruited in the microenvironment [L. Chen et al. 2017]. The last step is the resolution of the issue by tissue repair and remodeling by monocytes. This is made possible by the switching from pro-inflammatory to anti-inflammatory signals in the inflammatory environment, promoting the recruitment of monocytes and inhibiting recruitment of neutrophils [Medzhitov 2008]. In the case of infection, if the acute inflammatory response fails to eliminate the pathogen, the inflammatory process persists with the presence of macrophages and T cells in the tissue and a chronic inflammatory state occurs [Medzhitov 2008]. The chronic inflammatory process that plays a central role in some of the most challenging diseases, including cancers, rheumatoid arthritis, heart diseases, diabetes, asthma, and

even Alzheimers. Complex genetic and environmental interactions contribute to the development of chronic inflammatory diseases. Autoimmunity is characterized by dysregulation of the adaptive immune system as well as the pathogenic role of innate immunity and is associated with several chronic inflammatory diseases. Studies have shown the importance of microbiota in the development of autoimmunity [Yurkovetskiy, Pickard, and Chervonsky 2015] but also the genetic impact of several autoimmune diseases [Zenewicz et al. 2010]. Chronic inflammation is thought to promote cancer development. Today, between 5% and 10% of cancer cases are thought to be triggered by mutation and up to 15% by inflammation; the origin of the 80% left is still unknown [Brücher and Jamall 2014]. Cancer is a complex and heterogeneous disease affecting several cell populations in many localization and tissues. The tumor microenvironment (TME) is a complex network not only composed of malignant cells but also stromal cells. Communications among tumor and stromal cells create a distinct cellular environment that plays a significant role in tumor development and progression. In solid tumors, fibroblasts in the TME secreting chemokines and growth factors contribute to tumor growth and affect the extracellular matrix environment that helps tumor to progress [Allen and Jones 2011]. Studies have shown the impact of metabolism in TME, particularly hypoxia that induce angiogenesis, and invasion [Allen and Jones 2011]. Since it is an inflamed environment, we can find immune cells infiltrating the TME. Leukocyte infiltration of solid tumors was first described in the 1800s by Virchow. Proinflammatory cytokines, chemokines, and adhesion molecules, which regulate the recruitment of leukocytes, are frequently observed in the TME. Some leukocytes including cytotoxic T cells and NK cells have a pro-inflammatory and anti-tumor role [DeNardo, Andreu, and Coussens 2010; Gavin P. Dunn, Old, and R. D. Schreiber 2004] whereas other leukocytes such as regulatory T cells and macrophages play an anti-inflammatory and pro-tumoral role promoting cancer immune evasion and cancer progression [DeNardo, Andreu, and Coussens 2010].

For my thesis work I was interested in studying communication processes in one particular network which is breast cancer microenvironment.

1.2 Human Breast Cancer

1.2.1 Factors of incidence

Breast cancer is the second most common cancer worldwide with nearly 1.7 million new cases in 2012 and is the first cause of mortality by cancer among women (http://globocan.iarc.fr/Default.aspx). In the literature, many factors are known to have an incidence on the risk to develop breast cancer. Some mutations, particularly in BRCA1/2, EGFR, and p53 genes result in an increased risk of occurrence of breast cancer [M.-C. King et al. 2003; Malkin et al. 1990; Sun et al. 2017]. However, it concerns only a small proportion of tumors, less than 30% of breast cancers. On the other hand, exposure to endogenous hormones (estrogen) increases the risk of breast cancer occurrence [Travis and Key 2003]. During the last decades, many groups have pointed out the higher risk of developing breast cancer induced by using exogenous hormones such as hormone replacement therapies (HTR). Moreover, the relative risk of breast cancer in current users increases with increasing duration of use of HRT [Li et al. 2003]. Additionally, environmental signals play a role in modifying the incidence of breast cancer. Danaei et al. have studied the impact of several environmental factors (*e.g.* cigarette smoke, diet, obesity) on the incidence of cancers worldwide. They showed that alcohol use, overweight and obesity, and physical inactivity have a joint incidence on 21% of all breast cancer deaths worldwide [Danaei et al. 2005].

The diversity of factors involved in the appearance of breast cancer is a first observation of the complexity of this disease. Another important layer is the heterogeneity of breast cancer subtypes.

1.2.2 Breast cancer subtypes and inter-tumor heterogeneity

1.2.2.1 Classification

Breast cancer has been suggested to be a heterogeneous disease, and multiple classifications exist to better characterize this disease and improve treatments and care of the patients. The first classification of breast cancer relies on the histopathological

status of the disease. It is divided into more than 20 types with the most important being invasive ductal carcinomas (IDCs), not otherwise specified (NOS), and invasive lobular carcinoma (ILC). The grade of the disease can also be taken into account in the classification of breast cancer. Several scores measure the disease state such as Eston-Ellis grade, Nottingham prognostic index, or tumor, lymph nodes and metastasis status (TNM). They are based on measurement of the tumor growth and development, or the lymph node invasion status [Sinn and Kreipe 2013; Viale 2012]. Based on the molecular and transcriptional profile of breast cancers, different subtypes have been identified and correlated with clinical outcome [Koboldt et al. 2012; Prat, Pineda, et al. 2015; Viale 2012]. Six breast cancer subtypes have been established based on expression of hormone receptors (HR) which are estrogen receptor (ER) and progesterone receptor (PR), expression of HER2 (human epidermal growth factor 2), and Ki-67 protein immunoreactivity:

- Luminal A breast cancer is hormone-receptor positive (estrogen-receptor and/or progesterone-receptor positive), but negative for HER2 and have low level of Ki67 immunoreactivity. It is also characterized by a genomic stability.

- Luminal B breast cancer is hormone-receptor positive as Luminal A but is characterized by less genomic stability with some amplification (HER2), deletions and mutations (P53). It can be either HER2-positive or negative with high levels of Ki67 immunoreactivity.

- HER2enriched breast cancer has amplification of ERBB2 and many other genes. It is defined by positive expression of HER2 and no expression of the hormone receptors (ER, PR).

- Triple-Negative (TNBC) or Basallike breast cancer is defined based on the absence of expression of hormone receptors (ER, PR) and HER2. TNBC have a high genomic instability.

- Normal Breastlike group is similar normal breast epithelium in transcriptomic analyses.

- Claudinlow breast cancer is characterized by low expression of cell-to-cell communication proteins (claudins), no/low markers of luminal differentiation and a high expression of epithelial to mesenchymal transition (EMT) markers, immune response genes and cancer stem-cell markers. These tumors are only high grade and are less frequent (12-14% of cancers)

These breast cancer classifications highlight the heterogeneity of the disease, at multiple layers: localisation, grade, molecular profile. Additionally, they have been linked to distinct clinical outcome.

1.2.2.2 Diversity of behavior and outcome

Tumor complexity is due to the heterogeneity of the disease which impacts the clinical behavior and outcome of the patients [Koren and Bentires-Alj 2015]. The molecular subtypes of breast cancer correlate with different clinical outcomes and response to treatment [Prat, J. S. Parker, et al. 2010; Prat, Pineda, et al. 2015; Troester et al. 2004]. Troester et al. compared basal and luminal BC cell lines and showed that molecular subtypes of BC have a subtype-specific response to chemotherapies which was validated by *in vivo* data [Troester et al. 2004]. PAM50, a 50-gene qPCR assay, has been identified as a predictive marker of pathological complete response (pCR) regarding chemotherapy response. This predictive marker was shown to reflect the intrinsic molecular classification and its correlation to clinical outcome [Y.-R. Liu et al. 2016; Prat, Pineda, et al. 2015].

Luminal A cancers are low-grade, tend to grow slowly and have the best prognosis and long-term survival while luminal B cancers prognosis is slightly worse. This difference of prognosis was suggested to be due to a variation in response to estrogen therapy between luminal A and B [Rivenbark, OConnor, and Coleman 2013; Sørlie et al. 2003]. Triple-Negative or basal-like breast cancers are more aggressive with high rates of cell proliferation and have poor clinical outcomes. As they do not express hormone receptors neither HER2, herceptin and hormone therapies cannot be used. Patients with claudin-low breast cancer have poor recurrence-free and overall survival outcomes, this cancer not being responsive to chemotherapy treatments [Prat, J. S. Parker, et al. 2010]. HER2-enriched breast cancers are associated

with a poor clinical outcome. As they are ER negative, they are not treated with anti-estrogen receptor therapies. However, survival of HER2$^+$ breast cancer (HER2-enriched, Luminal B) improved thanks to herceptin-targeted therapy, in addition to adjuvant chemotherapy [Cortés et al. 2012; Mukai 2010].

Although the molecular classification of breast cancer help to characterize the disease and defined adapted therapies, the patient outcomes are disparate. The observed variation in treatment efficacy has been connected to heterogeneity in the cellular composition of individual tumors and significant heterogeneity in immune composition is observed across subtypes as well as patients [Dushyanthen et al. 2015; García-Teijido et al. 2016]. This highlights the importance of taking into account the molecular subtypes as well as the intra-tumoral heterogeneity when studying breast cancer networks and communications.

1.2.3 Intra-tumor heterogeneity

Two distinct but complementary theories describe the origin of tumor cells heterogeneity, the cancer stem cell (CSC) hypothesis [Meacham and Morrison 2013] and the clonal evolution and selection model [Greaves and Maley 2012]. CSCs originate from single cells possessing specific characteristics regarding cell plasticity. Those cells undergo tumor-reprogramming processes via multiple molecular alterations through a specific hierarchy and have indefinite self-renew potential that drive tumor growth. These mechanisms drive temporal intra-tumor heterogeneity. The clonal evolution/selection model is based on clonal expansion by natural selection and adaptation to tissue microenvironments. The factors contributing to clonal expansion promotes certain cellular characteristics allowing cancer cell proliferation in hypoxia environments. Depending on the local microenvironment, the clonal expansion wont be promoting the same clones, contributing to spatial heterogeneity. In the majority of the cases intra-tumor heterogeneity is clonal-based, however it has been shown in the literature that some areas of the tumor can be morphologically distinct with different repertoires of genetic aberrations [Greaves and Maley 2012; Martelotto et al. 2014]. Intra-tumoral heterogeneity is a complex interplay between CSCs genetic and epigenetic mutations and clonal evolution promoting develop-

ment and evolution of breast cancer to metastasis. Several studies have revealed genetic differences between primary breast tumors and their metastases [Bonsing et al. 2000; Kuukasjärvi et al. 1997; Pandis et al. 1998; Torres et al. 2007; C. Wu et al. 2009]. Genetic and epigenetic modifications can be caused by external factors such as cigarette smoke, UV lights, chemotherapy agents and/or the microenvironment during the development and growth of the tumor contributing to the temporal heterogeneity of breast cancers [Martelotto et al. 2014]. Studying intra-tumor heterogeneity could have clinical benefits since we observe treatment failures due to therapeutic selection of cancer cells harboring resistance mechanisms [Turner and Reis-Filho 2012].

Both inter-tumoral and intra-tumoral heterogeneity make breast cancer a complex disease. Tumor cells evolve in a specific microenvironment (including non-tumoral cells) that display specific signaling that can be hijacked by the tumor to promote its progression and survival [Poli, Fagnocchi, and Zippo 2018].

1.2.4 Tumor microenvironment

TME is a complex network composed of cancer cells, stromal cells, endothelial cells, immune cells as well as components of the extracellular matrix (ECM). As described above, the TME shows high level of spatiotemporal heterogeneity which is partly due to alterations of the microenvironment. In normal breast, epithelial and stromal cells communications are essential to inhibit tumor growth and proliferation [Quail and Joyce 2013]. However, in breast cancer, communication between cancer cells and non-malignant cells infiltrating the TME promotes heterogeneity, growth and proliferation of the disease [Quail and Joyce 2013]. Understand the composition of the tumor microenvironment and what are the interactions that promote development and resistance of the disease could help define better therapies. The TME is not only impacted by the presence of tumor cells, but it is also involved in the development of the disease, in different ways. Specific changes happen in the breast tumor microenvironment that regulate progression to invasion and metastasis, for instance increase of fibroblast proliferation and ECM remodeling [Bonnans, Chou, and Werb 2014]. Stromal cells can create a permissive microenvironment for tu-

morigenesis.[Mao et al. 2013]. We also observe cell-to-cell signaling changes. Genes encoding for secreted proteins and cell surface receptors are found differentially expressed in epithelial and stromal cells during breast tumor progression [Allinen et al. 2004]. Paracrine signaling takes place through secretion of soluble factors by cancer cells, fibroblasts and other cells of the TME. Allinen et al. performed a molecular characterisation of breast cancer microenvironment. They compared normal epithelial and stromal cells to cancer epithelial cells and infiltrating stromal cells. High expression of CXCL12 and CXCL14 by myoepithelial and myofibroblast were found in the TME. These chemokines are involved in cell proliferation, differentiation, migration, and invasion of breast cancer cell lines. Several signaling pathways involved in the interplay between tumor infiltrating cells and cancer cells promote tumor growth, metastatic spread or even drug resistance. TGF-β signaling in breast TME plays an important part in tumorigenesis. It has implication in angiogenesis, recruitment of endothelial cells, monocytes and macrophages, and activation of fibroblasts. TGF-β also suppress T cell immunosurveillance and cytotoxic activity [Scheel et al. 2011; Taylor, Lee, and Schiemann 2011]. Breast tumor microenvironment represents a social network where cells produce and interpret a diversity of signals promoting cancer cells progression. Figure 1.3 represent in a schematic view these interactions between the cells of the breast environment. Cancer cells cross-talk with endothelial cells, fibroblasts and immune cells such as macrophages and T cells, using specific signaling including TGF-β, growth factors and inflammatory cytokines.

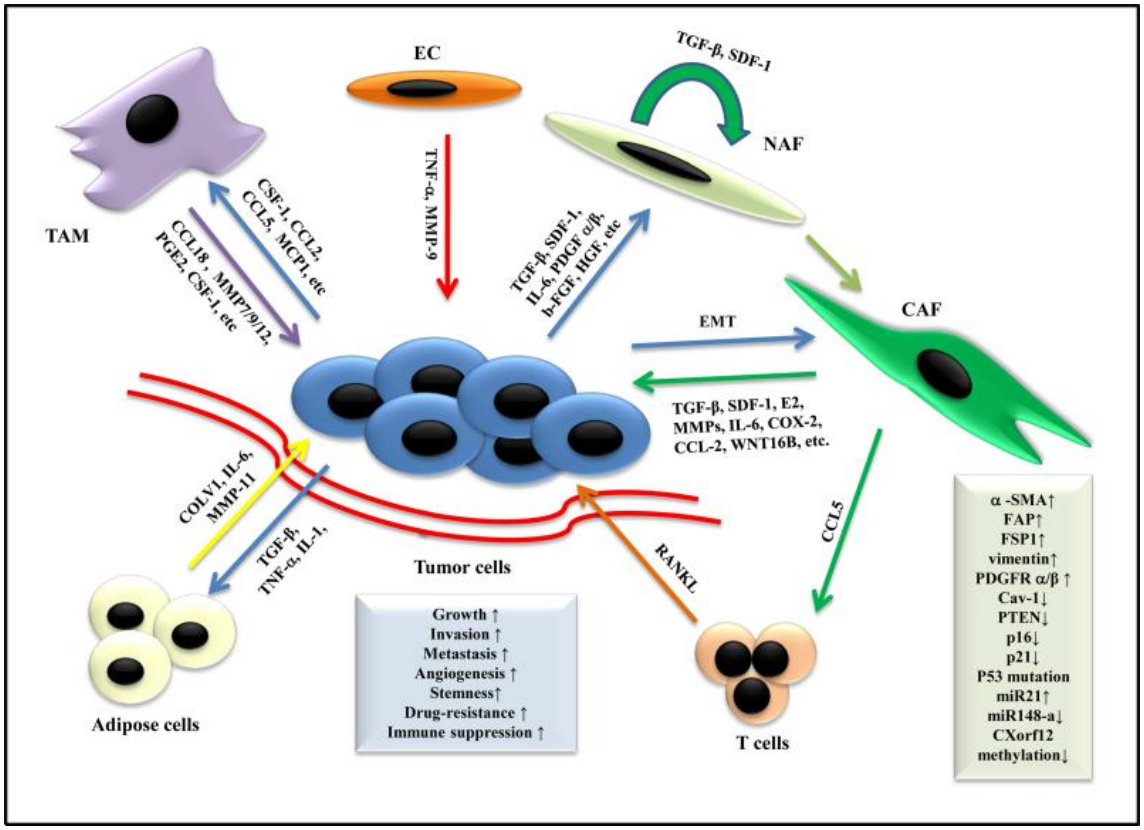

Figure 1.3: Schematic representation showing the role of stromal cells in microenvironment and breast cancer progression. The tumor microenvironment is a dynamic composite of cells broadly categorized as multiple components of non-stromal and stromal cells, where tumor cells thrive. Stromal cells promote tumor growth, invasion, and metastasis by secreting multiple cytokines, chemokines, growth factors, etc. Moreover, tumor cells also affect the phenotype of stromal cells. From Mao et al. 2013.

1.2.5 Inflammatory environment

At the beginning of cancer studies, the immune system was not considered as playing a role in cancer development neither on the clinical outcome of patients. In breast microenvironment, immune cells play a role of immunosurveillance, by killing potential cancer cells before they became a cancer. However, the immunosurveillance of immune cells put a selective pressure on cancer cells that develop resistance mechanisms and escape immune surveillance or generate an immunosuppressive environment [Gavin P. Dunn, Bruce, et al. 2002]. This implies changes in the cell-to-cell

interaction network formed by the cells of the TME. Only recently, immune evasion has been recognized as a hallmark of BC which is enabled by three major characteristics being (epi)genetic modifications and clonal selection of cancer cells, and tumor-promoting inflammation [Hanahan and Weinberg 2011]. Now, it is well known that the TME is composed of different immune cell populations such as T and B lymphocytes, natural killers (NK), and myeloid cells including macrophages, myeloid derived suppressor cells (MDSCs), and dendritic cells (DCs). Cellular crosstalk between different leukocyte subsets infiltrating the breast cancer TME induces either pro- or antitumor functions driving immune-mediated anti- or pro-tumor activities in the microenvironment [D. S. Chen and Mellman 2013; DeNardo, Andreu, and Coussens 2010]. Distinct populations of tumor-infiltrating lymphoid and myeloid cells have been linked to different prognosis in BC patients [Kroemer et al. 2015]. While breast tumor infiltration by $CD8^+$ T cells was associated with patient survival and response to therapy [DeNardo, Brennan, et al. 2011; Mahmoud et al. 2011; Seo et al. 2013], regulatory $CD4^+FOXP3^+$ T cells support pro-tumor immunity and are associated with a poor prognosis in some cases of breast carcinoma [Ibrahim et al. 2014; Yeong et al. 2017; Zhou et al. 2017]. Myeloid cells localized in pre- and malignant tissues release amount of cytokines, soluble factors and other inflammatory molecules. These signals contributing to tissue remodelling, angiogenesis, and suppression of anti-tumor immunity [Stockmann et al. 2014]. If MDSCs have been characterized as regulator of the immune system [Gabrilovich and Nagaraj 2009], they also play a role in cancer development and metastasis. MDSCs and cancer cells interaction *via* IL-6/STAT3 and NOTCH signaling induce CSCs development [Peng et al. 2016]. Cancer cells also secrete molecules influencing the microenvironment towards pro-tumoral and pro-inflammatory environment. Ghirelli et al described the activation of pDC *via* GM-CSF and IL-6 secretion by breast tumor cells that was linked to a worse prognosis [Ghirelli et al. 2015]. Over the past years, new therapies have been developed targeting the immune system in cancer. As described by the concept of hot versus cold tumor, the diversity of TILs infiltration levels in tumors may impact the efficacy of immunotherapies [L. Chen et al. 2017; Spranger 2016; Wargo et al. 2016]. In breast cancer, level of TILs is variable across BC subtypes

and high levels of TILs are correlated with increased expression of the checkpoint molecule programmed cell death 1 ligand (PD-L1). Immunotherapy treatments rely on therapeutic antibodies targeting immune checkpoint molecules that have co-stimulatory or co-inhibitory functions. Clinical trials on TNBC show some positive results. For instance, monotherapies targeting programmed cell death 1 (PD-1) and one of its ligand CD274 (PD-L1) which have an inhibitory interaction in metastatic TNBC and showed between 4.7% and 23% of overall response rate (Figure 1.4)[Tan 2018]. Despite some treatment successes, the response seen in patients is limited, especially in other subtypes such as luminal, drawing attention to the need of better understanding the immune components of the TME.

Breast Cancer Subtype	Trial	Phase	Drug	No. of Patients Screened/ Enrolled	No. (%) With PD-L1 Positivity	No. Evaluable	Outcomes	References
TNBC PD-L1–positive	KEYNOTE-012 NCT01848834	Ib	Pembrolizumab	111/32	65 (58.6% of screened)	27	ORR: 18.5%; 1 CR, 4 PRs	Nanda et al (SABCS 2014, SABCS 2016, *JCO* 2016)[3-5]
TNBC	KEYNOTE-086 NCT02447003 Cohort A	II	Pembrolizumab	386/170	Unselected	170	ORR: 4.7%; 1 CR, 7 PRs	Adams et al (ASCO 2017)[10]
TNBC PD-L1–positive	KEYNOTE-086 NCT02447003 Cohort B	II	Pembrolizumab	167/52	79 (47% of screened)	52	ORR: 23%; 2 CRs, 10 PRs	Adams et al (ASCO 2017)[11]
TNBC PD-L1–positive	GO27831 NCT01375842	Ia	Atezolizumab	54 enrolled	21	21	ORR: 19%; 2 CRs, 2 PRs	Emens et al (AACR 2015)[6]
TNBC	GO27831 NCT01375842	Ia	Atezolizumab	115 enrolled	72 (63% of enrolled)	112	ORR: 10%; 3 CRs, 8 PRs	Schmid et al (AACR 2017)[7]
TNBC	JAVELIN NCT01772004	Ib	Avelumab	All comers: 266/168	Unselected	58	ORR: 5.2%; 3 PRs	Dirix et al (SABCS 2015; BCRT 2018)[8,9]
ER-positive/ HER2-negative PD-L1–positive	KEYNOTE-028 NCT02054806	Ib	Pembrolizumab	248/48	48 (19.4% of screened)	25	ORR: 12%; 3 PRs	Rugo et al (SABCS 2015; CCR 2018)[12,13]
HR-positive/ HER2-negative	JAVELIN NCT01772004	Ib	Avelumab	All comers: 266/168	Unselected	72	ORR: 2.8%; 2 PRs	Dirix et al (SABCS 2015; BCRT 2018)[8,9]
HER2-positive	JAVELIN NCT01772004	Ib	Avelumab	All comers: 266/168	Unselected	26	ORR: 0%	Dirix et al (SABCS 2015; BCRT 2018)[8,9]

Abbreviations: AACR, American Association of Cancer Research; ASCO, American Society of Clinical Oncology; BCRT, Breast Cancer Research and Treatment; CCR, Clinical Cancer Research; CR, complete response; ER, estrogen receptor; HR, hormone receptor; *JCO, Journal of Clinical Oncology*; ORR, overall response rate; PR, partial response; SABCS, San Antonio Breast Cancer Symposium; TNBC, triple-negative breast cancer.

Note: ORR is defined by RECIST version 1.1.

Figure 1.4: Clinical trials of checkpoint inhibitors as monotherapy in metastatic breast cancer. From Tan 2018.

1.3 Antigen presenting cells

Antigen presenting cells (APCs) are key players of the immune system communication/social interactions and infiltrate the tumor microenvironment. Professional APCs include dendritic cells (DCs), B cells, and macrophages [Parkin and Cohen 2001]. These peculiar cells are the sentinels of the body and have an extremely important role as messenger of the immune system. They patrol many tissues and are able to trigger the adaptive immune response by presenting exogenous antigens through MHC class II molecules. This complex is then presented to T cells that recognize antigens *via* their TCR. These interactions lead to activation of T cells.

Here, we will focus on monocytes, macrophages and DCs which are mononuclear phagocytes distinguished on the basis of their morphology, function and origin.

1.3.1 Monocytes and macrophages

Monocytes are present in all vertebrates. In humans, these cells represent 10% of the nucleated cells in the blood. They arise from myeloid precursor cells in primary lymphoid organs. Two main human monocyte subpopulations are defined as $CD14^{+}$ and $CD14^{low}CD16^{+}$ monocytes. The first category can be further subdivided into distinct populations of $CD14^{+}CD16^{+}$ and $CD14^{+}CD16^{-}$ monocytes that have differential capacities to secrete key inflammatory cytokines upon in vitro stimulation [Sánchez-Torres et al. 2001]. Monocytes and their progeny display various physiological processes including both DC-like and macrophage-like activities. They are able to promote angiogenesis and arteriogenesis [Ginhoux and Jung 2014]. Upon inflammation, in tissues, monocytes can differentiate into tissue-resident macrophages and especially in cancer they can give rise to tumor associated macrophages [Wynn, Chawla, and Pollard 2013].

Macrophages are myeloid immune cells that are characterized by avid phagocytosis. They are found in all tissues and have functions on various mechanisms such as development, tissue homeostasis, wound healing and tissue repair through immune responses to pathogens [Wynn, Chawla, and Pollard 2013]. Tissue macrophages have two distinct origins even though the majority of macrophages that reside in healthy

tissues are established prenatally and show self-maintenance properties [Hashimoto et al. 2013]. As exposed before, macrophages can also derive from tissue-infiltrating monocytes [McGovern et al. 2014; Wynn, Chawla, and Pollard 2013]. In inflammatory condition, studies have delineated the activation of macrophages in response to various signals which exhibit distinct phenotypes called M1 and M2 [Gordon 2003; Sica and Mantovani 2012]. M1 macrophages express high levels of proinflammatory cytokines, produce reactive nitrogen and oxygen intermediates, promote Th1 response, and are able to kill microbes and tumor cells. In contrast, M2 macrophages promotes tissue remodeling and cancer progression. They are also characterized by immunoregulatory functions and efficient phagocytic activity. M1-M2 macrophages are also distinct in their chemokine expression profiles [Sica and Mantovani 2012]. Tumor-associated macrophages secrete growth factors in the TME, promote breast cancer progression and correlate with poor prognosis [Mao et al. 2013].

1.3.2 Dendritic cells

DCs were first described in mice by R. Steinman and Z. Cohn in 1973 [Steinman and Z. A. Cohn 1973]. These peculiar cells are essential sentinels and messenger between the innate and adaptive immune system. DCs are bone marrow-derived cells present in blood, lymphoid organs and tissues. When patrolling the body, the "immature" DCs can sense pathogen-associated and danger-associated signals and capture antigens. They are specialized antigen-presenting cells: they uptake antigens with high efficiency *via* different mechanisms including phagocytosis, micropinosis and endocytosis and present them through MHC class II molecules. DCs are able to present antigenic peptides complexed to MHC class I molecules to $CD8^+$ T cells which will differentiate into cytotoxic killer cells capable of eliminating infected cells, damaged cells and even tumor cells [J. Banchereau and Steinman 1998]. Upon activation, DCs migrate to lymphoid organs to initiate adaptive immune response by interacting with T and B cells.

1.3.2.1 Notion of subset

First described as a largely homogeneous population distributed throughout the body, dendritic cells (DC) are, in fact, composed of distinct subtypes each specialized to respond to particular pathogens and to interact with specific subsets of T cells. Heterogeneity of the DCs have been described by generating the transcriptional profiles of mouse and human leukocytes (ImmGen) [Collin, McGovern, and Haniffa 2013]. Several subsets of DCs were characterized based on their ontogeny, phenotypic and functional specialization. All human DCs express high levels of MHC class II (HLA-DR) and lack typical lineage markers CD3 (T cell), CD19/20 (B cell) and CD56 (NK cell). The different subpopulations of DCs are defined as HLA-DR^+ $lineage^-$ cells. Several positive DC lineage markers identifies DCs as either "myeloid" or "plasmacytoid" and exclude monocytes expressing CD14 and CD16 markers [Haniffa, Collin, and Ginhoux 2013]. Two types of "classical" or "myeloid" DCs from "plasmacytoid" DCs can be distinguished across all mammalian species by looking at the differential expression of interferon regulatory factors 8 and 4 (IRF8 and IRF4) [Collin and Bigley 2018]. These three subsets derive from common myeloid progenitors (Figure 1.5). Each subset of DCs can be identified by the expression of surface markers and the secretion of various cytokines [Collin and Bigley 2018] (Figure 1.6).

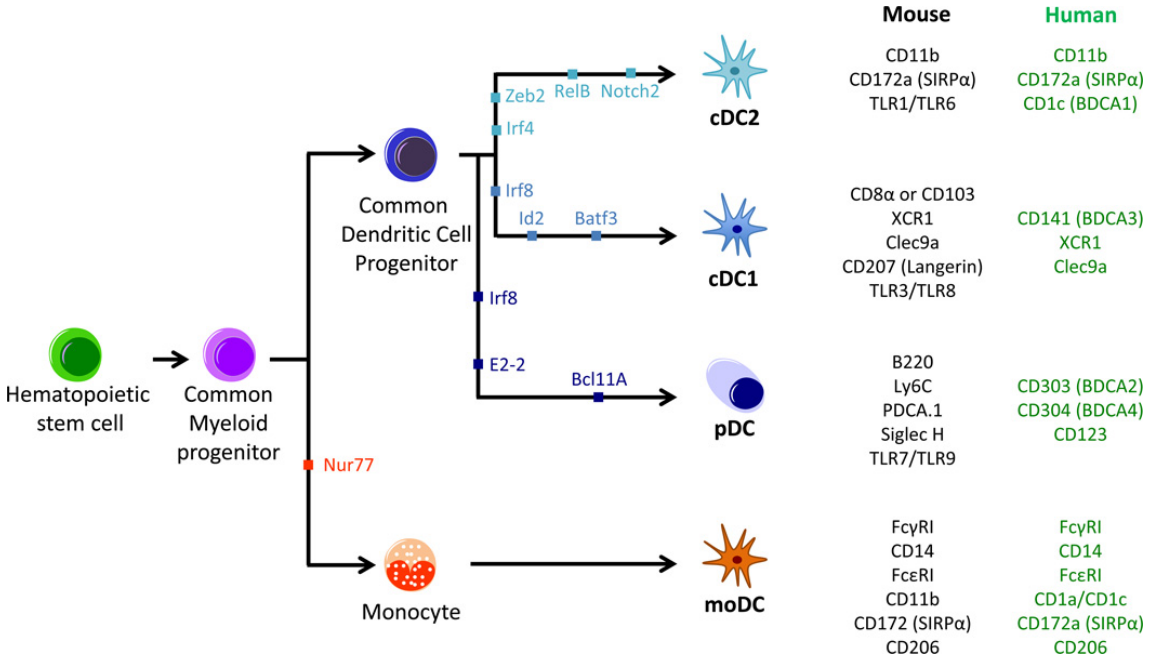

Figure 1.5: Monocytes and DCs classification. From Gardner and Ruffell 2016.

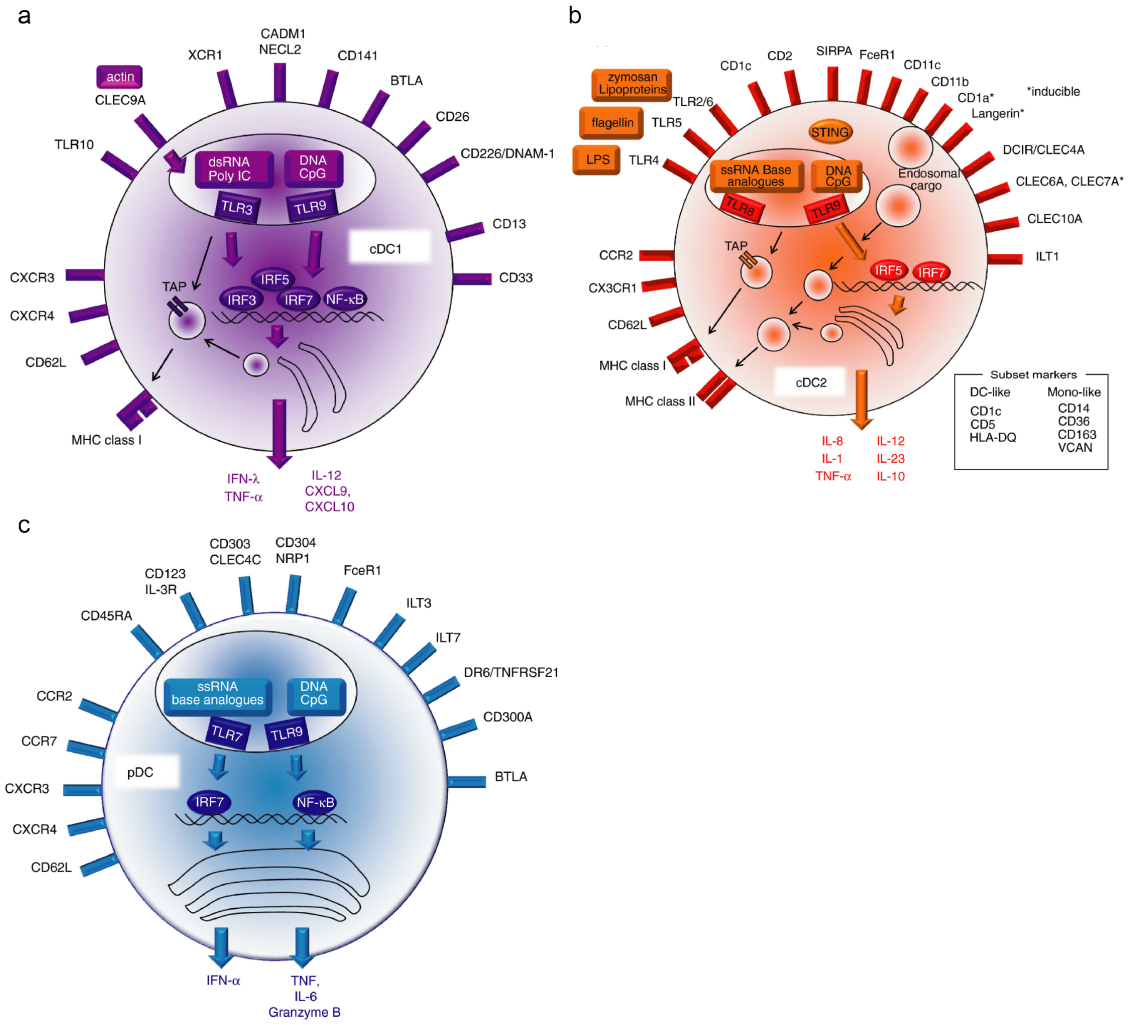

Figure 1.6: Human dendritic cell subsets. Features of the principal human dendritic cell (DC) subsets. Diagrams of the main surface markers, pathogen sensors and responses of (a) classical DC1 (cDC1) and (b) cDC2 ; (c) plasmacytoid DC (pDC). Data are principally drawn from observations on freshly isolated blood DC and do not capture the variety of responses possible following inflammatory activation. From Collin and Bigley 2018.

1.3.2.2 Classical DCs

In humans, the two subsets of classical DCs (cDCs) can be characterized in part by expression of BDCA-1 (CD1c) and BDCA-3 (CD141) in peripheral blood (Fig6 a-b). Haniffa et al also found these two subsets in other peripheral tissues such as liver, skin and lung [Haniffa, Shin, et al. 2012]. Human myeloid cDC1s are present

at approximately one-tenth the frequency of cDC2s in steady-state blood and tissues [Granot et al. 2017; Guilliams et al. 2016; Haniffa, Shin, et al. 2012; Heidkamp et al. 2016; Ziegler-Heitbrock et al. 2010]. Thanks to expression profiling, additional markers have been identified across species to characterize each population of myeloid DCs. These markers include CLEC9A, CADM1, BTLA, XCR1 and CD26 for $CD141^+$ myeloid cDC1, and CD2, FcεR1 and SIRPA for $CD1c^+$ myeloid cDC2 (Figure 1.5 and 1.6 a-b) [Collin and Bigley 2018]. cDC2s excel in $CD4^+$ T cell priming [L. Cohn et al. 2013; Jin et al. 2014] and promote T helper type 17 (Th17)- and T helper type 2 (Th2)-biased immune responses to extracellular pathogens [Persson et al. 2013; Schlitzer et al. 2013]. After stimulation, they can produce high amount of IL-12 which is known to drive IFNγproduction and promote cytotoxicity in primed naive T cells [Nizzoli et al. 2013]. cDC1s have a high capacity to crosspresent antigens *via* MHC class I to induce T helper type 1 (Th1) responses and natural killer responses via IL-12 expression. However, cDC1s express lower levels of IL-12 in comparison to cDC2 [Collin and Bigley 2018; Haniffa, Shin, et al. 2012; Poulin et al. 2010]. Myeloid cDC1s are also able to present viral and intracellular antigens and produce type III interferons (IFNλ)[Collin and Bigley 2018].

1.3.2.3 Plasmacytoid pre-DC

In 1997, Grouard et al and Olweus et al. discovered a $Lin^-HLA\text{-}DR^+$ plasmacytoid cell in human peripheral blood and lymphoid tissues, such as spleen and lymph nodes [Grouard et al. 1997; Olweus et al. 1997]. These cells were distinct from known myeloid DCs. At that time, they were named plasmacytoid T cells or plasmacytoid monocytes due to their expression of CD4, CD45RA, and their round shape and morphology resembling plasma cells [Grouard et al. 1997; Olweus et al. 1997]. However they did not express any T cell antigen, CD3, neither the myeloid antigens CD11b, CD11c, CD13, and CD33 while they have a high MHC-II expression when put in culture with monocytes. Upon culture with IL-3 and CD40L, plasmacytoid cells were shown to differentiate into cells with a mature DC morphology with dentrites [Cella et al. 1999; Colonna, Trinchieri, and Y.-J. Liu 2004; O'Doherty et al. 1994; Siegal et al. 1999]. As they were able to induce Th1 or Th2 responses after

activation by various stimuli, these cells were called plasmacytoid dendritic cells (pDCs). In 1999, Siegal et al. and Cella et al. definitively identified the pDCs of peripheral blood and secondary lymphoid organs as being the same population as natural interferon-producing cells previously described and responsible for type I interferon production in peripheral blood in response to most viruses [Cella et al. 1999; O'Doherty et al. 1994; Siegal et al. 1999]. pDCs play a role in viral infections and against bacterial and fungal pathogens. Upon recognition of nucleic acids from pathogens, pDCs produce massive amounts of type I and some quantities of type III interferons and acquire the capacity to present antigen. Production of type I interferons by human pDCs impact various cell types of the immune system including NK cells, DCs, T cells and even B cells. Indeed, it activates NK cells cytolytic activity against infected cells, and it promotes differentiation, maturation and immunostimulatory functions of DCs. Combined with IL-6 expression by pDCs, it induces B cells differentiation into plasma cells and production of immunoglobulin and induces early T cell activation markers, long-term T cell survival, IFNλproduction and Th1 differentiation [Colonna, Trinchieri, and Y.-J. Liu 2004].

1.3.2.4 Emerging subsets of DC

Recently, the evolution of RNA-sequencing techniques and single-cell isolation and analysis helped in defining emerging subpopulations of DCs. Two single-cell RNA-seq studies shed light on the heterogeneity of DCs subpopulations in blood. See et al. characterized a new subset of DC precursors called ["early pre-DC"], expressing CD33, CD45RA and CD123 markers [See et al. 2017]. Those cells present myeloid DC characteristics of inferior type I interferon production, higher IL-12 production and greater $CD4^+$ T cell allo-stimulatory capacity. In parallel, Villani et al. have characterized an other DC subpopulation with similar characteristics. This new population is $CD123^+$ resembling pDC but also express myeloid cDC antigens including CD11c, CD33 (SIGLEC3) and CX3CR1, AXL and SIGLEC6 (CD327). Though they were labelled AS DCs [Villani et al. 2017]. A new DC subset, called DC4, was described as distinct from nonclassical monocytes transcriptomic profile [Villani et al. 2017] and closer to a dendritic cell subset, although it resembles $SLAN^+$ cells

which are a controversial population called DCs or $CD16^+$ nonclassical monocyte in literature [Collin and Bigley 2018]. Their transcriptional profile is reminiscent of $SLAN^+$ cells with lower CD11b, CD14 and CD36 but higher expression of CD16.

1.3.3 Inflammatory DC (Monocyte-derived inflammatory DC)

In inflammatory skin context such as eczema [Wollenberg et al. 1996] or psoriasis [Wollenberg et al. 1996; Zaba, Krueger, and Lowes 2009] and inflammatory fluids including tumor ascites, one specific subpopulation of monocyte-derived DC (Mo-DC) was identified and called inflammatory DCs (infDCs). They present a DC morphology and phenotype with expression of CD11c, CD1c, FceR1, CD206, IRF4 cells and MHC class II expression (HLA-DR) suggesting they have the ability to activate T cells. Nonetheless, infDCs do not express CD16 and CD163 but they express CD14 at their surface at a lower level than macrophages [Segura and Amigorena 2013]. This peculiar cells can stimulate antigen-specific naive $CD4^+$ T cells during pathogen infection and induce Th differentiation [León, López-Bravo, and Ardavín 2007; Nakano et al. 2009; Segura, Touzot, et al. 2013]. infDCs can express key cytokines and chemokines that are crucial for T cell polarization [Plantinga et al. 2013; H. A. Schreiber et al. 2013]. infDCs are also able to migrate from the site of infection to draining lymph nodes in a CCR7-dependent manner [Segura and Amigorena 2013].

1.3.4 Plasticity of APC

Antigen presenting cells are composed of a variety of cell populations that are heterogenous. These subsets of cells have distinct origin and functions but importantly, one key feature is their plasticity regarding various stimuli and environments. Whether it is macrophages, monocytes or each subset of DCs, we can observe different spectra of activation and Th polarizations in response to environmental stimuli. As described previously, macrophages are extremely plastic cells, they exhibit a huge functional diversity and can undergo M1 or M2 activation depending on the disease and tissue as it was shown in vitro [Sica and Mantovani 2012]. Concerning DCs, the

ability of cDC1 and cDC2 to activate and polarize T cells into different Th profiles has been shown to depend on the activator they encounter. The type of pathogen sensed by DCs can induce a differential gene expression profile which impact their functions [Huang et al. 2001]. Alculumbre et al recently demonstrated that pDCs are plastic cells that can differentiate into two subsets with distinct phenotypes, morphology and functions [Alculumbre et al. 2018]. Those subsets appear only after activation with specific factors such as influenza virus infection.

If the type of stimuli sensed by APCs shapes their phenotype and functions toward a specific and adapted immune response, it may probably be the case of the tumor microenvironment. As we introduce previously, breast cancer is an heterogenous disease fashioned by the interaction of malignant and various non-malignant cells forming a peculiar cellular microenvironment. Since APCs are plastic cells, we can wonder whether the breast TME modulates the APC phenotype and how it can impact the communication and signaling between these key players of the immune system and cells in this specific network.

1.3.5 Communication in TME

One key feature of cellular communication is the expression of ligands and receptors by the cells. The interaction between these molecules convey a message to the cell and induce specific responses. APCs express at their membrane surface various receptors implicated in sensing pathogens and danger signals. pDCs express Toll-Like Receptors (TLRs) to sense pathogens. DCs are able to sense pathogen-associated molecular patterns (PAMP) *via* Pattern Recognition Receptors (PRRs), TLRs and C-type Lectin Receptors (CLRs) such as CLEC9A in DC1 (Figure 1.6). They also express various ligands inducing immune responses such as cytokines and chemokines. The sensing of various stimuli impacts the differentiation of cells and their functions [Dalod et al. 2014; Huang et al. 2001; Y. J. Liu 2001; Pulendran, Palucka, and Jacques Banchereau 2001; Soumelis et al. 2015; Stagg and Allard 2013]. For instance, in response to various signals, macrophages may undergo classical M1 activation *via* stimulation by TLR ligands and IFNγ or alternatively M2 activation *via* stimulation by IL-4 and IL-13. Among those ligands and receptors,

one category is particularly interesting. It is immune checkpoint molecules which are regulators of immune activation. They play a key role in maintaining immune homeostasis and preventing autoimmunity. In cancer, immune checkpoint mechanisms are often activated to suppress the nascent anti-tumor immune response. It has been shown that cancer cells can express inhibitory checkpoints suppressing T cell activation [Ott, Hodi, and Robert 2013](Figure 1.7). In recent years, immune checkpoint mechanisms became central targets of anti-cancer immunotherapies.

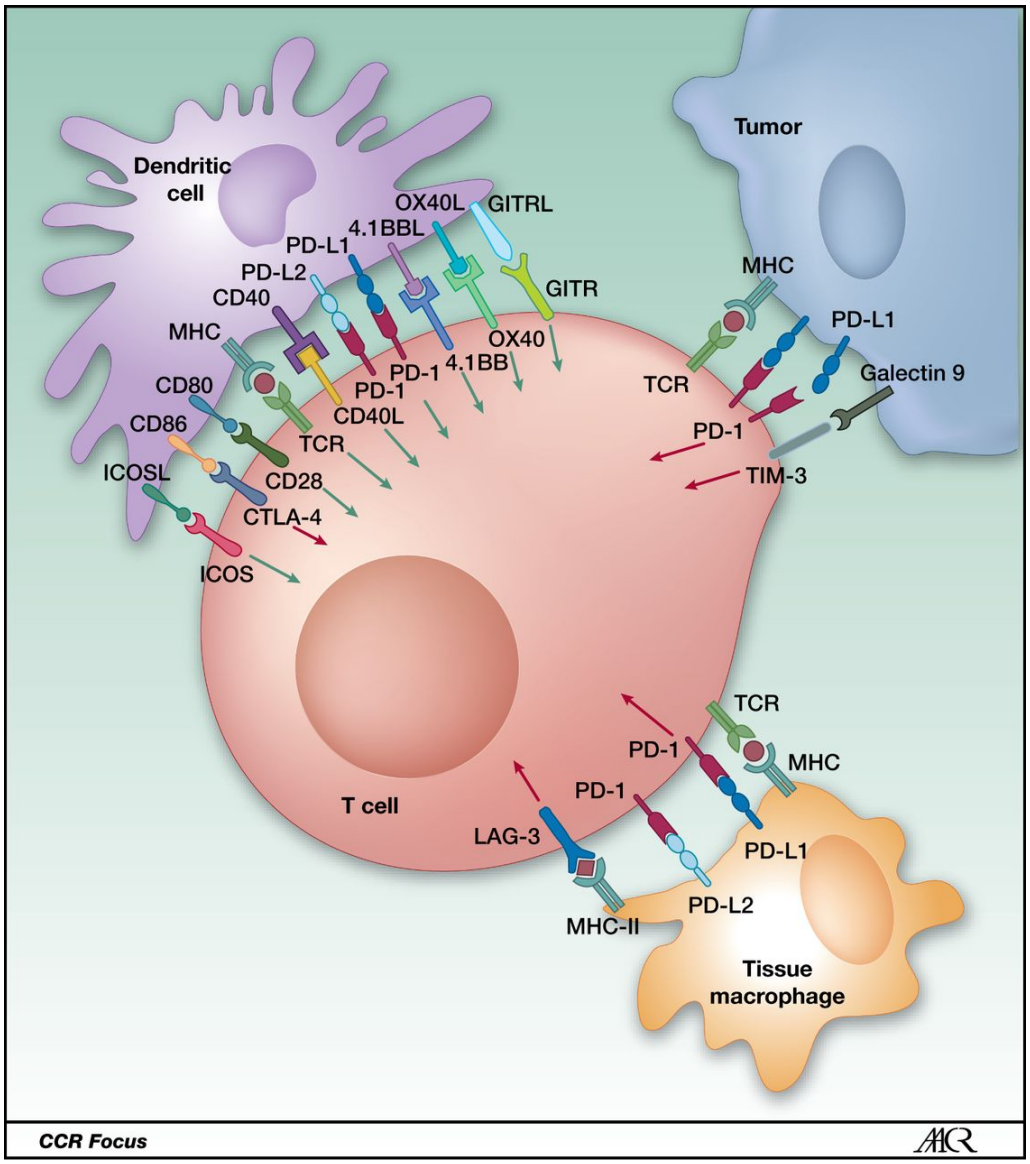

Figure 1.7: Immune checkpoint interactions between T cells, APCs and cancer cells in the tumor microenvironment. From Ott, Hodi, and Robert 2013.

1.4 How can we study the communication between cells in the TME?

1.4.1 Challenges

The tumor microenvironment is a complex network which can be decomposed in multiple layers of information: tissue specificity, cellular infiltration, cell plasticity, soluble factors present in the environment, genetic and epigenetic modifications. This network evolves in time and space. To reconstruct cell-to-cell signaling, a general problem arises that all reconstructed signals hypotheses are generated from partial information due to technical limitations including the experimental design used, the access to biological material, the number of parameters monitored. Taking into account the combinatorial aspect of communication and response to signal, this make a huge network analyse with infinite combinations not necessarily validated experimentally. Simplification of the network is a first step to understand communication between cells in the TME. It appears to represent a challenge to study how the TME acts on cell-to-cell interactions, especially between APCs, and how it affects their functions in this specific context.

One way to understand the communication between two entities, is to study the expression of the messages (ligands) and if they can be deciphered (by receptors, downstream pathways) under different conditions. The modulation of messages expression in the environment can be diverse: up-regulation (higher expression), down-regulation (lower expression), blockade, inhibition, or activation. To monitor the expression of specific proteins localized at the surface of cells, one possibility is the use of fluorescence flow cytometry. Fluorescence-activated cell sorting (FACS) is commonly used for identifying cell population such as human DCs [Guilliams et al. 2016]. FACS enables to identify population *via* fluorescent antibodies targeting specific surface markers but also other proteins such as surface receptors, immune checkpoints, chemokines or cytokines. Advances through cytometry by time-of-light now enable 30 to 40 antigens to be analyzed simultaneously [Guilliams et al. 2016]. Other techniques based on protein targeting via antibodies can be used to monitor

expression of ligands and receptors by cells. This includes bead-based (*e.g.* Cytometric bead array) and electrochemiluminescence systems (*e.g.* Luminex). However, the major limitation of all of these techniques is that they allow to monitor only several proteins at a time and the amount biological material required to perform these experiments. In recent years, development of high throughput sequencing techniques and bioinformatic tools enabled biologists to generate molecular profiles of cells. Breast cancer subtypes were identified using transcriptomics data [Curtis et al. 2012]. Dendritic cells were also characterized at the molecular level in blood and tissues, in human and mouse [Ginhoux and Guilliams 2016; Guilliams et al. 2016; Haniffa, Collin, and Ginhoux 2013]. With such large amount of data, it is possible to study changes in signaling pathways of APCs in a certain environment such as breast TME which contribute to understand how the communication network of APCs is influenced by breast cancer.

1.4.2 Bioinformatics to study cell-to-cell communication

1.4.2.1 Transcriptomic profiles, information providers

The transcriptome refers to the ensemble of messenger RNA (mRNA) molecules transcribed from expressed genes in an organism. It also describe the group of mRNA transcripts produced in a particular cell or tissue type. The transcriptome actively changes, depending on many factors, including stage of development and environmental conditions. The study of transcriptomes can be use to dissect signaling information and compare gene expression differences between two environments such as TME and healthy tissue. From the analysis of a transcriptome, we can reveal genes differentially regulated between at least two conditions. Therefore, we can derive a gene signature which combines several genes with specific patterns of expression characterizing cells in one condition (*e.g.* subsets of cell, disease state, tissue localization) or genes corresponding to a biological process (*e.g.* signaling pathways, response to a stimulus, cellular function). These signatures can have different applications. In clinics, gene signatures can be used to perform either prediction of disease outcome (*i.e.* predictive signature), prediction of the effect of

a treatment (*i.e.* prognostic signature) or classification of disease phenotypes and severity (*i.e.* diagnostic). Gene signatures characterizing cell populations can be used to deconvolute bulk expression datasets to estimate the proportion of cell infiltration in a specific context. Several methods are based on this concept such as CIBERSORT [A. M. Newman et al. 2015]. In the manuscript, subset-specific gene signatures refer to genes that have an up-regulated expression in a subpopulation of cells compared to all other populations of the study. It can also refer to a list of genes linked to a biological function or concept (*e.g.* signaling pathway, costimulatory molecules) and with a differential expression pattern between conditions of the study.

Two different techniques enable generation of transcriptomic profiles of organisms: gene-expression profiling microarrays and RNA-sequencing (RNA-seq). Microarrays can be used to measure the expression of thousands of genes at the same time, as well as to provide gene expression profiles, which describe changes in the transcriptome in response to a particular condition or treatment [Liotta and Petricoin 2000; Mills et al. 2001]. mRNA molecules are purified from both experimental and reference samples. A step of reverse transcription converts mRNAs into complementary DNA (cDNA), and each sample is labeled with a fluorescent probe of a different color. Then, the cDNAs of the samples are bound to the microarray slide via hybridization. Following hybridization, the microarray is scanned to measure the expression of each gene printed on the slide (Figure 1.8). Standardized protocols are established to analyze the data even though many bioinformatic tools are available [Selvaraj and Natarajan 2011].

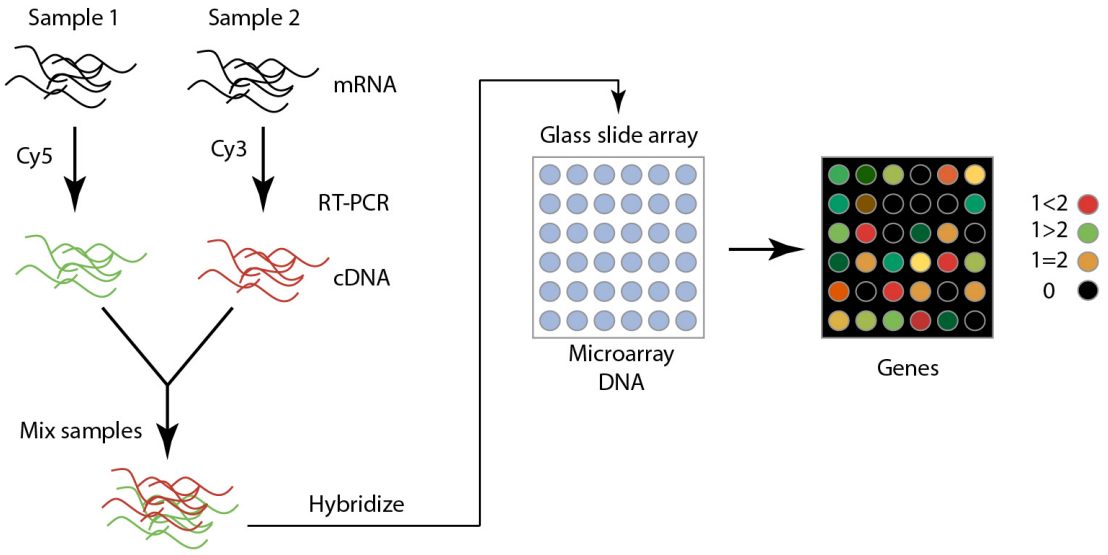

Figure 1.8: Gene-expression profiling microarray protocol. Adapted from Ortuño et al. 2011.

Public databases are a wealth of information, more than 1500 datasets of expression profiling by array of human immune cells are found in GEO database (National Center for Biotechnology Information NCBI, https://www.ncbi.nlm.nih.gov/gds/). Transcriptomic profiles of mice and human immune cells are available in literature (BioGPS, ImmGen https://www.immgen.org/) [Collin, McGovern, and Haniffa 2013; C. Wu et al. 2009]. These profiles have been generated from cells coming from various tissue origin (*e.g.* blood, skin, lymph nodes, spleen), species (*e.g.* human, mouse), and experimental conditions (healthy, disease, activation *via* diverse molecules). Hence, these resources are helpful to study gene expression linked to communication pathways in a variety of conditions. Regarding APCs and especially DCs, several gene expression datasets of human DC subsets are available (Figure 1.9). However, majority of the datasets were generated from blood or skin DCs but not from tumor microenvironment-infiltrating cells.

Authors	DOI	Year	Cell type(s)	Tissue type	Number of samples	Technique	Link for dataset
Chaussabel D, Semnani RT, McDowell MA, Sacks D et al.	10.1182/blood-2002-10-3232	2003	Macrophages, DC	blood, exposure to parasites	28	microarray	GSE360
Lindstedt M, Lundberg K, Borrebaeck CAK.	10.4049/jimmunol.175.8.4839	2005	pDC, BDCA1+ DC, BDCA3+ DC, CD16+ DC	tonsil, blood	21	microarray	E-TABM-34
Széles L, Póliska S, Nagy G, Szatmari I et al.	10.1210/me.2010-0215	2010	monocyte-derived DC, dermal DC (DDC), Langerhans cells (LCs), blood CD1c+ DC	skin, blood	12	microarray	GSE23618
Frankenberger M, Hofer TP, Marei A, Dayyani F et al.	10.1002/eji.201141907	2012	classical monocytes (CD14++CD16-), CD16 positive monocytes (CD14+16++ and CD14++CD16+), and CD1c+ CD19- DCs	blood	9	microarray	GSE34515
Hutter C, Kauer M, Simonitsch-Klupp I, Jug G et al.	10.1182/blood-2012-02-410241	2012	CD207+/CD1a+ Langerhans cell histiocytosis (LCH), epidermal LCs, myeloid DC (mDC1) and pDCs	skin, bone, mucosa, peripheral blood	17	microarray	GSE35340
Haniffa M, Shin A, Bigley V, McGovern N et al.	10.1016/j.immuni.2012.04.012	2012	CD14+ DC, CD1c+ DC, CD1c+CD141+ DC, CD141+ DC, CD14+ mono, CD16+ mono, pDC	skin, blood	49	microarray	GSE35457
Segura E, Touzot M, Bohineust A, Cappuccio A et al.	10.1016/j.immuni.2012.10.018	2013	inflammatory DC and macrophages, CD14+CD16- monocytes, CD14dim CD16+ monocytes and BDCA1+ DC	inflammatory ascites (ovarian cancer), blood (healthy donors)	22	microarray	GSE40484
Mabbott NA, Baillie JK, Brown H, Freeman TC et al.	10.1186/1471-2164-14-632	2013	primary cells	-	745	microarray	GSE49910
Harman AN, Bye CR, Nasr N, Sandgren KJ et al.	10.4049/jimmunol.1200779	2013	monocyte-derived DCs (MDDC) Reference, CD1a DDC, CD14 DDC, CD1a LC, CD14 DDC Cultured, pDC Cultured, CD14 monocytes, mDC Cultured, CD14 monocytes Cultured, CD16 monocytes Cultured, CD16 monocytes, mDC, pDC	skin, blood	62	microarray	GSE32648
Harman AN, Bye CR, Nasr N, Sandgren KJ et al.	10.4049/jimmunol.1200779	2013	immature model MDDCs, mature model MDDCs, MUTZ3 LCs, CD14+ monocytes, CD16/M-DC8+ monocytes/DCs, CD11c+ blood myeloid, CD1a expressing DDCs, CD14 expressing DDCs, CD1a expressing epidermal LCs	skin, blood	24	microarray	GSE32400
Banchereau R, Baldwin N, Cepika AM, Athale S et al.	10.1038/ncomms6283	2014	IFNa and IL4 DCs stimulated with microbial components for 6hr	blood	77	microarray	GSE44719
Banchereau R, Baldwin N, Cepika AM, Athale S et al.	10.1038/ncomms6283	2014	IFNa DCs and IL4 DCs exposed to H1N1, heat killed S. aureus, or heat killed S. enterica (HKSE) for 1h, 2h, 6h, 12h, or 24h	blood	120	microarray	GSE44720
Banchereau R, Baldwin N, Cepika AM, Athale S et al.	10.1038/ncomms6283	2014	IL4 DCs and monocytes stimulated by 13 human vaccines and LPS for 6hr	blood	128	microarray	GSE44721
Banchereau R, Baldwin N, Cepika AM, Athale S et al.	10.1038/ncomms6283	2014	see GSE44719, GSE44720, GSE44721, GSE56744,	blood	413	microarray	GSE44722
Banchereau R, Baldwin N, Cepika AM, Athale S et al.	10.1038/ncomms6283	2014	BDCA1+ mDCs and BDCA3+ mDCs stimulated with vaccines for 6 hr	blood	88	microarray	GSE56744
Balan S, Ollion V, Colletti N, Chelbi R et al.	10.4049/jimmunol.1401243	2014	CD141- XCR1- CD34-DC, CD141+ XCR1- CD34-DC, XCR1+ CD34-DC, XCR1- CD34-DC, CD1c blood DC , XCR1 blood DC, CD34-MoDC, blood pDC	coord blood, peripheral blood - treated w/ PIC, LPS or R848, untreated	74	microarray	GSE57671
McGovern N, Schlitzer A, Gunawan M, Jardine L et al.	10.1016/j.immuni.2014.08.006	2014	Macrophages, LCs, CD14+ cells	skin (dermal and epidermal)	11	microarray	GSE60317
Artyomov MN, Munk A, Gorvel L, Korenfeld D et al.	10.1084/jem.20131675	2015	LCs (epidermal Langerhan Cells), CD1a(dim)CD141+ (CD141+ dermal cells), CD14+ (CD14+ dermal cells), CD1a(dim)CD141- (CD141-CD14- dermal cells)	skin	17	microarray	GSE66355
Carpentier S, Vu Manh TP, Chelbi R, Henri S et al.	10.1016/j.jim.2016.02.023	2016	DCs, LCs, macrophages	reanalysis (human + mouse)	-	microarray	GSE74316
Goudot C, Coillard A, Villani AC, Gueguen P et al.	10.1016/j.immuni.2017.08.016	2017	IL-34 + IL-4 + TNFa mo-DC, IL-34 + IL-4 + TNFa mo-Mac, MSCF + IL-4 + TNFa mo-DC, MSCF + IL-4 + TNFa mo-Mac, GMCSF + IL-4 mo-DC	blood	30	microarray	GSE102046
Helft J, Anjos-Afonso F, van der Veen AG, Chakravarty P et al.	10.1016/j.celrep.2017.06.075	2017	MLP derived cDC1, CMP derived cDC1	umbilical cord blood	7	microarray	GSE98957
Breton G, Zheng S, Valieris R, Tojal da Silva I et al.	10.1084/jem.20161135	2016	BDCA-1+ cDCs, BDCA-3+ cDCs, cord blood CD172a-pre-cDCs, cord blood CD172a+ pre-cDCs	umbilical cord blood, bone marrow, peripheral blood	16	RNA-seq	GSE88858
Bakdash G, Buschow SI, Gorris MA, Halilovic A et al.	10.1158/0008-5472.CAN-15-1695	2016	BDCA1+ DC, BDCA1+CD14+ , Monocyte	blood	9	RNA-seq	GSE75042
Tirosh I, Izar B, Prakadan SM, Wadsworth MH 2nd et al.	10.1126/science.aad0501	2016	Malignant, immune, stromal, and endothelial cells	metastatic melanoma	4645 single cells, 19 patients	scRNA-seq	GSE72056
See P, Dutertre CA, Chen J, Günther P et al.	10.1126/science.aag3009	2017	(Lin)(CD3/14/16/19/20/34)–CD45+CD135+HLA-DR+CD123+CD33+ cells (DC compartment)	peripheral blood	710 single cells	scRNA-seq	GSE98052, GSE98011, GSE80171
Villani AC, Satija R, Reynolds G, Sarkizova S et al.	10.1126/science.aah4573	2017	DC and monocytes subsets	blood	2422 single cells, 1 donor	scRNA-seq	GSE94820
Goudot C, Coillard A, Villani AC, Gueguen P et al.	10.1016/j.immuni.2017.08.016	2017	Blood CD14+ monocytes	blood	425 and 431 single cells, 2 donors	scRNA-seq	GSE103544

Figure 1.9: Table of human DCs and monocytes transcriptomic profile datasets available in the literature.

For this thesis project, we strived to study APC subpopulations which are rare cells in the tumor microenvironment. Studies have shown that RNA-seq have better

sensitivity than microarrays [Mortazavi et al. 2008]. Another limitation of array technology is the detection of genes for which there are corresponding probes only. Since we were studying more than two conditions taking into account the tissue (tumor and non-invaded tissue), the cancer subtype, and different subpopulations of APCs, we used RNA-seq technologies to generate the transcriptomic profiles of tumor-infiltrating APC subpopulations. Transcriptomics have moved rapidly from expression arrays of bulk populations to single cell RNA-sequencing. High-throughput sequencing technologies are now common use in biology. By sequencing steady-state mRNAs in a sample, we can obtain short sequence of reads corresponding to all mRNAs. RNA-seq enables detection of alternative splicing [Griffith et al. 2010; Trapnell, B. A. Williams, et al. 2010; L. Wang et al. 2010], RNA editing [Picardi et al. 2010] and novel transcripts [Robertson et al. 2010; Trapnell, B. A. Williams, et al. 2010], but most importantly, quantification of gene expression profiling and quantification of the differential expression levels of transcripts during development or under different conditions such as healthy or disease state. Only small 10 pg to 1 ng of RNA is necessary to perform RNA-seq. Following purification of picograms of mRNAs isolated from samples of interest, the mRNAs are reverse transcribed into cDNA. Then, the cDNA is fragmented, adaptors are ligated to the short sequences by random priming and amplified before sequencing (Figure 1.10). Afterwards, the reads are aligned to the reference genome and several tools are available for this purpose including Bowtie [Langmead et al. 2009], TopHat (which builds on BowTie results to align splice junctions) [Trapnell, Pachter, and Salzberg 2009; Trapnell, Roberts, et al. 2012], and STAR [Dobin et al. 2013]. RNA-seq produces large and complex datasets and their interpretation is not straightforward. Analysis methodology is critical to interpreting the data. It encompasses several key steps to analyze sequencing data or microarrays or RNA-seq, including quality control of the data and data normalization. Gene length and nucleotide composition as well as library size could induce technical biases in RNA-seq. Many effort have been done to improve normalization methods in order to tackle such biases [Dillies et al. 2013; Risso et al. 2014].

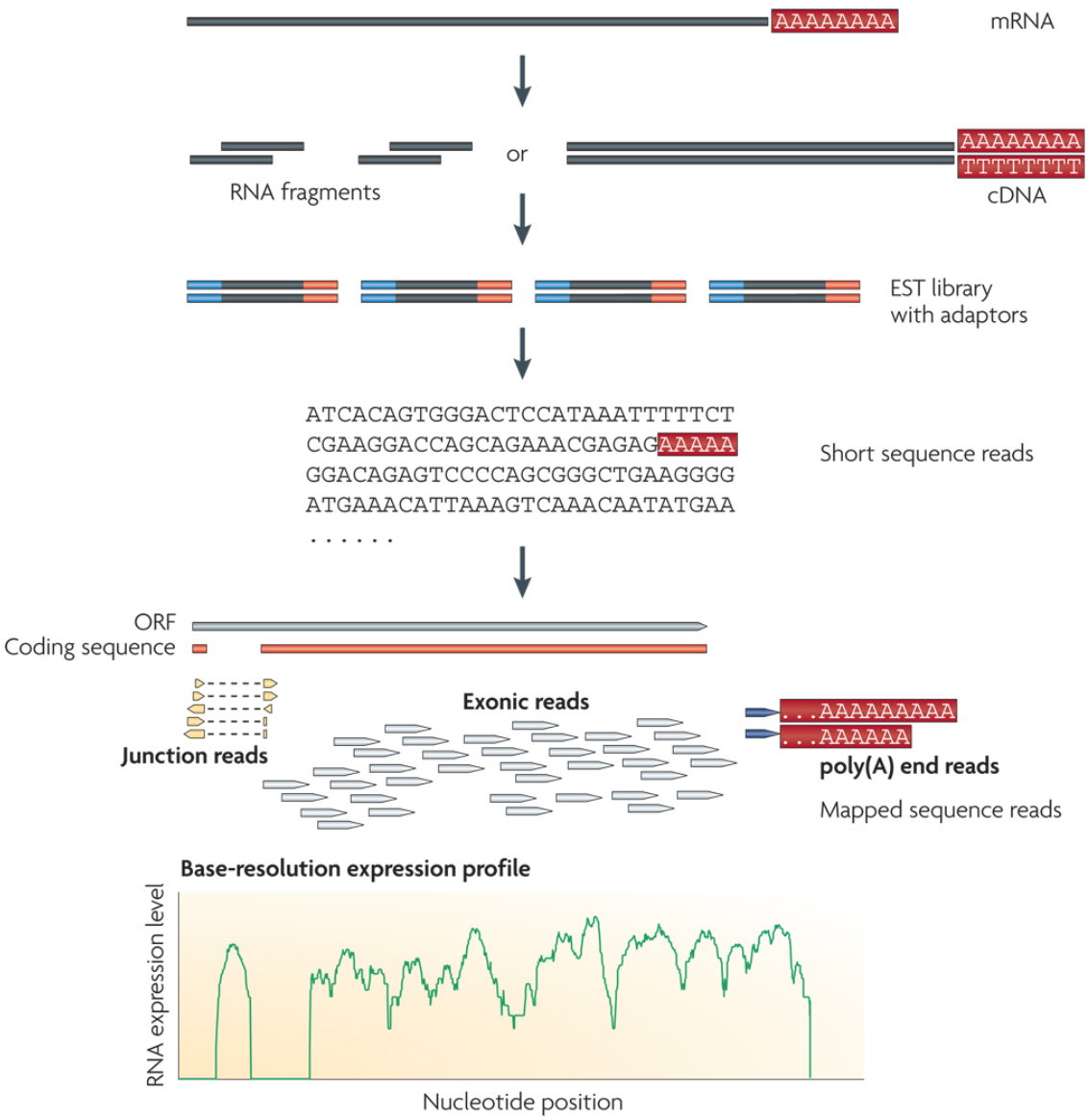

Figure 1.10: RNA-seq experiment protocol (From Z. Wang, Gerstein, and Snyder 2009).

1.4.2.2 Tools to study communication

Nowadays, biostatistic and bioinformatic tools are essential to analyse large scale data and draw hypothesis on biological processes. From cell transcriptional profiles it is possible to extract a lot of information regarding the expression of genes coding for proteins involved in diverse cellular pathways. Additionally, the differential gene expression analysis of these profiles is helpful to decipher how an environment impacts the transcriptional profile of specific cell populations. Different algorithms

and tools are dedicated to differential expression analyses regarding the technology used to generate the transcriptomic profiles. Tools such as limma [Ritchie et al. 2015] are widely used to analyze gene-expression profiling microarray data. It is less unanimous for RNA-seq data analysis. RNA-seq data can be represented as read count matrices, with a non-normal distribution. The different methods of differential expression analysis fit models to the data following either a poisson distribution or a negative-binomial distribution which is more accurate for RNA-seq data [Dillies et al. 2013; Risso et al. 2014]. Tools such as edgeR or DESeq2 in R software have then become gold-standard methods for differential gene expression analysis of RNA-seq data [Conesa et al. 2016; Love, Huber, and Anders 2014; Robinson, McCarthy, and Smyth 2010]. They implement negative-binomial model fitting with variance estimation to perform differential testing of gene expression. These methods enable the detection of differentially expressed genes (DEGs) between several conditions (*e.g.* disease state versus healthy state or between cell types).

From the DEG list, we can perform functional enrichment tests to infer which biological functions are affected by one condition versus another and whether these functions are up- or down-regulated for each condition. A great majority of functions, processes and signaling pathways are gathered in databases as Gene Ontology (GO), KEGG, DAVID, and Reactom [Ashburner et al. 2000; Croft et al. 2011; Dennis et al. 2003; Kanehisa and Goto 2000]. In the TME, a few studies have analyzed macrophages and dendritic cells profiles [Ojalvo, W. King, et al. 2009; Pyfferoen et al. 2017]. Ojalvo et al. compared invasive and general TAMs purified from mice with carcinomas [Ojalvo, W. King, et al. 2009]. Using gene-expression profiling arrays, they identified 1457 differentially regulated transcripts between the two populations of TAMs. They also showed that invasive TAMs present genes enriched in Wnt signaling pathway. These results highlight the role of transcriptomic analyses in deciphering cellular communication and functions in specific context such as cancer.

In parallel, if we consider that gene regulation is part of a specific intra-cellular communication network, one step of transcriptomic analysis is functional network inference to reconstruct genes networks in each cell population studied. The ARACNe algorithm was developed by Manolin to this purpose [Margolin et al. 2006]. It is

based on mutual information which measures the degree of statistical dependency between two variables. It enables the identification of candidate interactions by estimating pairwise gene expression profile mutual information. When linked to functional inference, this helps to understand the gene expression and regulation inside cells which correspond to the processing of the message, coding and decoding, as well as the response.

Chapter 2

Objectives of the thesis

This project started from the hypothesis that the tumor microenvironment modulates the intra- and intercellular communication network formed by APCs. These modifications would have consequences on the interaction between the tumor and the host immune system and *a fortiori* on the tumor development. Unfortunately, several limits exist in the literature concerning the study of rare APCs in tissue context. APC subpopulations have been characterized in different tissues (*e.g.* blood, spleen, skin), diseases (*e.g.* cancer, autoimmune diseases), organisms (*e.g.* mouse, human). However, in breast cancer, only macrophages and cDC2 have been studied [Ojalvo, Whittaker, et al. 2010; Wargo et al. 2016] and no comparison has been made either between tumoral tissue (T) and non-malignant tissue which we call juxtatumor (J), or between different breast cancer subtypes. Our general objective was to understand the impact of the breast tumor microenvironment on DCs subsets using system-level analysis.

2.1 First objective: identify subsets of DCs and infer their biological functions in breast cancer using RNA-seq transcriptional profiles.

In the first part of my thesis work, I aimed at identifying DC subpopulations in the breast tumor microenvironment. More precisely, the project focused on the identification and characterization of biological functions of DCs subpopulations isolated from breast tumors of two different subtypes: Luminal (LBC) and Triple-Negative (TNBC) which is of worst prognosis. Since APCs are rare cells in the breast TME, we wanted to define tumor-infiltrating APCs subsets at a higher resolution than what has been done in the literature. Using RNA-seq technology, we generated the molecular profile of these cells and wanted to infer the biological functions. In a first step, the goal of this study was to decipher how the TME modulate the transcriptional profile of APC subsets by comparing APC transcriptional profiles in tumors and juxtatumors and linking the variation of gene expressions to biological functions. In a second step, we assessed the impact of the breast tumor heterogene-

ity on DCs and Monomacs. To do so, we compared the transcriptional profile of APCs subset isolated from two types of breast cancer, LBC, and TNBC. Finally, since we had studied the breast tumor microenvironment and its potential impact on APC subsets communication network, we wondered what was the link between the characterization of each specific APC populations and the clinical outcome. Are there any differences at the population level between clinical outcome, and in different TME, depending on the breast cancer subtype? From the extraction of specific gene lists that characterize each population of APCs identified in breast TME, we aimed to link the subset- and context-specific signatures to the patient outcome.

2.2 Second objective: reconstruct intercellular communication networks

In a second part we studied the cellular communications in order to understand how cells integrate signals from their environment. To do so, we aimed at creating a simple communication score based on cell transcriptomic profiles. This score could be applied to microarray data as well as RNA-seq data. It will be part of a tool including a manually curated database of ligand and receptors interactions and a collection of transcriptional profiles of primary cells publicly available in BioGPS [Mabbott et al. 2013].

Chapter 3

Results

3.1 Article 1: Adjustment of dendritic cells to the breast-cancer microenvironment is subset specific

The TME is composed of a wide variety of cell types that influence tumor progression and immune evasion. DCs are APCs that can infiltrate most cancer types. They can have a protective role in anti-tumor immunity but conversely, they can also promote immunosuppression [DeNardo, Barreto, et al. 2009; Faget et al. 2012; Ghirelli et al. 2015]. The influence of the TME on the diversity and plasticity of these APCs remains poorly explored. During my thesis, I analyzed large-scale RNA sequencing profiles of tumor-infiltrating APCs in 8 luminal (LBC) and 4 triple-negative (TNBC) breast cancer samples, in close collaboration with Paula Michea, post-doctoral fellow in the lab.

Based on previous analysis performed in the lab and on the basis of published studies of human DC subsets on other tissues such as peripheral blood or skin [Bronte et al. 2016; Guilliams et al. 2016; Zaba, Krueger, and Lowes 2009], we studied four DCs subsets and macrophages at the phenotypic and transcriptional level in breast cancer. By comparing the transcriptomes of those APCs from tumor sample and from non-cancerous (juxtatumoral) tissue of the same patients, we identified tumor-specific gene signatures for each APC subset that were linked to distinct biological functions such as cell migration in pDCs. Furthermore, we observed substantial differences between the APC profiles in TNBC and LBC unveiling the impact of tumor microenvironment and not only the tissue imprint or the ontogeny on the behavior of APCs. Interestingly, the pDC signature was linked to a better disease-free survival in LBC but not in TNBC patients, which implicates that the outcome associated with the pDC signature is context-dependent.

In conclusion, we found that transcriptional reprogramming of tumor-infiltrating APCs is subset-specific, suggesting a complex interplay between ontogeny and tissue imprinting in conditioning DC diversity in the TME. The signatures we generated are particularly relevant for the identification of biological pathway activation and

novel biomarkers in APC subsets.

Link to the article: https://www.nature.com/articles/s41590-018-0145-8

Adjustment of dendritic cells to the breast-cancer microenvironment is subset-specific

Paula Michea[1,2#], Floriane Noël[1,2,3#], Eve Zakine[1,2], Urszula Czerwinska[1,2,4,8], Philemon Sirven[1,2], Omar Abouzid[1,2], Christel Goudot[1,2], Alix Scholer-Dahirel[1,2], Anne Vincent-Salomon[5,6], Fabien Reyal[7], Sebastian Amigorena[1,2], Maude Guillot-Delost[1,2], Elodie Segura [1,2], and Vassili Soumelis[1,2*].

Author affiliations:

1 Institut Curie, PSL Research University, France

2 INSERM, UMR 932, F-75005, Paris, France

3 Université Paris Sud, Université Paris-Saclay, F-91405, Orsay, France

4 INSERM, U900, F-75005, Paris, France ; Mines Paris Tech, France

5 Institut Curie, Service de pathologie, F-75005, Paris, France

6 INSERM, U934, F-75005, Paris, France

7 Département de Recherche Translationnelle, INSERM, UMR 932, Residual Tumor & Response to Treatment Laboratory (RT2Lab), F-75005, Paris, France ; Institut Curie, Département de Chirurgie, Paris, France

8 Centre de Recherches Interdisciplinaires, Paris Descartes, F-75005 Paris, France

#Contribute equally to this study

*Corresponding author vassili.soumelis@curie.fr

The functions and transcriptional profiles of dendritic cells (DCs) result from the interplay between ontogeny and tissue imprinting. How tumors shape human DCs is unknown. Here we used RNA-based next generation sequencing to systematically analyze the transcriptomes of plasmacytoid pre-DC (pDC), cDC1-enriched cells, cDC2, $CD14^{+}$DC, and monocyte/macrophages from human primary luminal breast cancer (LBC) and triple-negative breast cancer (TNBC). By comparing tumor tissue with non-invaded tissue from the same patients, we found that 85% of the genes upregulated in DCs in LBC were specific to each DC subset. However, all DC subsets in TNBC commonly showed enrichment for the interferon pathway, but those in LBC did not. Finally, we defined transcriptional signatures specific for tumor DC subsets with a prognostic effect on their respective breast-cancer subtype. We conclude that the adjustment of DCs to the tumor microenvironment is subset specific and can be used to predict disease outcome. Our work also provides a resource for the identification of potential targets and biomarkers that might improve antitumor therapies.

Dendritic cells (DCs) are antigen-presenting cells (APCs) specialized in triggering adaptive immune responses through T cell activation[1]. Different subsets of DCs were defined based on their ontogeny, phenotype and anatomical location[2, 3]. Advances in high throughput technologies have improved DCs classification, by identifying novel subset-specific markers and molecular signatures[4]. At steady state, studies in mice and human suggest that ontogeny is a predominant factor in defining DC subsets identity[5, 6, 7, 8]. For instance, studies on plasmacytoid pre-DCs (pDCs)[9], conventional DC1 ($CD141^+$DC) and cDC2 ($CD1c^+$DC) from human blood and tonsils, revealed that pDCs clustered first by ontogeny independently of their tissue of origin[10]. Instead, cDC1 and cDC2 were more sensitive to tissue localization as tonsil cDC1 clustered closer to tonsil cDC2 rather than blood cDC1[10]. Tissue imprinting also influence DCs function. Gut but not spleen DC induce T cell homing back to the gut through a retinoic acid- CCR9- and $\alpha4\beta7$-dependent mechanism[11]. This suggests a complex interplay between ontogeny and tissue imprinting, the relative contribution of which remains a matter of debate.

During inflammation, complex signals must be integrated by various DC subsets, which may change their function and molecular features[12, 13, 14, 15, 16, 17]. DC subset diversity itself is also modified by inflammation, with the appearance of monocyte-derived inflammatory DCs, which are absent in homeostatic conditions[18]. In humans, inflammatory DCs were characterized in psoriatic skin[19, 20], ovarian cancer ascites and rheumatoid arthritis synovial fluid[21]. DCs infiltrate most cancer types. They have a protective role in anti-tumor immunity through the expression of co-stimulatory molecules and inflammatory cytokines, and by inducing T cell activation[22, 23]. Conversely, DCs also promote immunosuppression by secreting anti-inflammatory cytokines[24, 25, 26, 27] or by expressing negative immune checkpoint molecules, which are currently targeted by promising anti-tumor therapies[28, 29]. DC plasticity

to various tumor microenvironments (i.e tissue imprinting), as well as specialized ontogeny-driven DC functions, may contribute to such a molecular and functional heterogeneity.

In this study, we performed a systematic comparative transcriptomic study of DC subsets in human primary breast cancer and matched non-involved juxta-tumor tissue. We found that transcriptional reprogramming of tumor-infiltrating DCs was DC subset-specific, suggesting a complex interplay between ontogeny and tissue imprint in conditioning DC diversity in the tumor microenvironment. Our results also provide high-quality large-scale datasets of primary tumor-infiltrating DC, which constitute a valuable resource to the biomedical community.

Results

Phenotypically distinct APCs infiltrate human breast cancer

DCs infiltrating breast cancer tissues were identified by multicolor flow cytometry based on previous human DC subset studies[20]. Because this was the first in depth characterization of DC subsets in human breast cancer, we performed preliminary analyses to validate our strategy. After standard gating to eliminate debris, doublets and dead cells, we selected $CD45^+$ cells to efficiently exclude $CD45^-$ cells, which are mainly tumor cells and fibroblasts (**Supplementary Fig. 1a**). We used a lineage (Lin) panel to exclude $CD3^+$ T cells, $CD19^+$ B cells and $CD56^+$ cells (**Supplementary Fig. 1a**). CD14 expression was analyzed independently of the lineage channel to efficiently identify $CD14^+$ DC, which were reported in cancer [20, 21, 30, 31, 32]. In Lin^- cells, we next gated on $CD11c^+HLA\text{-}DR^{hi}$ cells to exclude $CD11c^+HLA\text{-}DR^{-/lo}$ myeloid-derived suppressor cells (MDSC)[33]. $HLA\text{-}DR^+CD123^+$ pDCs were identified in the $CD11c^-$ gate (**Supplementary Fig. 1a**).

In the Lin^-CD45^+ gate we identified four distinct $CD11c^+$ cell populations defined by their CD1c and CD14 expression (**Fig 1a**). Based on a recent standardized nomenclature for blood DC subsets[34], $CD1c^+CD14^-$ cells matched the cDC2 definition, $CD1c^-CD14^-$ cells contained cDC1, and $CD1c^-CD14^+$ cells were monocyte/macrophages (hereafter MonoMacs) (**Fig. 1a**). We also identified a $CD1c^+CD14^+$ cell population that co-expressed monocytes and macrophage markers such as CD14, CD64, CD163 and cDC2 markers like CD1c, CD206 and FcεRI (**Fig. 1b and Supplementary Fig. 1b**). Because these $CD1c^+CD14^+$ cells were phenotypically distinct from MonoMacs, and because they were not systematically distinguished in previous studies [34], we refer to them hereafter as $CD14^+$ DCs. $CD56^+CD14^+$ cells were reported as interferon-producing killer dendritic cells (IKDC) in the context of cancer [35], later shown to correspond to activated NK cells[36]. A similar $CD56^+CD14^+$ phenotype was previously described on a fraction of healthy blood monocytes[37]. We detected

93 $CD56^+CD14^+$ cells in breast cancer samples (18% of $CD45^+CD3^-CD19^-$ live cells)
94 (**Supplementary Fig. 1c**). Because of their controversial nature, we excluded them using
95 CD56 in our lineage cocktail (**Supplementary Fig. 1c**).
96 Clec9A could not be used to identify cDC1, as it was degraded during enzymatic digestion of
97 the tissue (**Supplementary Fig 1d**). CD141 (BDCA3) was promiscuously expressed by all
98 DCs, including pDCs and MonoMacs (**Fig 1b**). However, $CD141^{hi}$ cells were found only in
99 the $CD1c^-CD14^-$ population (Fig. 1b), hence they were highly enriched in cDC1. Because
100 $CD141^{hi}$ cells were too few (<100 cells/sample) and rare (5-50% of $CD141^{hi}$ from $CD1c^-$
101 $CD14^-$ cells in only half of the patients) to enable further separation into subsets, we
102 designated the $CD1c^-CD14^-$ cell subset as "cDC1-enriched" (cDC1e) and used it for further
103 molecular characterization. MonoMacs, $CD11c^+HLADR^{-/lo}$, $CD14^+$DC, cDC2 and cDC1e did
104 not express CD16 (**Fig. 1b and data not shown**). CD32B, described on a non-inflammatory
105 subset of cDC2 in blood[38], was highly expressed by MonoMacs, $CD14^+$DC and cDC2, but not
106 cDC1e. AXL, which is expressed by blood DC precursors and cDC2, was mainly expressed
107 by cDC2, $CD14^+$DCs and MonoMacs in breast tumors (**Fig 1b**). This indicates a clear
108 discrepancy in DC markers between blood and breast tissue.
109 To examine the morphology of tumor APCs, we sorted and analyzed them for cytological
110 features. pDCs presented a typical plasmacytoid morphology[9], while cDC2, cDC1e and
111 $CD14^+$DCs had a dendritic morphology with high nuclear-to-cytoplasmic ratio, and,
112 compared to pDCs, a less basophilic cytoplasm (**Fig 1c**). MonoMacs presented an acidophilic
113 cytoplasm with abundant vacuoles (**Fig 1c**), as commonly observed in this population.
114 We quantified the distinct APC subsets across 22 luminal breast cancer (LBC) samples.
115 MonoMacs were the most abundant (median of 6.1% of $CD45^+$ cells) followed by $CD14^+$DC,
116 and pDC (0.5% and 0.3% among $CD45^+$ cells, respectively). cDC1e and cDC2 were the less
117 numerous APC (0.2% of $CD45^+$ cells) (**Fig. 1d**). This phenotypic analysis identified and

quantified 5 APC populations infiltrating human breast cancer: MonoMac, cDC2, CD14^{+}DC, pDC and cDC1e.

Tumor-infiltrating DC are enriched in human blood DC signatures

Because the number of APCs from primary breast cancer samples obtained after sorting was very low (range: 2-12,000 cells), we adapted a protocol aimed to obtain robust RNA sequencing (RNA-seq) transcriptomes from rare cell populations (**Supplementary Fig. 1e**). We only analyzed cell populations with more than 100 events. We generated RNA-seq profiles of pDC, cDC2, cDC1e, CD14^{+}DC and MonoMac from 13 LBC patients (**Supplementary Table 1**), with 44 transcriptomes passing all quality controls (**Supplementary Table 2** and **Methods**). In average, 60.5% of reads were mapped to the reference transcriptome across all samples. After filtering and normalization of the RNA-seq raw data, we obtained an average of 14,417 expressed genes.

To verify the identity of each of the subsets at the RNA level in relation to the flow cytometric analysis, we checked the expression of various subset-specific and shared DC markers (**Fig. 1e**). As expected, pDCs had high expression of *IL3RA*, *CLEC4C* and *TLR9*; cDC2 had high expression of *CD1A*, *CD1B* and *FCER1A* (FcεRI); *CLEC9A*, *XCR1* and *BATF3*, all markers of cDC1, were preferentially expressed in cDC1e; MonoMacs had high expression of *CD14*, *MERTK* and *TLR4*; and CD14^{+}DC shared the expression of *FCER1A* and CD14 with cDC2 and MonoMacs, respectively (**Fig. 1e**). Gene set enrichment analyses using public datasets indicated that breast cancer cDC2, cDC1e, and MonoMac were enriched in blood cDC2, cDC1 (CD141^{hi}), and CD14^{+} dermal mononuclear phagocytes (DMP) and MonoMac genes, respectively (**Fig. 1f**). Hence, robust transcriptional profiles confirmed the identity of the main DC subsets and MonoMacs infiltrating breast cancer.

Tumor-infiltrating DC harbor subset-specific signatures

We performed differential analysis between pDC, cDC2, cDC1e, CD14^{+}DC and MonoMac, and identified 5,132 differentially expressed genes (DEG) in at least one subset compared to all other APC ($P< 0.05$) (**Fig. 2a**). We then applied a post-hoc test, to extract the upregulated genes for each APC, that we defined as subset-specific signatures. From a total of 662 subset-specific genes 490 corresponded to pDC, 88 to cDC1e, 40 to MonoMacs and 4 to cDC2. We found no genes specific to CD14^{+}DC (**Fig. 2b**).

Among the 10 most significant DEG, the oncogene *TCL1A* and the anti-apoptotic ZFAT, were found in the pDC signature; the glutamate receptor *GRIP, and the cytokines CCL22* and *IFNL1* (IL-29) in the cDC2 signature; the plasma membrane proteins *IL1RL1* (IL33R or ST2), and *XCR1* in the cDC1e signature and *ASAH1* and *ME1,* two RNA encoding for fatty acid biosynthesis enzymes, in the MonoMac signature (**Supplementary Table 3**).

We then inferred functions linked to each subset-specific signature (**Method**s; **Fig. 2d**). From a total of 29 pathways (False Discovery Rate (FDR) <0.05), the most significantly enriched in the pDC gene-network was "anatomical structure involved in morphogenesis" (FDR = $2{,}7\text{x}10^{-07}$), including *EPHB1*, *VEGFB* and *VASH2* (**Fig. 2e,f**). Two pathways were enriched in cDC1e network, both linked to hematopoiesis, which included *KIT*, *IL9R*, *CSF1* (M-CSF) and *ITGA2B* (**Fig. 2e,f**). "PI3K signaling" was the only pathway enriched in the MonoMac signature (IGF1, SEPP1, HTR2B) **(Fig. 2e,f**). Thus, subset-specific genes were identified for LBC-infiltrating pDC, cDC2, cDC1e and MonoMac. Importantly, no pathway directly linked to immune function was differentially enriched in any of those subsets.

DC plasticity to the tumor microenvironment is subset-specific

To determine how tumor-infiltrating APC adapt to their microenvironment, we analyzed matched juxta-tumoral (non-malignant) tissue from 8 donors. pDC, cDC2, cDC1e, CD14^{+}DC

and MonoMac populations described in the tumors were also identified in the juxta-tumoral tissue, but with decreased frequency among the $CD45^+$ cells compared to the tumor, which was statistically significant for pDC (P = 0.078) and cDC1e (P = 0.039) (**Fig. 3a** and **Supplementary Fig. 2a**). We generated transcriptional profiles for each APC subset in the juxta-tumoral tissue following the RNA-seq workflow used for the tumor DC subsets and the transcriptomes were generated in parallel, ran in the same batch as their tumor counterpart and matched for each patient (**Supplementary Fig. 2b)**. We compared tumor and juxta-tumor transcriptome for each APC subset (**Supplementary Fig. 2b)**. We identified 607 DEG for pDC, 348 DEG for $CD14^+$DC, 236 DEG for MonoMacs, 45 DEG for cDC1e, and 22 DEG for cDC2 resulting in a total of 1,258 DEG (FDR<0.05; Log2 fold change (FC) >1) that were kept for further analysis (**Fig. 3b**). DEG from all DC subsets were increased in the tumor as compared to the juxta-tumor (**Fig. 3b**). We identified 7 genes with highest significance (FDR= 1,72x10-17– $4{,}1x10^{-10}$) in $CD14^+$DC compared to DEG from other APC subsets, which included the secretoglobulin, *TFF1* and *TFF3*, which have a function in mucosal healing. Conversely, DEG from MonoMacs were mostly upregulated in juxta-tumor (195 DEG) as compared to tumor (41 DEG) samples. Among the genes most significantly upregulated in juxta-tumor MonoMacs was CD163L, which is associated with M2 polarization (**Fig. 3b**).

Among the top five most increased transcripts in the tumor APCs compared to juxta-tumor, we detected CD5 in pDCs (**Fig. 3c**) and the secretoglobulins *SCGB2A2* and *SCGB1D2* in cDC2. *SCGB2A2* was also found in the top 5 DEG of $CD14^+$DC and pDC in the tumor versus juxta-tumor comparison (**Fig. 3c and Supplementary Fig. 2b**). *TNFRSF13B* (also named TACI), a TNF receptor superfamily protein, was among top 5 DEG upregulated in tumor compared to juxta-tumor cDC1e, whereas the chemokine *CCL7* was highly upregulated in

tumor compared to juxta-tumor MonoMacs (**Fig. 3b**). *AGR2* was among the top upregulated genes in tumor compared to juxta-tumor cDC2, CD14^{+}DC and MonoMacs (**Fig. 3b**).

We next analyzed whether the DEG between tumor and juxta-tumor APCs were shared across subsets. Strikingly, most of the genes were differentially expressed exclusively in one (1074 genes) or two (184 genes) subsets (**Fig. 3d**). Only 21 DEG were shared with two other subsets, and none with three or four (**Fig. 3d, e**). This indicated that the tumor-induced transcriptional reprogramming of APC is subset-specific.

The differential expression of *SCGB2A2* a gene previously associated to mammary epithelial tumor cells[39, 40], raised questions regarding its tumor- versus immune cell-specificity[41]. We excluded the possibility of a contamination by tumor cell mRNA based on our stringent gating strategy (**Supplementary Fig. 1** and **Fig. 1a**), and on the observation that epithelial-specific mRNA, such as *EPCAM*, were not detected among DEG in tumor pDCs (**Supplementary Fig. 2b**). Considering that *SCGB2A2* was detected in a transcriptome analysis of blood pDC from healthy donors [42], these observations suggest that pDC might express *SCGB2A2* mRNA endogenously at steady state and in inflammatory conditions. In conclusion, we showed that DCs adapt to the tumor microenvironment in a subset-specific manner.

Immune pathways are absent from APC tumor-emerging genes of APC

For each APC, we analyzed the functions linked to tumor-emerging genes (DEG upregulated), meaning enriched in tumor, as compared to juxta-tumor APC. Pathway enrichment analysis identified “actomyosin structure organization”, and “proteinaceous extracellular matrix”, in pDC, “receptor protein tyrosine kinase signaling” in CD14^{+}DC, and “kinetochore” in MonoMacs (**Fig. 4a**). Major genes driving enriched pathway included the growth factor *CTGF* in pDC, *AGR2* in CD14^{+}DC, and the mitotic checkpoint *BUB1* in

MonoMac (**Fig. 4b**). Because we did not identify any immune function enrichment with this unbiased approach, we specifically investigated the expression of immune checkpoints important in anti-tumor immunity[28,29]. Out of 19 positive and 15 negative immune checkpoints (**Methods**), we found the following that were differentially expressed in tumor as compared to juxta-tumor APC: *TNFRSF14* (HVEM) in pDC, *VTCN1* (B7-H4) and *CEACAM6* in cDC2 and CD14^{+}DC, and *CEACAM6* in MonoMacs (**Fig. 4c**). In conclusion, tumor-emerging genes from LBC APC are poorly linked to immune functions.

Transcriptomics profile of tumor APC depends on breast cancer subtype

In order to evaluate the impact of tumor type on DC transcriptional profile, we generated the transcriptomes of pDC, cDC2 and CD14^{+}DC from four TNBC samples and of cDC1e and MonoMac from four TNBC samples (**Supplementary Fig. 3 and Supplementary Table 1**). Principal component analysis of tumor DC transcriptional profiles using the 500 most variant genes indicated that DCs clustered based on cancer subtype rather than by DC subset (**Fig. 5a**), suggesting a differential tumor imprint on DC. pDC separated from the other APC subsets in both cancer types (**Fig. 5a**). To identify the genes upregulated in TNBC compared to LBC for each DC subset, we performed differential analysis (FDR<0.05, LogFC>1). MonoMacs had the highest number of DEG (2,930 genes), followed by CD14^{+}DC (2,662 genes) and pDC (1,434 genes) (**Fig. 5b**). cDC1e (605 genes) and cDC2 (521 genes) were the less impacted by the tumor type (**Fig. 5b).** The majority of DEG (65% of up-regulated genes in TNBC compared to LBC) were exclusively upregulated in one DC subset (**Fig. 5c**). Four DEG *(IFNL1*, *IFNB1* and *ISG2* and *ISG15)*, all associated to the IFN pathway, were upregulated in TNBC compared to LBC (**Fig. 5d**). These data indicate that two different types of cancer had a major impact on the transcriptome of infiltrating DC and MonoMac.

TNBC promotes a shared immune-related signature in DC

PDC had the highest number of enriched pathways (166) in comparison to others APC (**Fig. 6a**). MonoMac, cDC2 and $CD14^+$DC shared 49%, 36% and 29% of their enriched pathways with at least another subset, respectively (**Fig. 6a**). In contrast, cDC1e shared only 6% of their enriched pathways with other subsets (**Fig. 6a**). These results suggest that enriched pathways in TNBC APCs were mostly subset-specific, indicating a functional specialization for each subset.

We then focused on the pathways that were commonly enriched in APCs in TNBC. We identified 38 pathways, including those linked to immune-related functions, that were shared with at least another APC subset (**Fig. 6b and Supplementary Fig. 4a**). In particular, "chemokine activity", "cytokine activity", "cytokine receptor binding" and "IL-10 signaling" were shared between cDC2 and $CD14^+$DC (**Supplementary Fig. 4a**). Type 1 IFN related pathways, such as "IFNα/β signaling" and "negative regulation of viral life cycle" were commonly enriched in all DC subsets (**Fig. 6b**). From all type 1 IFN related pathways, we selected the significantly enriched genes, including *IFNB1*, *ISG15* and *ISG20* and classified them into distinct metagenes according to their contribution to IFN production or the IFN response (**Supplementary Fig. 4b**). Because both metagenes were strongly correlated across all TNBC samples (**Fig. 6c**) we pooled them into a single "IFN pathways" metagene, which was increased in all APCs in TNBC compared to APC in LBC (Fig. 6d). As a control, the "ECM organization pathway" metagene (**Supplementary Fig. 4c**) was significantly increased only in TNBC MonoMacs (**Fig. 6d**). We also analyzed the expression of a "costimulatory" metagene (**Supplementary Fig. 4d**) that was significantly increased only in TNBC cDC2 (**Fig. 6d**) and highly correlated with IFN pathways metagene (r=0,72, P=5,33x10^{-11}) (**Fig. 6e**). When analyzing the dependency of individual checkpoint genes with the IFN pathways metagene, we found that genes such as *CD48* (SLAMF2) in pDC, *CD80* in cDC2, and

SLAMF1 in cDC1e highly correlated with IFN pathways (**Fig. 6f**). In contrast, *TNFSF4* in pDC, *TIMD4* in cDC2, and *CD70* in CD14^{+}DC were not correlated with the IFN pathway metagenes (**Fig. 6f**). This reveals two groups of checkpoint molecules that are differentially associated to the IFN pathways (**Supplementary Fig. 4e**). Thus, the APC transcriptomes in TNBC strongly differs from that of APC in LBC, with a common IFN pathway upregulated in all TNBC APC, revealing a specific contribution of TNBC to APC reprograming.

Subset-specific signatures of tumor APC predict breast cancer survival

In order to assess whether the APC subset-specific signatures may have a prognostic impact, we took advantage of the publicly available dataset from whole breast cancer transcriptome METABRIC, which includes patient survival clinical annotation[43]. Because of the differences in the APC transcriptional profiles, we separately investigated LBC and TNBC datasets. We calculated a Z-score for each APC subset-specific signature[44] (**Supplementary Fig. 5a**). We found that high pDC, cDC2 and cDC1e scores significantly predicted disease-free survival in LBC (P = 0.0018, 0.0183, and 0.0111, and Hazard Ratio (HR) of 1.45, 1.32, and 1.35, respectively) (**Fig. 7a**). On the contrary, a high MonoMac score was linked to bad prognosis in LBC (P = 0.005; HR= 0.72), and TNBC (P = 0.0079; HR: 0.58) (**Fig. 7a**). A high cDC1e score was linked to good prognosis in TNBC (P = 0.0083; HR: 1.72), with an increased significance than for LBC (**Fig. 7a**). pDC and cDC2 scores had no prognostic value in TNBC (**Fig. 7a**), suggesting various signatures may have a different clinical impact according to the DC subset and the breast cancer type.

A CD103^{+}DC gene signature was reported to correlate with good prognosis in several tumor types, including breast cancer[44]. Using the METABRIC dataset, we found that the CD103^{+}DC gene signature score had significant impact on LBC survival (HR: 1.58; P<0.01) (**Fig. 7b**), but not on TNBC prognosis (**Fig. 7b**). We then assessed the prognostic value of blood pDC

292 signature[7]. Blood pDC signature score had no significant impact on LBC nor TNBC survival
293 outcome (**Fig. 7c**). Hence, prognostic significance was most efficiently reached in a given
294 tumor using DC signatures generated from the same tumor type. Last, no prognostic value
295 associated to the common IFN signature was found TNBC patients (**Fig. 7d**), showing that
296 subset-specific signatures harbored more prognostic information than a shared signature.
297 We then determined whether subset-specific signatures could be independently associated to
298 survival when integrated with the Nottingham Prognostic Index (NPI), a reference clinical
299 score determining survival[45]. We observed that all significant scores in univariate analysis
300 were kept in the multivariate analysis in LBC: pDC (P = 0.0072; HR=1.37), cDC2 (P =
301 0.0041; HR=1.27), cDC1e (P = 0.0041; HR=1.39), MonoMac (P = 0.025; HR=0.77) and in
302 TNBC: cDC1e (P = 0.0058; HR=1.76), MonoMac (P = 0.049; HR=0.67) (**Table 1**),
303 indicating that subset-specific APC signatures in LBC and TNBC were independent
304 prognostic factors associated to disease-free survival. These results demonstrate the relevance
305 of generating subset and breast cancer type-specific signatures to predict clinical outcome.

Discussion

Here we have used DC-specific markers to identify resident DC populations (cDC2, cDC1, pDC), MonoMacs and subsets that share many features with previously described inflammatory DCs ($CD14^+$DCs)[2, 21] to provide a broad and systematic coverage of currently identified APC subsets in two types of breast cancer (LBC and TNBC).

Our analysis revealed pDC as the most distinct APC subtype, as reported before in various tissues and species[5, 6, 7, 10, 46, 47]. We propose that part of such pDC-specific signature is determined by ontogeny, as supported by a number of genes identified in the pDC signatures independently of the tissue type, such as *CLEC4C*, GZMB, and *TCF4*[6, 7, 10]. Other pDC signature genes such as the basal membrane laminins *LAMA4*, *LAMB1* and *LAMC1*, not previously associated to a pDC-specific signature[6, 7], might be attributed to tissue imprint, or a combined effect between ontogeny and tissue-driven factors. Contrary to pDC, $CD14^+$DC and cDC2 had a very close similarity to other subsets. Comparative analyses of DC subsets across multiple studies may uncover conserved, ontogeny-determined signatures, as opposed to more plastic and environmental-driven transcriptional modifications.

In high-throughput studies of tumor-infiltrating APC in the mouse[48, 49, 50], only two had performed a comparison of tumor and non-tumor tissue[48, 50], but have focused on a single APC population: $CD11b^+$DC[53] or macrophages[48, 50], and did not systematically compare diverse APC in regards to their adaptation to a tumor context. Here, by systematically comparing the tumor and the juxta-tumor non-involved tissue for each APC subset transcriptome, we uncovered emergent features in tumor-infiltrating as compared to the non-tumor tissue APC. This imprinting was different for distinct APC subsets, both qualitatively and quantitatively, indicating that in breast cancer there is no unique signature that could be attributed to tissue imprinting, as was previously suggested in other anatomical sites[6, 7, 8]. We

propose that the effect of the tissue microenvironment on innate immune cells should be considered and interpreted in close interaction with subset-specific molecular features.

Recently, cDC1 was proposed as the main APC subset driving antitumor response in mice tumor models in a type 1 IFN-dependent manner[44, 51, 52]. In our study, cDC1e expressing *XCR1* and *CLEC9A*, as well as other cDC1-specific markers, had no increase in genes related to DC activation or antigen presentation, as compared to the other APC signatures, neither in LBC nor in TNBC. Moreover, all human APC transcriptome from TNBC, and not only cDC1e, were enriched IFN response and IFN production genes indicating that, at least in human breast cancer, all DC can upregulate an IFN signature. Further experiments are needed to determine whether cDC1 is key to antitumor immune responses in humans.

Tumors have been segregated based on their low versus high immune infiltrate ("cold" versus "hot" tumors)[53]. The first was characterized by a low T cell infiltration, and an increase in angiogenic and extracellular matrix factors[54, 55]. The second had higher T cell infiltrates and increased chemokine and type 1 IFN expression[51, 54, 55]. Both tumor types were associated with distinct mechanisms of immune escape[53, 54, 55]. The breast cancer subtypes investigated here, TNBC and LBC, have high and poor immune infiltrate, respectively[56]. LBC DCs, and especially LBC pDCs, were enriched in "vascular wound healing" and "extracellular matrix" pathways, whereas TNBC DC subsets were enriched in immune signatures, including IFN pathways. Hence, our findings identify DCs as another level of immune-based stratification of tumors. This could serve to study the differential contribution of DC subsets in mechanisms of immune escape across different tumor types.

TNBC is a rare and more aggressive breast cancer subtype[57]. Clinical trials using checkpoints blockers are ongoing in TNBC with promising results[14, 58]. Hence, there is a major interest in precisely characterizing the immune compartment in these patients**.** Here, we provide a detailed analysis of APC subsets in TNBC. In particular, cDC1e but not pDC or cDC2-

355 specific signatures were predictors of survival in TNBC in contrast to LBC. Hence, our data
356 can be exploited to identify TNBC-specific prognostic signatures, as well as promising targets
357 to better direct immune checkpoint-targeting therapies.
358 Overall, our study provides a detailed and comprehensive molecular profiling of tumor-
359 infiltrating DC subsets and MonoMac in human cancer, which may serve as a reference
360 dataset to increase biological knowledge on DC in disease context. Our findings shed light on
361 the rules dictating DC diversity and adaptation to complex microenvironments, such as in
362 cancer, through transcriptional reprograming. Our data will help to dissect the individual
363 contribution of DC subsets to anti-tumor immunity, and provide a valuable resource to
364 identify potential targets and biomarkers to better direct cancer immunotherapies.
365

ACCESSION CODES

RNAseq data that support the findings of this study have been deposited in NCBI Sequence Read Archive (SRA) with the accession code PRJNA380940 (https://www.ncbi.nlm.nih.gov/bioproject/?term=380940)

ACKNOWLEDGMENTS

We thank the Institut Curie Cytometry Core facility for cell sorting. We thank INSERM U932, particularly C. Laurent and A.S. Hamy-Petit for bioinformatics advice, and S. Alculumbre and P. Vargas for helpful discussions. F. Noël was supported by a fellowship from the French Ministry of Research. This work was supported by funding from INSERM (BIO2012-02, BIO2014-08, HTE2016), Fondation pour la Recherche Médicale, ANR-10-IDEX-0001-02 PSL* and ANR-11-LABX-0043, European Research Council (IT-DC 281987) and CIC IGR-Curie 1428, INCA EMERG-15-ICR-1, la Ligue contre le cancer (labellisation EL2016.LNCC/VaS). High-throughput sequencing has been performed by the ICGex NGS platform of the Institut Curie supported by grants ANR-10-EQPX-03 (Equipex) and ANR-10-INBS-09-08 (France Génomique Consortium), InCA from ANR ("Investissements d'Avenir" program), by the Canceropole Ile-de-France and by the SiRIC-Curie program - SiRIC Grant "INCa-DGOS- 4654".

AUTHOR CONTRIBUTION

P.M. designed and performed experiments, analyzed results and wrote the manuscript. F.N. performed bioinformatics analyses and wrote the manuscript. E.Z., U.C. and C.G. analyzed results P.S. and O.A. performed experiments. A.S.-D. contributed to project management. A.V.-S. contributed to clinical project management, pathology review and provided clinical samples. F.R. contributed to clinical project management. M.G.-D. contributed to project management and revised the manuscript. S.A. and E.S. provided strategic advice and revised the manuscript. V.S. designed experiments, supervised the research and wrote the manuscript.

COMPETING FINANCIAL INTERESTS

The authors declare no conflict of interests

References

1. Banchereau, J. & Steinman, R.M. Dendritic cells and the control of immunity. *Nature* **392**, 245-252 (1998).

2. Collin, M., McGovern, N. & Haniffa, M. Human dendritic cell subsets. *Immunology* **140**, 22-30 (2013).

3. Mildner, A. & Jung, S. Development and function of dendritic cell subsets. *Immunity* **40**, 642-656 (2014).

4. Shay, T. & Kang, J. Immunological Genome Project and systems immunology. *Trends Immunol* **34**, 602-609 (2013).

5. Miller, J.C. *et al*. Deciphering the transcriptional network of the dendritic cell lineage. *Nat Immunol* **13**, 888-899 (2012).

6. Heidkamp, G.F. *et al*. Human lymphoid organ dendritic cell identity is predominantly dictated by ontogeny, not tissue microenvironment. *Sci Immunol* **1** (2016).

7. Haniffa, M. *et al*. Human tissues contain CD141hi cross-presenting dendritic cells with functional homology to mouse CD103+ nonlymphoid dendritic cells. *Immunity* **37**, 60-73 (2012).

8. Watchmaker, P.B. *et al*. Comparative transcriptional and functional profiling defines conserved programs of intestinal DC differentiation in humans and mice. *Nat Immunol* **15**, 98-108 (2014).

9. Liu, Y.J. IPC: professional type 1 interferon-producing cells and plasmacytoid dendritic cell precursors. *Annu Rev Immunol* **23**, 275-306 (2005).

10. Lindstedt, M., Lundberg, K. & Borrebaeck, C.A. Gene family clustering identifies functionally associated subsets of human in vivo blood and tonsillar dendritic cells. *J Immunol* **175**, 4839-4846 (2005).

11. Mora, J.R. *et al*. Selective imprinting of gut-homing T cells by Peyer's patch dendritic cells. *Nature* **424**, 88-93 (2003).

12. Huang, Q. *et al*. The plasticity of dendritic cell responses to pathogens and their components. *Science* **294**, 870-875 (2001).

13. Pulendran, B., Palucka, K. & Banchereau, J. Sensing pathogens and tuning immune responses. *Science* **293**, 253-256 (2001).

14. Stagg, J. & Allard, B. Immunotherapeutic approaches in triple-negative breast cancer: latest research and clinical prospects. *Ther Adv Med Oncol* **5**, 169-181 (2013).

15. Liu, Y.J. Dendritic cell subsets and lineages, and their functions in innate and adaptive immunity. *Cell* **106**, 259-262 (2001).

16. Dalod, M., Chelbi, R., Malissen, B. & Lawrence, T. Dendritic cell maturation: functional specialization through signaling specificity and transcriptional programming. *EMBO J* **33**, 1104-1116 (2014).

17. Soumelis, V., Pattarini, L., Michea, P. & Cappuccio, A. Systems approaches to unravel innate immune cell diversity, environmental plasticity and functional specialization. *Curr Opin Immunol* **32**, 42-47 (2015).

18. Segura, E. & Amigorena, S. Inflammatory dendritic cells in mice and humans. *Trends Immunol* **34**, 440-445 (2013).

19. Wollenberg, A., Haberstok, J., Teichmann, B., Wen, S.P. & Bieber, T. Demonstration of the low-affinity IgE receptor Fc epsilonRII/CD23 in psoriatic epidermis: inflammatory dendritic epidermal cells (IDEC) but not Langerhans cells are the relevant CD1a-positive cell population. *Arch Dermatol Res* **290**, 517-521 (1998).

20. Zaba, L.C., Krueger, J.G. & Lowes, M.A. Resident and "inflammatory" dendritic cells in human skin. *J Invest Dermatol* **129**, 302-308 (2009).

21. Segura, E. *et al*. Human inflammatory dendritic cells induce Th17 cell differentiation. *Immunity* **38**, 336-348 (2013).

22. Dunn, G.P., Bruce, A.T., Ikeda, H., Old, L.J. & Schreiber, R.D. Cancer immunoediting: from immunosurveillance to tumor escape. *Nat Immunol* **3**, 991-998 (2002).

23. Bell, D. *et al*. In breast carcinoma tissue, immature dendritic cells reside within the tumor, whereas mature dendritic cells are located in peritumoral areas. *J Exp Med* **190**, 1417-1426 (1999).

24. DeNardo, D.G. & Coussens, L.M. Inflammation and breast cancer. Balancing immune response: crosstalk between adaptive and innate immune cells during breast cancer progression. *Breast Cancer Res* **9**, 212 (2007).

25. Ghiringhelli, F. *et al*. CD4+CD25+ regulatory T cells inhibit natural killer cell functions in a transforming growth factor-beta-dependent manner. *J Exp Med* **202**, 1075-1085 (2005).

26. Faget, J. *et al*. ICOS-ligand expression on plasmacytoid dendritic cells supports breast cancer progression by promoting the accumulation of immunosuppressive CD4+ T cells. *Cancer Res* **72**, 6130-6141 (2012).

27. Ghirelli, C. *et al*. Breast Cancer Cell-Derived GM-CSF Licenses Regulatory Th2 Induction by Plasmacytoid Predendritic Cells in Aggressive Disease Subtypes. *Cancer Res* **75**, 2775-2787 (2015).

28. Topalian, S.L., Drake, C.G. & Pardoll, D.M. Immune checkpoint blockade: a common denominator approach to cancer therapy. *Cancer Cell* **27**, 450-461 (2015).

29. Chen, D.S. & Mellman, I. Oncology meets immunology: the cancer-immunity cycle. *Immunity* **39**, 1-10 (2013).

30. Angel, C.E. *et al*. Cutting edge: CD1a+ antigen-presenting cells in human dermis respond rapidly to CCR7 ligands. *Journal of immunology (Baltimore, Md. : 1950)* **176**, 5730-5734 (2006).

31. Bakdash, G. *et al*. Expansion of a BDCA1+CD14+ Myeloid Cell Population in Melanoma Patients May Attenuate the Efficacy of Dendritic Cell Vaccines. *Cancer research* **76**, 4332-4346 (2016).

32. McGovern, N. *et al*. Human dermal CD14(+) cells are a transient population of monocyte-derived macrophages. *Immunity* **41**, 465-477 (2014).

33. Bronte, V. *et al*. Recommendations for myeloid-derived suppressor cell nomenclature and characterization standards. *Nat Commun* **7**, 12150 (2016).

34. Guilliams, M. *et al*. Unsupervised High-Dimensional Analysis Aligns Dendritic Cells across Tissues and Species. *Immunity* **45**, 669-684 (2016).

35. Taieb, J. *et al*. A novel dendritic cell subset involved in tumor immunosurveillance. *Nat Med* **12**, 214-219 (2006).

36. Caminschi, I. *et al*. Putative IKDCs are functionally and developmentally similar to natural killer cells, but not to dendritic cells. *J Exp Med* **204**, 2579-2590 (2007).

37. Krasselt, M., Baerwald, C., Wagner, U. & Rossol, M. CD56+ monocytes have a dysregulated cytokine response to lipopolysaccharide and accumulate in rheumatoid arthritis and immunosenescence. *Arthritis research & therapy* **15**, R139 (2013).

38. Villani, A.C. *et al*. Single-cell RNA-seq reveals new types of human blood dendritic cells, monocytes, and progenitors. *Science* **356** (2017).

39. Grunewald, K. *et al*. Mammaglobin gene expression: a superior marker of breast cancer cells in peripheral blood in comparison to epidermal-growth-factor receptor and cytokeratin-19. *Lab Invest* **80**, 1071-1077 (2000).

40. Han, J.H. *et al*. Mammaglobin expression in lymph nodes is an important marker of metastatic breast carcinoma. *Arch Pathol Lab Med* **127**, 1330-1334 (2003).

41. Kowalewska, M., Chechlinska, M., Markowicz, S., Kober, P. & Nowak, R. The relevance of RT-PCR detection of disseminated tumour cells is hampered by the expression of markers regarded as tumour-specific in activated lymphocytes. *Eur J Cancer* **42**, 2671-2674 (2006).

42. Novershtern, N., Regev, A. & Friedman, N. Physical Module Networks: an integrative approach for reconstructing transcription regulation. *Bioinformatics* **27**, i177-185 (2011).

43. Curtis, C. *et al*. The genomic and transcriptomic architecture of 2,000 breast tumours reveals novel subgroups. *Nature* **486**, 346-352 (2012).

44. Broz, M.L. *et al*. Dissecting the tumor myeloid compartment reveals rare activating antigen-presenting cells critical for T cell immunity. *Cancer Cell* **26**, 638-652 (2014).

45. Galea, M.H., Blamey, R.W., Elston, C.E. & Ellis, I.O. The Nottingham Prognostic Index in primary breast cancer. *Breast Cancer Res Treat* **22**, 207-219 (1992).

46. Gautier, E.L. *et al*. Gene-expression profiles and transcriptional regulatory pathways that underlie the identity and diversity of mouse tissue macrophages. *Nat Immunol* **13**, 1118-1128 (2012).

47. Robbins, S.H. *et al*. Novel insights into the relationships between dendritic cell subsets in human and mouse revealed by genome-wide expression profiling. *Genome Biol* **9**, R17 (2008).

48. Franklin, R.A. *et al*. The cellular and molecular origin of tumor-associated macrophages. *Science* **344**, 921-925 (2014).

49. Ojalvo, L.S., Whittaker, C.A., Condeelis, J.S. & Pollard, J.W. Gene expression analysis of macrophages that facilitate tumor invasion supports a role for Wnt-signaling in mediating their activity in primary mammary tumors. *J Immunol* **184**, 702-712 (2010).

50. Pyfferoen, L. *et al*. The transcriptome of lung tumor-infiltrating dendritic cells reveals a tumor-supporting phenotype and a microRNA signature with negative impact on clinical outcome. *Oncoimmunology* **6**, e1253655 (2017).

51. Fuertes, M.B. *et al*. Host type I IFN signals are required for antitumor CD8+ T cell responses through CD8{alpha}+ dendritic cells. *J Exp Med* **208**, 2005-2016 (2011).

52. Salmon, H. *et al*. Expansion and Activation of CD103(+) Dendritic Cell Progenitors at the Tumor Site Enhances Tumor Responses to Therapeutic PD-L1 and BRAF Inhibition. *Immunity* **44**, 924-938 (2016).

53. Wargo, J.A., Reddy, S.M., Reuben, A. & Sharma, P. Monitoring immune responses in the tumor microenvironment. *Curr Opin Immunol* **41**, 23-31 (2016).

54. Gajewski, T.F., Schreiber, H. & Fu, Y.X. Innate and adaptive immune cells in the tumor microenvironment. *Nat Immunol* **14**, 1014-1022 (2013).

55. Spranger, S. & Gajewski, T.F. Tumor-intrinsic oncogene pathways mediating immune avoidance. *Oncoimmunology* **5**, e1086862 (2016).

56. Stanton, S.E., Adams, S. & Disis, M.L. Variation in the Incidence and Magnitude of Tumor-Infiltrating Lymphocytes in Breast Cancer Subtypes: A Systematic Review. *JAMA Oncol* **2**, 1354-1360 (2016).

57. Foulkes, W.D., Smith, I.E. & Reis-Filho, J.S. Triple-negative breast cancer. *N Engl J Med* **363**, 1938-1948 (2010).

58. Bianchini, G., Balko, J.M., Mayer, I.A., Sanders, M.E. & Gianni, L. Triple-negative breast cancer: challenges and opportunities of a heterogeneous disease. *Nat Rev Clin Oncol* **13**, 674-690 (2016).

581 **Figure legends**

582

583 **Figure 1 Phenotypic and molecular characterization of innate APC infiltrating breast**
584 **cancer tissue. a**, Representative flow cytometry contour plots showing the gate strategy to
585 distinguish DC subsets from MonoMac, and their frequency in breast cancer samples. **b**,
586 Representative histograms of mean fluorescent intensity of CD141, CD16, CD163, AXL, and
587 CD32B expression by the indicated APC subset in breast cancer samples (n=3 donors with
588 similar results). **c**, Representative Giemsa-staining of cytospin preparation to analyze the
589 morphology of FACS-sorted APC from tumor (n=3 donors with similar results). **d**, Frequency
590 of APC subsets determined by flow cytometry, among total live cells (left), and $CD45^+$cells
591 (right) (n=22 donors). Median is shown in red. **e** Boxplots showing the gene expression as
592 Log_2 (Read counts +1) of DC selective markers by tumor-isolated APC. Color code
593 represents each APC subset. Box limits indicate 1^{st} quartile, median and 3^{rd} quartile. Each dot
594 represents a sample. **f**, BubbleMap analysis showing the enrichment of indicated APC public
595 signatures (***Carpentier et al.***[59]) in pairwise comparisons of tumor-isolated APC
596 transcriptomes. Frameworks indicates the expected signature enrichment. The legend
597 indicates color intensity and size code for Normalized Enrichment Score (NES) and False
598 Discovery Rate (FDR), respectively. **e,f** Transcriptomics data are from 6-10 tumor-isolated
599 APC (pDC n= 8, cDC2 n=10, cDC1e n=6, $CD14^+$DC n=9, and MonoMac n=11).

600

601 **Figure 2 Subset-specific signatures defining tumor APC. a**, Pie chart showing the
602 proportion of differentially expressed genes (DEG) (up/down) among tumor-isolated APC
603 subset after one-way ANOVA test, and Tukey post-hoc correction ($P < 0.05$). **b**, Bar plots
604 indicate the number of differentially upregulated genes in one subset versus all the others
605 (left), and the heatmap (right) the relative expression of each gene as z-score. **c**,

606 Bioinformatics pipeline used to perform functional inference from subset-specific gene
607 signatures. **d**, Functional network inference showing the most significantly overrepresented
608 biological pathway in pDC, cDC1e, and MonoMac gene signatures from tumor (FDR <0.05).
609 Color code represent distinct pathways. Node size reflects P-value, as specified. **(e)** Boxplots
610 showing the expression as Log_2 (Read counts +1) of indicated genes from the most
611 significantly enriched pathways found in **e** for pDC, cDC1e, and MonoMac. Color code
612 represents each APC subset. Box limits indicate 1st quartile, median and 3rd quartile. Each dot
613 represents a sample. **d, e** Transcriptomics data used for network inference analysis are from:
614 pDC n= 8, cDC1e n=6, and MonoMac n=11.
615
616 **Figure 3 Tumor-emergent genes from innate APC are subset-specific**. **a**, Frequency of
617 APC subsets as determined by flow cytometry, among CD45$^+$ or total live cells, between
618 tumor (black), and juxta-tumor (grey) from luminal breast cancer (LBC) samples (n=8 paired-
619 donors). Median is shown in red. *P<0.05, **P <0.01 (two-tailed Wilcoxon-test). **b**, Volcano
620 plots show the DEG (FDR < 0.05) between tumor and juxta-tumor for each APC subset
621 transcriptome. Genes upregulated in the tumor (T) are in black (Log_2 (Fold change) > 1), and
622 in the juxta-tumor (J) in grey (Log_2 (Fold change) < -1). Number of DEG for each condition is
623 indicated. **c**, Barplots show the Log_2 (Fold change) value from the top five upregulated (black)
624 or downregulated (grey) DEG in the tumor for each APC subset **d**, Venn diagram showing
625 total DEG between tumor and juxta-tumor from each subset. The number of shared DEG by
626 all subset is in the center of the diagram. **e**, Barplots showing the number of DEG unique (0)
627 or shared with another subset (1,2, 3, or 4). The total number of DEG per section is indicated.
628 Colors represent the DEG for the corresponding subset. (**b**-**e**) DEG are from: pDC n=3, cDC2
629 n=4; cDC1e n=4, CD14+DC n=3, MonoMac n=5 independent matched-donors from LBC
630 samples) obtained by likelihood ratio test from edgeR R package.

631

632 **Figure 4 Absence of immune function among enriched pathways from tumor-**
633 **upregulated genes. a**, Functional network inference results for pDC, $CD14^{+}$DC and
634 MonoMac gene signatures from luminal breast cancer (LBC) (FDR <0.05). Color code
635 represent distinct pathways. Node size reflects P-value, as specified. **b**, Boxplots showing the
636 expression as Log_2 (Read counts +1) of the indicated genes from the most significantly
637 enriched pathways found in a for pDC, $CD14^{+}$DC, and MonoMac from LBC **c**, Boxplots
638 showing the expression as Log_2 (Read counts +1) of the checkpoints genes: *VTCN1*,
639 *CEACAM6*, and *TNFRSF14* between tumor and matched-juxta-tumor from LBC. The entire
640 list of checkpoints is listed in *Online Method*. Only checkpoint genes differentially expressed
641 in at least one subset were shown. * P <0.05, **P<0.01, *** P <0.005; **** P <0.001
642 (likelihood ratio test from edgeR R package). (a-c) Transcriptomic data are from: pDC n=3,
643 cDC2 n=4; cDC1e n=4, CD14+DC n=3, MonoMac n=5 independent matched-donors from
644 LBC samples). (b-c) Color code represents tumor (black) and juxta-tumor (grey). Box limits
645 indicate 1^{st} quartile, median and 3^{rd} quartile. Each dot represents a sample.
646

647 **Figure 5 Transcriptional profile of innate APC subset is breast-cancer subtype**
648 **dependent. a**, Principal Component Analysis (PCA) showing the clustering of transcriptional
649 profiles of innate APC subsets isolated from LBC and TNBC tumors. The 500 most variant
650 genes were used and PC1 and PC2 projected. The variance for each axis is indicated. The
651 same PCA colored by subset (left), and by breast cancer type (right) is shown. **b**, Volcano
652 plots show the DEG for each subset (FDR P value < 0.05). Genes upregulated in the triple-
653 negative breast cancer (TNBC) are in black (Log_2 (Fold change) > 1), and in the luminal
654 breast cancer (LBC) in grey (Log_2 (Fold change) < -1). The number of DEG for each
655 condition is described. **c**, Venn diagram of total DEG upregulated in TNBC, show the shared

DEG for each subset. **d**, Boxplots showing the expression as Log_2 (Read counts +1) of the four genes upregulated in TNBC compared to LBC by all APC subsets (from Venn diagram core). Color code represents the tumor type. Box limits indicate 1st quartile, median and 3rd quartile. Each dot represents a sample. * P <0.05, ** P <0.01, *** P <0.005. (likelihood ratio test from edgeR R package). (**a**-**d**) Transcriptomics data are from 6-10 LBC donors (pDC n= 8, cDC2 n=10, cDC1e n=6, $CD14^+$DC n=9, and MonoMac n=11), and from 3-4 TNBC donors (pDC n= 3, cDC2 n=3, cDC1e n=4, $CD14^+$DC n=3, and MonoMac n=4).

Figure 6 Type-1 IFN pathway is upregulated in all TNBC-APC subsets. a, Functional pathways analysis from up-regulated DEG in TNBC APC, and the resulting number of genes. Pie chart indicate the percentage of shared (black) or specific (grey) pathways **b**, Heat map showing the relative significance as -Log(FDR) in enriched pathways (FDR <0.05) shared between at least two APC subsets. highlighted immune pathways are in red. IFN metagenes were extracted from significantly enriched pathways and divided in IFN production, and IFN response. **c**, Scatterplot showing the correlation between IFN response and IFN production (Log2 (expression)) of all APC subsets isolated from LBC or TNBC. **d**, Violin plots showing IFN pathways, ECM organization and Costimulatory metagene expression for each APC subset from LBC, and TNBC. *P<0.05, ** P <0.01, *** P <0.005, ns >0.05 (two-sided Wilcoxon test). **e**, Scatterplot showing the correlation between IFN pathways and Costimulatory metagenes (Log2(expression)) of all APC subsets isolated from LBC or TNBC. **f**, Scatterplot showing the correlation between IFN pathway metagene and individual costimulatory genes: *CD48*, *CD80*, *SLAMF1*, *TNFSF4*, *TIMD4*, *CD70* (Log2 (expression)) for the indicated APC from LBC, and TNBC. **c-f** LBC (green) or TNBC (blue). **c,d,f** Correlation coefficient and p-value are indicated on the plot (Pearson correlation test). LBC

680 data are from: pDC n= 8, cDC2 n=10, cDC1e n=6, CD14^{+}DC n=9, and MMAC n=11, and
681 TNBC data from:(pDC n= 3, cDC2 n=3, cDC1e n=4, CD14^{+}DC n=3, and MMAC n=4.
682
683 **Figure 7 Subset-specific signatures are linked to distinct disease-free survival depending**
684 **on the subset and breast cancer type. a**, Kaplan–Meier plots indicating the probability of
685 disease-free survival on time, associated to the corresponding subset score in LBC (up), and
686 TNBC (down) patients. High expression of subset-specific signatures ratio was colored
687 regarding the corresponding subset. Log-rank test *P*-val and Hazard Ratio (HR) are written on
688 each plot **c**, Kaplan–Meier plot indicate the probability of disease-free survival on time,
689 associated to previously reported CD103^{+}DC signature[44] in LBC (up) and TNBC (down)
690 patients. High expression of CD103^{+}DC signature Z-score was colored in brown. Log-rank
691 test p-val and Hazard Ratio (HR) are written. **d**, Kaplan–Meier plot indicate the probability of
692 disease-free survival on time, associated to previously reported pDC signature[7] in LBC (up)
693 and TNBC (down) patients. High expression of pDC signature Z-score was colored in brown.
694 Log-rank test p-val and Hazard Ratio (HR) are written. e, Kaplan–Meier plot indicate the
695 probability of disease-free survival on time, associated to the APC common IFN signature
696 score in TNBC patients. High expression of IFN signature Z-score was colored in brown.
697 Log-rank test p-val and Hazard Ratio (HR) are written. * P <0.05, ** P <0.005, *** P
698 <0.001, NS P >0.05. (**a**-**e**) Transcriptomics data are from METABRIC public dataset (LBC
699 n=1043, and TNBC n=259).
700

Table 1: Multivariate Cox regression of predictors of disease-free survival influencing the disease-free survival of breast cancer patients.

	LBC		TNBC	
Variables	HR	p-value	HR	p-value
pDC signature and NPI				
NPI > 5.4	1	-	-	-
NPI ≤ 5.4	0.31	**7.5e-13**	-	-
pDC signature ratio High	1	-	-	-
pDC signature ratio Low	1.37	**0.0072**	-	-
cDC2 signature and NPI				
NPI > 5.4	1	-	-	-
NPI ≤ 5.4	0.3	**1.8e-13**	-	-
cDC2 signature ratio High	1	-	-	-
cDC2 signature ratio Low	1.27	**0.041**	-	-
cDC1e signature and NPI				
NPI > 5.4	1	-	1	-
NPI ≤ 5.4	0.29	**7.6e-14**	0.27	**1.1e-09**
cDC1e signature ratio High	1	-	1	-
cDC1e signature ratio Low	1.39	**0.0041**	1.76	**0.0058**
MMAC signature and NPI				
NPI > 5.4	1	-	1	-
NPI ≤ 5.4	0.31	**5.9e-13**	0.28	**3.9e-09**
MMAC signature ratio High	1	-	1	-
MMAC signature ratio Low	0.77	**0.025**	0.67	**0.049**

NPI, Nottigham Prognostic Index; HR, Hazard Ratio; p-value < 0.05 marked in bold font shows statistical significant.

ONLINE METHODS

Human samples and patient characteristics

Fresh samples of tumor and juxta-tumor (exempt of malignant tumor cells) tissues of untreated breast cancer patients were obtained from Hôpital de l'Institut Curie (Paris) in accordance with Institut Curie ethical guidelines. Luminal and triple-negative breast cancer types were included in the study according to the hormonal receptor status. Patient characteristics are summarized in Supplementary Table 2.

Single cell suspension from human samples

Tumor and juxta-tumor tissue were cut into small pieces and digested in CO_2-independent medium (Gibco) containing 5% FBS (HyClone) 2mg/mL collagenase I (C0130, Sigma), 2mg/mL hyaluronidase (H3506, Sigma) and 25 μg/mL DNAse (Roche) by three round of 15 min incubation in agitation at 37°C. The samples were filtered on a cell strainer 40μm (Fischer Scientific) and diluted in PBS 1X (Gibco) supplemented with 1% decomplemented human serum (BioWest), and EDTA 2 mM (Gibco). After centrifugation, cells were resuspended in the same medium and counted before being assessed by flow cytometry or sorted.

Antibodies and cell sorting

For phenotypical characterization, single cell suspension was stained with the following anti-human antibodies: CD3-Alexa700 (557943; clone: UCHT1) CD19-Alexa700 (557921; clone: HIB19), CD56-Alexa700 (557919; clone: B159) or -BUV737 (564448; clone: NCAM16.2), CD163-BV786 (741003; clone: GHI/61), CD11c-PECy5 (551077; clone:B-ly6) or -PE-CF594 (562393; clone:B-ly6), CD123-BV650 (563405; clone: 7G3), HLA-DR-BUV395 (564040; clone: G46-6), and CD45 APC-Cy7 (557833; clone: 2D1) from BD. CD14-Qdot605

(Q10013; clone: TüK4) from Life Technologies. CD14-BV605 (301833; clone:M5E2), CD16-BV510 (302047 clone: 3G8), CD123-PE-Cy7 (306010; clone: 6h6), CD1c-PE (331506; clone: L161), and HLA-DR BV711 (307643; clone: L243) from Biolegend. CD1c-PerCP-eFluor710 (46-0015-42; clone: L161), FceR1-APC (17-5899-42; clone: AER-37) from eBioscience. AXL-AlexaFluor488 (FAB154G; clone: 108724), and CD32B-APC (FAB1330A; clone: 190723) from R&D. CD141-PE (130-098-841; clone: AD5-14H12) from Miltenyi Biotec. For DC sorting, we used the following antibodies: CD45-BV570 (304033; clone: HI30) from Biolegend, CD14-FITC (555527; clone: 10.1) from BD, and HLA-DR-APCeFluor780 (47-9956-42; clone: LN3) from eBioscience instead of the corresponding marker. Single cell suspension was of tumor-digested cells were sorted in a BD FACS Aria III upgrade using the purity mode, a 100µm nozzle loop, and at low pressure (20psi). DC subsets were sorted in eppendorf tubes containing RPMI+5% FBS (HyClone) for morphological analysis. Once the morphology for each subset validated, and because of the low numbers of tumor-infiltrating APC, we directly sorted tumor-APC in TCL buffer (Qiagen) supplemented with 1% of β-Mercaptoethanol (SIGMA) for RNA-seq experiments.

Morphological analysis

Sorted cells were subjected to cytospin and colored with May-Grunwald/Giemsa staining. Pictures were taken with a ProgRes SpeedXT core 5 Microscope Camera (JENOPTIK) on a Leica DM 4000 B microscope.

RNA sequencing

General RNA-seq workflow was summarized in *Supplementary Fig. 1*. Briefly, RNA from sorted cells (>100 cells) was extracted by using Single Cell RNA Purification Kit (Norgen Bioteck), including on-column DNase (Qiagen) digestion, as described by the manufacturer's

protocol. RNA integrity was confirmed with RNA 6000 Pico Kit (Agilent Technologies) in BioAnalyzer. cDNA was generated with SMARTer Ultra Low input RNA for Illumina Sequencing-HV(Clontech), following manufacturer's protocol. 14 cycles were used to amplify cDNA. Quantity and quality of cDNA was assessed with Qubit dsDNA high sensitivity (Thermofisher), and Agilent Bioanalyzer using nanochip (Agilent Technologies), respectively. Multiplexed pair-end libraries 50nt-length, were obtained using Nextera XT kit (Clontech). Sequencing was performed in a same batch in Illumina HiSeq 2500 using an average depth of 15 million reads, 50nt-length reads per samples were obtained. Library, sequencing, and quality control of the sequencing were performed by the NGS facility at Institut Curie.

RNA-seq data pre-processing

Reads were mapped to the human genome reference (hg19/GRCh37) using Tophat2 software version 2.0.6[60]. Gene expression values were quantified as read counts using HTSeq-count[61]. We filtered out genes with less than five read counts in at least 25% of samples, and normalized the raw data using RUVg method (RUVSeq R package)[62]. This method identifies technical noise based on negative control genes that should be affected by unwanted variations but not affected by biological effects of interest. We selected the 5,000 less variant genes as negative control genes. From the 82 samples sequenced, only two were excluded from this study, corresponding to tumor and juxta-tumor pDC. These sampled were expressing low levels of pDC-specific markers, and high expression of macrophage markers.

For exploratory analyses, we performed Principal Component Analysis (PCA) of the 500 most variant genes, based on inter-quartile range method (IQR) (EMA R package)[63], of APC transcriptomes from LBC and TNBC tumor samples. Data were log2-transformed, centered

and scaled. PCA was performed using the FactoMineR R package. Z-score of log2-transformed gene expression, scaled by gene, were represented in a heatmap color.

Geneset enrichment analysis

We selected APC specific genesets from literature[59] and perform enrichment analysis on our dataset selected LBC-T samples. To do so, we used BubbleMap module of the BubbleGUM software which perform GSEA analyses with multiple testing correction[64].

Statistical analysis

Significant differences in the APC frequency from total live cells or the $CD45^+$ cells, were performed using ANOVA, followed by a post-hoc test. For paired samples in the tumor versus juxta-tumor comparison of APC we performed a Wilcoxon test, by using the GraphPad Prism 6.0.

To generate subset-specific signature of APC for each condition, we performed one-way ANOVA differential analysis test on the Log2 expression data of the five APC. We kept only the genes differentially expressed between at least two subsets (P <0.05). We then performed a Tukey post-hoc test to select genes exclusively expressed in one subset compared to all the others, (P <0.05). Those upregulated genes were defined as the subset-specific signature.

To identify genes that vary between tumor and juxta-tumor, for each APC separately, we performed pairwise comparison of gene expression matched samples using the generalized linear model (GLM) likelihood ratio test of EdgeR R package[65]. Only DEG with FDR < 0.05 and Log2 FC > 1 were considered as differentially expressed. The same analysis was applied to find differentially expressed genes between TNBC and LBC samples for each subset.

Metagenes expression was defined as the median expression in Log2 of the genes of interest in each sample. Differential expression analysis of metagenes was done using non-paired

Wilcoxon test. Correlations were assessed using Pearson correlation test, and a threshold of $P < 0.05$.

All RNA-seq statistical analyses were performed using R software (Version 3.2.3).

Regulatory network and functional inference

We extracted the gene expression matrix for each subset, and each comparison. The conditions were as followed: 1) all subsets versus all other subsets in LBC, and 2) in TNBC. 3) tumor versus juxta-tumor in LBC, and 4) TNBC versus LBC, for each subset separately. We then load the matrix on cytoscape software version 3.4.0. One analysis per subset was performed. Network inference was performed using ARACNe application, which is based on mutual information theory[66, 67]. The parameters used in ARACNe were, Mutual information Algorithm Type: Variable Bandwith. We used a transcription factor (TF) list for Hub/TF Definition from the dataset Fantom[68]. Mutual information Threshold was 0.5. We next, utilized the ClueGO Application[69] (to determine pathway enrichment in each network. Public datasets only from "Experimental evidence" of Gene Ontology (GO) – Biological process-GOA, - Cellular Component-GOA, - ImmuneSystemProcess-GOA, - Molecular Function-GOA, (updated date: 15.01.2017), InterPro dB: Protein Domains (updated date: 03.11.2015), Reactome (updated date: 20.01.2017), and WikiPathways (updated date: 20.01.2017) were used. Go Term Fusion option was selected. Only pathways with a "Benjamini-Hochberg" (BH) adjusted p-val below 0.05 were kept.

Checkpoint expression analysis

The presence of the following immune checkpoints was analyzed among DEG in tumor versus juxta-tumor samples, for each subset. Positive checkpoint genes included: CD40, CD70, CD80, CD83, TNFSF9, also named 4-1BBL, ICOSL, SEMA4A, TIMD4, C10orf54

known as VISTA or B7-H5, TNFRSF13C, also named BAFFR, TNFSF13, also named APRIL, TNFSF13, also named as HVEML, CD84, CD48, TNSF4, also named OX40L, and PVR, also named as CD155. Negative immune checkpoint genes included: CD274, also named PD-L1, CD276, also named B7-H3, PDCD1LG2, also named PD-L2, BTLA, LGALS1, LGALS3, LGALS9, CD279, also known as PD1, CEACAM6, and CD209, also named DC-SIGN.

Clinical outcome of subset-specific signature score in public breast cancer dataset

METABRIC is a public dataset[43] of transcriptomic data of breast tumor samples with clinical data associated. From this dataset, we selected samples from LBC (n=1043) and TNBC (n=259) according to the expression of receptors ER, PR and HER2. To study the clinical outcome of patients we considered the ones with the label "d-d.s" and "a" in the "last follow up status" variable. Similar to previous report[44], we calculated a Z-score of APC subset-specific signatures that we generated from our breast cancer RNA-seq data, as follows:

$$log_2Ratio = log_2\left(\frac{\overline{Signature\ UP}}{\overline{Signature\ DOWN}}\right)$$

$$Zscore\ ratio = \frac{log_2Ratio - \overline{log_2Ratio}}{sd(log_2Ratio)}$$

To assess predictive value of the CD103$^+$DC reported in *Broz et al.*[44], we applied the same Z-score, based on CD103$^+$DC signature as the "signature UP" and CD103$^-$DC signature as the "signature DOWN". CD103$^+$DC and CD103$^-$DC signatures contained 9 and 16 genes respectively[44].

To assess predictive value of the pDC signature reported in *Haniffa et al.*[7], we applied the same Z-score, based on pDC up-regulated genes as the "signature UP" and pDC down-regulated genes as the "signature DOWN". pDC UP and pDC DOWN signatures contained 440 and 524 genes respectively.

To assess predictive value of the IFN signature found in TNBC-APC, we performed a Z-score on Log2 mean expression of: IFNL1, IFNB1, ISG15, and ISG20. We performed univariate cox analysis to assess the link between subset-specific signature ratio expression, and disease-free survival. We divided the subset-specific Z-score ratio expression in two groups: "high" or "low", according to the median value. Kaplan-Meier curves were generated using survminer R package. Multivariate cox analysis was performed to link subset-specific signatures and the clinical prognostic parameter, Nottingham Prognostic Index (NPI)[45], to disease-free survival.

Life Science Reporting Summary

Further information on Online Methods are available in the Nature Research Reporting Summary.

Data availability

RNAseq data that support the findings of this study have been deposited in NCBI Sequence Read Archive (SRA) with the accession code PRJNA380940 (https://www.ncbi.nlm.nih.gov/bioproject/?term=380940)

Method References

59. Carpentier, S. *et al*. Comparative genomics analysis of mononuclear phagocyte subsets confirms homology between lymphoid tissue-resident and dermal XCR1(+) DCs in mouse and human and distinguishes them from Langerhans cells. *J Immunol Methods* **432**, 35-49 (2016).

60. Kim, D. *et al*. TopHat2: accurate alignment of transcriptomes in the presence of insertions, deletions and gene fusions. *Genome Biol* **14**, R36 (2013).

61. Anders, S., Pyl, P.T. & Huber, W. HTSeq--a Python framework to work with high-throughput sequencing data. *Bioinformatics* **31**, 166-169 (2015).

62. Risso, D., Ngai, J., Speed, T.P. & Dudoit, S. Normalization of RNA-seq data using factor analysis of control genes or samples. *Nat Biotechnol* **32**, 896-902 (2014).

63. Servant, N. *et al*. EMA - A R package for Easy Microarray data analysis. *BMC Res Notes* **3**, 277 (2010).

64. Spinelli, L., Carpentier, S., Montanana Sanchis, F., Dalod, M. & Vu Manh, T.P. BubbleGUM: automatic extraction of phenotype molecular signatures and comprehensive visualization of multiple Gene Set Enrichment Analyses. *BMC Genomics* **16**, 814 (2015).

65. Robinson, M.D., McCarthy, D.J. & Smyth, G.K. edgeR: a Bioconductor package for differential expression analysis of digital gene expression data. *Bioinformatics* **26**, 139-140 (2010).

66. Margolin, A.A. *et al*. ARACNE: an algorithm for the reconstruction of gene regulatory networks in a mammalian cellular context. *BMC Bioinformatics* **7 Suppl 1**, S7 (2006).

67. Basso, K. *et al*. Reverse engineering of regulatory networks in human B cells. *Nat Genet* **37**, 382-390 (2005).

68. Joshi, A. *et al*. Technical Advance: Transcription factor, promoter, and enhancer utilization in human myeloid cells. *J Leukoc Biol* **97**, 985-995 (2015).

69. Bindea, G. *et al*. ClueGO: a Cytoscape plug-in to decipher functionally grouped gene ontology and pathway annotation networks. *Bioinformatics* **25**, 1091-1093 (2009).

Figure 1

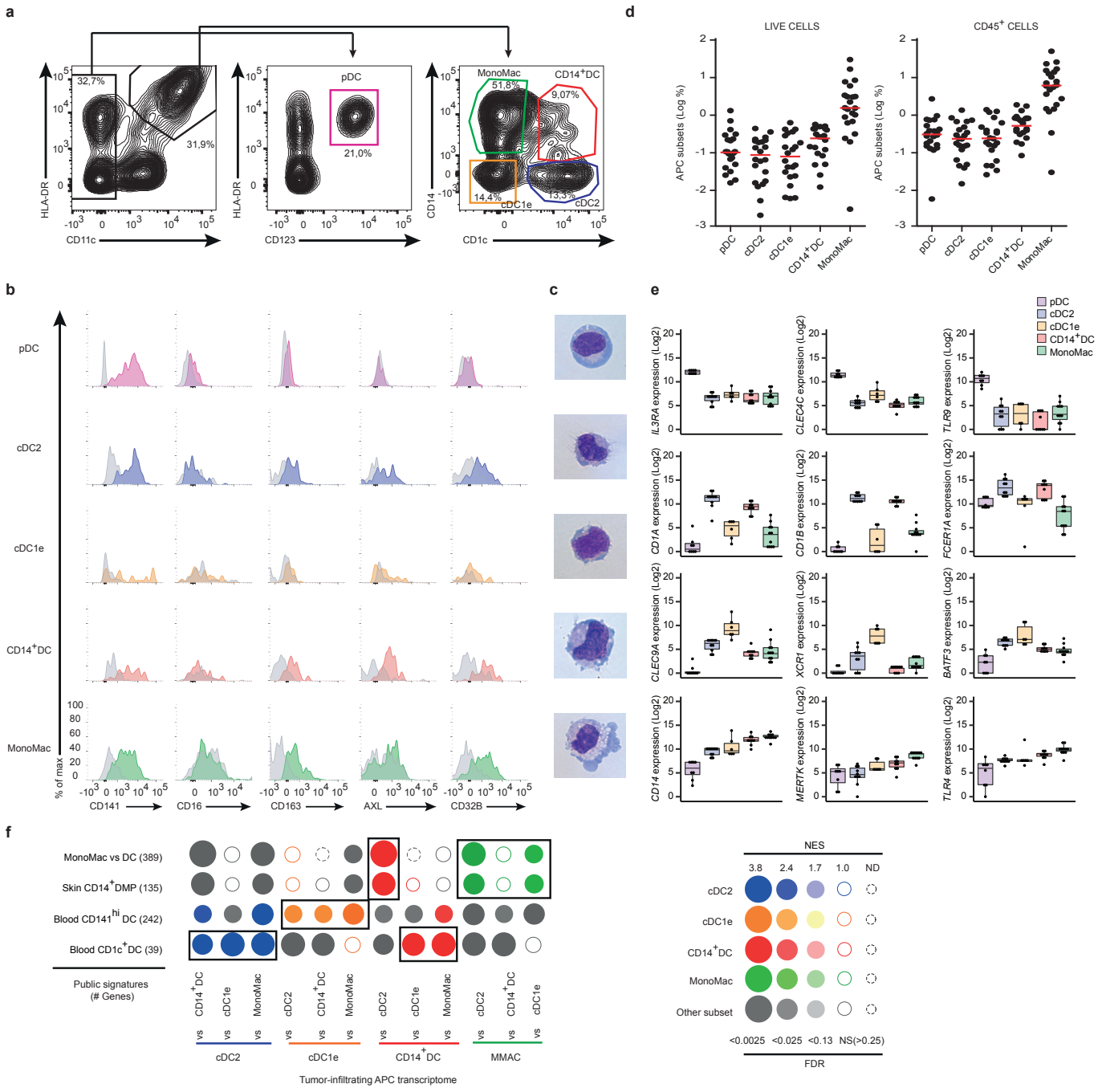
a
HLA-DR
CD11c
32,7%
31,9%
pDC
21,0%
CD123
CD14
CD1c
MonoMac
51,8%
CD14+DC
9,07%
14,4%
cDC1e
13,3%
cDC2
d
LIVE CELLS
CD45+ CELLS
APC subsets (Log %)
pDC
cDC2
cDC1e
CD14+DC
MonoMac
b
pDC
cDC2
cDC1e
CD14+DC
MonoMac
% of max
CD141
CD16
CD163
AXL
CD32B
c
e
pDC
cDC2
cDC1e
CD14+DC
MonoMac
IL3RA expression (Log2)
CLEC4C expression (Log2)
TLR9 expression (Log2)
CD1A expression (Log2)
CD1B expression (Log2)
FCER1A expression (Log2)
CLEC9A expression (Log2)
XCR1 expression (Log2)
BATF3 expression (Log2)
CD14 expression (Log2)
MERTK expression (Log2)
TLR4 expression (Log2)
f
MonoMac vs DC (389)
Skin CD14+DMP (135)
Blood CD141hi DC (242)
Blood CD1c+DC (39)
Public signatures
(# Genes)
CD14+DC
cDC1e
MonoMac
cDC2
vs
cDC2
cDC1e
CD14+DC
MMAC
Tumor-infiltrating APC transcriptome
NES
3.8
2.4
1.7
1.0
ND
cDC2
cDC1e
CD14+DC
MonoMac
Other subset
<0.0025
<0.025
<0.13
NS(>0.25)
FDR

Figure 2

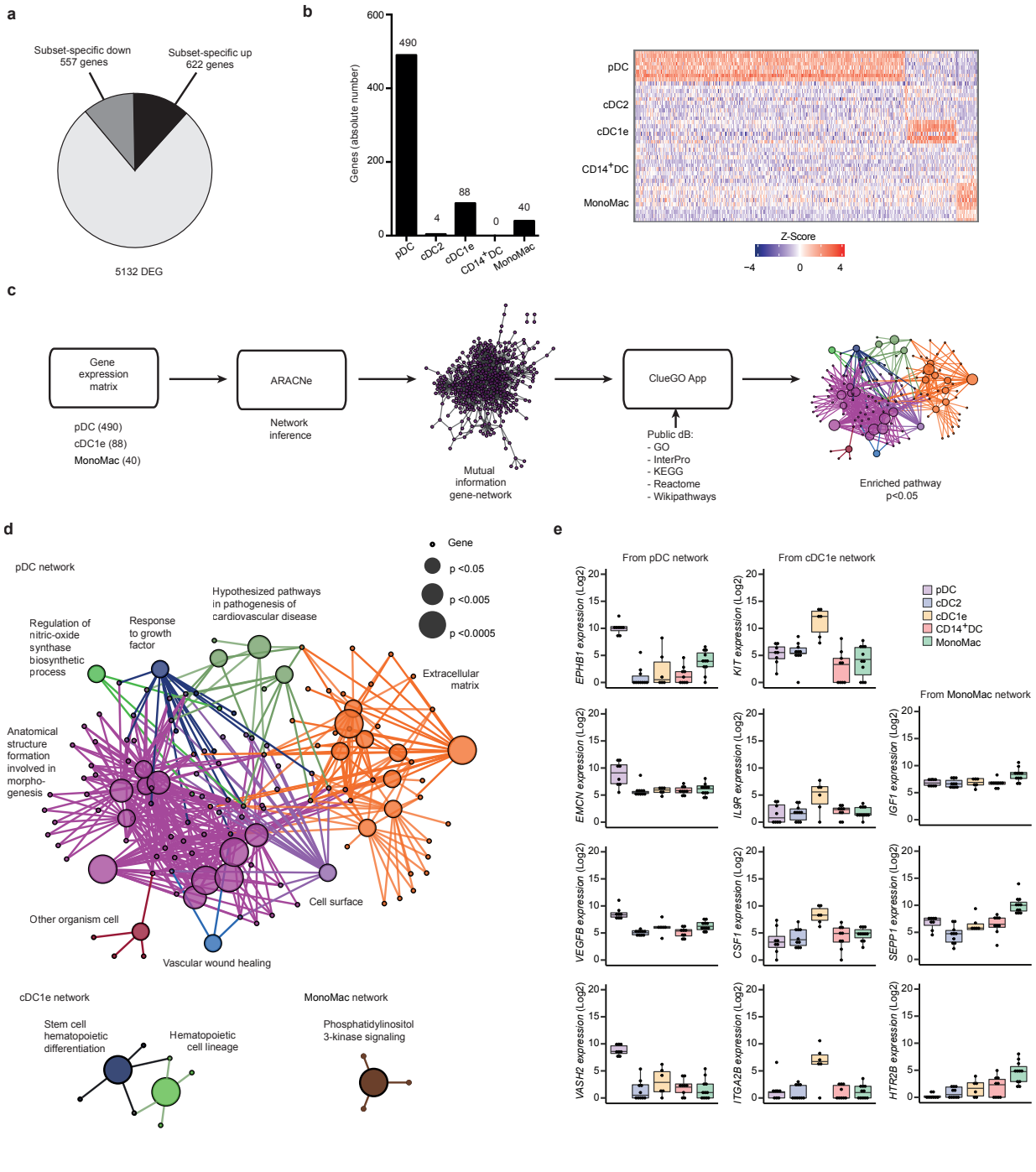
a
Subset-specific down
557 genes
Subset-specific up
622 genes
5132 DEG
b
Genes (absolute number)
600
400
200
0
490
4
88
0
40
pDC
cDC2
cDC1e
CD14+DC
MonoMac
pDC
cDC2
cDC1e
CD14+DC
MonoMac
Z-Score
−4
0
4
c
Gene expression matrix
pDC (490)
cDC1e (88)
MonoMac (40)
ARACNe
Network inference
Mutual information gene-network
ClueGO App
Public dB:
- GO
- InterPro
- KEGG
- Reactome
- Wikipathways
Enriched pathway
p<0.05
d
pDC network
Gene
p <0.05
p <0.005
p <0.0005
Hypothesized pathways in pathogenesis of cardiovascular disease
Regulation of nitric-oxide synthase biosynthetic process
Response to growth factor
Extracellular matrix
Anatomical structure formation involved in morpho-genesis
Cell surface
Other organism cell
Vascular wound healing
cDC1e network
Stem cell hematopoietic differentiation
Hematopoietic cell lineage
MonoMac network
Phosphatidylinositol 3-kinase signaling
e
From pDC network
From cDC1e network
From MonoMac network
pDC
cDC2
cDC1e
CD14+DC
MonoMac
EPHB1 expression (Log2)
KIT expression (Log2)
EMCN expression (Log2)
IL9R expression (Log2)
IGF1 expression (Log2)
VEGFB expression (Log2)
CSF1 expression (Log2)
SEPP1 expression (Log2)
VASH2 expression (Log2)
ITGA2B expression (Log2)
HTR2B expression (Log2)

Figure 3

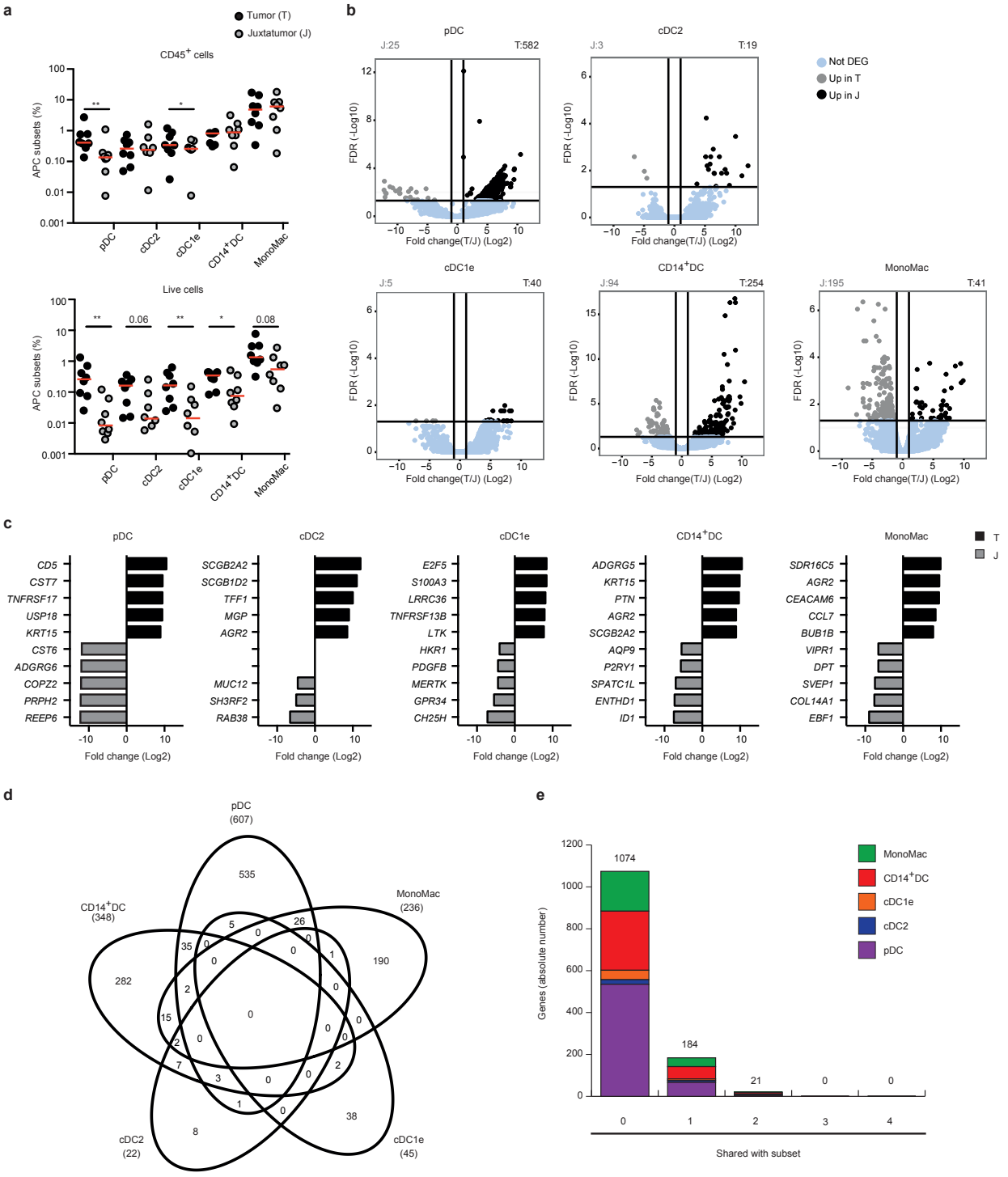
a
Tumor (T)
Juxtatumor (J)
CD45+ cells
APC subsets (%)
pDC
cDC2
cDC1e
CD14+DC
MonoMac
Live cells
b
pDC
cDC2
cDC1e
CD14+DC
MonoMac
Not DEG
Up in T
Up in J
FDR (-Log10)
Fold change(T/J) (Log2)
c
T
J
Fold change (Log2)
d
pDC (607)
CD14+DC (348)
MonoMac (236)
cDC2 (22)
cDC1e (45)
e
Genes (absolute number)
Shared with subset

Figure 4

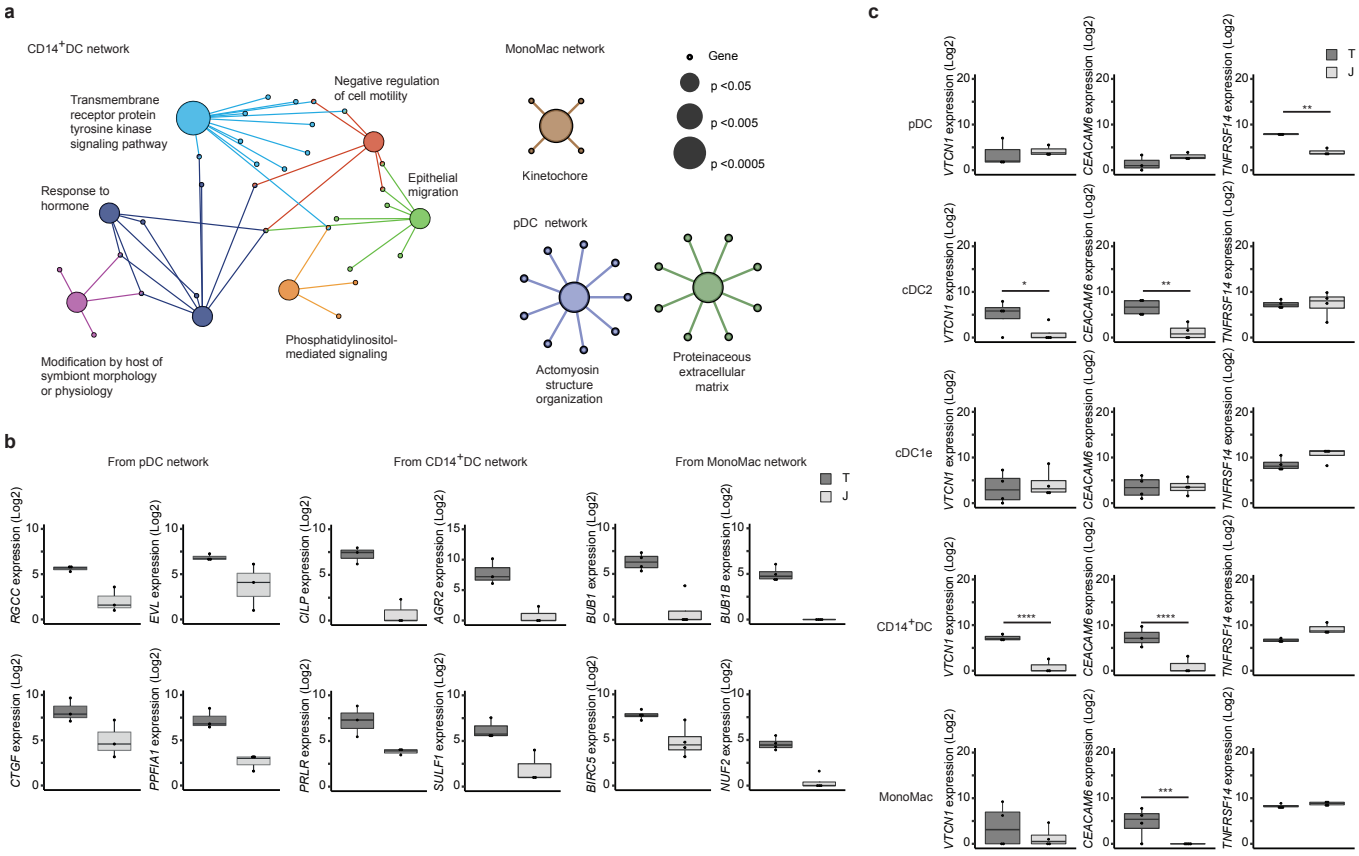
a
CD14+DC network
Transmembrane receptor protein tyrosine kinase signaling pathway
Negative regulation of cell motility
Epithelial migration
Response to hormone
Phosphatidylinositol-mediated signaling
Modification by host of symbiont morphology or physiology
MonoMac network
Kinetochore
pDC network
Actomyosin structure organization
Proteinaceous extracellular matrix
Gene
p <0.05
p <0.005
p <0.0005
b
From pDC network
From CD14+DC network
From MonoMac network
T
J
RGCC expression (Log2)
EVL expression (Log2)
CILP expression (Log2)
AGR2 expression (Log2)
BUB1 expression (Log2)
BUB1B expression (Log2)
CTGF expression (Log2)
PPFIA1 expression (Log2)
PRLR expression (Log2)
SULF1 expression (Log2)
BIRC5 expression (Log2)
NUF2 expression (Log2)
c
pDC
cDC2
cDC1e
CD14+DC
MonoMac
VTCN1 expression (Log2)
CEACAM6 expression (Log2)
TNFRSF14 expression (Log2)

Figure 5

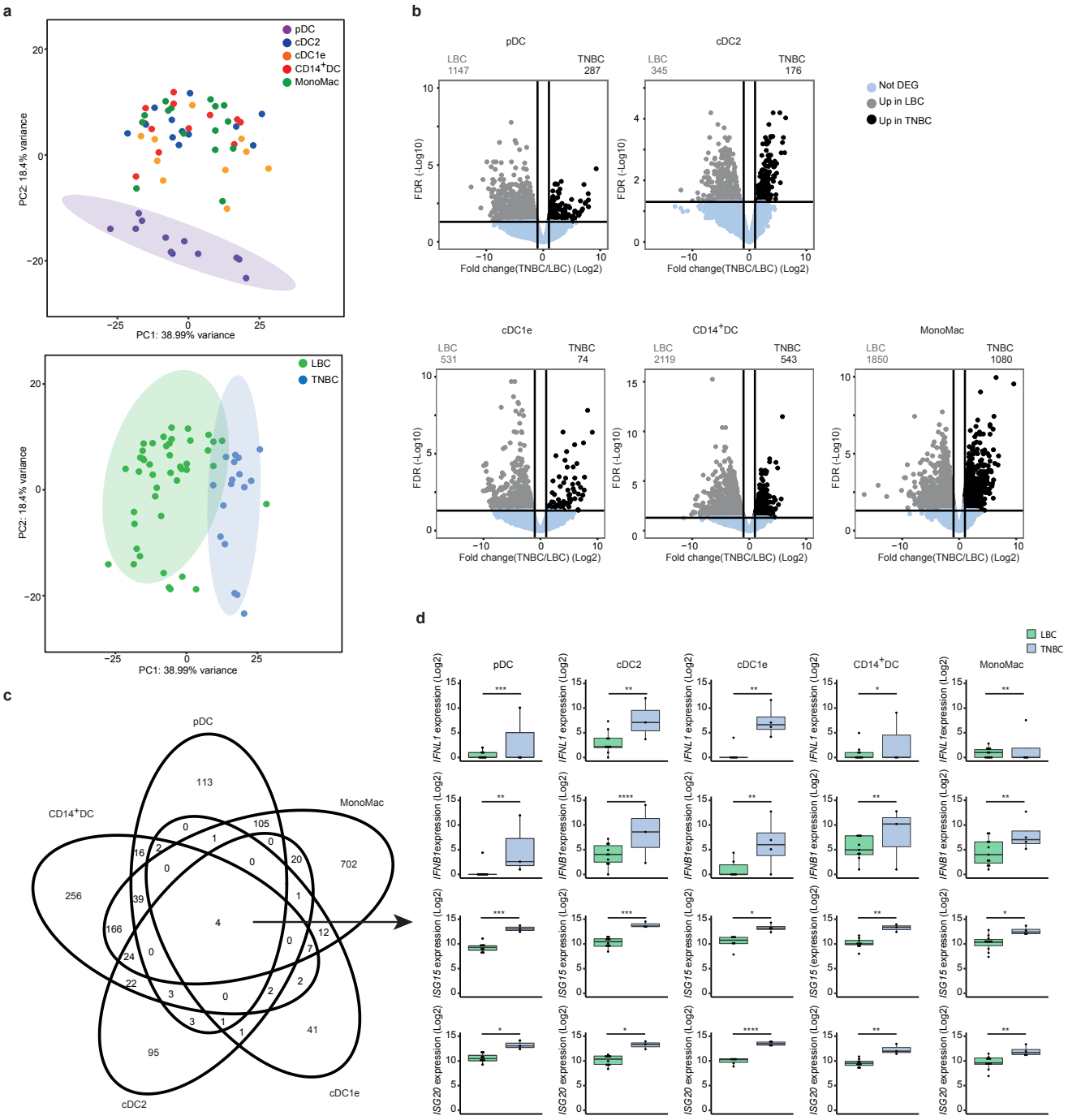
a
pDC
cDC2
cDC1e
CD14+DC
MonoMac
PC2: 18.4% variance
PC1: 38.99% variance
LBC
TNBC
b
pDC
cDC2
cDC1e
CD14+DC
MonoMac
Not DEG
Up in LBC
Up in TNBC
FDR (-Log10)
Fold change(TNBC/LBC) (Log2)
c
pDC
cDC2
cDC1e
CD14+DC
MonoMac
d
IFNL1 expression (Log2)
IFNB1 expression (Log2)
ISG15 expression (Log2)
ISG20 expression (Log2)

Figure 6

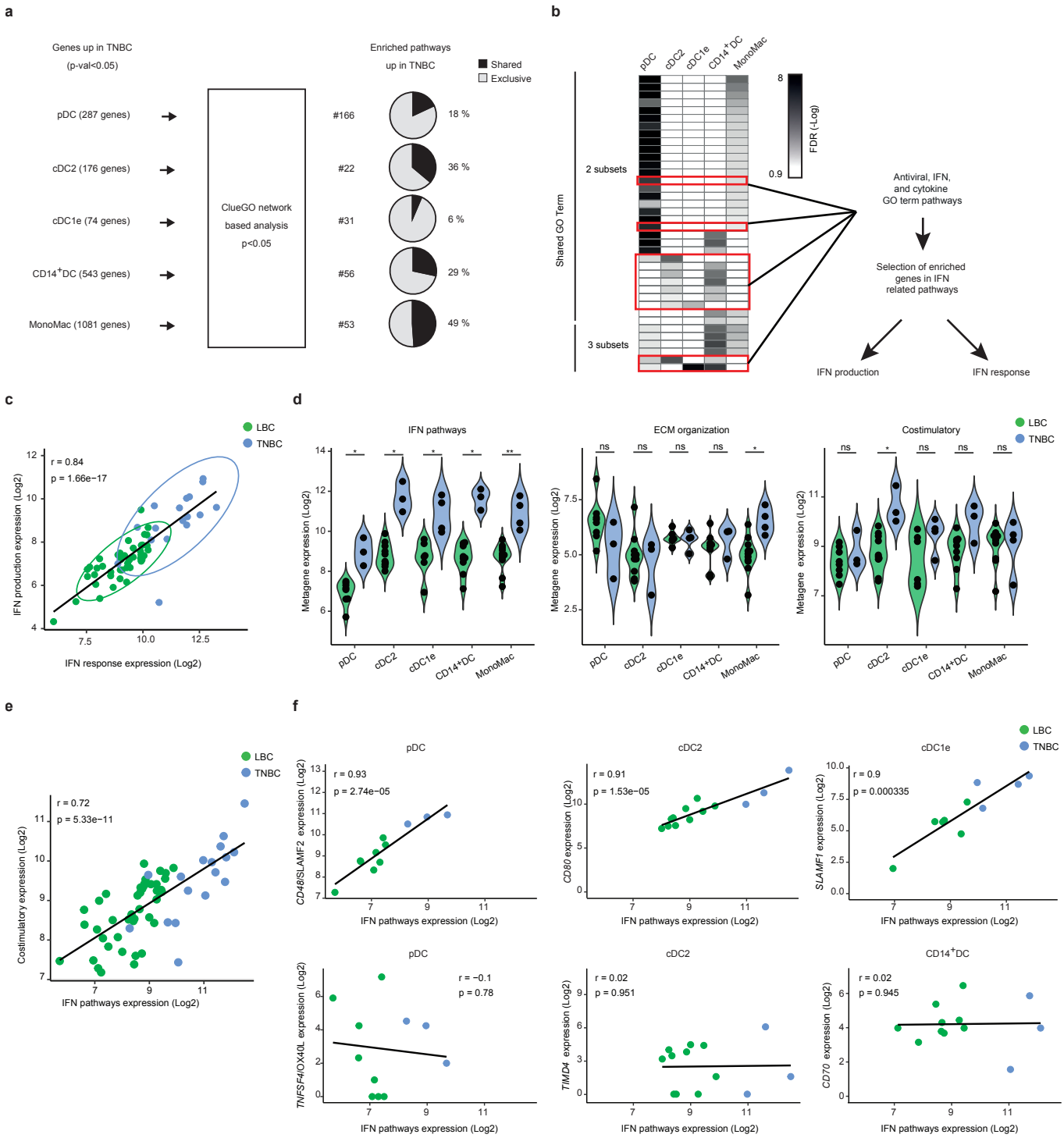
a
Genes up in TNBC
(p-val<0.05)
pDC (287 genes)
cDC2 (176 genes)
cDC1e (74 genes)
CD14+DC (543 genes)
MonoMac (1081 genes)
ClueGO network
based analysis
p<0.05
Enriched pathways
up in TNBC
Shared
Exclusive
#166
18 %
#22
36 %
#31
6 %
#56
29 %
#53
49 %
b
pDC
cDC2
cDC1e
CD14+DC
MonoMac
8
0.9
FDR (-Log)
2 subsets
3 subsets
Shared GO Term
Antiviral, IFN,
and cytokine
GO term pathways
Selection of enriched
genes in IFN
related pathways
IFN production
IFN response
c
LBC
TNBC
r = 0.84
p = 1.66e−17
IFN production expression (Log2)
IFN response expression (Log2)
d
IFN pathways
ECM organization
Costimulatory
Metagene expression (Log2)
ns
*
**
pDC
cDC2
cDC1e
CD14+DC
MonoMac
e
LBC
TNBC
r = 0.72
p = 5.33e−11
Costimulatory expression (Log2)
IFN pathways expression (Log2)
f
pDC
cDC2
cDC1e
CD14+DC
r = 0.93
p = 2.74e−05
r = 0.91
p = 1.53e−05
r = 0.9
p = 0.000335
r = −0.1
p = 0.78
r = 0.02
p = 0.951
r = 0.02
p = 0.945
CD48/SLAMF2 expression (Log2)
CD80 expression (Log2)
SLAMF1 expression (Log2)
TNFSF4/OX40L expression (Log2)
TIMD4 expression (Log2)
CD70 expression (Log2)
IFN pathways expression (Log2)

Figure 7

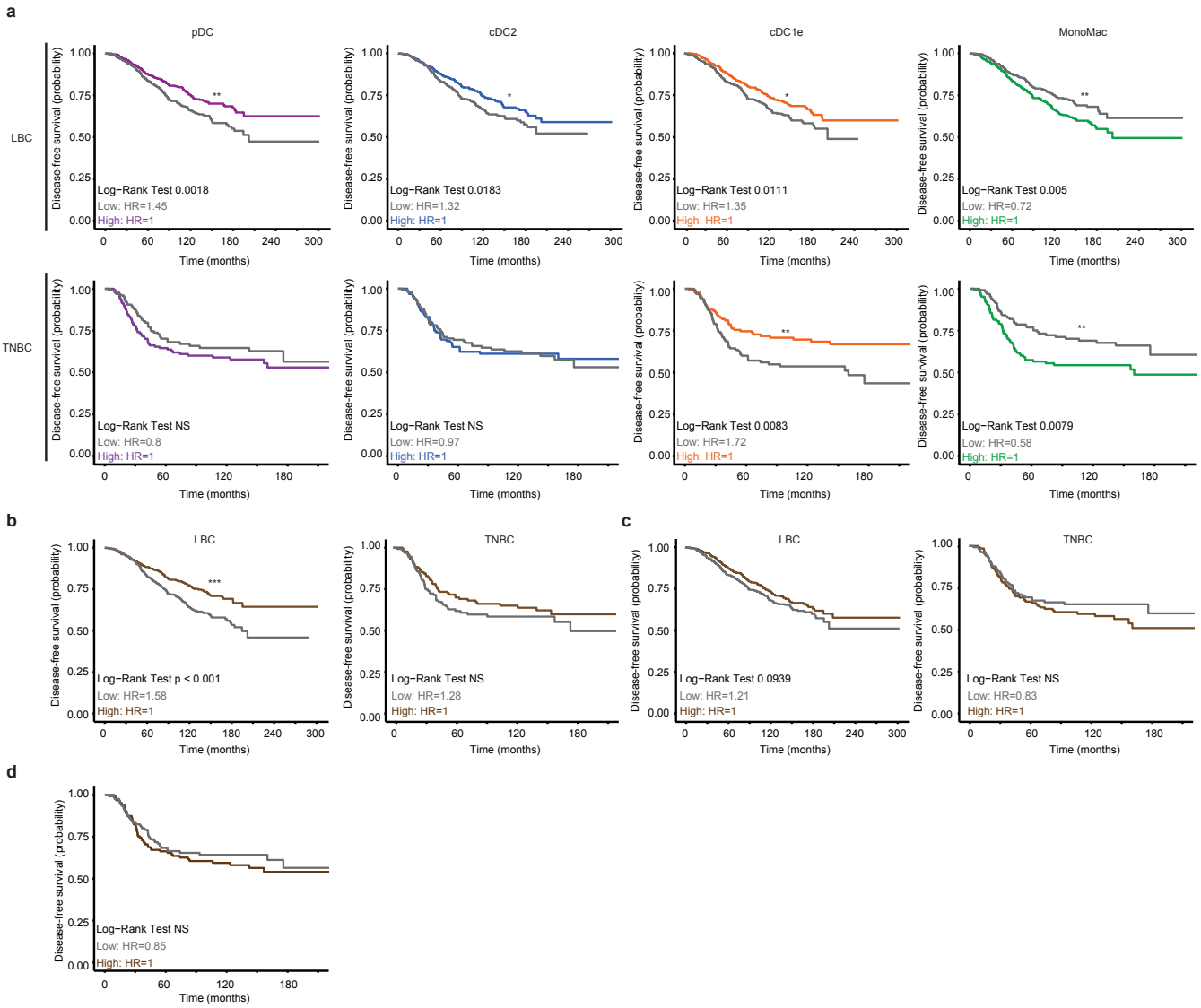
a
pDC
cDC2
cDC1e
MonoMac
LBC
TNBC
Disease-free survival (probability)
Time (months)
Log−Rank Test 0.0018
Low: HR=1.45
High: HR=1
Log−Rank Test 0.0183
Low: HR=1.32
High: HR=1
Log−Rank Test 0.0111
Low: HR=1.35
High: HR=1
Log−Rank Test 0.005
Low: HR=0.72
High: HR=1
Log−Rank Test NS
Low: HR=0.8
High: HR=1
Log−Rank Test NS
Low: HR=0.97
High: HR=1
Log−Rank Test 0.0083
Low: HR=1.72
High: HR=1
Log−Rank Test 0.0079
Low: HR=0.58
High: HR=1
b
LBC
TNBC
Log−Rank Test p < 0.001
Low: HR=1.58
High: HR=1
Log−Rank Test NS
Low: HR=1.28
High: HR=1
c
LBC
TNBC
Log−Rank Test 0.0939
Low: HR=1.21
High: HR=1
Log−Rank Test NS
Low: HR=0.83
High: HR=1
d
Log−Rank Test NS
Low: HR=0.85
High: HR=1

Supplementary Fig. 1

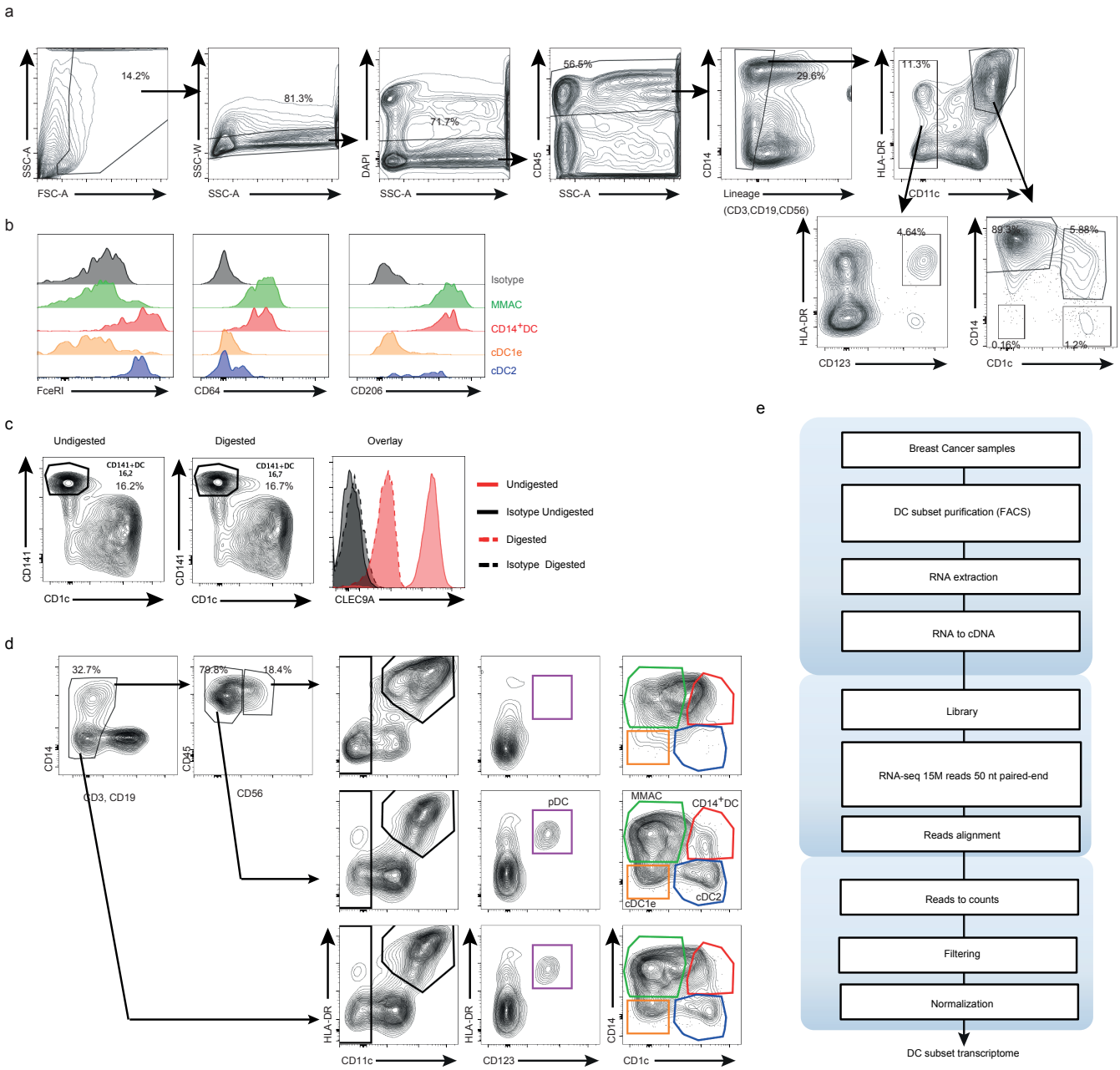

Supplementary Fig. 3

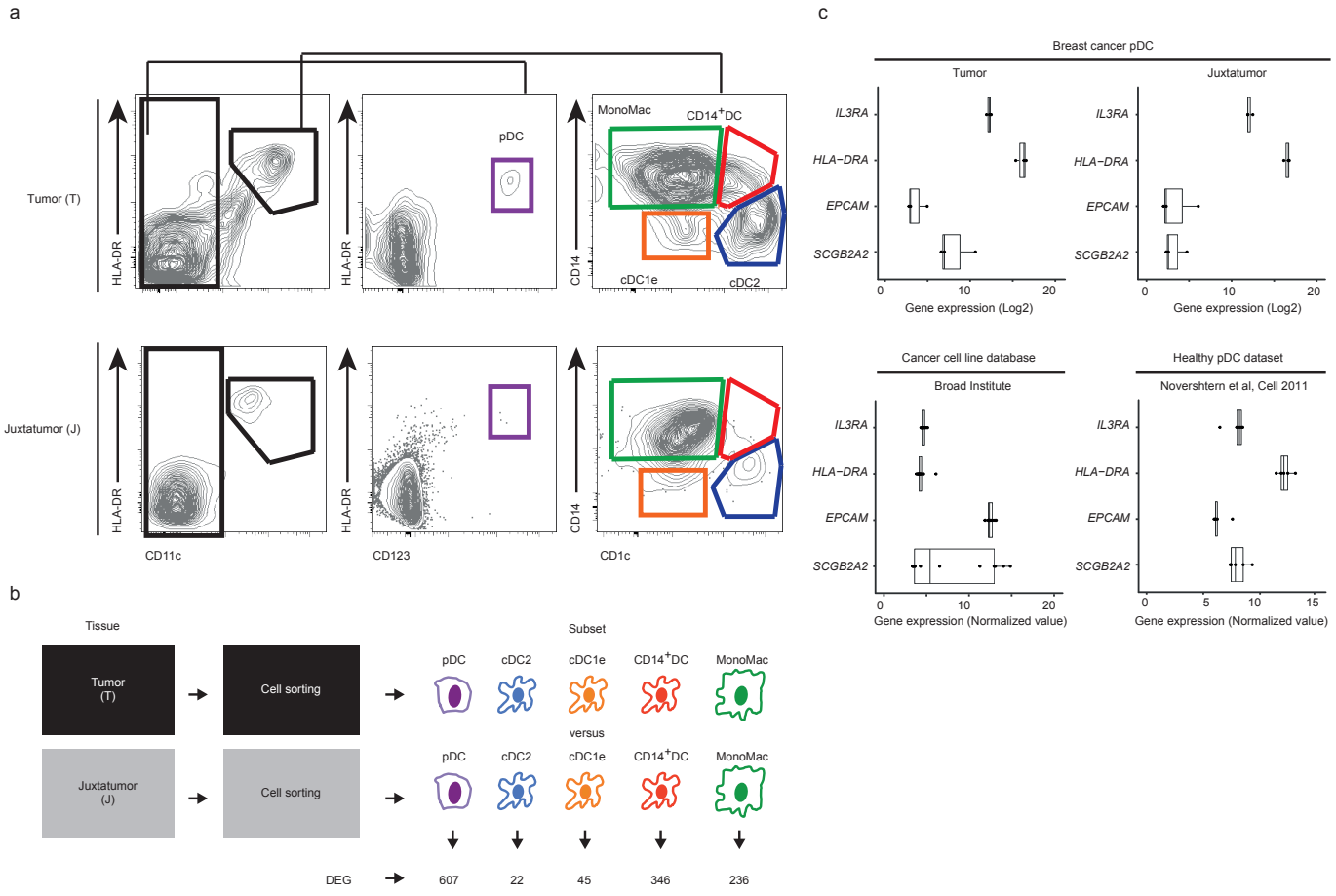

Supplementary Fig. 5

a

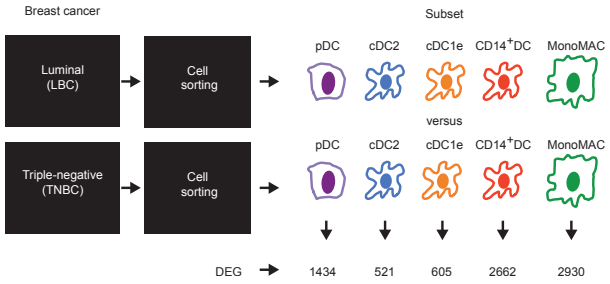

Supplementary Fig. 6

a

SHARED BIOLOGICAL PATHWAYS UP IN TNBC

	GO ID	GOTerm
2 subsets	GO:0044391	ribosomal subunit
	GO:0003010	Ribosome
	GO:0030529	intracellular ribonucleoprotein complex
	GO:0071291	Metabolism of amino acids and derivatives
	GO:0975956	Nonsense Mediated Decay (NMD) independent of the Exon Junction Complex (EJC)
	GO:0072312	rRNA processing
	GO:0168273	Influenza Viral RNA Transcription and Replication
	GO:0156902	Peptide chain elongation
	GO:2408557	Selenocysteine synthesis
	GO:0156842	Eukaryotic Translation Elongation
	GO:0072764	Eukaryotic Translation Termination
	GO:0975957	Nonsense Mediated Decay (NMD) enhanced by the Exon Junction Complex (EJC)
	GO:0927802	Nonsense-Mediated Decay (NMD)
	GO:0168255	Influenza Life Cycle
	GO:0015934	large ribosomal subunit
	GO:2408522	Selenoamino acid metabolism
	GO:0015935	small ribosomal subunit
	GO:6791226	Major pathway of rRNA processing in the nucleolus and cytosol
	GO:0072689	Formation of a pool of free 40S subunits
	GO:0168254	Influenza Infection
	GO:0005739	mitochondrion
	GO:0044429	mitochondrial part
	GO:0031967	organelle envelope
	GO:1903901	negative regulation of viral life cycle
	GO:0008009	chemokine activity
	GO:0005125	cytokine activity
	GO:0005126	cytokine receptor binding
	GO:6783783	Interleukin-10 signaling
	GO:0051924	regulation of calcium ion transport
	GO:0046425	regulation of JAK-STAT cascade
	GO:0005761	mitochondrial ribosome
	GO:0005759	mitochondrial matrix
3 subsets	GO:5389840	Mitochondrial translation elongation
	GO:5368287	Mitochondrial translation
	GO:5368286	Mitochondrial translation initiation
	GO:5419276	Mitochondrial translation termination
	GO:0909733	Interferon alpha/beta signaling
	GO:0045071	negative regulation of viral genome replication

Shared GO Term

b

«IFN PATHWAYS» GENELIST

IFN production	IFN response
IFNB1	ISG15
IFNI1	ISG20
OASL	IFIT1
TRIM21	IFIT2
USP18	IFIT3
KLF4	IFI35
MT2A	IFITM1
PDE2A	IFITM2
CDK1	IFITM3
CHMP4B	CCL2
S100A8	CCL3
S100A9	CCL4
CREB3	CCL5
CRYAB	CCL19
CSNK2A2	CXCL10
EGR3	CXCL11
	CCL20
	CXCL9
	OAS1
	APOBEC3A
	APOBEC3C
	APOBEC3G
	ENC1
	VEGFA
	SRI
	CD80
	FPR1
	SLPI
	AIF1
	BCL2
	KLF4
	TAF9
	TREM2
	UBD
	AURKB
	BNIP3L
	CD38
	GCLC
	LGALS3
	MAD2L1
	PPIF
	TIMP1
	CKLF

c

«COSTIMULATORY» GENELIST

CD40
CD70
CD80
CD83
CD86
CD209/DC-SIGN
TNFSF9/4-1BBL
ICOSLG
SEMA4A
TIMD4
C10orf54/VISTA
TNFRSF13C/BAFFR
TNFSF13/APRIL
TNFSF14/HVEML
SLAMF1
CD84/SLAMF5
CD48/SLAMF2
TNFSF4/OX40L
HLA-DRA
HLA-DRB1
HLA-DRB3
HLA-DRB4
HLA-DRB5
HLA-DRB7
PVR

e

«ECM ORGANIZATION» GOTERM USED TO BUILT METAGENE

GO ID	GOTerm
GO:0030198	Extracellular matrix organization

d

HEATMAP OF CORRELATIONS BETWEEN «IFN PATHWAYS» METAGENE AND COSTIMULATORY CHECKPOINTS IN EACH SUBSET

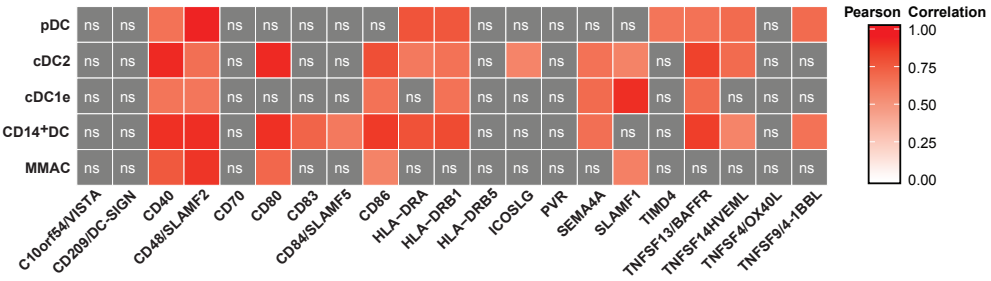

Supplementary Fig. 7

a

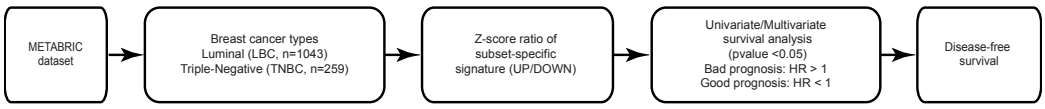

Supplementary Figure 1

Phenotypic characterization of innate APC infiltrating breast cancer tissue

a, Flow cytometry contour plots showing the entire gate strategy utilized to distinguish tumor-infiltrating APC in LBC. **b**, Histograms of mean fluorescent intensity of FcεR1, CD64 and CD206 expression by the indicated APC subsets in LBC samples. Isotype control is shown in grey. **c**, Representative flow cytometry contour plots from DAPI-CD45+cells comparing APC subset gates from CD3-, CD19-, CD56+ (upper row), CD3-, CD19-, CD56- (middle row), and directly from CD3-, CD19- (lower row) in LBC samples. Middle row corresponds to the strategy use in this study. **d**, Representative flow cytometry contour plots showing the frequency of cDC1 expressing CD141 markers in digested or undigested PBMC from healthy donors. Histograms shows the mean fluorescent intensity of CLEC9A expression at the surface of undigested (solid line) or digested (dashed line) blood cDC1. Specific staining is in red and the isotype control in black. **e**, Scheme showing the pipeline used to generate tumor-infiltrating APC transcriptome from breast cancer samples. **a** one representative donor out of 22 with similar results, **b** one representative donor out of 15 with similar results, **c, d** one representative donor out of 3 with similar results.

Supplementary Figure 3

Comparison of tumor versus juxta-tumor APC infiltrating LBC

a, Representative flow cytometry contour plots from DAPI-CD45+Lin- cells showing the indicated APC subsets in tumor (upper panel), and juxta-tumor (lower panel) samples from LBC patients. **b**, Schema showing the pipeline and number of DEG obtained from each indicated APC tumor versus juxta-tumor LBC. **c**, Box plots showing the RNA expression of IL3RA, HLA-DRA, EPCAM, and SCGB2A2 by tumor and juxta-tumor pDC transcriptome from this study (upper panels), breast cancer cell line database from Broad Institute (lower left), and pDC dataset from healthy donor blood (*Novershtern, et al 2011*).

Supplementary Figure 5

Comparison of tumor-infiltrating APC from TNBC versus LBC

a, Schema showing the pipeline and number of DEG obtained from each indicated APC from tumor TNBC versus tumor LBC.

Supplementary Figure 6

a, Extended list of enriched pathways and corresponding GO term from genes upregulated in TNBC versus LBC that were shared with 2 or 3 subsets, as indicated. **b**, Genes included in the IFN pathway metagene separated in IFN production and IFN response that were used for the analyses in Fig. 6 c-f. **c**, Genes included in the costimulatory metagene used for the analysis in Fig. 6 d,e. **d**, Heat map indicating the correlation coefficient between the indicated costimulatory gene, and the IFN pathway metagene for each APC subset from LBC and TNBC, as indicated. **e**, GO term associated to the ECM organization metagene used for the analyses in Fig. 6 f.

Supplementary Figure 7

a, Schema showing the pipeline used to analyze disease-free survival of the indicated subset-specific signature in the METABRIC public dataset.

Supplementary Table S1: Clinical information of the patients included in RNA-seq analysis

DEMOGRAPHY	Groups	N	%
Female		17	100
Age	< 60	4	23.5
	61-70	5	29.4
	> 71	8	47.1
EXTENSION			
Size (mm)	< 20	5	29.4
	21-40	7	41.2
	> 41	5	29.4
Lymph Nodes (LN) involvement	LN+	11	64.7
	LN-	6	35.3
HISTOLOGICAL SUBTYPE			
Invasive Ductal		9	53
Invasive Lobular		4	23.5
Mixed ductal/lobular		3	17.6
Papillary		1	5.9
Elston Ellis (EE) GRADE			
I		0	0
II		6	35.3
III		11	64.7
MOLECULAR SUBGROUP			
Triple negative, TN (hormone receptor and HER2 negative)		4	23.5
Luminal B, LB (hormone receptor and HER2 positive or negative)		13	76.5

Supplementary table S2: Sample description for RNA-seq analysis

Cancer type	Tissue type	Subset	Donor (absolute number)	Donor ID
LBC	T	pDC	8	D1, D2, D3, D6, D7, D11, D13, D15
		cDC2	10	D1, D2, D3, D6, D7, D8, D9, D11, D13, D15
		cDC1e	6	D6, D7, D8, D11, D13, D15
		CD14posDC	9	D1, D2, D3, D6, D7, D9, D11, D13, D15
		MMAC	11	D1, D2, D3, D5, D6, D7, D8, D9, D10, D13, D17
	J	pDC	3	D1, D2, D15
		cDC2	4	D6, D8, D9, D15
		cDC1e	4	D6, D8, D13, D15
		CD14posDC	3	D6, D9, D15
		MMAC	5	D5, D6, D7, D8, D10
TNBC	T	pDC	3	D4, D14, D16
		cDC2	3	D4, D14, D16
		cDC1e	4	D4, D12, D14, D16
		CD14posDC	3	D4, D14, D16
		MMAC	4	D4, D12, D14, D16

Supplementary Table 3: Top 10 subset-specific DEG from LBC samples

pDC	cDC2	cDC1e	MonoMac
TCL1A	*CCL22*	*SIGLEC17P*	*ADAP2*
NLRP7	*CLEC17A*	*CLNK*	*MS4A7*
ZFAT	*GRIP1*	*MS4A2*	*NXF3*
FAM129C	*IFNL1*	*CLEC9A*	*LINC01094*
CUX2		*CATSPER1*	*ASAH1*
GZMB		*SLC45A3*	*DAB2*
SMIM6		*XCR1*	*IGSF21*
ZDHHC17		*LAX1*	*ME1*
CLEC4C		*SH3RF2*	*PLA2G15*
CRYM		*IL1RL1*	*DLEU7*

3.2 ICELLNET: Reconstruction of intercellular communication networks using transcriptomic profiles

The second results will be presented as a manuscript that will be soon finalized for submission. It is entitled "ICELLNET: Reconstruction of intercellular communication networks using transcriptomic profiles". For this collaborative work, I was involved in the development of a systematic transcriptomic-based approach for cell communication network reconstruction. Indeed, cell-to-cell communication is essential to transfer information between cells with different functions and sensing capabilities. Intercellular communication coordinates the activities of diverse cell types required for complex processes such as embryogenesis, tissue remodelling during inflammation and wound healing, and immune responses. Currently, there is no systematic method to reconstruct cell-to-cell communication in a qualitative and quantitative manner.

In this study, we developed ICELLNET, a tool integrating prior information on ligand/receptor interactions, and cell-specific gene expression data and representing quantitative and qualitative aspects of cell-to-cell communication as connectivity maps. ICELLNET can be automatically applied to any cell population level transcriptomic profile in order to estimate and quantify its communication with over 12 other cell types. We applied this method to tumor cells, innate and adaptive immune cells (*e.g.* DCs, T cells, B cells, NK), epithelial, and stromal cells. By analyzing an original de novo generated dataset of human dendritic cells, we identified and experimentally validated IL-10 as a major regulator of the systems-level DC intercellular connectivity.

Our approach to assess cell connectivity may provide a valuable tool to evaluate the impact of a specific context on cell-to-cell communication, especially in inflammatory microenvironment such as cancer. In future perspectives, ICELLNET applications could lead to important biological insight and helping to direct pharmacological manipulation.

Title: ICELLNET: reconstruction of intercellular communication networks using transcriptomic profiles

Short title: DC connectivity

Author names: Irit Carmi-Levy[1,2,*], Antonio Cappuccio[1,2*], Maximilien Grandclaudon[1,2*], Floriane Noël[1,2], Coline Trichot[1,2], Fanny Coffin[1,3,4], Philippe Hupé[1,3,4,5] and Vassili Soumelis[1,2,†].

Affiliations:

1. Institut Curie, 26 rue d'Ulm, 75005 Paris, France; 2. Inserm U932, Department of Immunology, Paris, France; 3. Inserm U900, Paris, France; 4. Mines ParisTech, Fontainebleau, France; 5. CNRS, UMR144, Paris, France

*These authors contributed equally to this work

†Lead Contact: correspondence and requests for materials should be addressed to VS (vassili.soumelis@curie.fr)

Abstract word count: 135

Introduction: 310

Results: 2221

Discussion: 1043

Methods: 1821

Figures: 4

Supplementary Figures: 6

Tables: 1

Supplementary Table files: 3

References: 42

Scientific category: Immuno-biology, system's biology

Key points

- Systems level approach predicted that endogenous DC-derived IL-10 but not TNF controls DC communication with multiple target cells
- We experimentally validated that IL-10 significantly affects DC communication outcome with keratinocytes, neutrophils, and pDC

Abstract

Intro

Cell-to-cell communication is at the basis of the higher-order organisation observed in tissues, organs, and organisms. It is critical to coordinate the function of diverse cell types involved in complex biological processes, such as embryogenesis, tissue formation and renewal, and efficient immune responses. In the literature, there is no method developed to reconstruct intercellular communication networks in a quantitative and qualitative manner.

Here, we developed ICELLNET, a transcriptomic-based tool to reconstruct intercellular communication networks. This original quantitative method integrating ligand-receptor interactions, and cell-type specific gene expression, can be automatically applied to any cell population level transcriptomic profile. In this study, it predicted that IL-10 controls up to 12 communication channels connecting DCs to immune, epithelial, and stromal cells, four of which were experimentally validated.

Our results reveal that a single factor can shape systems level cellular connectivity, which has important implications in the physiopathology and pharmacological manipulation of multicellular processes.

Introduction

Cell-to-cell communication is essential to transfer information between cells with different functions and sensing capabilities. Intercellular communication is critical to coordinate the function of diverse cell types involved in complex biological processes, such as embryogenesis, tissue regeneration, and immune responses. For example, this allows innate immune cells, such as dendritic cells (DCs), to alert neighbouring cells after having sensed a threat through specialized innate receptors (1, 2). Numerous studies have established important cross-talks between distinct types of immune cells. However, inflammatory networks involve numerous cell-cell communications, which collectively determine the nature and outcome of the response (3, 4). Few attempts were made to reconstruct systems level immune inter-cellular networks, using literature-based approaches to enumerate possible connections between different cell types (5, 6). In such networks, nodes are cell-types, and edges correspond to ligand/receptor interactions forming a communication channel between two cell-types. This structure introduces three fundamental quantitative dimensions, which collectively shape the global functional output of a given cell network: 1) the number of different connections one cell type can form concurrently with other cell types, 2) the intensity of the communication between two cell types, 3) the efficiency of the communication reflected by information-induced modifications in the state or function of a target cell.

Currently, there is no systematic method to reconstruct cell-to-cell communication in a qualitative and quantitative manner. Given the multiplicity of possible communications between a given cell type and other cells, we reckoned that large-scale datasets could provide a valuable source of information in order to estimate cell communication.

In this study, we developed ICELLNET, a systematic transcriptomic-based approach for cell communication network reconstruction. This method can be automatically applied to any cell population level transcriptomic profile in order to estimate and quantify its communication with over 15 other cell types. We applied this method to tumor cells and various types of immune cells. By analyzing an original de novo generated dataset of human dendritic cells, we identified and experimentally validated IL-10 as a major regulator of the systems level DC intercellular connectivity.

Results

Development of ICELLNET, a transcriptomic-based communication score

We developed a quantitative and qualitative bioinformatics approach by integrating prior information on ligand/receptor interactions, and cell-specific expression data (**Figure 1A**). We developed an automatized tool in R script, ICELLNET, to perform the score computation and network reconstruction that we can apply to any cell type transcriptomic profiles. In a first step, we manually curated a database of ligand-receptor interactions containing 244 entries (**Supplementary Table S2B**). The quantification of intercellular communication consisted of scoring the intensity of each ligand/receptor interaction between two cell types with known expression profiles. Whenever needed, we took into account the requirements for multiple ligand units, or receptor chains, using logical rules. The score of an individual ligand/receptor interaction was computed as the product of their expression levels respectively by the source and by the target cell. These individual scores were then combined into a global metric assessing the overall exchange of information between the cell types of interest (**Figure 1A**). As putative cellular targets, we selected 12 cell types known to be present in an inflamed tissue microenvironment (**Figure 1B**). Cell-specific gene expression data was obtained using a database from human primary cells (12, 13). As cells of interest, we selected from literature a dataset of SUM149 human inflammatory breast cancer cell line transfected with siRNA targeting tazarotene-induced gene 1 (TIG1), a potential tumorigenic gene identified in inflammatory breast cancer (Wang et al. Cancer Res 2013). By taking into account all the individual ligand/receptor interactions, we developed a visualization tool by reconstructing the intercellular communication networks. In these directed graphs, nodes represent cell types, the width of the edges connecting two cell types is proportional to a global measure of the intensity of the communication between them and the arrows indicate the direction of communication from ligand to receptor (**Figure 1A and see methods**). Such connectivity maps enable to visualize the communication between cell types in a quantitative and qualitative manner. Generated for the two conditions (siTIG1 versus control), they demonstrated that SUM149 cells have a higher communication score with neutrophils, macrophages and monocytes. On the contrary, the lowest communication score is toward B cells. We can also observe an increase of communication score towards B cells in the siTIG1 condition compared to control (**Figure 1B**).

115 ***IL-10 controls an intercellular communication module in LPS-activated dendritic cells***

116 After using a tumor cell model to test the connectivity map reconstruction, we wanted to
117 assess if ICELLNET tool would allow us to characterize cellular communication using the
118 immune system as a model. Particularly, we were interested in studying communication of
119 resting and perturbed immune cells. To explore the role of autocrine loops, we cultured LPS-
120 activated human monocyte-derived DCs in the presence or absence of blocking antibodies
121 (Abs) to the TNF and IL-10 receptors (αTNFR and αIL10R). No effect on cell viability was
122 observed (**Figure S1**). The most prominent effect of LPS on DC hallmark maturation markers
123 was observed at the mRNA level in the time frame of 4 to 8 hours following activation (11).
124 We performed large-scale microarray analysis after 4 and 8 hours of culture of DC with LPS,
125 with and without blocking Abs to TNF and IL-10 receptors (**Figure 2A**). To identify
126 expression patterns determined specifically by each loop, we scored every differentially
127 expressed gene according to its ability to separate the experimental condition LPS+αTNFR or
128 LPS+αIL10R, respectively, from all of the other conditions considered as a single statistical
129 group. At 4 hours, we could detect relatively small numbers of genes with expression patterns
130 specific for the condition LPS+αTNFR or LPS+αIL10R (**Figure 2B**). At 8 hours, while only
131 77 genes exhibited significant separability when the TNF loop was blocked, blocking the IL-
132 10 loop led to a transcriptional signature comprising 1432 genes (**Figure 2B and C**). These
133 quantitative differences led us to focus on the IL-10 loop signature at 8 hours. Some of the
134 genes in this signature (ARHGAP22, CSF2, CD163L1 and MLXIP for example) showed a
135 remarkably large separability score (**Figure 2B and C**). By using various pathway analysis
136 resources, we found that the TNF loop signature is enriched in functions involving the
137 activation of different receptors (GPCR, rhodopsin-like and P2Y) (**Figure 3**). Applying the
138 same methods to the IL-10 loop signature, a highly significant enrichment was found in
139 annotation terms related to cytokine-cytokine receptor interactions, and positive regulation of
140 cell communication (**Figure 2D and E**). These results were robust to changes in the empirical
141 threshold used to define the IL10 loop signature, consistent with a robust biological signal
142 (**supplementary table 1E-H**).

143 We then screened the IL-10 and TNF loop signatures to systematically identify extracellular
144 molecules mediating cell communication through ligand/receptor interactions. We were able
145 to extract 47 ligands and 23 receptors from the IL-10 loop signature, while only 3 ligands and
146 5 receptors from the TNF loop signature (**Figure 2F**).

Despite extensive studies of both TNF and IL-10 in the context of innate immunity, their different contribution to DC intercellular communication could not be predicted a priori at this systems level. It was particularly striking that communication was controlled specifically by IL-10, although TNF has strong pro-inflammatory actions (7) which could have suggested a decreased cell communication in the absence of this cytokine.

The IL-10 loop signature comprised a variety of cytokines, chemokines, growth factors, and membrane ligands (**table 1**). Although some of the communication molecules in the loop signature were known to depend on IL-10 (for example CD80, GM-CSF and GCSF), many of them had weak or no prior association to IL-10 function (e.g. CLCF1 and TNFSF15), and would not have been captured by a strategy exclusively based on prior knowledge. We selected four important immunoregulatory molecules from the IL-6- and IL-12-families, and further validated expression at the protein level in 24h culture DC supernatants using cytometric bead array (CBA) and ELISA (**Figure 2G**). Interestingly, exogenous IL-10 downregulated several targets that were instead up-regulated by blocking the IL-10 loop (**Figure S3**).

Systems level reconstruction of dendritic cell intercellular communication networks

After establishing the possibility of increased DC communication in the absence of the IL-10 loop, we set out to identify the putative cellular partners in the local inflammatory microenvironment. We applied ICELLNET to reconstruct the intercellular networks between DCs and the putative target cells (**Figure 3A and Figure S4**). Focusing on individual ligand/receptor interactions connecting DCs with the putative target cells, we observed that certain ligands, such as TNF, could potentially act on many cellular partners (**Figure 3B**), consistent with a pleiotropic effect (14). However, other interactions pointed to crosstalk between DCs and specific targets, for example IL19 and IL36G with keratinocytes; TNFSF18 with NK cells; CD70 with T and B cells (**Figure 3B**). The connectivity maps, generated for every DC experimental condition, demonstrated an increase of the global communication score in all 12 channels, when comparing LPS-activated DC to resting (medium) DC (**Figure 3C and Figure S4B**). Importantly, these maps revealed that blocking the IL-10 loop determined the largest amplification of DC communication with all 12 cellular targets, while the blocking of TNF loop in LPS-activated DC had a minor effect on the global communication score (**Figure 3C and figure S4B**). **Supplementary table 3A-L** details the

top contributing communication molecules in each DC-target cell channel. Quantification of in-flow communication, as obtained by reversing the directionality of cell-to-cell interactions, showed that communication towards LPS-activated DC was also increased with respect to resting (Med) cells (**Figure S4C and D**). However, we observed a trend of decreased in-flow communication for LPS+αIL-10R-DC, relative to LPS-DC or LPS+αTNFR-DC (**Figure S4C and D**), indicating that IL-10 specifically controls out-flow communication of DCs.

Experimental validation of multiple IL-10-dependent communication channels

To assess communication efficiency, i.e how increased connectivity translates into functional changes in target cells, we turned to experimental validation of predicted communication channels using immunological assays adapted to output response of each cell type. Due to its physiopathological relevance, we first investigated the DC-T cell axis through co-culture experiments of T cells with DCs treated by LPS with or without TNFR and IL10R blocking antibodies (Figure 3- figure supplement 1). We found that naive CD4 T cells, when co-cultured with LPS-DC in the absence of the IL-10 loop, globally increased and shifted their pattern of cytokine secretion, as compared to LPS-DC, while blocking the TNF loop had almost no effect (**Figure 4A**). Similar results were obtained with memory T cells (**Figure 4B**).

Since the IL10/IL10R pathway could have a direct effect on T helper cells during the differentiation process, we verified that the observed T helper polarization was indeed due to the IL-10 loop blockade in the DCs, and not to a direct effect on T cells (**Figure S5B**). Indeed, remaining IL10R blocking antibodies after the DCs washes could have act directly on T cells during DC-T co-culture. By adding IL10R antibodies during DC-T co-culture (not only to during DC activation) we could show that IL10R antibodies in our setting would not have any direct effect on T cell polarization.

Among the factors best explaining the secretion profile of T cells determined by LPS+αIL10R-DCs, we observed a remarkable emergence of Th17 cytokines (**Figure 4C**), in line with recent murine studies (15-17). Strikingly, IL-9 was also increased (**Figure 4C**), and produced by a T cell population distinct from Th17 cells producing IL-17A alone or co-expressed with IL-9 and IFN-g (**Figure 4D**). This provides the first demonstration that LPS-

activated DCs, in the absence of an IL-10 loop, determine a Th17 and Th9 polarization in human, both of which participate in host defense and autoimmunity (18, 19).

Through a paired DC/T dataset, we detected correlations between specific DC outputs from the IL-10 loop signature and specific T helper cytokines (**Figure 4E and Figure S6**). IL-9 secretion from T cells strongly correlated with pro-inflammatory cytokines produced by DCs such as IL-12p70, again illustrating the link between communication molecules made by DC, and modifications in T cell behaviour.

We then aimed at validating the model-based hypothesis of an increased communication between DC and multiple cell types. We considered three additional types of target cells: keratinocytes, plasmacytoid DCs (pDC) and neutrophils. Similar to T cells, these cell types play key roles in the inflammatory microenvironment and had an increased global communication score. Target cells were cultured with DC-derived supernatants, and their activation assessed by qRT-PCR or FACS. LPS-DC supernatant induced marginal keratinocyte activation, as assessed by the expression of TNF, IL-1β and this was not affected by αTNFR (**Figure 5A**). However, blocking the IL-10 loop dramatically increased both factors (**Figure 5A**), validating a potent DC to keratinocyte communication controlled by IL-10. This extends DC-induced keratinocyte activation (20, 21) to the context of bacterial infection.

The DC-pDC communication channel was also controlled by IL-10, since LPS+aIL10R-DC supernatants activated pDCs (as assessed by CD86, HLA-DR, and ICOSL surface expression), in comparison to LPS-DCs (**Figure 5B**). DC-induced activation of pDC and keratinocytes was not due to the presence of residual αIL10R (**Figure S5C and D**). DC-pDC crosstalk was suggested to be important in antiviral (22), antibacterial (23), and antitumor (24) immune responses. Through our systems approach, we now show that IL-10 controls DC-pDC connectivity.

Neutrophils contribute to DC migration to infection sites and to their subsequent activation (25, 26). Reciprocally, it was proposed that DCs can promote neutrophil survival (27).

LPS-DC supernatant induced only a mild activation of neutrophils (as evaluated by rapid upregulation of CD11b with concomitant downregulation of CD62L), while LPS+αIL10R-DC supernatants led to a strong activation of neutrophils (**Figure 5C**), establishing an IL-10 loop control of DC-neutrophils communication.

For all the above-mentioned communication channel, we aimed at getting further mechanistic insight. First, we performed control experiments using exogenous LPS that formally excluded a direct effect of LPS at the concentrations found in the DC supernatants (**Figure S5A**). We then considered ligand-receptor interactions showing high intensity, and thus more likely to mediate cellular crosstalk as observed with the LPS+αIL10R-DC supernatants (**supplementary table 3A-L**). We blocked, in each DC communication channel, 4 of ligands, known as potential activators of the target cell type: GCSF, GM-CSF, IL-6 and TNF for neutrophils, IL-19, IL-36 gamma, OSM and TNF for keratinocytes, and G-CSF, GM-CSF, TNF and IL-12 for pDCs. Importantly, blocking TNF alone in the LPS+αIL10R-DC supernatant was sufficient to inhibit keratinocyte, pDC and neutrophil activation (**Figure 5A-C**). By comparing the predicted communication intensities with a global score describing the activation level of keratinocytes, pDC and neutrophils, we observed a qualitative agreement (**Figure 5D**), demonstrating increased communication efficiency. In all cases, the maximal activation of the target cells was determined by the condition LPS + αIL10R.

Discussion

In this study, we demonstrated that a single molecule, IL-10, was able to control intercellular communication between DC and multiple immune and non-immune cells. DC are central to immune responses in health and disease, and have the ability to orchestrate and/or modulate the function of many cell types, including CD4 and CD8 T cells (2, 28), NK cells (29), γδ T cells (30), neutrophils (27), as well as other DC subsets (22, 24). Our findings reveal that these multiple connections may be collectively regulated by one molecule, in a coordinated manner. This indicates a level of regulation that could not be captured by conventional methods isolating pair-wise cell cross-talks, and calls for systems approaches. Previous research in this direction showed, for example, that systems approaches can be successfully applied to reconstruct the global cell cross-talk in the stem cell niche (31). In our study, we add an essential component, in the form of perturbations on purified cell cultures, in order to address mechanisms regulating the connectivity of immune cells.

One key element of systems approaches to intercellular communication is our *a priori* knowledge of the possible ligand-receptor interactions triggering a transduction process. Such information can be retrieved, for example, through automatic literature mining (31). However, this method makes it difficult to control the publication quality, and may fail to capture the requirements for complex interactions involving hetero dimeric receptors. In our work, the

information on the relevant ligand-receptor interactions was curated manually, which allowed taking into account the quality of publications, as well as up-to-date knowledge on the different chains of heterodimeric and heterotrimeric receptors.

Once the molecular mediators of possible cell-to-cell interactions were identified, we turned to assessing their cell-specific expression. To this end, we identified BioGPS as a particularly suitable resource, because it integrates transcriptional profiles of over twenty human primary cell types generated with the same Affymetrix platform (12). While previous applications of BioGPS allowed identifying specific tissue-related genes (32, 33), we show as an original use of this resource the possibility to simulate cell cross-talks in diverse microenvironments. The fact that BioGPS includes transcriptional profiles for both steady state and activated cells indicates that a predicted communication channel would not be specific (and restricted) to a given activation cell state. Our ability to provide functional validation of many of the predicted cellular cross-talks indicates the robustness of the method, and warrants application to other cellular types.

After retrieving a set of ligand-receptor interactions and cell-specific transcriptomics expression, we faced the problem of quantifying the intensity of communication between any pair of cell types. To score individual ligand/receptor interactions, we used the product of their expression values consistent the law of mass action, commonly assumed in biochemical models (34). Such individual scores give rise to a complex multigraph with potentially hundreds of edges connecting any two cell types. To reduce this complexity, we introduced a global score summing up the intensity of all the individual channels. This greatly simplifies the interpretation and visualization of intercellular networks, but also introduces some arbitrariness when choosing to combine the individual scores. Notwithstanding, all the predicted cellular targets could be experimentally verified, which led us to gain new insight on the role of TNF and IL-10 auto-regulatory loops during bacterial activation of DC. Exogenous TNF functional effect on dendritic cells has been described by many. It was found to induce maturation (35) and more specifically – induce and increase surface costimulatory molecules such as CD40, CD80, CD86, CD83 and HLA-DR (35-37). Exogenous IL-10, however, was found to have an opposite effect on the expression of these costimulatory molecules and led to their downregulation (8) (38). Contrasting effects on DC development were also described when comparing TNF to another anti-inflammatory cytokine, TGF beta (39). Taken together, one might expect to find contradicting effects of the TNF and IL-10 endogenous loops on DC, with an opposite directionality of gene regulation, including

communication molecules. Our data, however, uncover a very different scenario. Distinct and non-overlapping set of genes were controlled by either loop, and the intercellular communication function was regulated almost exclusively by the IL-10 loop.

We identified IL-10 as a molecular switch able to regulate the connectivity of DC with 12 other cell types, and thereby to modify their activation and functional states. IL-10 was already shown to regulate DC-derived inflammatory cytokines and chemokines, in particular IL-12 (8, 40). Through our systems approach, we identified a large number of communication molecules not previously associated to IL-10 function. Most importantly, we could demonstrate that endogenous DC-derived IL-10 governs the global connectivity of DC with multiple cell types, subsequently affecting their activation state, which brings new insight into how IL-10 regulates inflammation. We propose that the intensity and efficiency of communication may constitute a novel paradigm underlying the regulation of inflammatory processes, with increased intercellular connectivity being associated to enhanced inflammation. This warrants further studies in disease settings, in vivo and ex vivo, in order to precisely define the physiopathological relevance to specific inflammatory disorders.

Interestingly, IL-10 functions as an auto-regulatory switch controlling the structure and intensity of communication within cell networks while it was not predicted to be a direct effector on other cell types (**Supplementary table S3A-L**). On the contrary, TNF was predicted and validated to be a direct effector in most communication channels, leading to activation of target cells, while in the context of a feedforward loop it did not play a major role in determining the intensity of the global communication network. Thus, IL-10 and TNF act at different hierarchical levels to regulate cell-cell communication: IL-10 as an upstream molecular switch, TNF as a downstream effector communication molecule. This may have implications to understand the impact of IL-10 and TNF targeting in inflammation.

Our study revealed that connectivity within cell networks could be controlled by a single molecule. This predicts that, within the inflammatory microenvironment, the impact of targeted therapies to soluble mediators or surface receptors may be much broader than anticipated, due to a global re-programming of intercellular communication. Our systems and quantitative approach to cell connectivity may provide a valuable tool to evaluate such impact. Future studies should prove useful in identifying other regulators of immune cell connectivity in various physiopathological contexts, leading to important biological insight and helping to direct pharmacological manipulation.

Methods

Purification of Peripheral blood mononuclear cells (PBMCs) from adult blood

Fresh blood samples were collected from healthy donors and obtained from Hôpital Crozatier Établissement Français du Sang (EFS), Paris, France, in conformity with Institut Curie ethical guidelines. In agreement with EFS rules, all informed consent and consent to publish were obtained. PBMCs were isolated by centrifugation on a Ficoll gradient (Ficoll-Paque PLUS, GE Healthcare Life Sciences).

Monocyte-derived dendritic cells generation and activation

Monocytes were selected from PBMCs using antibody-coated magnetic beads and magnetic columns according to manufacturer's instructions (CD14 MicroBeads, MiltenyiBiotec). To generate immature DCs, CD14+ cells were cultured for 5 days with IL-4 (50 ng/mL) and GM-CSF (10 ng/mL) in RPMI 1640 Medium, GlutaMAX (Life Technologies) with 10% FCS. Monocyte-derived DCs were pre-treated for one hour with mouse IgG1 (20 µg/mL, R&D Systems), mouse anti-IL10R blocking antibody (10 µg/mL, R&D Systems) or mouse anti-TNFα Receptors 1 and 2 (10 µg/mL, R&D Systems) (see Figure 1-Figure Supplement 4B) and then cultured with medium or LPS (100 ng/mL, LPS-EB Ultrapure, activates TLR4 only, Invivogen) for 24 hours. DCs from donors which responded to (a) LPS and (b) IL-10R blocking antibody, as evaluated by maturation markers, were included in this study. The following cytokines were measured in culture supernatants by CBA (BD Bioscience): IL-6, IL-12p70 and OSM. IL-23 was measured using ELISA (eBioscience).

Gene expression profiling

Monocyte-derived DCs were pre- treated with blocking Abs as described above for one hour and then cultured with medium or LPS (100 ng/mL, Invivogen) for additional 4 or 8 hours. Total RNA was extracted using the RNeasy micro kit (Qiagen). Samples were then amplified and labelled according to the protocol recommended by Affymetrix for hybridization to Human Genome U133 Plus 2.0 arrays.

The gene expression profiles generated for this publication have been deposited in NCBI's Gene Expression Omnibus and are accessible through GEO Series accession number GSE89342 (http://www.ncbi.nlm.nih.gov/geo/query/acc.cgi?acc=GSE89342).

Purification of naive CD4+ T lymphocytes.

368 $CD4^+$T lymphocytes were purified from PBMCs by immunomagnetic depletion with the
369 human $CD4^+$T cell Isolation KitII (MiltenyiBiotec), followed by staining with allophyco-
370 cyanin-anti CD4 (VIT4 ; MiltenyiBiotec), phycoerythrin-anti-CD45RA (BD), fluorescein-
371 isothiocyanate-anti-CD45RO (BD Bioscience) and phycoerythrin-7-anti-CD25 (BD
372 bioscience). Naive $CD4^+$T cells sorting of $CD4^+CD45RA^+CD45RO^-CD25^-$ had a purity of
373 over 99% with a FACSAria (BD Bioscience).

374 ***DC- T cells Coculture assays.***

375 To analyze T cell polarization, 24 hours activated DC and T cells were incubated in 96 well
376 plates at a DC/T ratio 1:5 in Xvivo15 medium (Lonza). After 6 days, T cells were
377 resuspended in fresh Xvivo15 medium at a concentration of 1 million cells per ml and
378 restimulated with anti-CD3/CD28 beads (life Technologies) at a ratio bead/cell 1:1.
379 Supernatants of T cells were collected after 24 hours of restimulation. The following
380 cytokines were measured in naive culture supernatants by CBA (BD Bioscience) according to
381 the manufacturer's instructions: IL-2, IL-3, IL-4, IL-9, IL-10, IL-17A, IL-17F and IFN-γ.
382 Additional cytokines were measured in memory T cells supernatant: IL-5, IL-13 TNF and
383 GM-CSF.

384 Cytokines producing cells were analyzed by intracellular staining after addition of brefeldinA
385 (10ug/mL) during the last 3 hours of the 5 hours restimulation in PMA and ionomycine
386 respectively 100ng/mL and 500ng/ml. Cells were stained 30 minutes with the yellow live
387 dead kit (Invitrogen). Finally, cells were fixed and permeabilized using the Staining Buffer
388 Set (eBioscience) and stained with anti-IL9, anti-IFNg, and anti-IL17A (ebioscience), and
389 analyzed by flow cytometry (BD Fortessa).

390 ***Measurement of surface molecules expression by plasmacytoid dendritic cells***

391 In order to enrich plasmacytoid dendritic cells (pDCs), cells expressing CD3, CD9, CD14,
392 CD16, CD19, CD34, CD56, CD66b and glycophorin A were depleted from PBMCs using
393 magnetic sorting (Human Pan-DC Pre-Enrichment Kit, StemCell Technologies), pDCs were
394 then sorted on a FACS Vantage instrument (BD Biosciences). pDCs were cultured for 24
395 hours at 37°C and 5% CO_2 with medium RPMI 1640 Medium, GlutaMAX (Life
396 Technologies) with 10% FCS, GM-CSF (10 ng/mL) used as a positive control or DC
397 supernatants. Cells were stained for 15 min at 4°C using a FITC-anti-CD86 (BD), an APC-

anti-ICOSL (R&D Systems) and Alexa-Fluor-700-anti-HLA-DR (Biolegend) or with the corresponding isotypes. Cells were analyzed on a LSR II instrument (BD Biosciences).

Measurement of adhesion molecules expression at the Neutrophil surface

Whole-blood samples were obtained from healthy donors from Hôpital Crozatier Établissement Français du Sang (EFS), Paris, France, in conformity with Institut Curie ethical guidelines. Blood samples were stimulated for an hour at 37°C with medium, LPS (100 ng/mL) used as a positive control or DC supernatants. Cells were stained at 4°C for 15 min with an APC-anti-Human-CD62L (clone DREG-56, BD Pharmingen), a BV650-anti-Human-CD11b (BioLegend) and a PE-anti-Human-CD15 (MiltenyiBiotec) or with the corresponding isotypes. Erythrocytes were lysed with 1X BD Pharm Lyse Solution (BD Pharmingen), white cells were resuspended in PBS supplemented with 1% human serum and 2 mM EDTA and analyzed on a LSR Fortessa instrument (BD Biosciences).

Real-time quantitative RT-PCR

The keratinocyte cell line HaCaT was cultured in DMEM (Gibco) supplemented with 10% FBS and 1% penicillin/streptomycin. Cells were cultured with medium, LPS (100 ng/ml), or with DC supernatant diluted 1:10 for 4h. Total RNA was extracted by RNeasy Mini kit (Qiagen). RNA was then transcribed to cDNA using Superscript II reverse transcriptase based on the manufacture's protocol (Invitrogen). The Taqman method was used for real-time PCR with primers from Life technologies. The expression of mRNA was normalized to the geometrical mean of 3 house-keeping genes: β-actin, GAPDH and RPL34. HaCaT cells were negative for Mycoplasma contamination, standardized and regular tests were performed by PCR for mycoplasma detection.

Statistical analysis of gene expression data

Expression data were normalized with Plier. Transcriptomics analysis was performed in a Matlab environment. For independent filtering, we used the function *geneverfilter,* which calculates the variance of each probe across the samples and identifies the ones with low variance. Probes with variance less than 40^{th} percentile were filtered out because poorly informative. Differential analysis was performed using an ANOVA test (function *anova1*) at 4 hours and 8 hours. P-values were adjusted for multiple testing using the Benjamini-Hochberg correction using the function *mafdr*. Adjusted p-values <5% were considered significant (see **supplementary table 1A-B**). To detect genes whose expression pattern was specific for the

conditions LPS, LPS+αIL10R, or LPS+ αTNFR, we used the function *rankfeature.* This function returns a separability score based on binary classification, which measures how well each gene separates a given experimental condition from all the others based on its expression profile. By inspecting the distribution of the separability score over all differentially expressed genes, we determined an empirical cutoff of 4. Genes with separability score larger than this cut off (**supplementary table 1C-E**) were further analyzed for functional interpretation using the Molecular Signature Database (41) (**supplementary table 1F-H)**. The following databases were considered: KEGG, REACTOME and BIOCARTA. To compute the enrichment of the TNF and IL10 loop signatures in genes annotated in the GO term "positive regulation of cell communication" (GO:0010647) (**supplementary table 2A),** we performed a standard hypergeometric test.

Reconstruction of inter-cellular networks

To reconstruct the inter-cellular communication networks, we systematically extracted a list of ligands and receptors contained in the genes whose expression pattern was specific for the condition LPS, LPS+αIL10R, or LPS+ αTNFR (see the section above). Surveying the literature for any potential interactions, we manually curated a ligand-receptor database using STRING (http://string-db.org/) and Ingenuity (http://www.ingenuity.com/) online tools to verify protein-protein interactions. Logical rules were applied to address requirement for multiple chains as well as multiple ligand subunits (http://www.genome.jp/kegg-bin/show_pathway?hsa04060).

The database of ligand-receptor interactions is contained in the **supplementary table 2B**. To get the cell-specific expression level of the receptors of the ligands of interest, we used a database of transcriptional data from human primary cells (12) (13) and a dataset of SUM149 inflammatory breast cancer cell line transcriptional profile from literature (Wang et al. Cancer Res 2013). All the cell-specific transcriptional profiles used in the analysis were generated with the U133 Plus 2.0 Array, which limits the platform-related bias. If multiple probes corresponded to the same receptor, we selected the optimal probe based on the Jetset optimality condition (42). The results are contained in **supplementary table 2C-E**. To score the intensity of a particular ligand-receptor interaction between DC and a given target cell, we considered the product of the expression of the ligand in DC and of the cognate receptor in the target cells. Formally, if l_j^i is the average expression level of ligand i by DC in the experimental condition j, and r_k^i is the average expression of the corresponding receptor by

cell type *k*, the intensity $s^i_{j,k}$ of the corresponding interaction was quantified by $s^i_{j,k} = l^i_j \cdot r^i_k$. For interactions requiring multiple components of the ligand and/or of the receptor, we considered a geometric average of the receptor components. For example, if a given interaction corresponding to ligand *i* required two chains of the receptor, the score was computed as $l^i_j \cdot \sqrt{r^{i,1}_k . r^{i,2}_k}$, where $r^{i,1}_k$ and $r^{i,2}_k$ are the expression levels of the two receptor chains in cell type *k*. To assign a global score $S_{j,k}$to the communication between DC in the condition *j* and cell type *k*, a composite score was defined by summing up the intensity of all the possible ligand-receptor interactions, i.e., $S_{j,k} = \sum_{i=1}^{N} s^i_{j,k}$, *N* being the total number of interactions. Four DC experimental conditions were considered: Medium (j=0), LPS (j=1), blocking TNF loop (j=2), blocking IL10 loop. To emphasize comparisons $S_{j,k}$ across the four conditions, the global scores $S_{j,k}$ were normalized to the Medium condition (*j*=0). Thus, the final scores $\overline{S_{j,k}}$ used to measure the communication intensity between DC in the condition *j* and the target cell *k* were computed using the following formula $\overline{S_{j,k}} = S_{j,k}/S_{0,k}.=\frac{\sum_{i=1}^{N} s^i_{j,k}}{\sum_{i=1}^{N} s^i_{0,k}}$. The scores corresponding to each interaction and each target cell in the experimental condition of IL10R blocking are provided in **supplementary table 3A-L**. The generation of the inflow connectivity maps was done by reversing the role of DC and their cellular targets. See supplementary figure 5. Global communication scores for both inflow and outflow connectivity maps are contained in **supplementary table 3M-N**.

Statistical analysis of DC-T cell protein data

All analyses have been generated with R 3.1. For principal component analysis (PCA) of the T cell secretion profile, a data matrix was formed whose rows corresponded to conditions and columns to the different cytokines (each column was scaled using *zscore*). PCA was done using the function *princomp*. When appropriate, a paired student t-test was performed. Significant differences were considered with $p<0.05$. The correlation heatmap based on Spearman was generated on the logged data. Correlations with p values<0.05 were considered as significant.

Calculation of the activation score of target cells

To compute a global activation score of keratinocytes, neutrophils and pDC, each activation marker output was first normalized in the range 0-1, 0 being to the untreated condition and 1 being to the maximum value observed in all the conditions. An average of the normalized

outputs corresponding to the same cell type was then considered. All of the measured factors, with the exception of CD62L in neutrophils, were positively correlated with cell activation. In order to make CD62L consistent with the other factors, we considered the reciprocal of its value. The numerical results are in the **supplementary table 3M-N**.

Acknowledgements

We wish to thank Franck Perez, Sebastian Amigorena, Yong-Jun Liu and Fivos Soumelis for insightful comments and discussions, the Institut Curie Flow Cytometry facility (Z. Maciorowsky), the Institut Curie Affymetrix facility (D. Gentien). This work was supported by funding from the Institut Curie, Agence Nationale pour la Recherche (ANR), Fondation pour la Recherche Médicale (FRM), the European Research Council (ERC starting grant 281987), ANR-10-IDEX-0001-02 PSL, ANR-11-LABX-0043, CIC IGR-Curie 1428 for V.S. EMBO and Institut Curie post-doctoral fellowships to ICL. ANRS and ARC fellowships to MG.

Conflict-of-interest statement

The authors declare no conflict of interest**.**

References

1. Banchereau J, et al. (2000) Immunobiology of dendritic cells. Annual review of immunology 18:767-811.

2. Guermonprez P, Valladeau J, Zitvogel L, Thery C, & Amigorena S (2002) Antigen presentation and T cell stimulation by dendritic cells. Annual review of immunology 20:621-667.

3. Valeyev NV, et al. (2010) A systems model for immune cell interactions unravels the mechanism of inflammation in human skin. PLoS computational biology 6(12):e1001024.

4. Neurath MF (2014) Cytokines in inflammatory bowel disease. Nature reviews. Immunology 14(5):329-342.

5. Shen-Orr SS, et al. (2009) Towards a cytokine-cell interaction knowledgebase of the adaptive immune system. Pacific Symposium on Biocomputing. Pacific Symposium on Biocomputing:439-450.

6. Frankenstein Z, Alon U, & Cohen IR (2006) The immune-body cytokine network defines a social architecture of cell interactions. Biology direct 1:32.

7. Blanco P, Palucka AK, Pascual V, & Banchereau J (2008) Dendritic cells and cytokines in human inflammatory and autoimmune diseases. Cytokine & growth factor reviews 19(1):41-52.

8. Moore KW, de Waal Malefyt R, Coffman RL, & O'Garra A (2001) Interleukin-10 and the interleukin-10 receptor. Annual review of immunology 19:683-765.

9. Corinti S, Albanesi C, la Sala A, Pastore S, & Girolomoni G (2001) Regulatory activity of autocrine IL-10 on dendritic cell functions. J Immunol 166(7):4312-4318.

10. Melillo JA, et al. (2010) Dendritic cell (DC)-specific targeting reveals Stat3 as a negative regulator of DC function. J Immunol 184(5):2638-2645.

11. Huang Q, et al. (2001) The plasticity of dendritic cell responses to pathogens and their components. Science 294(5543):870-875.

12. Wu C, et al. (2009) BioGPS: an extensible and customizable portal for querying and organizing gene annotation resources. Genome biology 10(11):R130.

13. Mabbott NA, Baillie JK, Brown H, Freeman TC, & Hume DA (2013) An expression atlas of human primary cells: inference of gene function from coexpression networks. BMC genomics 14:632.

14. Goetz FW, Planas JV, & MacKenzie S (2004) Tumor necrosis factors. Developmental and comparative immunology 28(5):487-497.

15. Pitt JM, et al. (2012) Blockade of IL-10 signaling during bacillus Calmette-Guerin vaccination enhances and sustains Th1, Th17, and innate lymphoid IFN-gamma and IL-17 responses and increases protection to Mycobacterium tuberculosis infection. J Immunol 189(8):4079-4087.

16. Zigmond E, et al. (2014) Macrophage-restricted interleukin-10 receptor deficiency, but not IL-10 deficiency, causes severe spontaneous colitis. Immunity 40(5):720-733.

17. Wilke CM, et al. (2011) Endogenous interleukin-10 constrains Th17 cells in patients with inflammatory bowel disease. Journal of translational medicine 9:217.

18. Stassen M, Schmitt E, & Bopp T (2012) From interleukin-9 to T helper 9 cells. Annals of the New York Academy of Sciences 1247:56-68.

19. Graeber KE & Olsen NJ (2012) Th17 cell cytokine secretion profile in host defense and autoimmunity. Inflammation research : official journal of the European Histamine Research Society ... [et al.] 61(2):87-96.

20. Tortola L, et al. (2012) Psoriasiform dermatitis is driven by IL-36-mediated DC-keratinocyte crosstalk. The Journal of clinical investigation 122(11):3965-3976.

21. Shimura C, et al. (2010) Dendritic cells express hematopoietic prostaglandin D synthase and function as a source of prostaglandin D2 in the skin. The American journal of pathology 176(1):227-237.

22. Kramer M, et al. (2010) Cross-talk between human dendritic cell subsets influences expression of RNA sensors and inhibits picornavirus infection. Journal of innate immunity 2(4):360-370.

23. Piccioli D, et al. (2009) Human plasmacytoid dendritic cells are unresponsive to bacterial stimulation and require a novel type of cooperation with myeloid dendritic cells for maturation. Blood 113(18):4232-4239.

24. Lou Y, et al. (2007) Plasmacytoid dendritic cells synergize with myeloid dendritic cells in the induction of antigen-specific antitumor immune responses. J Immunol 178(3):1534-1541.

25. Schuster S, Hurrell B, & Tacchini-Cottier F (2013) Crosstalk between neutrophils and dendritic cells: a context-dependent process. Journal of leukocyte biology 94(4):671-675.

26. Ludwig IS, Geijtenbeek TB, & van Kooyk Y (2006) Two way communication between neutrophils and dendritic cells. Current opinion in pharmacology 6(4):408-413.

27. Jiao J, et al. (2014) Central role of conventional dendritic cells in regulation of bone marrow release and survival of neutrophils. J Immunol 192(7):3374-3382.

28. Hivroz C, Chemin K, Tourret M, & Bohineust A (2012) Crosstalk between T lymphocytes and dendritic cells. Critical reviews in immunology 32(2):139-155.

29. Cooper MA, Fehniger TA, Fuchs A, Colonna M, & Caligiuri MA (2004) NK cell and DC interactions. Trends in immunology 25(1):47-52.

30. Scotet E, Nedellec S, Devilder MC, Allain S, & Bonneville M (2008) Bridging innate and adaptive immunity through gammadelta T-dendritic cell crosstalk. Frontiers in bioscience : a journal and virtual library 13:6872-6885.

31. Kirouac DC, et al. (2010) Dynamic interaction networks in a hierarchically organized tissue. Molecular systems biology 6:417.

32. Podobed PS, Alibhai FJ, Chow CW, & Martino TA (2014) Circadian regulation of myocardial sarcomeric Titin-cap (Tcap, telethonin): identification of cardiac clock-controlled genes using open access bioinformatics data. PloS one 9(8):e104907.

33. Romeu A & Arola L (2014) Classical dynamin DNM1 and DNM3 genes attain maximum expression in the normal human central nervous system. BMC research notes 7:188.

34. B I (2013) Mathematical Modeling in Systems Biology: An Introduction. .

35. Sallusto F & Lanzavecchia A (1994) Efficient presentation of soluble antigen by cultured human dendritic cells is maintained by granulocyte/macrophage colony-stimulating factor plus interleukin 4 and downregulated by tumor necrosis factor alpha. The Journal of experimental medicine 179(4):1109-1118.

36. Arrighi JF, Rebsamen M, Rousset F, Kindler V, & Hauser C (2001) A critical role for p38 mitogen-activated protein kinase in the maturation of human blood-derived dendritic cells

596 induced by lipopolysaccharide, TNF-alpha, and contact sensitizers. J Immunol 166(6):3837-
597 3845.

598 37. Trevejo JM, et al. (2001) TNF-alpha -dependent maturation of local dendritic cells is
599 critical for activating the adaptive immune response to virus infection. Proceedings of the
600 National Academy of Sciences of the United States of America 98(21):12162-12167.

601 38. Buelens C, et al. (1995) Interleukin-10 differentially regulates B7-1 (CD80) and B7-2
602 (CD86) expression on human peripheral blood dendritic cells. European journal of
603 immunology 25(9):2668-2672.

604 39. Yamaguchi Y, Tsumura H, Miwa M, & Inaba K (1997) Contrasting effects of TGF-
605 beta 1 and TNF-alpha on the development of dendritic cells from progenitors in mouse bone
606 marrow. Stem Cells 15(2):144-153.

607 40. D'Andrea A, et al. (1993) Interleukin 10 (IL-10) inhibits human lymphocyte interferon
608 gamma-production by suppressing natural killer cell stimulatory factor/IL-12 synthesis in
609 accessory cells. The Journal of experimental medicine 178(3):1041-1048.

610 41. Liberzon A, et al. (2011) Molecular signatures database (MSigDB) 3.0. Bioinformatics
611 27(12):1739-1740.

612 42. Li Q, Birkbak NJ, Gyorffy B, Szallasi Z, & Eklund AC (2011) Jetset: selecting the
613 optimal microarray probe set to represent a gene. BMC bioinformatics 12:474.

614

615 43.

616

Figure legends

Fig. 1: Development of a communication score based on transcriptomic profiles. (A) Pipeline used to create the intercellular communication score and network reconstruction. **(B)** Connectivity maps describing outgoing communication from SUM149 cells to primary cells in the conditions: siRNA control and siTIG1. The width of the edges corresponds to a global score combining the intensity of all the individual ligand/receptor interactions. A scale ranging from 400000 to 1600000, corresponding to minimum and maximum communication scores, is shown in the legend.

Fig. 2: IL-10R blocking activates a cell-to-cell communication module in LPS-stimulated DCs. (A) Depicted are the 4 experimental conditions for which transcriptomics was generated (n = 6). **(B)** Distribution of the separability score corresponding to the conditions LPS+αTNFR and LPS+αIL10R after 4 and 8 hours of cell culture. Genes with separability score ≥ 4 were included in each condition's signature. Bottom: separability criterion used to define the signatures. **(C)** Expression pattern of 4 example genes with high separability score from the IL-10 loop signature (means± SEM, n=6). (**D)** Top 3 KEGG and REACTOME annotation terms over-represented in the IL-10 loop signature, together with the number of hits and the enrichment significance. **(E)** log-transformed enrichment significance of the overlap between the TNF and IL10 loop signatures, with the Gene Ontology term "positive regulation of cell communication". (**F)** Gene products corresponding to ligands (white) and receptors (black) counted in each loop signature and plotted according to regulation directionality: upregulated (Up) or downregulated (Down). (**G)** Protein levels of IL-6, OSM, IL-23 and IL-12p70 (means ± SEM), demonstrating increased secretion in LPS+αIL-10R DC supernatant.

Fig. 3: IL-10 loop controls DC intercellular connectivity. **(A)** Flowchart illustrating the strategy used for intercellular networks reconstruction. **(B)** Expression values of 8 example ligands in DCs (means ± SEM) side-by-side with the expression of their cognate receptor in 12 different cell types from four compartments: epithelium, stroma, innate and adaptive immune cells. Color code indicates different compartments. Box plots show cell-specific expression of the receptors in control and stimulated conditions, as provided by the BioGPS database (supplementary table 2C-E) (**C)** Connectivity maps describing outgoing communication from DCs to putative target cells in the conditions: Med, LPS, LPS+αTNFR and LPS+αIL-10R. The width of the edges corresponds to a global score combining the

intensity of all the individual ligand/receptor interactions, normalized to the medium condition. A scale ranging from 1 to 7, corresponding to minimum and maximum communication scores, is shown in the legend.

Fig. 4: IL-10 but not TNF loop dictates T helper polarization by LPS-DC. (A-B) Supernatants of CD4+ naive (A) and memory (B) T cells, co-cultured with the indicated DCs, were analyzed for the presence of T helper cytokines by CBA: IL-2, IL-3, IL-4, IL-9, IL-10, IL-17A, IL-17F and IFN-γ (A) and all the above in addition to IL-5, IL-13 TNF and GM-CSF (B). Results are shown in a 2D PCA. Dots represent mean of 9 (A) or 6 (B) independent co-culture experiments. **(C)** Histogram representation (means ± SEM, n = 16) of 4 cytokines present in the supernatant of naive (white bars, left axis) or memory (black bars, right axis) supernatant. **(D)** CD4+ naive T cells were analyzed for IL-17A, IL-9 and IFNg production using intracellular staining FACS. Percentage of positive producers is given. Shown is one representative out of 3 independent experiments. **(E)**The matrix plot presents the significant (p value < 0.05) Spearman correlation values between DC soluble factors and T helper-secreted cytokines (9 independent co-culture experiments).

Fig. 5: IL-10 loop controls DC communication with keratinocytes, neutrophils and pDCs. (A) RT-PCR analysis of the expression of TNF and IL-1b mRNA in HaCat cells incubated with medium, LPS or with supernatant (diluted 1:10) of the indicated DCs for 4h. Blocking antibodies for the cytokines IL-19, IL-36g, OSM and TNF were added to LPS+αIL-10R-DC supernatant for 1h incubation before culturing with HaCat cells. Data represent mean ± SEM, n=4, * p<0.05. **(B-C)** Expression of maturation markers CD86, HLA-DR and ICOSL (B) or DC11b and CD62L (C) analyzed by flow cytometry with surface staining on pDCs (n=12) cultured with supernatant (diluted 1:10) of the indicated DC for 24h (b) and neutrophils (n=9) cultured with supernatant (diluted 1:100) of the indicated DC for 1h. Blocking antibodies for the cytokines GCSF, GM-CSF, TNF and IL-12 (for pDC) or IL-6 (neutrophils) were added to LPS+αIL-10R-DC supernatant for 1h incubation before culture. Each biological replicate comprised independent DC donor paired to independent pDCs / neutrophils donor. Data represent mean ± SEM, * p<0.05; ** p<0.01; *** p<0.001 (paired t-test). **(D)** For each target cell, we reduced the different activation markers to a single parameter normalized between 0 (Ø) and 1 (max) in the rectangles. The value 0 corresponds to the activation level induced by supernatants from untreated DC, while 1 corresponds to the maximum activation level from all the observed conditions. These experimentally validated

activation scores were in qualitative agreement with the model predictive intensity scores of communication between DC and the target cells, represented by the width of the edges.

Table 1: Communication factors in signatures by separability. Communication factors (ligands and receptors) identified in the signatures corresponding to the DC conditions LPS, LPS+αTNFR, LPS+αIL10R.

Table 1 : Communication factors in signatures by separability				
Factor	**Direction**	**LPS**	**LPS+αTNFR**	**LPS+αIL10R**
Ligand	**Down**	**EFNB1**	**ICOSLG**	**EFNA4, PLAU, SLIT1, WNT5B**
	Up	**PDGFA, PVR**	**PLAU, VCAN**	**AREG, C3, CCL1, CCL20, CCL3, CCL4, CD58, CD70, CD80, CLCF1, CSF1, CSF2, CSF3, EDN1, GAST, GUCA2A, HBEGF, ICOSLG, IFNB1, IGHG1, IL12A, IL12B, IL19, IL23A, IL36G, IL36RN, IL6, INHBA, JAG1, OSM, OSTN, PDGFB, RSPO4, SEMA4D, SEMA7A, TGFA, TNF, TNFSF10, TNFSF15, TNFSF18, TNFSF4, TNFSF9, TSLP**
Receptor	**Down**	**CXCR1**		**CCR2, CSF1R, FZD2, GFRA2, IFNGR1, IL17RA, IL17RB, LTBR, PLXNB2, TNFRSF6B**
	Up	**IL20RB, ITGAV, PDGFRA, NFRSF1B**	**CCR5, FZD5, ITGA9, LILRB1, MERTK**	**CALCRL, CCR7, CCRL2, CD40, GALR2, IL15RA, LMBR1L, NRP2, PLAUR, PRLR, TNFRSF18, TNFRSF4, TNFRSF9**

A

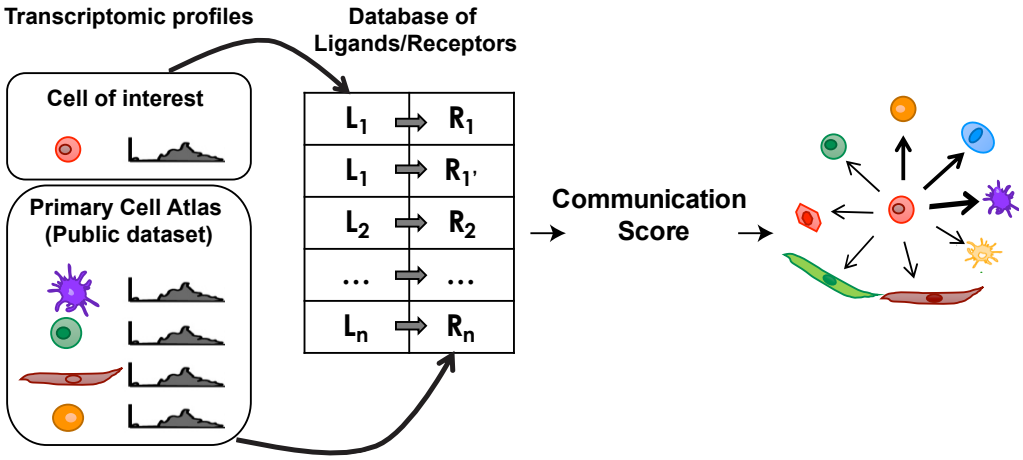
Transcriptomic profiles
Database of Ligands/Receptors
Cell of interest
Primary Cell Atlas (Public dataset)
L1 R1
L1 R1'
L2 R2
... ...
Ln Rn
Communication Score

B

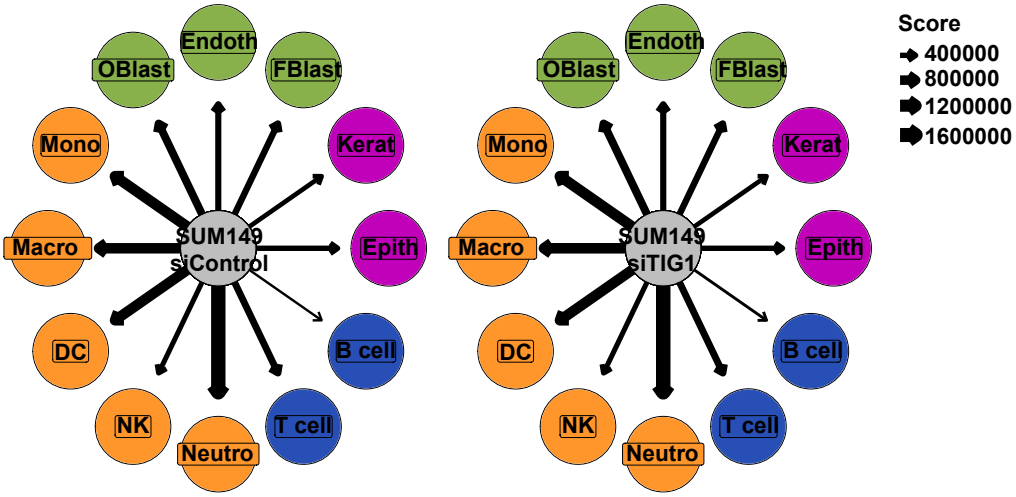
Endoth
OBlast
FBlast
Mono
Kerat
Macro
SUM149 siControl
Epith
DC
B cell
NK
Neutro
T cell
SUM149 siTIG1
Score
400000
800000
1200000
1600000

Figure 1

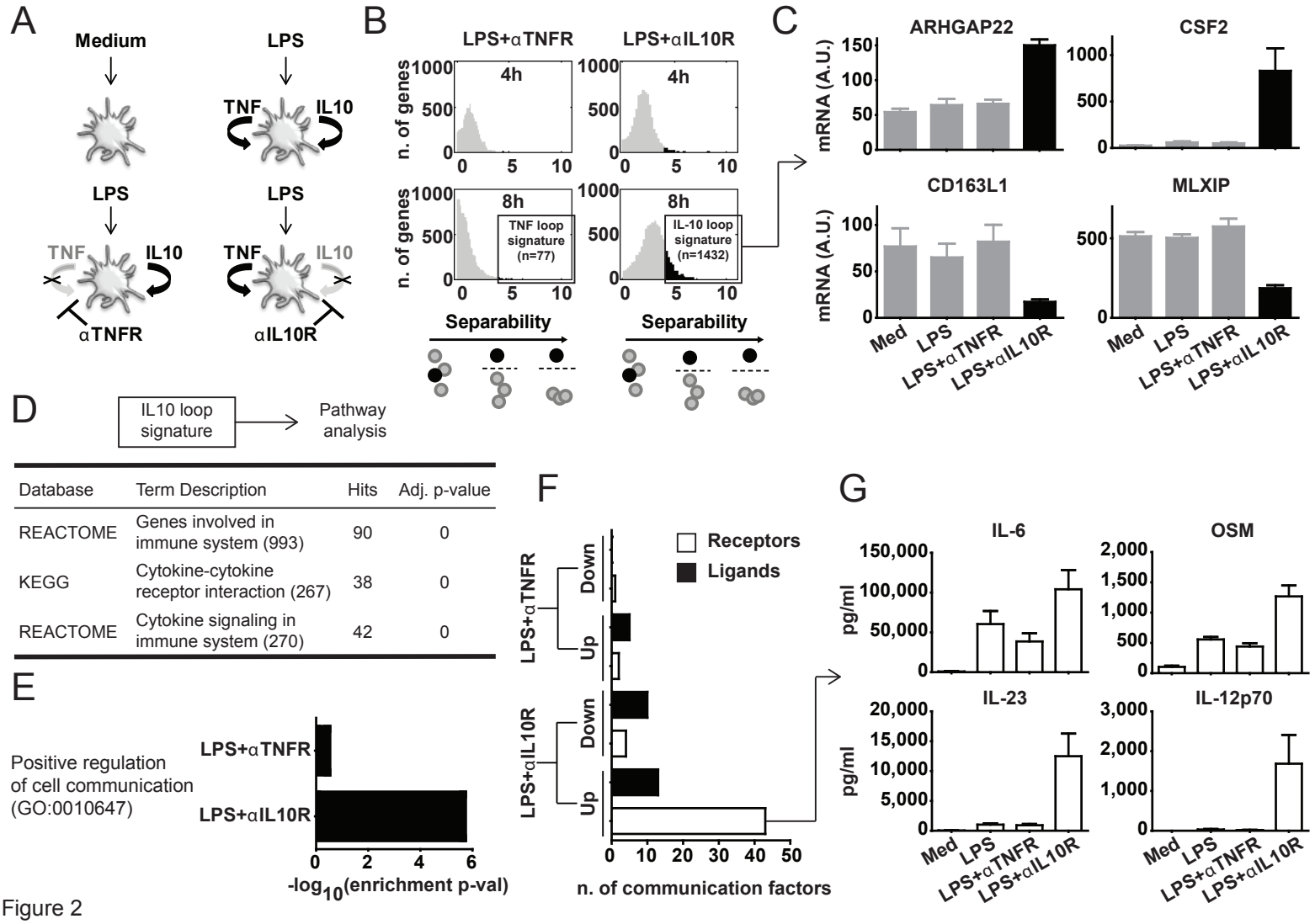
A
Medium
LPS
TNF
IL10
LPS
LPS
TNF
IL10
TNF
IL10
αTNFR
αIL10R
B
LPS+αTNFR
LPS+αIL10R
n. of genes
4h
8h
TNF loop signature (n=77)
IL-10 loop signature (n=1432)
Separability
C
ARHGAP22
CSF2
CD163L1
MLXIP
mRNA (A.U.)
Med
LPS
LPS+αTNFR
LPS+αIL10R
D
IL10 loop signature
Pathway analysis
Database
Term Description
Hits
Adj. p-value
REACTOME
Genes involved in immune system (993)
90
0
KEGG
Cytokine-cytokine receptor interaction (267)
38
0
REACTOME
Cytokine signaling in immune system (270)
42
0
E
Positive regulation of cell communication (GO:0010647)
LPS+αTNFR
LPS+αIL10R
-log10(enrichment p-val)
F
Receptors
Ligands
LPS+αTNFR
LPS+αIL10R
Down
Up
n. of communication factors
G
IL-6
OSM
IL-23
IL-12p70
pg/ml
Med
LPS
LPS+αTNFR
LPS+αIL10R

Figure 2

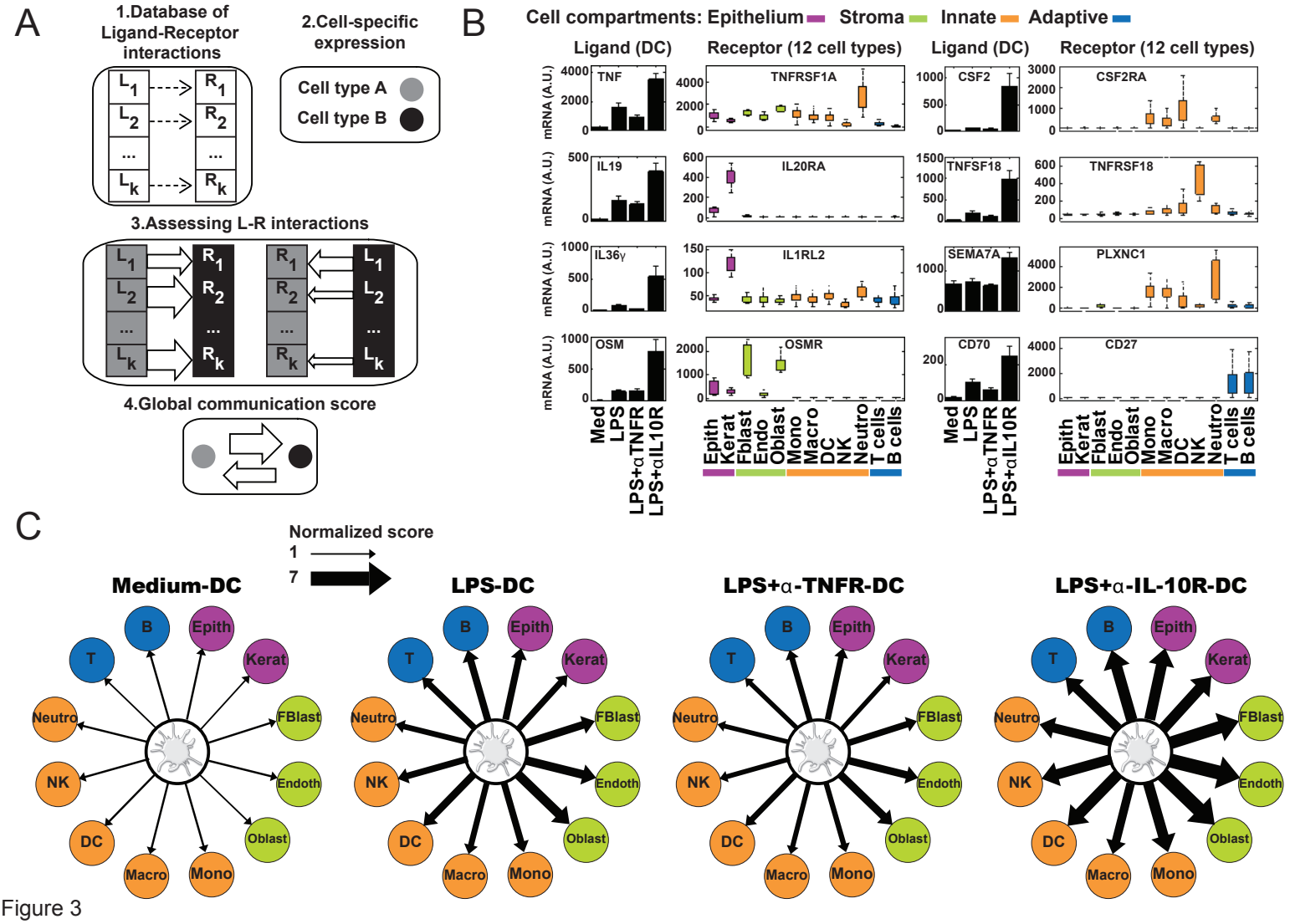
A
1.Database of Ligand-Receptor interactions
2.Cell-specific expression
Cell type A
Cell type B
3.Assessing L-R interactions
4.Global communication score
B
Cell compartments: Epithelium Stroma Innate Adaptive
Ligand (DC)
Receptor (12 cell types)
Ligand (DC)
Receptor (12 cell types)
mRNA (A.U.)
TNF
TNFRSF1A
CSF2
CSF2RA
IL19
IL20RA
TNFSF18
TNFRSF18
IL36γ
IL1RL2
SEMA7A
PLXNC1
OSM
OSMR
CD70
CD27
Med
LPS
LPS+αTNFR
LPS+αIL10R
Epith
Kerat
Fblast
Endo
Oblast
Mono
Macro
DC
NK
Neutro
T cells
B cells
C
Normalized score
1
7
Medium-DC
LPS-DC
LPS+α-TNFR-DC
LPS+α-IL-10R-DC
B
Epith
Kerat
FBlast
Endoth
Oblast
Mono
Macro
DC
NK
Neutro
T

Figure 3

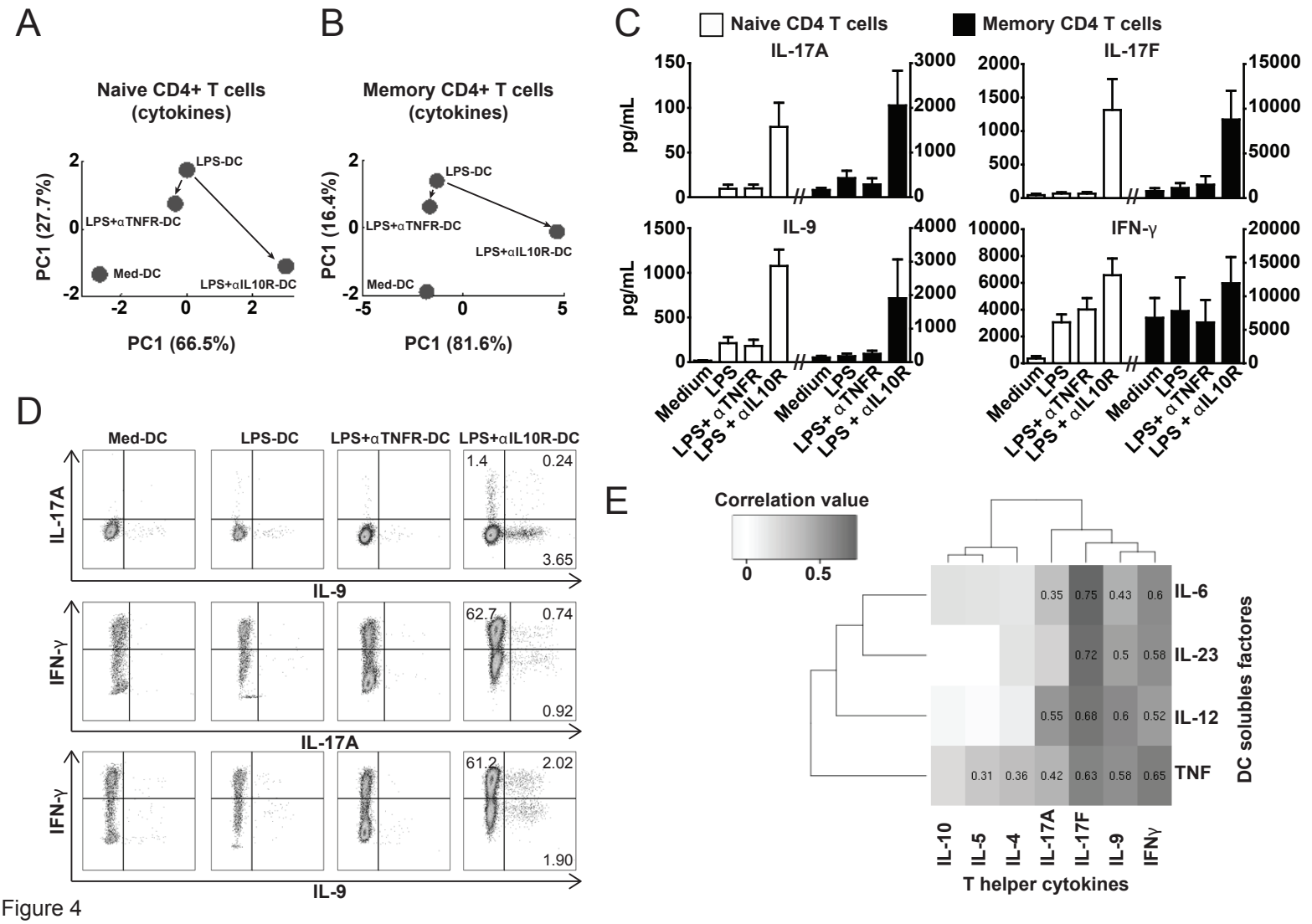
A
Naive CD4+ T cells (cytokines)
LPS-DC
LPS+αTNFR-DC
Med-DC
LPS+αIL10R-DC
PC1 (27.7%)
PC1 (66.5%)
B
Memory CD4+ T cells (cytokines)
LPS-DC
LPS+αTNFR-DC
LPS+αIL10R-DC
Med-DC
PC1 (16.4%)
PC1 (81.6%)
C
Naive CD4 T cells
Memory CD4 T cells
IL-17A
IL-17F
IL-9
IFN-γ
pg/mL
Medium
LPS
LPS+ αTNFR
LPS + αIL10R
D
Med-DC
LPS-DC
LPS+αTNFR-DC
LPS+αIL10R-DC
IL-17A
IL-9
IFN-γ
1.4
0.24
3.65
62.7
0.74
0.92
61.2
2.02
1.90
E
Correlation value
0
0.5
IL-6
IL-23
IL-12
TNF
DC solubles factores
IL-10
IL-5
IL-4
IL-17A
IL-17F
IL-9
IFNγ
T helper cytokines

Figure 4

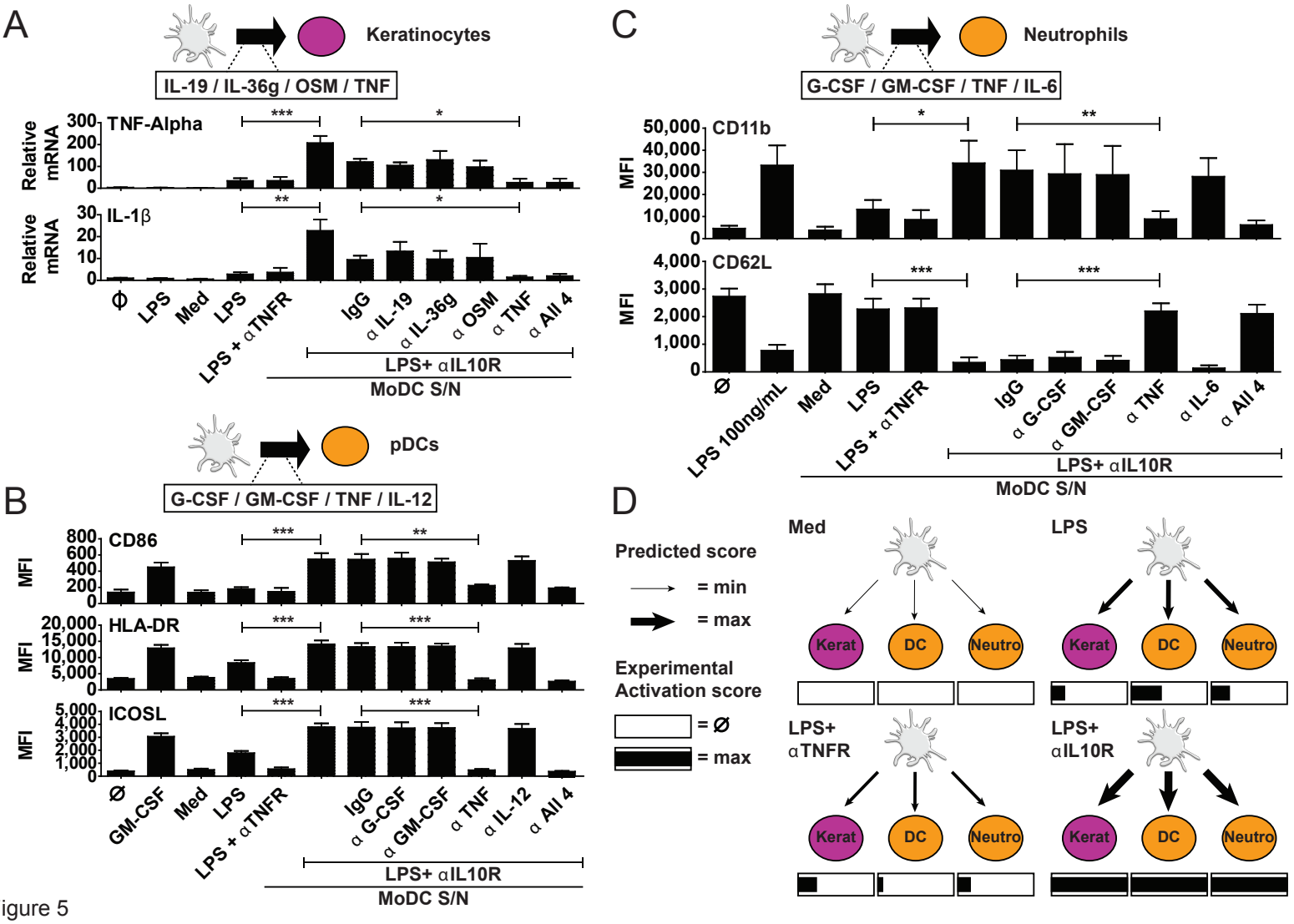
A
Keratinocytes
IL-19 / IL-36g / OSM / TNF
TNF-Alpha
IL-1β
Relative mRNA
Φ
LPS
Med
LPS
LPS + αTNFR
IgG
α IL-19
α IL-36g
α OSM
α TNF
α All 4
LPS+ αIL10R
MoDC S/N
B
pDCs
G-CSF / GM-CSF / TNF / IL-12
CD86
HLA-DR
ICOSL
MFI
Ø
GM-CSF
Med
LPS
LPS + αTNFR
IgG
α G-CSF
α GM-CSF
α TNF
α IL-12
α All 4
LPS+ αIL10R
MoDC S/N
C
Neutrophils
G-CSF / GM-CSF / TNF / IL-6
CD11b
CD62L
MFI
Ø
LPS 100ng/mL
Med
LPS
LPS + αTNFR
IgG
α G-CSF
α GM-CSF
α TNF
α IL-6
α All 4
LPS+ αIL10R
MoDC S/N
D
Predicted score
= min
= max
Experimental Activation score
= Ø
= max
Med
LPS
LPS+ αTNFR
LPS+ αIL10R
Kerat
DC
Neutro

Figure 5

Supplementary Figure Legends:

Figure S1: Viability is not affected by LPS activation or by receptor blocking antibodies. Cell viability of DC cultured 24 hours in the indicated blocking conditions were assessed by DAPI staining. Histograms represent the mean ± SEM of DAPI negative cell percentage.

Figure S2: Additional expression data analysis revealed distinct functions for the TNF-alpha and IL-10 loops. Listed are the top 3 functional annotations predicted/ proposed for the TNF-alpha loop signature with the matching corrected p-value by MSigDB (Liberzon et al., 2011).

Figure S3: Exogenous IL-10 inhibits LPS-induced secretion of factors for the IL-10 loop signature. Histogram representation (means ± SD) demonstrating inhibited secretion of four factors by LPS-DC in the presence of exogenous IL-10 (10ng/ml) or blocking IL10R. Data represent mean ± SD, n=7, * $p<0.05$, ** $p<0.01$, *** $p<0.001$ (paired t-test).

Figure S4: Quantification of global communication scores. (A) Numerical details related to the connectivity maps from DC to the selected target cells. Starting from 51 ligands present in one of the signatures corresponding to LPS, LPS+αTNFR, LPS+αIL10R, 96 possible ligand/receptor interactions were identified from our curated database. However, 4 ligand/receptor interactions could not be assessed because one of the components necessary for the interactions had been filtered out during pre-processing of DC data, or because it was not annotated in Jetset. **(B)** The global communication score from DC to target cells (see methods or details). The numerical values are contained in the supplementary table 2C-E. **(C)** Numerical details related to the connectivity maps from the selected target cells to DC. Criteria for excluding interactions were defined as for panel. **(D)** The global communication score from the target cells to DC (see methods or details). The numerical values are contained in the supplementary table 3M-N.

Figure S5: Observed effect on communication partner-cells is not due to the presence of residual αIL10R antibody or a potent LPS dose. (A) Neutrophils cultured for 1h with 1ng/ml LPS were not significantly activated compared to medium as assessed by surface expression of CD11b and CD62L by flow cytometry. Data represent mean ±SEM, n=3. **(B)** CD4 Naive T cells were pre-treated with blocking antibody for IL-10 receptor or a non-specific one and then put in culture with DC as indicated for 6d. After restimulation with anti-

CD3/anti-CD28 for 24h, supernatants were analyzed for the presence of IL-17F. Histogram represent means ± SEM (n= 4 donors). **(C)** HaCat cells were pre-treated with blocking antibody for IL-10 receptor or a non-specific one and then put in culture with DCs supernatant (diluted 1:10) as indicated for 4h. RNA was then extracted from cells and the expression of TNF and IL-1b was assayed using qRT-PCR. Data represent mean ±SD, n=4. **(D)** pDCs were pre-treated with blocking antibody for IL-10 receptor or a non-specific one and then put in culture with DCs supernatant (diluted 1:10) as indicated for 24h. Expression of maturation markers CD86 and ICOSL analysed by flow cytometry. Data represent mean ± SEM, n=6.

Figure S6: T cells polarization is linked to ligands found in the IL-10 loop signature. Correlation circle of a scaled PCA performed on the mean of DC outputs (grey line). 7 T-helper secreted cytokines were added to the graph (black dashed line) (n=10).

Supplementary Tables Legends:

Supplementary Table 1: (A,B) Lists of the differential expressed genes at 4 hours (A) or 8 hours (B), differential analysis was performed using an ANOVA test (function *anova1*) for these two time points. P-values were adjusted for multiple testing using the Benjamini-Hochberg correction using the function *mafdr*. Adjusted p-values <5% were considered significant. **(C, D, E)** List of genes whose expression pattern was specific for the conditions LPS (C), LPS+ αTNFR (D) or LPS+αIL10R (E), determined by the function *rankfeature* using a cutoff of 4. **(F, G, H)** Analysis of functional inference using the Molecular Signature Databases. Two cut-offs are presented, a more stringent cutoff (G) and a less stringent cutoff (H).

Supplementary Table 2: (A) List of the genes annotated in the GO term "positive regulation of cell communication" (GO:0010647) **(B)** Manually curated database of ligand and their corresponding receptors. The different receptor and ligand chains are detailed. **(C,D)** cell-specific expression level of the ligands (C) and receptors (D) of interest extracted from a database of transcriptional data from human primary cells . All the cell-specific transcriptional profiles used in the analysis were generated with the U133 Plus 2.0 Array, which limits the platform-related bias. If multiple probes corresponded to the same receptor, we selected the optimal probe based on the Jetset optimality condition. **(E)** Table showing the different abbreviations used in the analysis together with their full names.

Supplementary Table 3: (A-L) Scores corresponding to each interaction and each target cell in the experimental condition of IL10R blocking. The name of each target cell from A to L is indicated as the first entry of each table. **(M-N)** Global communication scores for both outflow (M) and inflow (N) connectivity maps. The inflow connectivity maps was done by reversing the role of DC and their cellular targets.

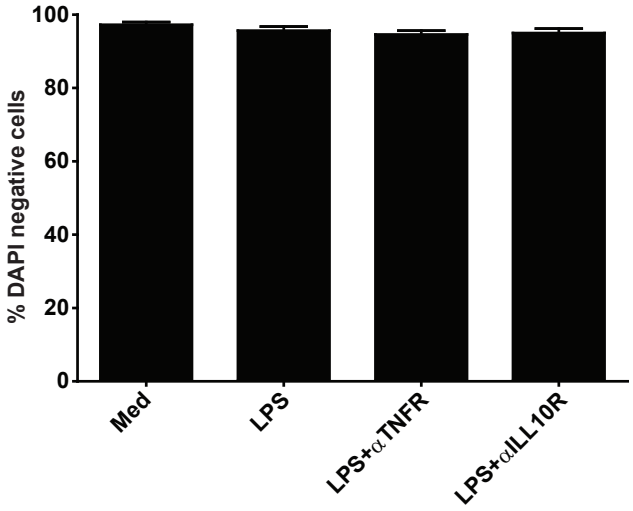
100
80
60
40
20
0
% DAPI negative cells
Med
LPS
LPS+αTNFR
LPS+αIL10R

Figure S1

Database	TermDescription	Hits	FDR
REACTOME	GPCR_LIGAND_BINDING	6	2.70E-02
REACTOME	CLASS_A1_RHODOPSIN_LIKE_RECEPTORS	5	4.00E-02
REACTOME	P2Y_RECEPTORS	2	4.62E-02

Figure S2

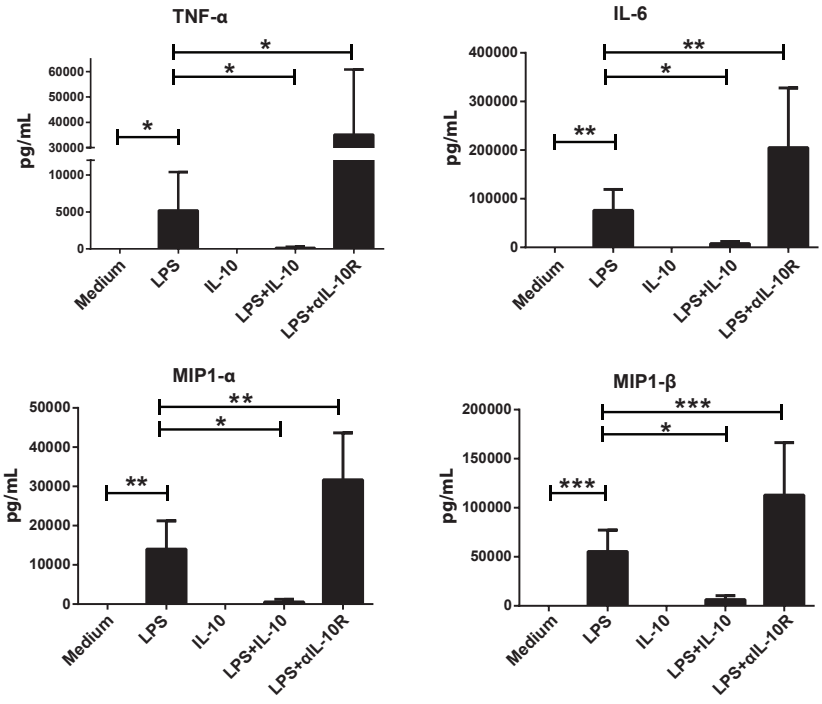
TNF-α
IL-6
MIP1-α
MIP1-β
pg/mL
Medium
LPS
IL-10
LPS+IL-10
LPS+αIL-10R

Figure S3

A

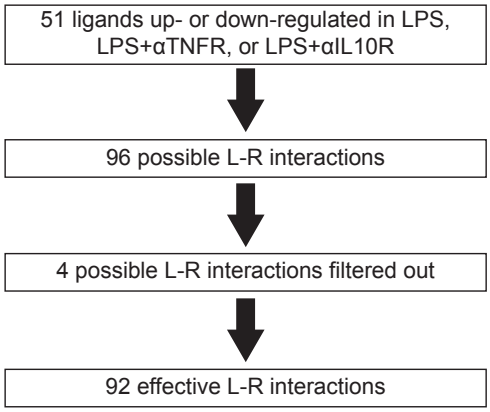

B

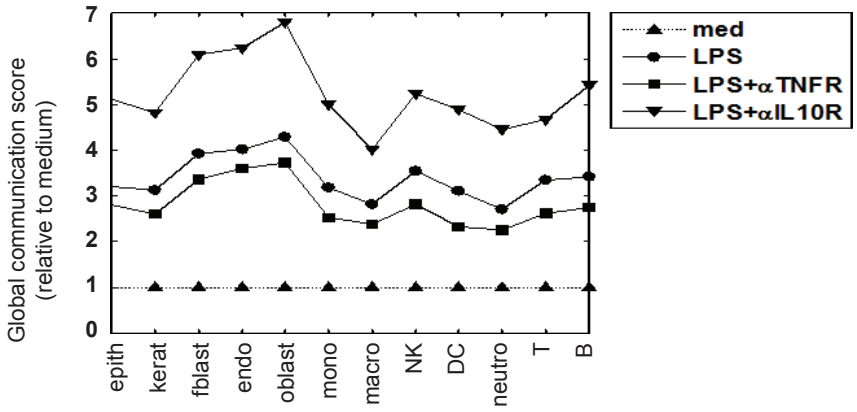

C

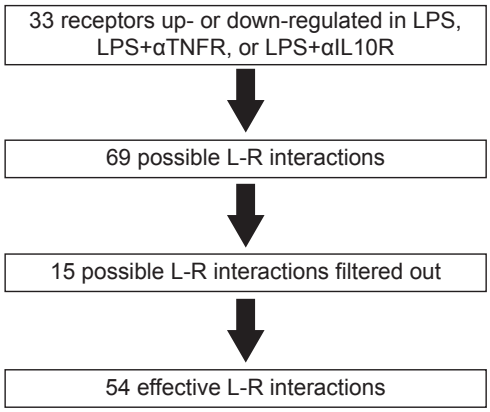

D

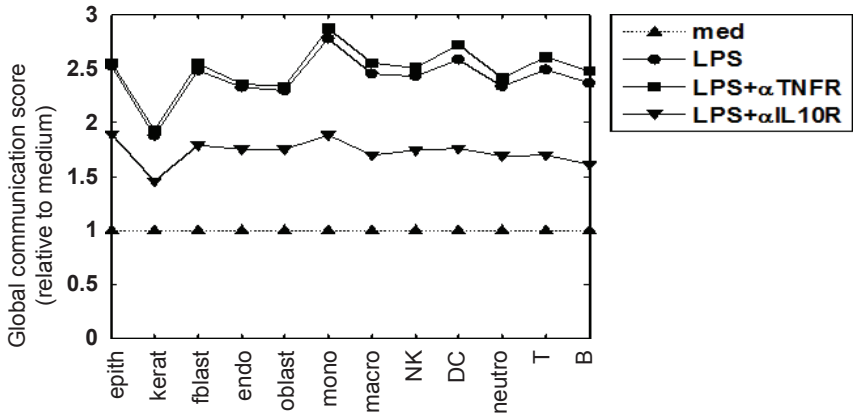

Figure S4

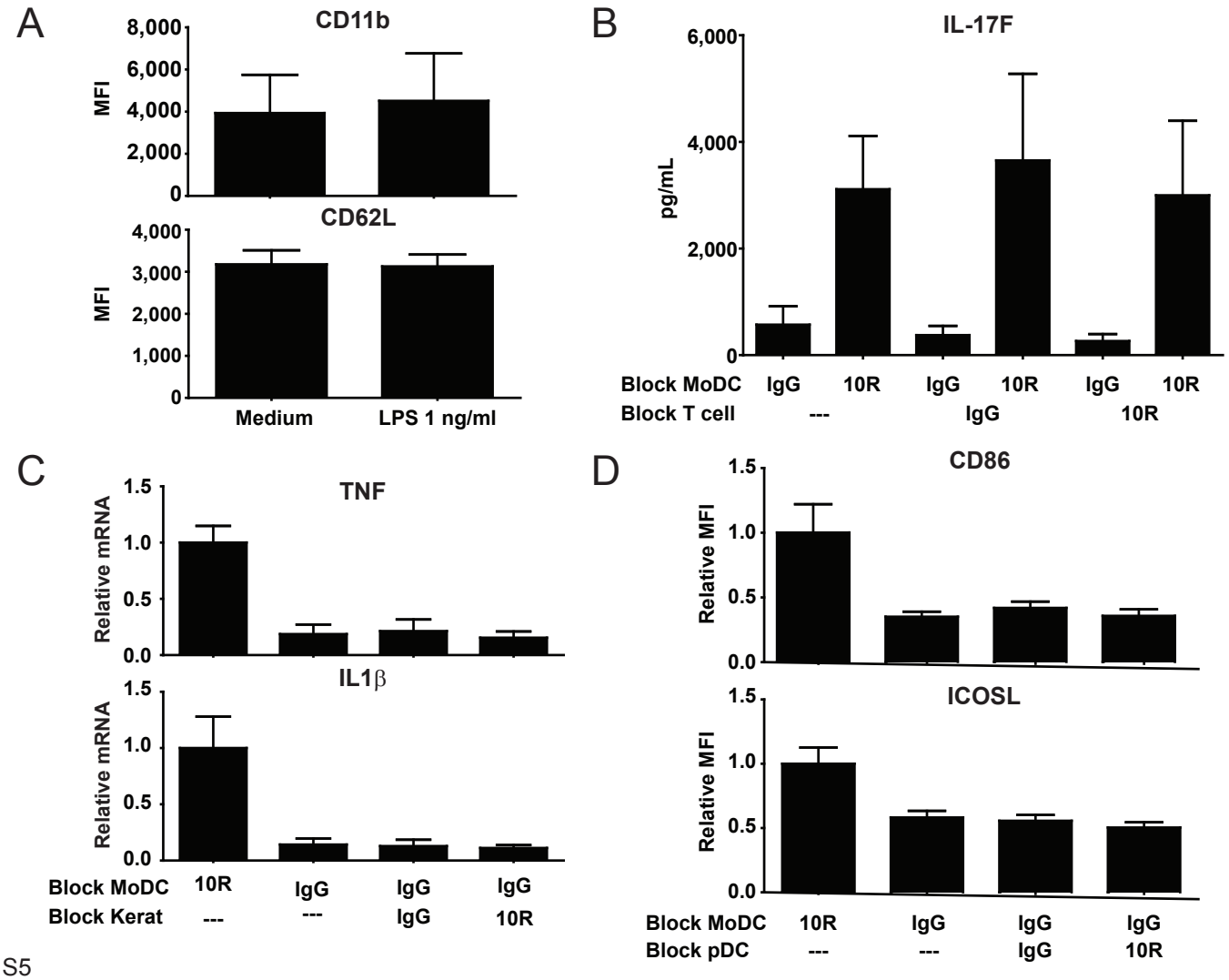
A
CD11b
MFI
8,000
6,000
4,000
2,000
0
CD62L
MFI
4,000
3,000
2,000
1,000
0
Medium
LPS 1 ng/ml
B
IL-17F
pg/mL
6,000
4,000
2,000
0
Block MoDC
IgG
10R
IgG
10R
IgG
10R
Block T cell

IgG
10R
C
TNF
Relative mRNA
1.5
1.0
0.5
0.0
IL1β
Relative mRNA
Block MoDC
10R
IgG
IgG
IgG
Block Kerat

IgG
10R
D
CD86
Relative MFI
ICOSL
Relative MFI
Block MoDC
10R
IgG
IgG
IgG
Block pDC

IgG
10R

Figure S5

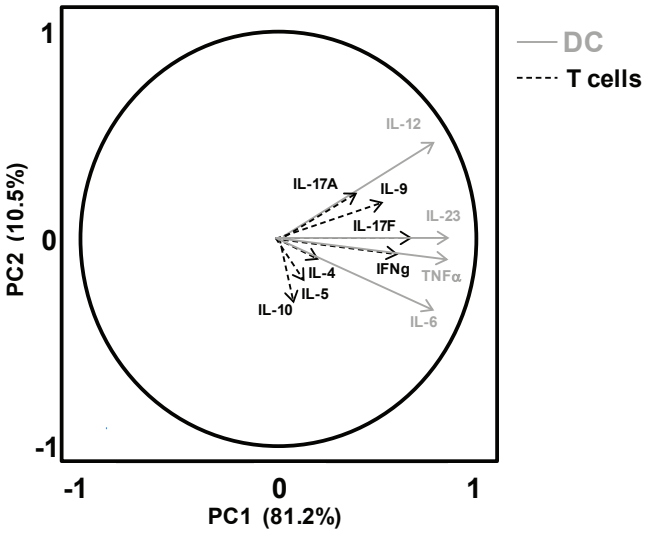
DC
T cells
IL-12
IL-17A
IL-9
IL-23
IL-17F
IFNg
TNFα
IL-4
IL-5
IL-10
IL-6
1
0
-1
PC2 (10.5%)
-1
0
1
PC1 (81.2%)

Figure S6

Chapter 4

General discussion et perspectives

Inflammation of a tissue induces changes in communication between cells creating a specific microenvironment [L. Chen et al. 2017]. The TME is a complex inflammatory network not only composed of malignant cells but also stromal and immune cells. Communications among tumor and stromal cells create a distinct cellular environment that plays a significant role in tumor development and progression [Tlsty and Coussens 2006]. In my thesis work, I aimed at understanding how the breast TME modulates the intra- and intercellular communication network formed by APCs, using a systems-level analysis.

First, I will discuss the relevance of characterizing APC subsets in breast cancer and how this work is positioned in relation to the literature. I will consider how cancer heterogeneity can impact cellular communications. Regarding the biological results I obtained, I will discuss the interferon signature found in TNBC. Additionally, I want to review the relevance of using transcriptomic data to study the intercellular communication and the microenvironmental impact on cellular behavior. I will include future perspectives on the use of a new technology that is single-cell RNA-seq to this field. Finally, I will discuss the interest and the complexity of understanding cell-to-cell communication and future developments that can be done to improve the ICELLNET tool.

4.1 Breast tumor-infiltrating APC subsets characterization

At the interface of innate and adaptive immunity, APCs are essential cells in triggering immune responses. Monocytes, macrophages and DCs present a diversity of cell types defined by their distinct phenotypes, functions and tissue localization [Collin, McGovern, and Haniffa 2013; Mildner and Jung 2014]. Several subsets have been characterized in tissues and inflammatory conditions [Mantovani et al. 2008; Segura and Amigorena 2013]. In the context of cancer, APCs and particularly DC subsets have not been described with a level of detail as we proposed in this work. In breast TME, we identified and characterized four subsets of DCs and a mix of monocytes and macrophages. pDC subset appears to be the most distinct subset

as described in other tissues [Hanahan and Weinberg 2011; Heidkamp et al. 2016; Lindstedt, Lundberg, and Borrebaeck 2005] while CD14+ DCs, apparented to inflammatory DCs [Segura, Touzot, et al. 2013], were close to cDC2 and Monomacs. The subset-specific signatures that we generated could be used in deconvolution tools, to mine publicly available transcriptomic datasets of bulk tissues. This enable to infer the immune infiltration and especially APC infiltration in breast cancer datasets as well as in other inflammatory contexts. These signatures could also be used to identify clusters of cells in single-cell RNA-seq (scRNA-seq) experiments. APCs are plastic and able to adapt to the inflammatory environment, such as during pathogen infection [Huang et al. 2001; Soumelis et al. 2015]. They can adapt according to a specific tissue-imprinting [Mora, Bono, et al. 2003]. At steady-state, however, the ontogeny is described as the predominant driver of DC subsets definition [Heidkamp et al. 2016; Miller et al. 2012]. When we compared LBC tumor- and juxta-tumor-infiltrating APC subsets, we observed that they display subset-specific transcriptional programs. This implies that APCs are able to integrate signals from the tumor and adapt their functions in a subset-dependent manner, highlighting the complex interplay between intrinsic origin of the cells and plasticity to their environment (*i.e.* tumor imprinting). This is a new vision of APC subset adaptation in a peculiar inflammatory microenvironment and it would be interesting to compare these results to APCs in other anatomical location under inflammatory conditions including invaded lymph nodes, other cancer types (*e.g.* lung cancer, head and neck cancer, lymphoma). These potential studies would shed new lights on the impact of tumor imprinting versus tissue imprinting and ontogeny on APC subset functional specialization.

4.2 Heterogeneity of tumors and impact on cellular communication

In the literature, the concept of “hot” versus “cold” tumors discriminates tumors according to the level of immune infiltration [Wargo et al. 2016]. Hot tumors present a greater T cell infiltration, chemokine and interferon expression, than cold tumors

which display lack of T cell infiltration, poor chemokine expression and minimal presence of defined immune inhibitory pathways [Gajewski, H. Schreiber, and Fu 2013]. LBCs display poor immune-infiltration on contrary to TNBCs [Stanton, Adams, and Disis 2016]. Comparing LBC tumor- and juxtatumor-infiltrating APC subsets transcriptional profiles, we did not reveal differential gene expression or functions related to immune signaling. In LBC tumor tissue, DCs do not integrate signals activating immune responses or inducing an immunosuppressive phenotype. Targeting DCs to activate them and induce anti-tumor response could have beneficial therapeutic aftermaths in LBC. On the other hand, we observed that all TNBC-infiltrating APC subsets up-regulate genes related to interferon pathways as compared to LBC-infiltrating APCs. At the light of our results and literature concepts, we can hypothesize that the heterogeneity of T cells infiltration across breast cancer subtypes modify the TME and its signaling network. Immune cell communication network is a component of the TME which has to be evaluated in order to better understand mechanisms of immune escape. As a future perspective, we want to compare APCs infiltrating cancers of a different anatomical location to find clues on the link between immune infiltration, signaling and APC subset-specific functions. We want to further study the adaptation of APC subsets in other cancer types to better understand the contributions of DCs and Monomacs to immune escape mechanisms. In the lab, we already generated transcriptional profiles of head and neck (HNSCC) tumor-infiltrating APC subsets, using the same strategy as in the breast. Analysis the three different cancer datasets (*i.e.* LBC, TNBC and HNSCC) would be a first step to evaluate how the tumor type influence the transcriptional reprogramming of APC subsets. It would also be insightful to transpose these results in another type of inflammatory disease such as autoimmune disease in order to see if APCs contribute to the inflammatory environment as in TNBC or if they are quite passive in term of immune-related functions as in LBC.

4.3 Myeloid cells and interferon, a potential therapeutic axis in TNBC?

One interesting biological feature we observed in TNBC-infiltrating APC transcriptome is the common interferon signature, which include genes related to interferon production and response with an increased expression of IFNλ (type III interferon) and IFNβ (type I interferon) in TNBC-infiltrating cDC2 and cDC1e (data not shown).

Interferons are cytokines produced by immune cells, such as dendritic cells and macrophages, following activation of innate sensors of pathogen infection, and lymphocytes. pDC are the "professional" interferon-producing cells since they constitutively express IRF7, an interferon regulatory factor. Myeloid or classical DC (mDC or cDC) also produce type I interferon, and Lauterbach et al. have shown that BDCA3$^+$ DCs from PBMCs stimulated with poly-IC are the main producers of type III interferon (IFNλ)[Lauterbach et al. 2010]. IFNγ is a potent proinflammatory cytokine secreted by CD4$^+$ Th1 lymphocytes, CD8$^+$ cytotoxic lymphocytes and NK cells.

In the context of cancer, some findings highlighted the important role and functions of type I interferons (IFNα and IFNβ) in antitumor immunity [Gough et al. 2012]. Endogenous interferon has also been shown to modulate the antitumor immune response [Gavin P Dunn et al. 2005]. In the context of TNBC tumors that fail to respond to chemotherapy, Doherty et al. showed that treatment with IFNβ represses thier cancer stem cell properties and could be used as a therapy in highly aggressive TNBC tumors [Doherty et al. 2017]. Regarding type III interferon, it can target tumor cells directly to inhibit proliferation, alter the cell cycle and induce apoptosis, as well as activate antitumor immunity [Stiff and Carson 2015].

Tumor cells, similarly to infiltrating innate immune cells and lymphocytes, are capable of producing type I interferon. Bidwell et al. described a novel immune-evasion mechanism whereby tumor cells suppressed their intrinsic secretion of type I interferon in order to metastasize successfully [Bidwell et al. 2012]. In mice, type I interferons can activate CD8$^+$ T cells and induce CTL activity [Diamond et al. 2011;

Fuertes et al. 2011]. However, it has been shown that $CD8^+$ T cells can produce IFNγ which promotes tolerogenic DCs [Jurgens et al. 2009; Mojic, Takeda, and Hayakawa 2017]. It would be interesting to perform further experiments to study the communication between interferon-producing DCs and $CD8^+$ T cells, to see if there is a feedback loop in interferon signaling in favor of tumor escape or antitumor immunity.

There is a certain interest of using interferon in cancer therapies, as it is seen in available patents and clinical trials using interferon DC-vaccine to activate T cell and induce a proper immune response [Baek et al. 2015; B. S. Parker, Rautela, and Hertzog 2016; Santini et al. 2000]. Trials of interferon therapies in solid malignancies such as melanoma, renal cell carcinoma and Kaposi sarcoma have met with varied success. The source, inducer, subtype, dose, duration and stability of the endogenous or exogenous IFN also have a major impact on outcome; as does the requirement for IFNα/β receptor (IFNAR) expression. The presence of IFNAR on T cells should be assessed to verify if type I interferon production by myeloid cells is efficient to induce activation of $CD8^+$ T cells in the TME. As suggested by Parker and collegues, the use of IFN therapy in combination with PD1targeted therapies could hold particular promise in the aggressive TNBC [B. S. Parker, Rautela, and Hertzog 2016]. This subtype of breast cancer expresses high levels of PDL1 and they have demonstrated an important role for IFN signaling in metastatic breast cancer, hence such a combination may hold great promise in a breast cancer subtype that currently has limited and untargeted treatment options. However, interferon therapies reach dose-limiting toxicities.

Finding interferon signature and correlation with checkpoint expression in myeloid cells gives hint for developing targeted therapies. However, further experiments and validation must be performed. Previously in the lab, Ghirelli et al. [Ghirelli et al. 2015] showed that IFNγ and IFNα were undetectable in breast cancer cell line supernatants. However, it would be relevant to check the level of interferons in supernatants of fresh human breast cancer samples, taking into account the complexity of the TME, and comparing LBC and TNBC. We could also consider performing a co-culture of blood DCs activated with interferon (type I and/or type III) or

tumor-infiltrating DCs and naive $CD8^+$ T cells. Then, we could study cytokines expression, T cell activation profile and DC profile using transcriptomic data analysis for instance.

4.4 Relevance of using transcriptomic data

We can argue that transcriptional profiles do not provide all information needed to assess the cell-to-cell communication. It only reveals what happen at the transcript level and not at the protein level which is the final message sensed by cells. However, it gives huge hint to infer the cellular functions impacted by a specific context and enable to study more than one molecule at a time. Using transcriptomic data of communication molecules, we were able to i) characterize tumor-infiltrating APC subsets and study their adaptation to breast TME, ii) derive subset-specific signature to assess the clinical outcome of patients, and iii) derive a communication score and find clues of cell-to-cell communication in response to specific stimuli that was experimentally validated. We can also monitor proteins to study intercellular communication but depending on the experimental setting we used, the number of parameters can become a limitation. Recently, a study described the social network architecture of immune cells and their altered communication associated with pathology using quantitative proteomics [Rieckmann et al. 2017].

4.5 Single-cell RNA-seq technology

Using single-cell RNA-seq (scRNA-seq), recent studies identified new subsets of DC in peripheral blood and proposed a new classification [See et al. 2017; Villani et al. 2017]. Single-cell technology is, indeed, a helpful tool to decipher cellular heterogeneity in tissues. In my thesis work, I analyzed APC transcriptomic profiles at the population-level, with a priori knowledge on the subset present in the breast TME. To go further on describing the heterogeneity of APCs in the context of breast cancer, we generated scRNA-seq profiles of immune cells from one sample of LBC. As preliminary results, I identified a cluster of DC which does not express genes

coding for lineage markers classically used to identify DCs [See et al. 2017; Villani et al. 2017] but express genes coding for maturation markers (*e.g.* CCR7) and checkpoint molecules (*e.g.* IDO) (Figure 4.1). In the literature, mature DCs have been characterized at the periphery of tumor but not in the tumor bed of carcinoma cells whereas tumor-infiltrating DCs exhibit an immature phenotype [Bell et al. 1999; Janco et al. 2015]. Upon maturation, DCs increase their efficacy to present processed antigens and consequently improve their capability to activate T cells [Dudek et al. 2013] whereas immature DCs found in tumors exhibit a tolerogenic phenotype, expressing PD-L1 and suppressing T cell activation [Krempski et al. 2011]. Complementary studies including experimental validation are required to define phenotype and functions of this population. If it corresponds to mature DCs, we will have to investigate why this particular LBC sample is infiltrated by mature DCs and we will need to experimentally validate the presence of this DC subset in breast cancer, for instance by FACS or processing and analysis of public single-cell datasets of immune cells infiltrating breast cancers [Azizi et al. 2018; Yin et al. 2018]. From the scRNAseq analysis, we can derive a specific gene signature for this small population. Mining public databases of breast cancer profiles with clinical outcome, as I performed in the first part of my thesis project, we can assess the correlation between this cluster of DCs and clinical outcome. These results would give cues on the relevance of targeting this population for the development of DC-targeted cancer therapy.

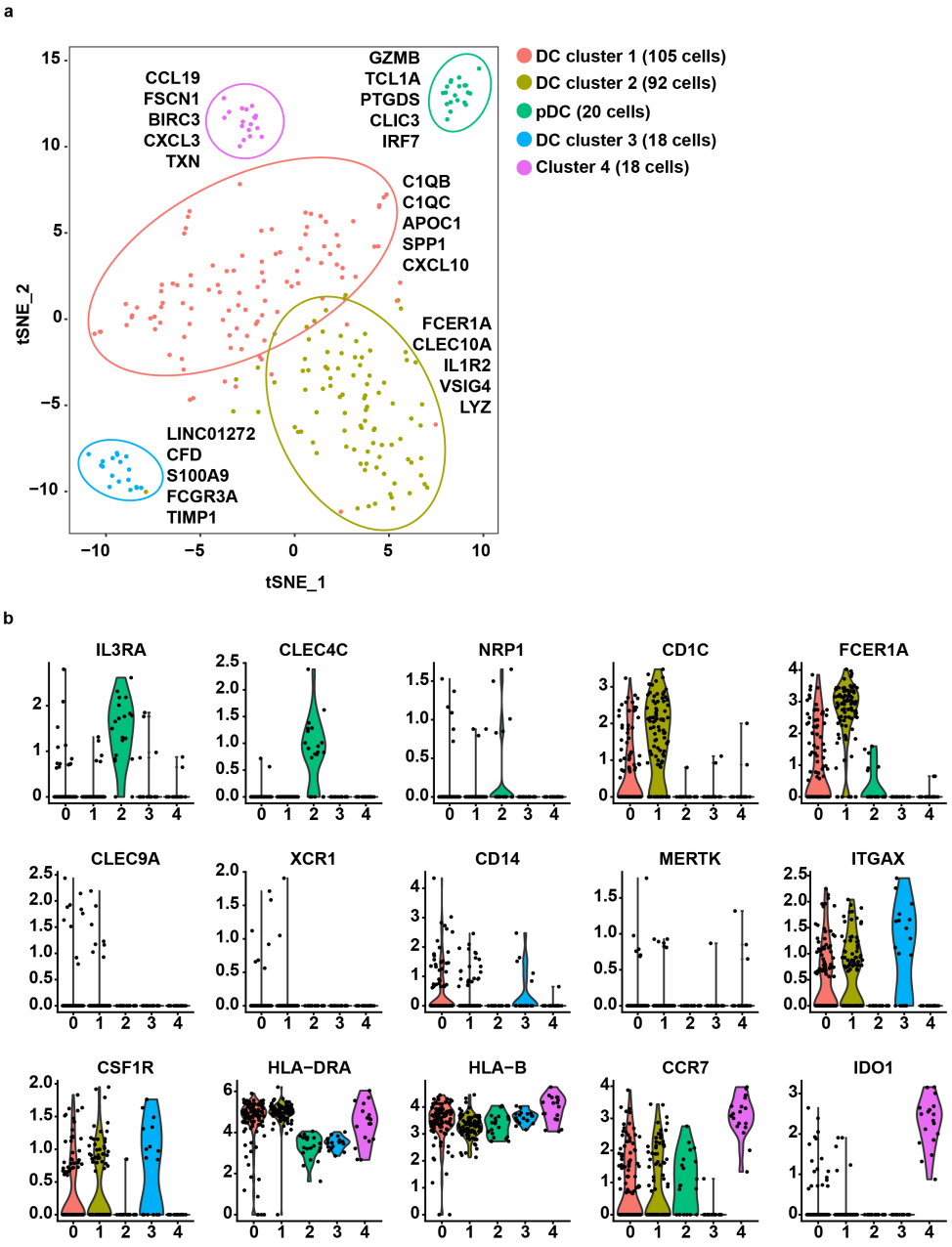

Figure 4.1: Characterization of breast tumor-infiltrating DC subsets using scRNA-seq (preliminary results). a: tSNE representation of DCs (n= 253 cells) purified from one LBC sample. Color code and ellipses indicate clusters identified by graph-based clustering, five top discriminator genes are listed next to each cluster. b: Violin plot representation of lineage markers expression in each cluster. Each dot represent a unique cell. Color code indicate the same clusters as in (a).

4.6 Complexity of intercellular communication, a challenge to study

Understanding cell-to-cell communication, and its underlying mechanisms that drive the development of cancer is essential. From a cell-to-cell communication view, mechanisms of tumor immune escape are poorly described due to the complexity and dynamic of the system: multiple cell types with distinct phenotypes and functions, multiple signals in this environment which impact cell functions and intercellular communication. To reduce this complexity, we introduced a global score summing up the intensity of all the individual channels. This greatly simplifies the interpretation and visualization of intercellular networks, but also introduces some arbitrariness when choosing to combine the individual scores. Moreover, the database of communication molecules was manually curated, despite the robustness and validity of the information it provides, the resource is focusing on immune interaction and is not exhaustive. It could be completed by adding molecules implicated in other communication modules such as cellular migration signaling. To follow up on characterizing APC subsets in the breast TME, we could also apply our ICELLNET score focusing only on immune checkpoint expression. We could generate *in silico* prediction of checkpoint activation or inhibition to assess the changes on the connectivity maps. In cancer, it can give clues on which checkpoint(s) could be an interesting target for immunotherapy development. In my thesis work, I applied the ICELLNET tool to datasets of cells from *in vitro* generated context. We hypothesize that the cellular communication network of stemming from various tissues (*e.g.* blood, skin, brain) and diseases (*e.g.* tumors, autoimmune disorders, pathogen infection) will harbour different communication patterns. As a long term future perspective, the integration of dynamical aspects of communications in the network reconstruction would give a more realistic view of cell-to-cell communication in the human body. Cells are not all frozen in one location but are able to migrate throughout the body. The interactions between cells then, appear to be part of a dynamic process in space and time which is not taken into account in most of cell-to-cell communication studies . Finally, the use of scRNA-seq data can be helpful to

decipher intercellular communication between individual cells but it is a challenging project in term of methodological development and biological interpretation [Rodda et al. 2018; Thurley, L. F. Wu, and Altschuler 2018; Yin et al. 2018].

Bibliography

Adedokun, Mary Olufunke, Comfort Wuraola Adeyemo, and Edith Oluwafunmilola Olorunsola (2010). "The Impact of Communication on Community Development". In: *Journal of Communication* 1.2, pp. 101–105. ISSN: 0976-691X. DOI: 10.1080/0976691X.2010.11884775. URL: https://doi.org/10.1080/0976691X.2010.11884775 (visited on 09/06/2018) (cit. on p. 28).

Alculumbre, Solana G. et al. (2018). "Diversification of human plasmacytoid predendritic cells in response to a single stimulus". eng. In: *Nature Immunology* 19.1, pp. 63–75. ISSN: 1529-2916. DOI: 10.1038/s41590-017-0012-z (cit. on p. 53).

Allen, Michael and J. Louise Jones (2011). "Jekyll and Hyde: the role of the microenvironment on the progression of cancer". en. In: *The Journal of Pathology* 223.2, pp. 163–177. ISSN: 1096-9896. DOI: 10.1002/path.2803. URL: https://onlinelibrary.wiley.com/doi/abs/10.1002/path.2803 (visited on 09/06/2018) (cit. on p. 35).

Allinen, Minna et al. (2004). "Molecular characterization of the tumor microenvironment in breast cancer". eng. In: *Cancer Cell* 6.1, pp. 17–32. ISSN: 1535-6108. DOI: 10.1016/j.ccr.2004.06.010 (cit. on p. 41).

Aristotle (2018). *Aristotle, Politics, Book 1, section 1253a*. URL: http://www.perseus.tufts.edu/hopper/text?doc=Perseus%3Atext%3A1999.01.0058%3Abook%3D1%3Asection%3D1253a (visited on 09/06/2018) (cit. on p. 27).

Ashburner, Michael et al. (2000). "Gene Ontology: tool for the unification of biology". In: *Nature genetics* 25.1, pp. 25–29. ISSN: 1061-4036. DOI: 10.1038/75556. URL: https://www.ncbi.nlm.nih.gov/pmc/articles/PMC3037419/ (visited on 09/08/2018) (cit. on p. 62).

Azizi, Elham et al. (2018). "Single-Cell Map of Diverse Immune Phenotypes in the Breast Tumor Microenvironment". eng. In: *Cell* 174.5, 1293–1308.e36. ISSN: 1097-4172. DOI: 10.1016/j.cell.2018.05.060 (cit. on p. 173).

Baek, Soyoung et al. (2015). "Therapeutic DC vaccination with IL-2 as a consolidation therapy for ovarian cancer patients: a phase I/II trial." eng. In: *Cellular & molecular immunology* 12.1, pp. 87–95. ISSN: 2042-0226 (Electronic). DOI: 10.1038/cmi.2014.40 (cit. on p. 171).

Banchereau, J. and R. M. Steinman (1998). "Dendritic cells and the control of immunity". eng. In: *Nature* 392.6673, pp. 245–252. ISSN: 0028-0836. DOI: 10.1038/32588 (cit. on p. 46).

Barolo, Scott and James W. Posakony (2002). "Three habits of highly effective signaling pathways: principles of transcriptional control by developmental cell signaling". en. In: *Genes & Development* 16.10, pp. 1167–1181. ISSN: 0890-9369, 1549-5477. DOI: 10.

1101/gad.976502. URL: http://genesdev.cshlp.org/content/16/10/1167 (visited on 09/06/2018) (cit. on p. 28).

Bee, Mark A. and Eli M. Swanson (2007). "Auditory masking of anuran advertisement calls by road traffic noise". In: *Animal Behaviour* 74.6, pp. 1765–1776. ISSN: 0003-3472. DOI: 10.1016/j.anbehav.2007.03.019. URL: http://www.sciencedirect.com/science/article/pii/S0003347207003314 (visited on 09/06/2018) (cit. on p. 30).

Bell, D. et al. (1999). "In breast carcinoma tissue, immature dendritic cells reside within the tumor, whereas mature dendritic cells are located in peritumoral areas". eng. In: *The Journal of Experimental Medicine* 190.10, pp. 1417–1426. ISSN: 0022-1007 (cit. on p. 173).

Bidwell, Bradley N et al. (2012). "Silencing of Irf7 pathways in breast cancer cells promotes bone metastasis through immune escape." eng. In: *Nature medicine* 18.8, pp. 1224–1231. ISSN: 1546-170X (Electronic). DOI: 10.1038/nm.2830 (cit. on p. 170).

Bindea, Gabriela et al. (2013). "Spatiotemporal dynamics of intratumoral immune cells reveal the immune landscape in human cancer". eng. In: *Immunity* 39.4, pp. 782–795. ISSN: 1097-4180. DOI: 10.1016/j.immuni.2013.10.003 (cit. on p. 32).

Bonnans, Caroline, Jonathan Chou, and Zena Werb (2014). "Remodelling the extracellular matrix in development and disease". In: *Nature reviews. Molecular cell biology* 15.12, pp. 786–801. ISSN: 1471-0072. DOI: 10.1038/nrm3904. URL: https://www.ncbi.nlm.nih.gov/pmc/articles/PMC4316204/ (visited on 09/06/2018) (cit. on p. 40).

Bonsing, Bert A. et al. (2000). "Allelotype analysis of flow-sorted breast cancer cells demonstrates genetically related diploid and aneuploid subpopulations in primary tumors and lymph node metastases". en. In: *Genes, Chromosomes and Cancer* 28.2, pp. 173–183. ISSN: 1098-2264. DOI: 10.1002/(SICI)1098-2264(200006)28:2<173::AID-GCC6>3.0.CO;2-1. URL: https://onlinelibrary.wiley.com/doi/abs/10.1002/%28SICI%291098-2264%28200006%2928%3A2%3C173%3A%3AAID-GCC6%3E3.0.CO%3B2-1 (visited on 09/06/2018) (cit. on p. 40).

Bronte, Vincenzo et al. (2016). "Recommendations for myeloid-derived suppressor cell nomenclature and characterization standards". eng. In: *Nature Communications* 7, p. 12150. ISSN: 2041-1723. DOI: 10.1038/ncomms12150 (cit. on p. 71).

Brücher, Björn Ldm and Ijaz S. Jamall (2014). "Epistemology of the origin of cancer: a new paradigm". eng. In: *BMC cancer* 14, p. 331. ISSN: 1471-2407. DOI: 10.1186/1471-2407-14-331 (cit. on p. 35).

Cella, M. et al. (1999). "Plasmacytoid monocytes migrate to inflamed lymph nodes and produce large amounts of type I interferon". eng. In: *Nature Medicine* 5.8, pp. 919–923. ISSN: 1078-8956. DOI: 10.1038/11360 (cit. on pp. 50, 51).

Chen, Daniel S. and Ira Mellman (2013). "Oncology meets immunology: the cancer-immunity cycle". eng. In: *Immunity* 39.1,

pp. 1–10. ISSN: 1097-4180. DOI: 10.1016/j.immuni.2013.07.012 (cit. on p. 43).

Chen, Linlin et al. (2017). "Inflammatory responses and inflammation-associated diseases in organs". In: *Oncotarget* 9.6, pp. 7204–7218. ISSN: 1949-2553. DOI: 10.18632/oncotarget.23208. URL: https://www.ncbi.nlm.nih.gov/pmc/articles/PMC5805548/ (visited on 09/06/2018) (cit. on pp. 34, 43, 167).

Ciaccio, Anna Laura and Tobias Bormann (2013). "The Sapir-Whorf hypothesis in the domain of colors: evidence from healthy and aphasic speakers". en. In: *Rivista Italiana di Filosofia del Linguaggio* 3, pp. 1–14. DOI: 10.4396/20131202. URL: http://www.rifl.unical.it/index.php/rifl/article/view/171/160 (visited on 09/06/2018) (cit. on p. 30).

Cohn, Lillian et al. (2013). "Antigen delivery to early endosomes eliminates the superiority of human blood BDCA3+ dendritic cells at cross presentation". eng. In: *The Journal of Experimental Medicine* 210.5, pp. 1049–1063. ISSN: 1540-9538. DOI: 10.1084/jem.20121251 (cit. on p. 50).

Collin, Matthew and Venetia Bigley (2018). "Human dendritic cell subsets: an update". In: *Immunology* 154.1, pp. 3–20. ISSN: 0019-2805. DOI: 10.1111/imm.12888. URL: https://www.ncbi.nlm.nih.gov/pmc/articles/PMC5904714/ (visited on 09/06/2018) (cit. on pp. 47, 49, 50, 52).

Collin, Matthew, Naomi McGovern, and Muzlifah Haniffa (2013). "Human dendritic cell subsets". In: *Immunology* 140.1, pp. 22–30. ISSN: 0019-2805. DOI: 10.1111/imm.12117. URL: https://www.ncbi.nlm.nih.gov/pmc/articles/PMC3809702/ (visited on 09/06/2018) (cit. on pp. 47, 58, 167).

Colonna, Marco, Giorgio Trinchieri, and Yong-Jun Liu (2004). "Plasmacytoid dendritic cells in immunity". eng. In: *Nature Immunology* 5.12, pp. 1219–1226. ISSN: 1529-2908. DOI: 10.1038/ni1141 (cit. on pp. 50, 51).

Conesa, Ana et al. (2016). "A survey of best practices for RNA-seq data analysis". eng. In: *Genome Biology* 17, p. 13. ISSN: 1474-760X. DOI: 10.1186/s13059-016-0881-8 (cit. on p. 62).

Cortés, Javier et al. (2012). "Pertuzumab Monotherapy After Trastuzumab-Based Treatment and Subsequent Reintroduction of Trastuzumab: Activity and Tolerability in Patients With Advanced Human Epidermal Growth Factor Receptor 2Positive Breast Cancer". en. In: *Journal of Clinical Oncology* 30.14, pp. 1594–1600. ISSN: 0732-183X, 1527-7755. DOI: 10.1200/JCO.2011.37.4207. URL: http://ascopubs.org/doi/10.1200/JCO.2011.37.4207 (visited on 09/06/2018) (cit. on p. 39).

Croft, David et al. (2011). "Reactome: a database of reactions, pathways and biological processes". eng. In: *Nucleic Acids Research* 39.Database issue, pp. D691–697. ISSN: 1362-4962. DOI: 10.1093/nar/gkq1018 (cit. on p. 62).

Curtis, Christina et al. (2012). "The genomic and transcriptomic architecture of 2,000 breast tumours reveals novel subgroups". In: *Nature* 486.7403, pp. 346–352. ISSN: 0028-0836. DOI: 10.1038/nature10983. URL:

https://www.ncbi.nlm.nih.gov/pmc/articles/PMC3440846/ (visited on 09/08/2018) (cit. on p. 56).

Dalod, Marc et al. (2014). "Dendritic cell maturation: functional specialization through signaling specificity and transcriptional programming". In: *The EMBO Journal* 33.10, pp. 1104–1116. ISSN: 0261-4189. DOI: 10.1002/embj.201488027. URL: https://www.ncbi.nlm.nih.gov/pmc/articles/PMC4193918/ (visited on 09/08/2018) (cit. on p. 53).

Danaei, Goodarz et al. (2005). "Causes of cancer in the world: comparative risk assessment of nine behavioural and environmental risk factors". eng. In: *Lancet (London, England)* 366.9499, pp. 1784–1793. ISSN: 1474-547X. DOI: 10.1016/S0140-6736(05)67725-2 (cit. on p. 36).

DeNardo, David G., Pauline Andreu, and Lisa M. Coussens (2010). "Interactions between lymphocytes and myeloid cells regulate pro-versus anti-tumor immunity". eng. In: *Cancer Metastasis Reviews* 29.2, pp. 309–316. ISSN: 1573-7233. DOI: 10.1007/s10555-010-9223-6 (cit. on pp. 35, 43).

DeNardo, David G., Jairo B. Barreto, et al. (2009). "CD4(+) T cells regulate pulmonary metastasis of mammary carcinomas by enhancing protumor properties of macrophages". eng. In: *Cancer Cell* 16.2, pp. 91–102. ISSN: 1878-3686. DOI: 10.1016/j.ccr.2009.06.018 (cit. on pp. 14, 71).

DeNardo, David G., Donal J. Brennan, et al. (2011). "Leukocyte Complexity Predicts Breast Cancer Survival and Functionally Regulates Response to Chemotherapy". en. In: *Cancer Discovery*. ISSN: 2159-8274, 2159-8290. DOI: 10.1158/2159-8274.CD-10-0028. URL: http://cancerdiscovery.aacrjournals.org/content/early/2011/03/17/2159-8274.CD-10-0028 (visited on 09/06/2018) (cit. on p. 43).

Dennis, Glynn et al. (2003). "DAVID: Database for Annotation, Visualization, and Integrated Discovery". In: *Genome Biology* 4.9, R60. ISSN: 1465-6906. URL: https://www.ncbi.nlm.nih.gov/pmc/articles/PMC193660/ (visited on 09/08/2018) (cit. on p. 62).

Diamond, Mark S et al. (2011). "Type I interferon is selectively required by dendritic cells for immune rejection of tumors." eng. In: *The Journal of experimental medicine* 208.10, pp. 1989–2003. ISSN: 1540-9538 (Electronic). DOI: 10.1084/jem.20101158 (cit. on p. 170).

Dillies, Marie-Agnès et al. (2013). "A comprehensive evaluation of normalization methods for Illumina high-throughput RNA sequencing data analysis". eng. In: *Briefings in Bioinformatics* 14.6, pp. 671–683. ISSN: 1477-4054. DOI: 10.1093/bib/bbs046 (cit. on pp. 60, 62).

Dobin, Alexander et al. (2013). "STAR: ultrafast universal RNA-seq aligner". en. In: *Bioinformatics* 29.1, pp. 15–21. ISSN: 1367-4803. DOI: 10.1093/bioinformatics/bts635. URL: https://academic.oup.com/bioinformatics/article/29/1/15/272537 (visited on 09/07/2018) (cit. on p. 60).

Doherty, Mary R et al. (2017). "Interferon-beta represses cancer stem cell properties

in triple-negative breast cancer." eng. In: *Proceedings of the National Academy of Sciences of the United States of America* 114.52, pp. 13792–13797. ISSN: 1091-6490 (Electronic). DOI: 10.1073/pnas.1713728114 (cit. on p. 170).

Dudek, Aleksandra M. et al. (2013). "Immature, Semi-Mature, and Fully Mature Dendritic Cells: Toward a DC-Cancer Cells Interface That Augments Anticancer Immunity". eng. In: *Frontiers in Immunology* 4, p. 438. ISSN: 1664-3224. DOI: 10.3389/fimmu.2013.00438 (cit. on p. 173).

Dunn, Gavin P., Allen T. Bruce, et al. (2002). "Cancer immunoediting: from immunosurveillance to tumor escape". eng. In: *Nature Immunology* 3.11, pp. 991–998. ISSN: 1529-2908. DOI: 10.1038/ni1102-991 (cit. on p. 42).

Dunn, Gavin P., Lloyd J. Old, and Robert D. Schreiber (2004). "The immunobiology of cancer immunosurveillance and immunoediting". eng. In: *Immunity* 21.2, pp. 137–148. ISSN: 1074-7613. DOI: 10.1016/j.immuni.2004.07.017 (cit. on p. 35).

Dunn, Gavin P et al. (2005). "A critical function for type I interferons in cancer immunoediting." eng. In: *Nature immunology* 6.7, pp. 722–729. ISSN: 1529-2908 (Print). DOI: 10.1038/ni1213 (cit. on p. 170).

Dushyanthen, Sathana et al. (2015). "Relevance of tumor-infiltrating lymphocytes in breast cancer". en. In: *BMC Medicine* 13.1. ISSN: 1741-7015. DOI: 10.1186/s12916-015-0431-3. URL: http://bmcmedicine.biomedcentral.com/articles/10.1186/s12916-015-0431-3 (visited on 09/06/2018) (cit. on p. 39).

Faget, Julien et al. (2012). "ICOS-ligand expression on plasmacytoid dendritic cells supports breast cancer progression by promoting the accumulation of immunosuppressive CD4+ T cells". eng. In: *Cancer Research* 72.23, pp. 6130–6141. ISSN: 1538-7445. DOI: 10.1158/0008-5472.CAN-12-2409 (cit. on pp. 14, 71).

Ferlazzo, Guido and Barbara Morandi (2014). "Cross-Talks between Natural Killer Cells and Distinct Subsets of Dendritic Cells". eng. In: *Frontiers in Immunology* 5, p. 159. ISSN: 1664-3224. DOI: 10.3389/fimmu.2014.00159 (cit. on p. 32).

Fuertes, M B et al. (2011). "Host type I IFN signals are required for antitumor CD8+ T cell responses through CD8{alpha}+ dendritic cells". In: *J Exp Med* 208.10, pp. 2005–2016. DOI: 10.1084/jem.20101159. URL: https://www.ncbi.nlm.nih.gov/pubmed/21930765 (cit. on p. 170).

Fuhrmann, Franziska et al. (2018). "Adequate immune response ensured by binary IL-2 and graded CD25 expression in a murine transfer model". In: *eLife* 5. ISSN: 2050-084X. DOI: 10.7554/eLife.20616. URL: https://www.ncbi.nlm.nih.gov/pmc/articles/PMC5201416/ (visited on 09/06/2018) (cit. on p. 32).

Gabrilovich, Dmitry I. and Srinivas Nagaraj (2009). "Myeloid-derived suppressor cells as regulators of the immune system". eng. In: *Nature Reviews. Immunology* 9.3, pp. 162–174. ISSN: 1474-1741. DOI: 10.1038/nri2506 (cit. on p. 43).

Gajewski, Thomas F., Hans Schreiber, and Yang-Xin Fu (2013). "Innate and adaptive immune cells in the tumor microenvironment". eng. In: *Nature Immunology* 14.10, pp. 1014–1022. ISSN: 1529-2916. DOI: 10.1038/ni.2703 (cit. on p. 169).

García-Teijido, Paula et al. (2016). "Tumor-Infiltrating Lymphocytes in Triple Negative Breast Cancer: The Future of Immune Targeting". eng. In: *Clinical Medicine Insights. Oncology* 10.Suppl 1, pp. 31–39. ISSN: 1179-5549. DOI: 10.4137/CMO.S34540 (cit. on p. 39).

Gardner, Alycia and Brian Ruffell (2016). "Dendritic Cells and Cancer Immunity". English. In: *Trends in Immunology* 37.12, pp. 855–865. ISSN: 1471-4906, 1471-4981. DOI: 10.1016/j.it.2016.09.006. URL: https://www.cell.com/trends/immunology/abstract/S1471-4906(16)30140-5 (visited on 09/06/2018) (cit. on p. 48).

Ghirelli, Cristina et al. (2015). "Breast Cancer Cell-Derived GM-CSF Licenses Regulatory Th2 Induction by Plasmacytoid Predendritic Cells in Aggressive Disease Subtypes". eng. In: *Cancer Research* 75.14, pp. 2775–2787. ISSN: 1538-7445. DOI: 10.1158/0008-5472.CAN-14-2386 (cit. on pp. 14, 32, 43, 71, 171).

Ginhoux, Florent and Martin Guilliams (2016). "Tissue-Resident Macrophage Ontogeny and Homeostasis". eng. In: *Immunity* 44.3, pp. 439–449. ISSN: 1097-4180. DOI: 10.1016/j.immuni.2016.02.024 (cit. on pp. 34, 56).

Ginhoux, Florent and Steffen Jung (2014). "Monocytes and macrophages: developmental pathways and tissue homeostasis". eng. In: *Nature Reviews. Immunology* 14.6, pp. 392–404. ISSN: 1474-1741. DOI: 10.1038/nri3671 (cit. on p. 45).

Gordon, Siamon (2003). "Alternative activation of macrophages". eng. In: *Nature Reviews. Immunology* 3.1, pp. 23–35. ISSN: 1474-1733. DOI: 10.1038/nri978 (cit. on p. 46).

Gosselin, David et al. (2014). "Environment drives selection and function of enhancers controlling tissue-specific macrophage identities". eng. In: *Cell* 159.6, pp. 1327–1340. ISSN: 1097-4172. DOI: 10.1016/j.cell.2014.11.023 (cit. on p. 34).

Gough, Daniel J et al. (2012). "Constitutive type I interferon modulates homeostatic balance through tonic signaling." eng. In: *Immunity* 36.2, pp. 166–174. ISSN: 1097-4180 (Electronic). DOI: 10.1016/j.immuni.2012.01.011 (cit. on p. 170).

Grandclaudon, Maximilien et al. (n.d.). "Th17 pathway and prognosis in Triple Negative breast cancer". In: *Manuscript in preparation* (cit. on p. 31).

Granot, Tomer et al. (2017). "Dendritic Cells Display Subset and Tissue-Specific Maturation Dynamics over Human Life". eng. In: *Immunity* 46.3, pp. 504–515. ISSN: 1097-4180. DOI: 10.1016/j.immuni.2017.02.019 (cit. on p. 50).

Greaves, Mel and Carlo C. Maley (2012). "Clonal evolution in cancer". eng. In: *Nature* 481.7381, pp. 306–313. ISSN: 1476-4687. DOI: 10.1038/nature10762 (cit. on p. 39).

Griffith, Malachi et al. (2010). "Alternative expression analysis by RNA sequencing". eng. In: *Nature Methods* 7.10, pp. 843–847. ISSN:

1548-7105. DOI: 10.1038/nmeth.1503 (cit. on p. 60).

Grouard, G. et al. (1997). "The enigmatic plasmacytoid T cells develop into dendritic cells with interleukin (IL)-3 and CD40-ligand". eng. In: *The Journal of Experimental Medicine* 185.6, pp. 1101–1111. ISSN: 0022-1007 (cit. on p. 50).

Guilliams, Martin et al. (2016). "Unsupervised High-Dimensional Analysis Aligns Dendritic Cells across Tissues and Species". eng. In: *Immunity* 45.3, pp. 669–684. ISSN: 1097-4180. DOI: 10.1016/j.immuni.2016.08.015 (cit. on pp. 50, 55, 56, 71).

Haan, Joke M. M. den, Ramon Arens, and Menno C. van Zelm (2014). "The activation of the adaptive immune system: Cross-talk between antigen-presenting cells, T cells and B cells". In: *Immunology Letters*. Dutch Society for Immunology 1964 2014 162.2, Part B, pp. 103–112. ISSN: 0165-2478. DOI: 10.1016/j.imlet.2014.10.011. URL: http://www.sciencedirect.com/science/article/pii/S016524781400220X (visited on 09/06/2018) (cit. on p. 32).

Hall, Edward T. (1976). *Beyond Culture* (cit. on p. 29).

Hanahan, Douglas and Robert A. Weinberg (2011). "Hallmarks of cancer: the next generation". eng. In: *Cell* 144.5, pp. 646–674. ISSN: 1097-4172. DOI: 10.1016/j.cell.2011.02.013 (cit. on pp. 43, 168).

Haniffa, Muzlifah, Matthew Collin, and Florent Ginhoux (2013). "Ontogeny and functional specialization of dendritic cells in human and mouse". eng. In: *Advances in Immunology* 120, pp. 1–49. ISSN: 1557-8445. DOI: 10.1016/B978-0-12-417028-5.00001-6 (cit. on pp. 47, 56).

Haniffa, Muzlifah, Amanda Shin, et al. (2012). "Human tissues contain CD141hi cross-presenting dendritic cells with functional homology to mouse CD103+ nonlymphoid dendritic cells". eng. In: *Immunity* 37.1, pp. 60–73. ISSN: 1097-4180. DOI: 10.1016/j.immuni.2012.04.012 (cit. on pp. 49, 50).

Hashimoto, Daigo et al. (2013). "Tissue-resident macrophages self-maintain locally throughout adult life with minimal contribution from circulating monocytes". eng. In: *Immunity* 38.4, pp. 792–804. ISSN: 1097-4180. DOI: 10.1016/j.immuni.2013.04.004 (cit. on p. 46).

Heidkamp, Gordon F. et al. (2016). "Human lymphoid organ dendritic cell identity is predominantly dictated by ontogeny, not tissue microenvironment". en. In: *Science Immunology* 1.6, eaai7677. ISSN: 2470-9468. DOI: 10.1126/sciimmunol.aai7677. URL: http://immunology.sciencemag.org/content/1/6/eaai7677 (visited on 09/06/2018) (cit. on pp. 50, 168).

Helmstetter, Caroline et al. (2015). "Individual T helper cells have a quantitative cytokine memory". eng. In: *Immunity* 42.1, pp. 108–122. ISSN: 1097-4180. DOI: 10.1016/j.immuni.2014.12.018 (cit. on p. 32).

Hivroz, Claire et al. (2012). "Crosstalk between T lymphocytes and dendritic cells". eng. In: *Critical Reviews in Immunology* 32.2, pp. 139–155. ISSN: 1040-8401 (cit. on p. 32).

Hooda, Yogesh and Philip M. Kim (2012). "Computational structural analysis of protein interactions and networks". eng. In:

Proteomics 12.10, pp. 1697–1705. ISSN: 1615-9861. DOI: 10.1002/pmic.201100597 (cit. on p. 32).

Huang, Q. et al. (2001). "The plasticity of dendritic cell responses to pathogens and their components". eng. In: *Science (New York, N.Y.)* 294.5543, pp. 870–875. ISSN: 0036-8075. DOI: 10.1126/science.294.5543.870 (cit. on pp. 53, 168).

Ibrahim, Ezzeldin M. et al. (2014). "The prognostic value of tumor-infiltrating lymphocytes in triple-negative breast cancer: a meta-analysis". eng. In: *Breast Cancer Research and Treatment* 148.3, pp. 467–476. ISSN: 1573-7217. DOI: 10.1007/s10549-014-3185-2 (cit. on p. 43).

Janco, Jo Marie Tran et al. (2015). "Tumor-Infiltrating Dendritic Cells in Cancer Pathogenesis". en. In: *The Journal of Immunology* 194.7, pp. 2985–2991. ISSN: 0022-1767, 1550-6606. DOI: 10.4049/jimmunol.1403134. URL: http://www.jimmunol.org/content/194/7/2985 (visited on 09/07/2018) (cit. on p. 173).

Jeong, H. et al. (2000). "The large-scale organization of metabolic networks". en. In: *Nature* 407.6804, pp. 651–654. ISSN: 1476-4687. DOI: 10.1038/35036627. URL: https://www.nature.com/articles/35036627 (visited on 09/06/2018) (cit. on p. 32).

Jin, Jun-O et al. (2014). "BDCA1-Positive Dendritic Cells (DCs) Represent a Unique Human Myeloid DC Subset That Induces Innate and Adaptive Immune Responses to Staphylococcus aureus Infection". In: *Infection and Immunity* 82.11, pp. 4466–4476. ISSN: 0019-9567. DOI: 10.1128/IAI.01851-14. URL: https://www.ncbi.nlm.nih.gov/pmc/articles/PMC4249336/ (visited on 09/06/2018) (cit. on p. 50).

Jurgens, Birgit et al. (2009). "Interferon-gamma-triggered indoleamine 2,3-dioxygenase competence in human monocyte-derived dendritic cells induces regulatory activity in allogeneic T cells." eng. In: *Blood* 114.15, pp. 3235–3243. ISSN: 1528-0020 (Electronic). DOI: 10.1182/blood-2008-12-195073 (cit. on p. 171).

Kanehisa, Minoru and Susumu Goto (2000). "KEGG: Kyoto Encyclopedia of Genes and Genomes". In: *Nucleic Acids Research* 28.1, pp. 27–30. ISSN: 0305-1048. URL: https://www.ncbi.nlm.nih.gov/pmc/articles/PMC102409/ (visited on 09/08/2018) (cit. on p. 62).

King, Mary-Claire et al. (2003). "Breast and ovarian cancer risks due to inherited mutations in BRCA1 and BRCA2". eng. In: *Science (New York, N.Y.)* 302.5645, pp. 643–646. ISSN: 1095-9203. DOI: 10.1126/science.1088759 (cit. on p. 36).

Koboldt, Daniel C. et al. (2012). "Comprehensive molecular portraits of human breast tumours". en. In: *Nature* 490.7418, pp. 61–70. ISSN: 0028-0836, 1476-4687. DOI: 10.1038/nature11412. URL: http://www.nature.com/doifinder/10.1038/nature11412 (visited on 09/06/2018) (cit. on p. 37).

Koren, Shany and Mohamed Bentires-Alj (2015). "Breast Tumor Heterogeneity: Source of Fitness, Hurdle for Therapy". eng. In: *Molecular Cell* 60.4, pp. 537–546. ISSN: 1097-4164. DOI: 10.1016/j.molcel.2015.10.031 (cit. on p. 38).

Krempski, James et al. (2011). "Tumor-Infiltrating Programmed Death Receptor-1+ Dendritic Cells Mediate Immune Suppression in Ovarian Cancer". en. In: *The Journal of Immunology*, p. 1100274. ISSN: 0022-1767, 1550-6606. DOI: 10.4049/jimmunol.1100274. URL: http://www.jimmunol.org/content/early/2011/05/06/jimmunol.1100274 (visited on 09/08/2018) (cit. on p. 173).

Kroemer, Guido et al. (2015). "Natural and therapy-induced immunosurveillance in breast cancer". eng. In: *Nature Medicine* 21.10, pp. 1128–1138. ISSN: 1546-170X. DOI: 10.1038/nm.3944 (cit. on p. 43).

Kuukasjärvi, T. et al. (1997). "Genetic heterogeneity and clonal evolution underlying development of asynchronous metastasis in human breast cancer". eng. In: *Cancer Research* 57.8, pp. 1597–1604. ISSN: 0008-5472 (cit. on p. 40).

Langmead, Ben et al. (2009). "Ultrafast and memory-efficient alignment of short DNA sequences to the human genome". In: *Genome Biology* 10.3, R25. ISSN: 1465-6906. DOI: 10.1186/gb-2009-10-3-r25. URL: https://www.ncbi.nlm.nih.gov/pmc/articles/PMC2690996/ (visited on 09/07/2018) (cit. on p. 60).

Lauterbach, Henning et al. (2010). "Mouse CD8α⁺ DCs and human BDCA3⁺ DCs are major producers of IFN-λ in response to poly IC". In: *The Journal of Experimental Medicine* 207.12, 2703 LP –2717. URL: http://jem.rupress.org/content/207/12/2703.abstract (cit. on p. 170).

León, Beatriz, María López-Bravo, and Carlos Ardavín (2007). "Monocyte-derived dendritic cells formed at the infection site control the induction of protective T helper 1 responses against Leishmania". eng. In: *Immunity* 26.4, pp. 519–531. ISSN: 1074-7613. DOI: 10.1016/j.immuni.2007.01.017 (cit. on p. 52).

Li, Christopher I. et al. (2003). "Relationship Between Long Durations and Different Regimens of Hormone Therapy and Risk of Breast Cancer". en. In: *JAMA* 289.24, pp. 3254–3263. ISSN: 0098-7484. DOI: 10.1001/jama.289.24.3254. URL: https://jamanetwork.com/journals/jama/fullarticle/196803 (visited on 09/06/2018) (cit. on p. 36).

Lindstedt, Malin, Kristina Lundberg, and Carl A. K. Borrebaeck (2005). "Gene family clustering identifies functionally associated subsets of human in vivo blood and tonsillar dendritic cells". eng. In: *Journal of Immunology (Baltimore, Md.: 1950)* 175.8, pp. 4839–4846. ISSN: 0022-1767 (cit. on p. 168).

Liotta, L. and E. Petricoin (2000). "Molecular profiling of human cancer". eng. In: *Nature Reviews. Genetics* 1.1, pp. 48–56. ISSN: 1471-0056. DOI: 10.1038/35049567 (cit. on p. 57).

Liu, Yi-Rong et al. (2016). "Comprehensive transcriptome analysis identifies novel molecular subtypes and subtype-specific RNAs of triple-negative breast cancer". eng. In: *Breast cancer research: BCR* 18.1, p. 33. ISSN: 1465-542X. DOI: 10.1186/s13058-016-0690-8 (cit. on p. 38).

Liu, Y. J. (2001). "Dendritic cell subsets and lineages, and their functions in innate and adaptive immunity". eng. In: *Cell* 106.3, pp. 259–262. ISSN: 0092-8674 (cit. on p. 53).

Liu, Yong-Jun et al. (2007). "TSLP: an epithelial cell cytokine that regulates T cell differentiation by conditioning dendritic cell maturation". eng. In: *Annual Review of Immunology* 25, pp. 193–219. ISSN: 0732-0582. DOI: 10.1146/annurev.immunol.25.022106.141718 (cit. on p. 32).

Love, Michael I, Wolfgang Huber, and Simon Anders (2014). "Moderated estimation of fold change and dispersion for RNA-seq data with DESeq2". In: *Genome Biology* 15.12. ISSN: 1465-6906. DOI: 10.1186/s13059-014-0550-8. URL: https://www.ncbi.nlm.nih.gov/pmc/articles/PMC4302049/ (visited on 09/08/2018) (cit. on p. 62).

Lysakova-Devine, Tatyana and Cliona O'Farrelly (2014). "Tissue-specific NK cell populations and their origin". eng. In: *Journal of Leukocyte Biology* 96.6, pp. 981–990. ISSN: 1938-3673. DOI: 10.1189/jlb.1RU0514-241R (cit. on p. 33).

Mabbott, Neil A. et al. (2013). "An expression atlas of human primary cells: inference of gene function from coexpression networks". In: *BMC Genomics* 14.1, p. 632. ISSN: 1471-2164. DOI: 10.1186/1471-2164-14-632. URL: https://doi.org/10.1186/1471-2164-14-632 (visited on 09/07/2018) (cit. on p. 68).

Mahmoud, Sahar M. A. et al. (2011). "Tumor-infiltrating CD8+ lymphocytes predict clinical outcome in breast cancer". eng. In: *Journal of Clinical Oncology: Official Journal of the American Society of Clinical Oncology* 29.15, pp. 1949–1955. ISSN: 1527-7755. DOI: 10.1200/JCO.2010.30.5037 (cit. on p. 43).

Malkin, D. et al. (1990). "Germ line p53 mutations in a familial syndrome of breast cancer, sarcomas, and other neoplasms". eng. In: *Science (New York, N.Y.)* 250.4985, pp. 1233–1238. ISSN: 0036-8075 (cit. on p. 36).

Mantovani, Alberto et al. (2008). "Cancer-related inflammation". eng. In: *Nature* 454.7203, pp. 436–444. ISSN: 1476-4687. DOI: 10.1038/nature07205 (cit. on p. 167).

Mao, Yan et al. (2013). "Stromal cells in tumor microenvironment and breast cancer". eng. In: *Cancer Metastasis Reviews* 32.1-2, pp. 303–315. ISSN: 1573-7233. DOI: 10.1007/s10555-012-9415-3 (cit. on pp. 41, 42, 46).

Margolin, Adam A. et al. (2006). "ARACNE: an algorithm for the reconstruction of gene regulatory networks in a mammalian cellular context". eng. In: *BMC bioinformatics* 7 Suppl 1, S7. ISSN: 1471-2105. DOI: 10.1186/1471-2105-7-S1-S7 (cit. on p. 62).

Martelotto, Luciano G. et al. (2014). "Breast cancer intra-tumor heterogeneity". eng. In: *Breast cancer research: BCR* 16.3, p. 210. ISSN: 1465-542X. DOI: 10.1186/bcr3658 (cit. on pp. 39, 40).

McGovern, Naomi et al. (2014). "Human dermal CD14 cells are a transient population of monocyte-derived macrophages". eng. In: *Immunity* 41.3, pp. 465–477. ISSN: 1097-4180. DOI: 10.1016/j.immuni.2014.08.006 (cit. on p. 46).

McNally, Luke, Sam P. Brown, and Andrew L. Jackson (2012). "Cooperation and the evolution of intelligence". en. In: *Proc. R. Soc. B* 279.1740, pp. 3027–3034. ISSN: 0962-8452, 1471-2954. DOI: 10.1098/rspb.2012.0206. URL: http://rspb.royalsocietypublishing.org/content/279/1740/3027 (visited on 09/06/2018) (cit. on p. 27).

Meacham, Corbin E. and Sean J. Morrison (2013). "Tumour heterogeneity and cancer cell plasticity". eng. In: *Nature* 501.7467, pp. 328–337. ISSN: 1476-4687. DOI: 10.1038/nature12624 (cit. on p. 39).

Medzhitov, Ruslan (2008). "Origin and physiological roles of inflammation". eng. In: *Nature* 454.7203, pp. 428–435. ISSN: 1476-4687. DOI: 10.1038/nature07201 (cit. on p. 34).

Mildner, Alexander and Steffen Jung (2014). "Development and function of dendritic cell subsets". eng. In: *Immunity* 40.5, pp. 642–656. ISSN: 1097-4180. DOI: 10.1016/j.immuni.2014.04.016 (cit. on p. 167).

Miller, Jennifer C et al. (2012). "Deciphering the transcriptional network of the DC lineage". In: *Nature immunology* 13.9, pp. 888–899. ISSN: 1529-2908. DOI: 10.1038/ni.2370. URL: https://www.ncbi.nlm.nih.gov/pmc/articles/PMC3985403/ (visited on 09/08/2018) (cit. on p. 168).

Mills, J. C. et al. (2001). "DNA microarrays and beyond: completing the journey from tissue to cell". eng. In: *Nature Cell Biology* 3.8, E175–178. ISSN: 1465-7392. DOI: 10.1038/35087108 (cit. on p. 57).

Mojic, Marija, Kazuyoshi Takeda, and Yoshihiro Hayakawa (2017). "The Dark Side of IFN-gamma: Its Role in Promoting Cancer Immunoevasion." eng. In: *International journal of molecular sciences* 19.1. ISSN: 1422-0067 (Electronic). DOI: 10.3390/ijms19010089 (cit. on p. 171).

Mora, J. Rodrigo and Ulrich H. von Andrian (2006). "T-cell homing specificity and plasticity: new concepts and future challenges". English. In: *Trends in Immunology* 27.5, pp. 235–243. ISSN: 1471-4906, 1471-4981. DOI: 10.1016/j.it.2006.03.007. URL: https://www.cell.com/trends/immunology/abstract/S1471-4906(06)00095-0 (visited on 09/06/2018) (cit. on p. 33).

Mora, J. Rodrigo, Maria Rosa Bono, et al. (2003). "Selective imprinting of gut-homing T cells by Peyer's patch dendritic cells". eng. In: *Nature* 424.6944, pp. 88–93. ISSN: 1476-4687. DOI: 10.1038/nature01726 (cit. on p. 168).

Mortazavi, Ali et al. (2008). "Mapping and quantifying mammalian transcriptomes by RNA-Seq". eng. In: *Nature Methods* 5.7, pp. 621–628. ISSN: 1548-7105. DOI: 10.1038/nmeth.1226 (cit. on p. 60).

Mukai, Hirofumi (2010). "Treatment strategy for HER2-positive breast cancer". eng. In: *International Journal of Clinical Oncology* 15.4, pp. 335–340. ISSN: 1437-7772. DOI: 10.1007/s10147-010-0107-0 (cit. on p. 39).

Nakano, Hideki et al. (2009). "Blood-derived inflammatory dendritic cells in lymph nodes stimulate acute T helper type 1 immune responses". eng. In: *Nature Immunology* 10.4, pp. 394–402. ISSN: 1529-2916. DOI: 10.1038/ni.1707 (cit. on p. 52).

Newman, Aaron M et al. (2015). "Robust enumeration of cell subsets from tissue expression profiles." In: *Nature methods* 12.MAY 2014, pp. 1–10. ISSN: 1548-7105. DOI: 10.1038/nmeth.3337. URL: http://www.nature.com/doifinder/10.1038/nmeth.3337%7B%5C%%7D5Cnhttp://www.ncbi.nlm.nih.gov/pubmed/25822800 (cit. on p. 57).

Newman, M. E. J. (2003). "The structure and function of complex networks". In: *SIAM Review* 45.2, pp. 167–256. ISSN: 0036-1445, 1095-7200. DOI: 10.1137/S003614450342480. URL: http://arxiv.org/abs/cond-mat/0303516 (visited on 09/06/2018) (cit. on p. 31).

Newport, M. J. et al. (1996). "A mutation in the interferon-gamma-receptor gene and susceptibility to mycobacterial infection". eng. In: *The New England Journal of Medicine* 335.26, pp. 1941–1949. ISSN: 0028-4793. DOI: 10.1056/NEJM199612263352602 (cit. on p. 29).

Niel, Guillaume van, Gisela D'Angelo, and Graça Raposo (2018). "Shedding light on the cell biology of extracellular vesicles". eng. In: *Nature Reviews. Molecular Cell Biology* 19.4, pp. 213–228. ISSN: 1471-0080. DOI: 10.1038/nrm.2017.125 (cit. on p. 26).

Niklas, Karl J. and Stuart A. Newman (2013). "The origins of multicellular organisms". eng. In: *Evolution & Development* 15.1, pp. 41–52. ISSN: 1525-142X. DOI: 10.1111/ede.12013 (cit. on p. 28).

Nizzoli, Giulia et al. (2013). "Human CD1c+ dendritic cells secrete high levels of IL-12 and potently prime cytotoxic T-cell responses". eng. In: *Blood* 122.6, pp. 932–942. ISSN: 1528-0020. DOI: 10.1182/blood-2013-04-495424 (cit. on p. 50).

O'Doherty, U. et al. (1994). "Human blood contains two subsets of dendritic cells, one immunologically mature and the other immature". eng. In: *Immunology* 82.3, pp. 487–493. ISSN: 0019-2805 (cit. on pp. 50, 51).

Ojalvo, Laureen S., William King, et al. (2009). "High-density gene expression analysis of tumor-associated macrophages from mouse mammary tumors". eng. In: *The American Journal of Pathology* 174.3, pp. 1048–1064. ISSN: 1525-2191. DOI: 10.2353/ajpath.2009.080676 (cit. on p. 62).

Ojalvo, Laureen S., Charles A. Whittaker, et al. (2010). "Gene Expression Analysis of Macrophages That Facilitate Tumor Invasion Supports a Role for Wnt-Signaling in Mediating Their Activity in Primary Mammary Tumors". en. In: *The Journal of Immunology* 184.2, pp. 702–712. ISSN: 0022-1767, 1550-6606. DOI: 10.4049/jimmunol.0902360. URL: http://www.jimmunol.org/content/184/2/702 (visited on 09/08/2018) (cit. on pp. 13, 67).

Okabe, Yasutaka and Ruslan Medzhitov (2016). "Tissue biology perspective on macrophages". eng. In: *Nature Immunology* 17.1, pp. 9–17. ISSN: 1529-2916. DOI: 10.1038/ni.3320 (cit. on p. 34).

Olweus, J. et al. (1997). "Dendritic cell ontogeny: a human dendritic cell lineage of myeloid origin". eng. In: *Proceedings of the National Academy of Sciences of the United States of America* 94.23, pp. 12551–12556. ISSN: 0027-8424 (cit. on p. 50).

Ortuño, Daniel et al. (2011). "Embryonic Neural Stem Cell Differentiation to Aldynoglia Induced by Olfactory Bulb Ensheathing Cell-Conditioned Medium". In: ISBN: 978-953-307-196-1. DOI: 10.5772/15239 (cit. on p. 58).

Ott, Patrick A., F. Stephen Hodi, and Caroline Robert (2013). "CTLA-4 and PD-1/PD-L1 Blockade: New Immunotherapeutic Modalities with Durable Clinical Benefit in Melanoma Patients". en. In: *Clinical Cancer Research* 19.19, pp. 5300–5309. ISSN: 1078-0432, 1557-3265. DOI: 10.1158/1078-0432.CCR-13-0143. URL: http://clincancerres.aacrjournals.org/content/19/19/5300 (visited on 09/07/2018) (cit. on p. 54).

Pandis, N. et al. (1998). "Cytogenetic comparison of primary tumors and lymph node metastases in breast cancer patients". eng. In: *Genes, Chromosomes & Cancer* 22.2, pp. 122–129. ISSN: 1045-2257 (cit. on p. 40).

Parker, Belinda S, Jai Rautela, and Paul J Hertzog (2016). "Antitumour actions of interferons: implications for cancer therapy." eng. In: *Nature reviews. Cancer* 16.3, pp. 131–144. ISSN: 1474-1768 (Electronic). DOI: 10.1038/nrc.2016.14 (cit. on p. 171).

Parkin, J. and B. Cohen (2001). "An overview of the immune system". eng. In: *Lancet (London, England)* 357.9270, pp. 1777–1789. ISSN: 0140-6736. DOI: 10.1016/S0140-6736(00)04904-7 (cit. on p. 45).

Paszek, Pawel et al. (2010). "Population robustness arising from cellular heterogeneity". en. In: *Proceedings of the National Academy of Sciences* 107.25, pp. 11644–11649. ISSN: 0027-8424, 1091-6490. DOI: 10.1073/pnas.0913798107. URL: http://www.pnas.org/content/107/25/11644 (visited on 09/08/2018) (cit. on p. 32).

Peng, Dongjun et al. (2016). "Myeloid-Derived Suppressor Cells Endow Stem-like Qualities to Breast Cancer Cells through IL6/STAT3 and NO/NOTCH Cross-talk Signaling". eng. In: *Cancer Research* 76.11, pp. 3156–3165. ISSN: 1538-7445. DOI: 10.1158/0008-5472.CAN-15-2528 (cit. on p. 43).

Persson, Emma K. et al. (2013). "IRF4 transcription-factor-dependent CD103(+)CD11b(+) dendritic cells drive mucosal T helper 17 cell differentiation". eng. In: *Immunity* 38.5, pp. 958–969. ISSN: 1097-4180. DOI: 10.1016/j.immuni.2013.03.009 (cit. on p. 50).

Picardi, Ernesto et al. (2010). "Large-scale detection and analysis of RNA editing in grape mtDNA by RNA deep-sequencing". eng. In: *Nucleic Acids Research* 38.14, pp. 4755–4767. ISSN: 1362-4962. DOI: 10.1093/nar/gkq202 (cit. on p. 60).

Plantinga, Maud et al. (2013). "Conventional and monocyte-derived CD11b(+) dendritic cells initiate and maintain T helper 2 cell-mediated immunity to house dust mite allergen". eng. In: *Immunity* 38.2, pp. 322–335. ISSN: 1097-4180. DOI: 10.1016/j.immuni.2012.10.016 (cit. on p. 52).

Poli, Vittoria, Luca Fagnocchi, and Alessio Zippo (2018). *Tumorigenic Cell Reprogramming and Cancer Plasticity: Interplay between Signaling, Microenvironment, and Epigenetics*. en. DOI: 10.1155/2018/4598195. URL: https://www.hindawi.com/

journals/sci/2018/4598195/abs/ (visited on 09/06/2018) (cit. on p. 40).

Poulin, Lionel Franz et al. (2010). "Characterization of human DNGR-1+ BDCA3+ leukocytes as putative equivalents of mouse CD8alpha+ dendritic cells". eng. In: *The Journal of Experimental Medicine* 207.6, pp. 1261–1271. ISSN: 1540-9538. DOI: 10.1084/jem.20092618 (cit. on p. 50).

Prat, Aleix, Joel S. Parker, et al. (2010). "Phenotypic and molecular characterization of the claudin-low intrinsic subtype of breast cancer". eng. In: *Breast cancer research: BCR* 12.5, R68. ISSN: 1465-542X. DOI: 10.1186/bcr2635 (cit. on p. 38).

Prat, Aleix, Estela Pineda, et al. (2015). "Clinical implications of the intrinsic molecular subtypes of breast cancer". eng. In: *Breast (Edinburgh, Scotland)* 24 Suppl 2, S26–35. ISSN: 1532-3080. DOI: 10.1016/j.breast.2015.07.008 (cit. on pp. 37, 38).

Pulendran, Bali, Karolina Palucka, and Jacques Banchereau (2001). "Sensing Pathogens and Tuning Immune Responses". en. In: *Science* 293.5528, pp. 253–256. ISSN: 0036-8075, 1095-9203. DOI: 10.1126/science.1062060. URL: http://science.sciencemag.org.gate2.inist.fr/content/293/5528/253 (visited on 09/07/2018) (cit. on p. 53).

Pyfferoen, Lotte et al. (2017). "The transcriptome of lung tumor-infiltrating dendritic cells reveals a tumor-supporting phenotype and a microRNA signature with negative impact on clinical outcome". eng. In: *Oncoimmunology* 6.1, e1253655. ISSN: 2162-4011. DOI: 10.1080/2162402X.2016.1253655 (cit. on p. 62).

Quail, DF and JA Joyce (2013). "Microenvironmental regulation of tumor progression and metastasis". In: *Nature medicine* 19.11, pp. 1423–1437. ISSN: 1078-8956. DOI: 10.1038/nm.3394. URL: https://www.ncbi.nlm.nih.gov/pmc/articles/PMC3954707/ (visited on 09/06/2018) (cit. on p. 40).

Raphael, Itay et al. (2015). "T cell subsets and their signature cytokines in autoimmune and inflammatory diseases". eng. In: *Cytokine* 74.1, pp. 5–17. ISSN: 1096-0023. DOI: 10.1016/j.cyto.2014.09.011 (cit. on p. 31).

Rieckmann, Jan C. et al. (2017). "Social network architecture of human immune cells unveiled by quantitative proteomics". en. In: *Nature Immunology* 18.5, pp. 583–593. ISSN: 1529-2916. DOI: 10.1038/ni.3693. URL: https://www.nature.com/articles/ni.3693 (visited on 09/07/2018) (cit. on p. 172).

Risso, Davide et al. (2014). "Normalization of RNA-seq data using factor analysis of control genes or samples". eng. In: *Nature Biotechnology* 32.9, pp. 896–902. ISSN: 1546-1696. DOI: 10.1038/nbt.2931 (cit. on pp. 60, 62).

Rissoan, M. C. et al. (1999). "Reciprocal control of T helper cell and dendritic cell differentiation". eng. In: *Science (New York, N.Y.)* 283.5405, pp. 1183–1186. ISSN: 0036-8075 (cit. on p. 31).

Ritchie, Matthew E. et al. (2015). "limma powers differential expression analyses for RNA-sequencing and microarray studies". eng. In: *Nucleic Acids Research* 43.7, e47. ISSN:

1362-4962. DOI: 10.1093/nar/gkv007 (cit. on p. 62).

Rivenbark, Ashley G., Siobhan M. OConnor, and William B. Coleman (2013). "Molecular and Cellular Heterogeneity in Breast Cancer". In: *The American Journal of Pathology* 183.4, pp. 1113–1124. ISSN: 0002-9440. DOI: 10.1016/j.ajpath.2013.08.002. URL: https://www.ncbi.nlm.nih.gov/pmc/articles/PMC5691324/ (visited on 09/06/2018) (cit. on p. 38).

Robertson, Gordon et al. (2010). "De novo assembly and analysis of RNA-seq data". eng. In: *Nature Methods* 7.11, pp. 909–912. ISSN: 1548-7105. DOI: 10.1038/nmeth.1517 (cit. on p. 60).

Robinson, Mark D., Davis J. McCarthy, and Gordon K. Smyth (2010). "edgeR: a Bioconductor package for differential expression analysis of digital gene expression data". In: *Bioinformatics* 26.1, pp. 139–140. ISSN: 1367-4803. DOI: 10.1093/bioinformatics/btp616. URL: https://www.ncbi.nlm.nih.gov/pmc/articles/PMC2796818/ (visited on 09/08/2018) (cit. on p. 62).

Rodda, Lauren B. et al. (2018). "Single-Cell RNA Sequencing of Lymph Node Stromal Cells Reveals Niche-Associated Heterogeneity". English. In: *Immunity* 48.5, 1014–1028.e6. ISSN: 1074-7613. DOI: 10.1016/j.immuni.2018.04.006. URL: https://www.cell.com/immunity/abstract/S1074-7613(18)30143-2 (visited on 09/07/2018) (cit. on p. 176).

Sánchez-Torres, Carmen et al. (2001). "CD16+ and CD16 human blood monocyte subsets differentiate in vitro to dendritic cells with different abilities to stimulate CD4+ T cells". en. In: *International Immunology* 13.12, pp. 1571–1581. ISSN: 0953-8178. DOI: 10.1093/intimm/13.12.1571. URL: https://academic.oup.com/intimm/article/13/12/1571/655166 (visited on 09/08/2018) (cit. on p. 45).

Santini, Stefano M et al. (2000). "Type I Interferon as a Powerful Adjuvant for Monocyte-Derived Dendritic Cell Development and Activity in Vitro and in Hu-Pbl-Scid Mice". In: *The Journal of Experimental Medicine* 191.10, 1777 LP –1788. URL: http://jem.rupress.org/content/191/10/1777.abstract (cit. on p. 171).

Scheel, Christina et al. (2011). "Paracrine and autocrine signals induce and maintain mesenchymal and stem cell states in the breast". eng. In: *Cell* 145.6, pp. 926–940. ISSN: 1097-4172. DOI: 10.1016/j.cell.2011.04.029 (cit. on p. 41).

Schlitzer, Andreas et al. (2013). "IRF4 transcription factor-dependent CD11b+ dendritic cells in human and mouse control mucosal IL-17 cytokine responses". eng. In: *Immunity* 38.5, pp. 970–983. ISSN: 1097-4180. DOI: 10.1016/j.immuni.2013.04.011 (cit. on p. 50).

Schreiber, Heidi A. et al. (2013). "Intestinal monocytes and macrophages are required for T cell polarization in response to Citrobacter rodentium". eng. In: *The Journal of Experimental Medicine* 210.10, pp. 2025–2039. ISSN: 1540-9538. DOI: 10.1084/jem.20130903 (cit. on p. 52).

See, Peter et al. (2017). "Mapping the human DC lineage through the integration of

high-dimensional techniques". eng. In: *Science (New York, N.Y.)* 356.6342. ISSN: 1095-9203. DOI: 10.1126/science.aag3009 (cit. on pp. 51, 172, 173).

Seebode, Christina, Janin Lehmann, and Steffen Emmert (2016). "Photocarcinogenesis and Skin Cancer Prevention Strategies". eng. In: *Anticancer Research* 36.3, pp. 1371–1378. ISSN: 1791-7530 (cit. on p. 30).

Segura, Elodie and Sebastian Amigorena (2013). "Inflammatory dendritic cells in mice and humans". eng. In: *Trends in Immunology* 34.9, pp. 440–445. ISSN: 1471-4981. DOI: 10.1016/j.it.2013.06.001 (cit. on pp. 52, 167).

Segura, Elodie, Maxime Touzot, et al. (2013). "Human inflammatory dendritic cells induce Th17 cell differentiation". eng. In: *Immunity* 38.2, pp. 336–348. ISSN: 1097-4180. DOI: 10.1016/j.immuni.2012.10.018 (cit. on pp. 52, 168).

Selvaraj, Saravanakumar and Jeyakumar Natarajan (2011). "Microarray Data Analysis and Mining Tools". In: *Bioinformation* 6.3, pp. 95–99. ISSN: 0973-2063. URL: https://www.ncbi.nlm.nih.gov/pmc/articles/PMC3089881/ (visited on 09/07/2018) (cit. on p. 57).

Seo, A. N. et al. (2013). "Tumour-infiltrating CD8+ lymphocytes as an independent predictive factor for pathological complete response to primary systemic therapy in breast cancer". eng. In: *British Journal of Cancer* 109.10, pp. 2705–2713. ISSN: 1532-1827. DOI: 10.1038/bjc.2013.634 (cit. on p. 43).

Shi, Fu-Dong et al. (2011). "Organ-specific features of natural killer cells". eng. In: *Nature Reviews. Immunology* 11.10, pp. 658–671. ISSN: 1474-1741. DOI: 10.1038/nri3065 (cit. on p. 33).

Sica, Antonio and Alberto Mantovani (2012). "Macrophage plasticity and polarization: in vivo veritas". eng. In: *The Journal of Clinical Investigation* 122.3, pp. 787–795. ISSN: 1558-8238. DOI: 10.1172/JCI59643 (cit. on pp. 46, 52).

Siegal, F. P. et al. (1999). "The nature of the principal type 1 interferon-producing cells in human blood". eng. In: *Science (New York, N.Y.)* 284.5421, pp. 1835–1837. ISSN: 0036-8075 (cit. on pp. 50, 51).

Sinn, Hans-Peter and Hans Kreipe (2013). "A Brief Overview of the WHO Classification of Breast Tumors, 4th Edition, Focusing on Issues and Updates from the 3rd Edition". eng. In: *Breast Care (Basel, Switzerland)* 8.2, pp. 149–154. ISSN: 1661-3791. DOI: 10.1159/000350774 (cit. on p. 37).

Sørlie, Therese et al. (2003). "Repeated observation of breast tumor subtypes in independent gene expression data sets". en. In: *Proceedings of the National Academy of Sciences* 100.14, pp. 8418–8423. ISSN: 0027-8424, 1091-6490. DOI: 10.1073/pnas.0932692100. URL: http://www.pnas.org/content/100/14/8418 (visited on 09/06/2018) (cit. on p. 38).

Soumelis, V. et al. (2015). "Systems approaches to unravel innate immune cell diversity, environmental plasticity and functional specialization." eng. In: *Current opinion in immunology* 32, pp. 42–47. ISSN: 0952-7915.

DOI: 10.1016/j.coi.2014.12.007. URL: http://europepmc.org/abstract/med/25588554 (visited on 09/07/2018) (cit. on pp. 53, 168).

Spranger, Stefani (2016). "Mechanisms of tumor escape in the context of the T-cell-inflamed and the non-T-cell-inflamed tumor microenvironment". eng. In: *International Immunology* 28.8, pp. 383–391. ISSN: 1460-2377. DOI: 10.1093/intimm/dxw014 (cit. on p. 43).

Stagg, John and Bertrand Allard (2013). "Immunotherapeutic approaches in triple-negative breast cancer: latest research and clinical prospects". en. In: *Therapeutic Advances in Medical Oncology* 5.3, pp. 169–181. ISSN: 1758-8359. DOI: 10.1177/1758834012475152. URL: https://doi.org/10.1177/1758834012475152 (visited on 09/07/2018) (cit. on p. 53).

Stanton, Sasha E., Sylvia Adams, and Mary L. Disis (2016). "Variation in the Incidence and Magnitude of Tumor-Infiltrating Lymphocytes in Breast Cancer Subtypes: A Systematic Review". eng. In: *JAMA oncology* 2.10, pp. 1354–1360. ISSN: 2374-2445. DOI: 10.1001/jamaoncol.2016.1061 (cit. on p. 169).

Steinman, R. M. and Z. A. Cohn (1973). "Identification of a novel cell type in peripheral lymphoid organs of mice. I. Morphology, quantitation, tissue distribution". eng. In: *The Journal of Experimental Medicine* 137.5, pp. 1142–1162. ISSN: 0022-1007 (cit. on p. 46).

Stiff, Andrew and William I I I Carson (2015). "Investigations of interferon-lambda for the treatment of cancer." eng. In: *Journal of innate immunity* 7.3, pp. 243–250. ISSN: 1662-8128 (Electronic). DOI: 10.1159/000370113 (cit. on p. 170).

Stockmann, Christian et al. (2014). "The Impact of the Immune System on Tumor: Angiogenesis and Vascular Remodeling". In: *Frontiers in Oncology* 4. ISSN: 2234-943X. DOI: 10.3389/fonc.2014.00069. URL: https://www.ncbi.nlm.nih.gov/pmc/articles/PMC3986554/ (visited on 09/07/2018) (cit. on p. 43).

Sun, Yi-Sheng et al. (2017). "Risk Factors and Preventions of Breast Cancer". eng. In: *International Journal of Biological Sciences* 13.11, pp. 1387–1397. ISSN: 1449-2288. DOI: 10.7150/ijbs.21635 (cit. on p. 36).

Takaba, Hiroyuki and Hiroshi Takayanagi (2017). "The Mechanisms of T Cell Selection in the Thymus". English. In: *Trends in Immunology* 38.11, pp. 805–816. ISSN: 1471-4906, 1471-4981. DOI: 10.1016/j.it.2017.07.010. URL: https://www.cell.com/trends/immunology/abstract/S1471-4906(17)30148-5 (visited on 09/06/2018) (cit. on p. 29).

Tan, AR (2018). *Checkpoint Inhibitors in Breast Cancer: Changing the Therapeutic Landscape*. en. URL: https://am.asco.org/checkpoint-inhibitors-breast-cancer-changing-therapeutic-landscape (visited on 09/06/2018) (cit. on p. 44).

Tay, Sava et al. (2010). "Single-cell NF-kappaB dynamics reveal digital activation and analogue information processing". eng. In: *Na-*

ture 466.7303, pp. 267–271. ISSN: 1476-4687. DOI: 10.1038/nature09145 (cit. on p. 32).

Taylor, Molly A., Yong-Hun Lee, and William P. Schiemann (2011). "Role of TGF- and the tumor microenvironment during mammary tumorigenesis". eng. In: *Gene Expression* 15.3, pp. 117–132. ISSN: 1052-2166 (cit. on p. 41).

Thompson, Dawn, Aviv Regev, and Sushmita Roy (2015). "Comparative analysis of gene regulatory networks: from network reconstruction to evolution". eng. In: *Annual Review of Cell and Developmental Biology* 31, pp. 399–428. ISSN: 1530-8995. DOI: 10.1146/annurev-cellbio-100913-012908 (cit. on p. 32).

Thurley, Kevin, Lani F. Wu, and Steven J. Altschuler (2018). "Modeling Cell-to-Cell Communication Networks Using Response-Time Distributions". English. In: *Cell Systems* 6.3, 355–367.e5. ISSN: 2405-4712. DOI: 10.1016/j.cels.2018.01.016. URL: https://www.cell.com/cell-systems/abstract/S2405-4712(18)30053-X (visited on 09/08/2018) (cit. on p. 176).

Tlsty, Thea D. and Lisa M. Coussens (2006). "Tumor Stroma and Regulation of Cancer Development". In: *Annual Review of Pathology: Mechanisms of Disease* 1.1, pp. 119–150. DOI: 10.1146/annurev.pathol.1.110304.100224. URL: https://doi.org/10.1146/annurev.pathol.1.110304.100224 (visited on 09/07/2018) (cit. on p. 167).

Torres, Lurdes et al. (2007). "Intratumor genomic heterogeneity in breast cancer with clonal divergence between primary carcinomas and lymph node metastases". eng. In: *Breast Cancer Research and Treatment* 102.2, pp. 143–155. ISSN: 0167-6806. DOI: 10.1007/s10549-006-9317-6 (cit. on p. 40).

Trapnell, Cole, Lior Pachter, and Steven L. Salzberg (2009). "TopHat: discovering splice junctions with RNA-Seq". en. In: *Bioinformatics* 25.9, pp. 1105–1111. ISSN: 1367-4803. DOI: 10.1093/bioinformatics/btp120. URL: https://academic.oup.com/bioinformatics/article/25/9/1105/203994 (visited on 09/07/2018) (cit. on p. 60).

Trapnell, Cole, Adam Roberts, et al. (2012). "Differential gene and transcript expression analysis of RNA-seq experiments with TopHat and Cufflinks". In: *Nature Protocols* 7.3, pp. 562–578. ISSN: 1754-2189. DOI: 10.1038/nprot.2012.016. URL: https://www.ncbi.nlm.nih.gov/pmc/articles/PMC3334321/ (visited on 09/07/2018) (cit. on p. 60).

Trapnell, Cole, Brian A. Williams, et al. (2010). "Transcript assembly and quantification by RNA-Seq reveals unannotated transcripts and isoform switching during cell differentiation". eng. In: *Nature Biotechnology* 28.5, pp. 511–515. ISSN: 1546-1696. DOI: 10.1038/nbt.1621 (cit. on p. 60).

Travis, Ruth C. and Timothy J. Key (2003). "Oestrogen exposure and breast cancer risk". eng. In: *Breast cancer research: BCR* 5.5, pp. 239–247. ISSN: 1465-542X. DOI: 10.1186/bcr628 (cit. on p. 36).

Troester, Melissa A. et al. (2004). "Cell-type-specific responses to chemotherapeutics in

breast cancer". eng. In: *Cancer Research* 64.12, pp. 4218–4226. ISSN: 0008-5472. DOI: 10.1158/0008-5472.CAN-04-0107 (cit. on p. 38).

Turner, Nicholas C. and Jorge S. Reis-Filho (2012). "Genetic heterogeneity and cancer drug resistance". eng. In: *The Lancet. Oncology* 13.4, e178–185. ISSN: 1474-5488. DOI: 10.1016/S1470-2045(11)70335-7 (cit. on p. 40).

Viale, G. (2012). "The current state of breast cancer classification". en. In: *Annals of Oncology* 23.suppl_10, pp. x207–x210. ISSN: 0923-7534. DOI: 10.1093/annonc/mds326. URL: https://academic.oup.com/annonc/article/23/suppl_10/x207/208302 (visited on 09/06/2018) (cit. on p. 37).

Villani, Alexandra-Chloé et al. (2017). "Single-cell RNA-seq reveals new types of human blood dendritic cells, monocytes, and progenitors". eng. In: *Science (New York, N.Y.)* 356.6335. ISSN: 1095-9203. DOI: 10.1126/science.aah4573 (cit. on pp. 51, 172, 173).

Wang, Claire Q. F. et al. (2013). "IL-17 and TNF synergistically modulate cytokine expression while suppressing melanogenesis: potential relevance to psoriasis". eng. In: *The Journal of Investigative Dermatology* 133.12, pp. 2741–2752. ISSN: 1523-1747. DOI: 10.1038/jid.2013.237 (cit. on p. 32).

Wang, Liguo et al. (2010). "A statistical method for the detection of alternative splicing using RNA-seq". eng. In: *PloS One* 5.1, e8529. ISSN: 1932-6203. DOI: 10.1371/journal.pone.0008529 (cit. on p. 60).

Wang, Zhong, Mark Gerstein, and Michael Snyder (2009). "RNA-Seq: a revolutionary tool for transcriptomics". eng. In: *Nature Reviews. Genetics* 10.1, pp. 57–63. ISSN: 1471-0064. DOI: 10.1038/nrg2484 (cit. on p. 61).

Wargo, Jennifer A. et al. (2016). "Monitoring immune responses in the tumor microenvironment". eng. In: *Current Opinion in Immunology* 41, pp. 23–31. ISSN: 1879-0372. DOI: 10.1016/j.coi.2016.05.006 (cit. on pp. 13, 43, 67, 168).

Williams, Eric (2011). "Environmental effects of information and communications technologies". eng. In: *Nature* 479.7373, pp. 354–358. ISSN: 1476-4687. DOI: 10.1038/nature10682 (cit. on p. 28).

Wollenberg, A. et al. (1996). "Immunomorphological and ultrastructural characterization of Langerhans cells and a novel, inflammatory dendritic epidermal cell (IDEC) population in lesional skin of atopic eczema". eng. In: *The Journal of Investigative Dermatology* 106.3, pp. 446–453. ISSN: 0022-202X (cit. on p. 52).

Wu, Chunlei et al. (2009). "BioGPS: an extensible and customizable portal for querying and organizing gene annotation resources". eng. In: *Genome Biology* 10.11, R130. ISSN: 1474-760X. DOI: 10.1186/gb-2009-10-11-r130 (cit. on pp. 40, 58).

Wynn, Thomas A., Ajay Chawla, and Jeffrey W. Pollard (2013). "Macrophage biology in development, homeostasis and disease". eng. In: *Nature* 496.7446, pp. 445–455. ISSN: 1476-4687. DOI: 10.1038/nature12034 (cit. on pp. 45, 46).

Yeong, Joe et al. (2017). "Higher densities of Foxp3+ regulatory T cells are associated with better prognosis in triple-negative

breast cancer". eng. In: *Breast Cancer Research and Treatment* 163.1, pp. 21–35. ISSN: 1573-7217. DOI: 10.1007/s10549-017-4161-4 (cit. on p. 43).

Yin, Jianhua et al. (2018). "Comprehensive analysis of immune evasion in breast cancer by single-cell RNA-seq". en. In: *bioRxiv*, p. 368605. DOI: 10.1101/368605. URL: https://www.biorxiv.org/content/early/2018/07/13/368605 (visited on 09/08/2018) (cit. on pp. 173, 176).

Yurkovetskiy, Leonid A., Joseph M. Pickard, and Alexander V. Chervonsky (2015). "Microbiota and autoimmunity: exploring new avenues". eng. In: *Cell Host & Microbe* 17.5, pp. 548–552. ISSN: 1934-6069. DOI: 10.1016/j.chom.2015.04.010 (cit. on p. 35).

Zaba, Lisa C., James G. Krueger, and Michelle A. Lowes (2009). "Resident and "inflammatory" dendritic cells in human skin". eng. In: *The Journal of Investigative Dermatology* 129.2, pp. 302–308. ISSN: 1523-1747. DOI: 10.1038/jid.2008.225 (cit. on pp. 52, 71).

Zenewicz, Lauren A. et al. (2010). "Unraveling the genetics of autoimmunity". eng. In: *Cell* 140.6, pp. 791–797. ISSN: 1097-4172. DOI: 10.1016/j.cell.2010.03.003 (cit. on p. 35).

Zhou, Yu et al. (2017). "Prognostic value of tumor-infiltrating Foxp3+ regulatory T cells in patients with breast cancer: a meta-analysis". In: *Journal of Cancer* 8.19, pp. 4098–4105. ISSN: 1837-9664. DOI: 10.7150/jca.21030. URL: https://www.ncbi.nlm.nih.gov/pmc/articles/PMC5706013/ (visited on 09/06/2018) (cit. on p. 43).

Ziegler-Heitbrock, Loems et al. (2010). "Nomenclature of monocytes and dendritic cells in blood". eng. In: *Blood* 116.16, e74–80. ISSN: 1528-0020. DOI: 10.1182/blood-2010-02-258558 (cit. on p. 50).

Zygmunt, Beata and Marc Veldhoen (2011). "T helper cell differentiation more than just cytokines". eng. In: *Advances in Immunology* 109, pp. 159–196. ISSN: 1557-8445. DOI: 10.1016/B978-0-12-387664-5.00005-4 (cit. on p. 31).

Annexes

A Article 1: collaborative work

Progenitor hypersensivity to FLT3L generates plasmacytoid dendritic cell islands in chronic myelomonocytic leukemia

Nolwenn Lucas,[1,2,3] Matthieu Duchmann,[1] Philippe Rameau,[4] Floriane Noël,[5] Paula Michea,[5] Véronique Saada,[3] Olivier Kosmider,[6,7] Gérard Pierron,[4] Martin E Fernadez-Zapico,[8,9] Matthew T. Howard,[8,9] Rebecca L. King,[8,9] Sandrine Niyongere,[10] M'boyba Khadija Diop,[1,4] Pierre Fenaux,[11] Raphael Itzykson,[11] Christophe Willekens,[1,3] Vincent Ribrag,[1,3] Michaela Fontenay,[6,7] Eric Padron,[10] Vassili Soumelis,[5] Nathalie Droin,[1,4] Mrinal M Patnaik,[12*] Eric Solary,[1,2,3*]

Running head: Clonal PDC in chronic myelomonocytic leukemia

1 – INSERM U1170, Gustave Roussy Cancer Center, Villejuif, France.
2 – Université Paris-Sud, Faculté de Médecine, Le Kremlin-Bicêtre, France
3 – Department of Hematology, Gustave Roussy Cancer Center, Villejuif, France;
4 - INSERM US23, CNRS UMS3655 Gustave Roussy Cancer Center, Villejuif, France.
5 - INSERM U932, Institut Curie, PSL Research University, Paris, France.
6 - Inserm U1016, CNRS UMR8104, Institut Cochin, Université Paris Descartes, Paris, France.
7 - Hôpital Cochin, Service d'hématologie biologique, Paris, France
8 - Schulze Center for Novel Therapeutics, Mayo Clinic, Rochester, MN 55905, USA.
9 - Department of Health Science Research, Mayo Clinic, Rochester, MN, 55905, USA.
10 - Malignant Hematology Department, H. Lee Moffitt Cancer Center, Tampa, FL, USA.
11 - Department of Hematology, Hopital Saint Louis, Universite Paris Diderot, Paris, France.
12 - Division of Hematology, Department of Medicine, Mayo Clinic, Rochester, MN, USA.

Correspondance to

Eric Solary
Gustave Roussy Cancer Center,
114 rue Edouard Vaillant
94805 Villejuif, France
Phone: 33 1 42 11 51 58
Fax: 33 1 42 11 52 40
email: eric.solary@gustaveroussy.fr

Mrinal Patnaik
Division of Hematology,
Department of Medicine,
Mayo Clinic,
Rochester, MN, USA.
Email: Patnaik.Mrinal@mayo.edu

Metrics

Title	115 characters
Running head	46 characters
Abstract	173 words
Text count	3,951 words
Figures / Tables	6 figures, 1 table
Supplemental material	Supplemental methods, 3 figures, 2 tables

Key Points

- Clonal CD123^{high} cells that infiltrate the bone marrow of chronic myelomonocytic leukemia patients are *bona fide* plasmacytoid dendritic cells.
- Their presence correlates with Ras pathway mutations, progenitor hypersensitivity to FLT-3L and an increased risk of leukemic transformation.

Abstract

Islands of CD123^{high} cells have been commonly described in the bone marrow of patients with chronic myelomonocytic leukemia (CMML). Using a multiparameter flow cytometry assay, we detected an excess of CD123^{+} mononucleated cells that are lineage-negative, CD45^{+}, HLA-DR^{+}, BDCA-2^{+}, BDCA-4^{+} in the bone marrow of 32/159 (20%) CMML patients. Conventional and electron microscopy, cell surface markers and gene expression analyses identify these cells as *bona fide* plasmacytoid dendritic cells (pDC). These cells belong to the leukemic clone, as demonstrated by whole exome sequencing of sorted monocytes and pDC. CD34^{+} cells collected from these patients generate pDC in response to low concentrations of FMS-like tyrosine kinase 3-ligand (FLT-3L). Somatic mutations in genes encoding proteins of the Ras pathway were identified in every pDC-rich patient. An excess of pDC, which respond to Toll-like receptor agonists by producing interferon alpha and interleukin-8, correlates with regulatory T cell accumulation and an increased risk of acute leukemia transformation. Collectively, these results suggest that clonal evolution of CMML with mutated Ras pathway can generate pDC that promote disease progression.

Introduction

Plasmacytoid dendritic cells (pDC) are bone-marrow derived cells whose development relies mostly on Fms-like tyrosine kinase 3 ligand (Flt-3L)[1] and the master transcription factor TCF4.[2] Mature pDC lack most of the lineage surface markers for B, T, NK cells and monocytes but express HLA-DR, CD123 (Interleukin-3 receptor alpha, IL-3R□), CD303 (BDCA2) and CD304 (BDCA4/Neuropilin-1).[3] These cells are the most important source of type I interferons (IFN-I) following recognition of viruses or nucleic acids through Toll-Like Receptor-7 (TLR7) and TLR9.[4] They can also capture, process, and present or cross-present antigens,[5] bridging innate and adaptive immune response.[6] pDC infiltrate a variety of human neoplasms.[7] In most cases, these tumor-associated pDC are defective in IFN-I production and exert a suppressive or tolerogenic function, primarily by inducing IL-10 producing regulatory T cells.[8-11] Paradoxically, a decrease in the number of circulating pDC can also be associated with disease progression.[12,13]

Chronic myelomonocytic leukemia (CMML) is a myeloid malignancy that arises from the age-related accumulation of somatic mutations in a hematopoietic stem or progenitor cell (HSPC).[14] This disease associates cellular dysplasia with proliferative features including monocytosis.[15] Although not specific, the high incidence of *TET2*, *SRSF2*, *ASXL1* and signaling mutations (*NRAS, KRAS* and *CBL*) is characteristic of this disease.[16-17] Myeloid progenitors commonly demonstrate hypersensitivity to granulocyte macrophage-colony stimulating factor (GM-CSF).[18-19] Median overall survival of CMML patients ranges between 15 and 30 months. Approximately 25% of these patients die from disease transformation into acute myeloid leukemia (AML).[20] Allogeneic stem cell transplantation is a potentially curative therapeutic option,[21] while cytoreductive drugs and hypomethylating agents have limited impact on long-term outcome.[22]

In the 1980s, pathologists identified the presence of irregular islands of CD123-positive cells in the bone marrow and tissues of a fraction of patients with acute and chronic myeloid neoplasms, with a strong predominance in CMML.[23-26] These cells were initially described as plasmacytoid T cells because of their plasma cell-like morphology and the expression of CD4,[27] then as plasmacytoid monocytes because of the expression of monocyte markers[28]. Their precise identity, the mechanisms

promoting their generation, and their impact on disease evolution had not been explored thus far.

We show that CD123$^+$ cells infiltrating the bone marrow of CMML patients are *bona fide* pDC according to the most recent classification.[29-30] The emergence of pDC islands is selectively observed in Ras-mutated CMML in which stem and progenitor cell differentiation into pDC has become hypersensitive to FLT3L. An increase in the number of pDC, which produce type I IFN and IL-8 upon TLR stimulation, correlates with an increased risk of leukemic transformation, bringing novel insights into CMML physiopathology.

Patients and methods

Cell collection. The two cohorts were approved by institutional review boards, disease diagnoses fulfilled the WHO 2016 classification criteria,[15] cytogenetic risk was evaluated according to the CMML-specific prognostic scoring system (CPSS),[31] and samples were collected with informed content. The French cohort characteristics are in **Table 1**. Cell collection and sorting procedures are in supplemental methods. The US cohort characteristics are in **Table S1**. Biopsies were obtained at diagnosis. Cytogenetic information was available on 198 (98%), while bone marrow mononucleated cell (BMNC) DNA was available on 167 (83%) patients and subjected to a 29 gene panel targeted capture assay.[32]

Flow cytometry

BMNC and PBMC were incubated for 15 min at room temperature with Fc blocking reagent (Miltenyi Biotech) before being stained for 45-60 min at 4°C with antibodies. Subsequent intracellular staining was obtained by cell fixation with Perm/Fix (BD Biosciences) for 20 min at room temperature and Perm/Wash washing before incubation with antibodies for 60 min at 4°C. Flow analysis was performed on a BD LSRFortessa X-20 with BD FACSDiva software (BD biosciences). pDC (**Figure S1** and supplemental methods) were quantified as the fraction of PBMC or BMMC, whose count was refined using a CD33 *vs* side structure (SSC) plot, which enables elimination of residual dysplastic immature myeloid cells. We used Kaluza (Beckman Coulter, Brea, California, USA) and ModFit LT (BD biosciences) softwares for

standard flow and CFSE experiments analyses, respectively. Antibodies and cell sorting methods are in supplemental methods.

Cell morphology and immunohistochemistry

Sorted pDC were analyzed on May-Grunwald Giemsa stained cytospins. For ultrastructural studies, they were fixed in 1.6 % glutaraldehyde (v/v in 0.1 M phosphate buffer) and post-fixed with 2 % osmium tetroxide (w/v in 0.1 M phosphate buffer). Following dehydration through a graded ethanol series, they were embedded in Epon™ 812 and ultrathin sections were stained with standard uranyl acetate and lead citrate. Images were taken using a Tecnai 12 electron microscope (FEI, Eindhoven, The Netherlands). Immunohistochemistry was performed on formalin-fixed and decalcified paraffin-embedded BM biopsies (details in supplemental methods).

pDC generation and stimulation

BMNC and PBMC (2.10^6 cells/mL) were incubated for 3 hours at 37°C with TLR agonists. After washing with cold PBS (Gibco), cells were stained extracellularly, fixed, permeabilized and stained intracellularly. Analysis of intracellular cytokines is in supplemental methods. To generate pDC, $CD34^+$ cells were cultured in X-vivo 15 (Lonza, Amboise, France) supplemented with insulin 10ng/mL, liposomes 20ng/mL, thrombopoietin (TPO 50ng/mL), Stem Cell Factor (SCF 50ng/mL), Fms-Like Tyrosine Kinase 3 ligand (FLT3L 100ng/mL), and Interleukin-3 (IL-3 20ng/mL) before flow cytometry detection and analysis of generated pDC (see supplemental methods)

Cytokine measurement in bone marrow supernatants

Fresh bone marrow samples were centrifuged at 150 G for 10 min. Supernatants were collected and frozen at -80°C until analysis using mesoscale (Meso Scale Diagnostics, Rockville, Maryland, USA) technology with two panels, including a 10-plex (IFNα, IL1Rα, MIF, FLT3-L, GM-CSF, CXCL12, VEGF, TNFα, IL10 et IL17a) and a 9-plex (: IL1b, IL6, IL8, IL4, IL2Rα, IFNγ, M-CSF, MIP-1β (CCL4), TPO) panels.

Exome and transcriptome analyses

Whole exome sequencing was performed on DNA collected from sorted bone marrow T-cells ($CD3^+$), monocytes ($CD14^+$) and pDC (Lin^- $HLA\text{-}DR^+$ $CD123^{high}$ $CD11c^-$ $BDCA4^+$). Total RNA was isolated from sorted cells with Single Cell RNA Purification Kit (Norgen Biotek Corp, Canada). Detailed methods are in supplemental material.

Statistical analyses

Given the number of samples, we used nonparametric tests, including Mann Whitney test to compare continuous variables, Fischer exact to compare categorical variables and Kendall's correlation test to compare ordinal variables. The Kaplan-Meier method was used to evaluate survival data from diagnosis to death or last news. Cumulative incidence of AML transformation was computed considering death as a competing risk and univariate and multivariate analyses performed with Fine & Gray's proportional subhazards model. Multivariate analysis was performed on all variables with significant impact in univariate analyses, followed by backward stepwise selection. All statistical analyses were two-sided, retaining $p<0.05$ as statistically significant and were realized with STATA or Prism 7.

Results

CD123-positive cells infiltrate hematopoietic tissues in a fraction of CMML patients

CD123-positive cells that form irregular nodules in the bone marrow of a fraction of CMML patients (**Figure 1A)** were suggested to be pDC. To further explore the presence of pDC in bone marrow aspirate and peripheral blood, we set up a multiparametric flow cytometry assay that detects lineage-negative ($CD3^-$, $CD14^-$, $CD15^-$, $CD16^-$, $CD19^-$, $CD24^-$), CD33-negative and CD11c-negative mononucleated cells expressing CD45, CD123, HLA-DR, BDCA-2, BDCA-4 and CD4 (**Figure 1B and S1)**. Compared to age-matched healthy donor controls (24 bone marrow and 34 peripheral blood), an increased fraction of these cells was detected in mononucleated cells collected from the bone marrow of 32/159 (20%) and the peripheral blood of 22/198 (11%) CMML patients, respectively (**Figure 1C, 1D and table 1**). The cut-off value defining an increased fraction of pDC in mononucleated

cells (mean + 2SD in age-matched control samples) was calculated to be 1.2% in the bone marrow and 0.6% in the peripheral blood, respectively (**Figure 1C, 1D and S2**). Analysis of 106 matched bone marrow and peripheral blood samples demonstrated that the fraction of pDC in mononucleated cells was always higher in bone marrow than in peripheral blood (median %pDC 0.32 [0.04-0.81] in bone marrow vs 0.10 [0.02-0.26] in peripheral blood, $p<0.0001$, Wilcoxon signed rank test, **Figure S2A**). Importantly, in patients whose pDC number was below the cut-off value (pDC-poor CMML patients), the fraction of pDC was significantly lower than in healthy donor tissues ($p=0.0002$ and $p=0.004$ in bone marrow and peripheral blood, respectively, **Figure S2B & S2C**). Comparison of cell surface marker staining index only detected a slightly lower expression of BDCA-2 in pDC-poor CMML samples (**Figure S2D to S2G**). A significant correlation was observed between the fraction of pDC measured in matched blood and bone marrow samples collected from 106 individual patients (linear regression, $R^2=0.75$, $p<0.001$; **Figure 1E**). This translated into a good agreement between pDC bone marrow and peripheral blood infiltration (91.5%, Cohen's kappa coefficient=0.66). Of these 106 cases, the 11 (10%) patients with an excess of pDC in peripheral blood had pDC excess in bone marrow, whereas 9 of the 20 patients with a pDC excess in bone marrow had a normal count in peripheral blood.

CD123-positive cells that infiltrate CMML bone marrow are *bona fide* pDC.

To further validate the presence of pDC in CMML patients using a rigorous definition, we sorted $CD45^+$, Lin^-, $HLA\text{-}DR^+$, $CD123^+$, $CD11c^-$, $BDCA\text{-}4^+$ cells from CMML patient bone marrow and performed Giemsa staining demonstrating a typical plasma cell-like morphology that included a round or oval shape, an eccentric nucleus, basophilic cytoplasm, and a pale Golgi zone known as the arcoplasm (**Figure 2A**). Electron microscopic analysis of these cells showed a well-developed rough endoplasmic reticulum (RER) in an electron-dense cytoplasm (**Figure 2B**) congruent with pDC. In some cases, we also noticed cytoplasmic hyaline inclusions made of aggregates of filaments (**Figure 2B, lower panels, arrow**). Flow cytometry analyses indicated that a small fraction of these cells (always lower than 16%) expressed AXL and, among $CD33^-$ AXL^- cells, a small fraction (25.4 +/- 17.7%, n = 17) expressed CD2 (**Figure 2C and Figure S2H and S2I**), two markers that were recently demonstrated to define independent cell populations.[29,30]

We then explored the ability of CMML pDC to produce IFN by intracellular flow cytometry analysis of mononucleated cells treated with brefeldin A, which induces the cytoplasmic retention of synthesized cytokines. With this method, IFN was detected in the cytoplasm of a fraction of bone marrow (**Figure 2D**) and peripheral blood (**Figure 2E**) pDC stimulated for 6 hours with a TLR7 agonist (the guanosine analog loxoribine, 2 mM) or a TLR9 agonist (CpG ODN2395, 1 μM). We also stimulated sorted pDC with either lipopolysaccharides (LPS, 1 μg/ml), or loxoribine (2 mM), or CpG ODN2395 (1 μM), or IL-3 (10 ng/ml) for 24 hours. Those collected from pDC-rich CMML patients secreted various amounts of IFN (**Figure 2F**), tumor necrosis factor (TNF) (**Figure 2G**), IL-6 (**Figure 2H**) and IL-8 (**Figure 2I**) in response to CpG ODN2395. All of them produced IL-8 in response to loxoribine (**Figure 2I**). None of these samples had any response to LPS (**Figure 2F-I**), compatible with the lack of TLR-4 expression in human pDC.[33]

Since pDC accumulation in solid tumors has been associated with an expansion of regulatory T cells (Tregs), we measured the fraction of $CD3^+$, $CD4^+$, $CD25^{high}$, $CD127^{low}$ Tregs (**Figure S1**) in bone marrow and peripheral blood mononucleated cells of CMML patients with and without excess pDC, and in healthy donors. The fraction of Tregs among T cells was significantly higher in the bone marrow and peripheral blood of CMML patients compared to healthy donors (**Figure 2J and 2K**). The fraction of TRegs among T cells was also significantly higher in the bone marrow **(Figure 2J)** and peripheral blood (**Figure 2K**) of pDC-rich bone marrow patients. A significant correlation between pDC infiltration and the fraction of Tregs was measured in bone marrow and peripheral blood, respectively (**Figure 2J and 2K**).

CMML pDC are close to healthy donor pDC

RNA-sequencing was performed in pDC sorted from pDC-rich (n=11) and poor (n=5) CMML bone marrow samples as well as pDC-rich (n=3) and pDC poor (n-4) CMML peripheral blood samples. Gene expression in these cells were similar to that observed in pDC sorted from age-matched healthy donors (n=7) (**Figure 3A**). More specifically, genes that are known to be highly expressed in healthy donor pDC, including *HLA-DR, CD123, CLEC4C (*BDCA2*), TLR9, TLR7, NRP1* (BDCA4), *IRF7*, *LILRA4* (ILT7) and *TCF4* (E2.2) genes were also highly expressed in CMML-associated pDC. CMML derived pDC expressed lower levels of *CD5, CD2*, and *SIGLEC6* genes that characterize the recently described "AS DC" (AXL^+ SIGLEC-6^+

Dendritic Cell) population and low levels of lineage specific genes (**Figure 3A**).[29] Of note, while *AXL* mRNA was expressed in all groups tested, low levels of the protein were detected by flow analysis (**Figure 3C**). Principal component analysis performed on the 500 most variable genes across pDC from different sample origin, did not distinguish pDC sorted from pDC-rich and -poor CMML bone marrow samples and from healthy donor bone marrow (**Figure 3B**).

We also performed differential gene expression analysis. To eliminate any batch effect, we focused on a series of simultaneously analyzed bone marrow pDC collected from pDC-rich CMML (n=6), pDC-poor CMML (n=4) and healthy donor (n=3) bone marrow samples. We detected 74 differentially expressed genes (DEG) between pDC-poor and pDC-rich CMML, 13 DEG between pDC-rich CMML and healthy-donor pDC, and 144 DEG between pDC-poor CMML and healthy-donor pDC. Unsupervised hierarchical clustering indicated that these genes could discriminate the three sample categories (**Figure 3C**). Gene Ontology enrichment analysis performed using over-representation test[34,35] demonstrated a trend toward enrichment in type I interferon signaling pathway, response to type I interferon and cellular defense response in pDC from pDC-rich compared to pDC-poor CMML.

pDC bone marrow infiltration correlates with increased leukemic transformation

Since pDC infiltration has been associated with a poor outcome in diverse solid tumors, we hypothesized that pDC-rich CMML had an inferior prognostic outlook in comparison to pDC-poor CMML. The follow-up was not sufficient to analyze the outcome of CMML patients whose pDC infiltration was prospectively evaluated by flow cytometry at diagnosis. Therefore, we performed this prognostic analysis on an independent retrospective cohort of 202 patients in which pDC were detected by immunohistopathology **(Table S1).** Bone marrow was considered as “pDC-rich” when > 5% of the bone marrow cellularity per field had $CD123^+$ and $TCL1^+$ cells. pDC infiltration measured in the peripheral blood of 56 of these patients by flow cytometry was in good accordance with immunohistochemistry analyses, *i.e.* pDC over 0.6% of peripheral blood mononucleated cells were detected only in patients with pDC > 5% in the bone marrow by immunohistochemistry (**Figure 4A**). pDC enrichment of CMML bone marrow was not statistically associated with overall survival outcomes, even

when higher percentages of pDC were used as cut-offs for being considered “pDC-rich” CMML (>10%, >25% and >50%) (not shown). However, pDC-rich CMML according to bone marrow immunohistochemistry was associated with a significantly higher cumulative incidence of leukemic transformation, considering death as a competing risk (**Figure 4B**, standardized hazard ratio 2.59 [95% confidence interval (CI) 1.21-5.51]; P=0.014). Importantly, an increased bone marrow infiltration with pDC remained an independent prognostic factor in multivariate analysis (sHR 3.3 [95% CI: 1.47-7.]; p=0.004), together with peripheral blood blast cell count and immature myeloid cell fraction (**Table S2**).

Bone marrow infiltrating pDC are detected in Ras-mutated CMML

Having demonstrated that $CD123^{high}$ cells that accumulate in the bone marrow of 20% of patients with CMML are *bona-fide* pDC, we wanted to determine if their accumulation was related to specific genetic events. Using a panel of 38 genes analyzed by NGS, we first identified similar gene alterations and variant allele frequencies in sorted peripheral blood monocytes and bone marrow pDC of two CMML patients, validating that pDC were part of the leukemic clone (not shown). In the cohort of patients analyzed by flow cytometry (French cohort), we noticed that CMML with pDC-rich bone marrow demonstrated a significantly higher incidence of *NRAS* + *KRAS* + *CBL* mutations in their sorted monocytes (**Table 1**). We validated this observation in the above-mentioned, independent cohort of 202 patients analyzed by immunohistochemistry (Mayo Clinic cohort), in which we observed a significant association between the presence of *NRAS* and *CBL* mutations analyzed in bulk bone marrow mononucleated cells and bone marrow enrichment in pDC (**Table S1**).

We then sorted bone marrow pDC, peripheral blood $CD14^{+}$ monocytes, and $CD3^{+}$ T cells from 10 CMML patients, one patient developing an $FLT3\text{-}ITD^{+}$ AML as a result of CMML transformation (sample #2202) and a patient with atypical CML, another MDS/MPN (#1996). All 12 cases displayed marrow pDC enrichment, thus enabling for the sorting of a sufficient amount of pDC to perform whole exome sequencing. Whole exome sequencing of each sorted cell population was performed (**Figure 5A and Table S2**). In every CMML patient, we detected at least one (7 cases) and sometimes two or more (5 cases) somatic mutations in genes encoding proteins of the Ras pathway. These heterogeneous mutations included variants in *NRAS*, *KRAS*,

NF1, *CBL*, *PTPN11* and *MAP2K1* genes (**Figure 5A**). A significant correlation was observed between variant allele frequencies measured in monocytes and in pDC (linear regression, r^2 =0.74, p<0.0001, **Figure 5B**). Nevertheless, some clonal heterogeneity could be detected, *e.g.* in sample #2048, *NRAS* ^{G13D} identified in sorted pDC was not detected in sorted monocytes (**Figure 5C)** whereas, of the three mutations of the Ras pathway detected in sample #1829, NRAS^{A59D} was almost exclusively identified in sorted monocytes (**Figure 5D)**. Patient #2202 developed *FLT3-ITD*-driven secondary AML with *NRAS*^{G12V} being mostly detected in sorted residual monocytes (**Figure S3A**). Finally, in one bone marrow sample (#2387), we were able to sort progenitor populations.[36,37] This sample was collected from the same patient as sample # 2062 with a 10.4 months interval between the two samples collection. Analysis of somatic mutations in sorted monocytes detected the loss of a KRAS^{G60V} subclone. Five other somatic mutations showed a similar variant allele frequency in every cell compartment (**Figure S3B**).

CD34$^+$ cells from pDC-rich CMML are hypersensitive to FLT-3L

We then analyzed the ability of CD34$^+$ cells from CMML patients to generate pDC *in vitro* by culturing these cells in the presence of SCF, TPO, IL-3 and FLT3L for 30 days.[38,39] From day 15 to day 25, CD34$^+$ cells from pDC-rich CMML demonstrated a significantly increased ability to generate pDC in culture when compared to CD34$^+$ cells from pDC-poor CMML, as shown by serial flow analysis of CD34$^+$cells-derived pDC (**Figure 6A and 6B**). Morphological analysis of the generated cells using conventional microscopy (**Figure 6C, left panel**) and electron microscopy (**Figure 6C, right panel**) confirmed pDC features. Analysis of somatic variants detected the same abnormalities with similar allele frequencies in sorted fresh pDC and pDC generated in culture from CD34$^+$ cells (**Figure 6D**). Under these culture conditions, CD34$^+$ cells from pDC-rich CMML also produced a greater number of pDC as compared to cord blood CD34$^+$ cells, usually tested for pDC generation *in vitro* (**Figure 6E & 6F**). We repeated the experiments in the absence or presence of increasing amount of FLT-3L, demonstrating the ability of CD34$^+$ cells from pDC-rich CMML to produce pDC in the absence of FLT-3L and to produce more pDC in response to low concentrations of FLT-3L (**Figure 6G**). Interestingly, the level of FLT-3L measured in the supernatant of bone marrow was observed to be significantly lower in CMML patients, and this decreased FLT-3L level was more significant in

pDC-rich CMML (**Figure 6H**).

Discussion

While the number of bone marrow pDC is decreased in a majority of CMML patients in comparison to age-matched healthy controls, an increased number of pDC is detected in the bone marrow of about 20% of these patients. All the studied patients with bone marrow pDC excess demonstrated genetic alterations of the oncogenic Ras pathway and their bone marrow $CD34^+$ cells were hypersensitive to FLT3-L when induced to differentiate into pDC. The accumulation of leukemic pDC also correlated with a higher rate of regulatory T cells in the bone marrow and peripheral blood and a higher risk of AML transformation.

The presence of $CD123^{high}$ cell islands in the bone marrow of a fraction of patients has long been identified in CMML and other myeloid neoplasms.[25,40,41] This pathologic finding is distinct from blastic plasmacytoid dendritic cell neoplasms (BPDCN), a rare clonal proliferation of pDC precursors that affects elderly people and involves alterations in *MYC, RB1* and *IKAROS* gene family members.[41] Because of their plasmacytoid morphology, $CD123^{high}$ cells were considered as pDC but a definitive proof of their identity was missing. Recent analyses have suggested that $CD123^{high}$ cell population was more complex than anticipated.[29,30] Flow analysis combined with conventional and electron microscopy, gene expression analyses and cytokine production profiling in response to TLR9 and TLR7 agonists, establish these cells as authentic pDC that can be distinguished from $CD123^{high}$ "AS DC" (AXL^+, $SIGLEC6^+$) or "pre-DC" cells.[42]

pDC are the main type I IFN-producing cells.[43] IFNα has demonstrated antineoplastic effects through the activation of pDC, cytotoxic T-cells and NK cells while having context-dependent effects of CD4 T cells[44] and therapeutic benefits of IFNα was demonstrated in myeloproliferative neoplasms.[45] In multiple myeloma, in which bone marrow pDC mediate immune deficiency and promote plasma cell growth and drug resistance, CpG oligodeoxynucleotides could restore pDC immune function and abrogate pDC-induced plasma cell growth.[46] We show that CMML-associated pDC could produce IFNα after stimulation with a TLR9 agonist, although at lower level than peripheral blood pDC from young healthy donors. CMML is a disease associated with ageing[17] and pDC from age-matched healthy donors also produced lower levels of IFNα than pDC from younger healthy donors. The heterogeneous level of IFNα produced by CMML pDC could indicate the differential amplification of

pDC subpopulations that diversely react to a given individual stimulus under control of a TNF autocrine and/or paracrine communication loop.[47] Therefore, pDC stimulation may not necessarily be sufficient to restore pDC immune function and generate therapeutically active levels of IFNα.

An alternative approach would be to inhibit the effect of cytokines produced by pDC. Cytokines produced by mature cells of the leukemic clone modulate normal and leukemic progenitor differentiation in a mouse model of myeloproliferative neoplasm,[48] a regulatory loop demonstrated to be a potential therapeutic target in chronic myeloid leukemia.[49] The heterogeneous production of IFNα by CMML associated pDC contrasts with IL-8 production, especially when these cells are stimulated with TLR7 agonists. While the primary function of this chemokine is the attraction and degranulation of neutrophils,[50] IL-8 can also promote the survival and self-renewal of hematopoietic stem cells. [51] Elevated IL-8 secretion has been detected in AML and MDS[52,53] and inhibition of its receptor CXCR2 could selectively inhibit the proliferation of MDS/AML cells,[54] indicating IL-8 as a potential therapeutic target in CMML patients with an excess of pDC.

Flt3-L and GM-CSF have a concerted effect on myeloid cell homeostasis[55] with Flt3-L supporting the development of pDC through TCF4 and IRF8 and GM-CSF antagonizing this effect through STAT5 activation.[56] Hypersensitivity to GM-CSF is a common feature of CMML myeloid progenitors,[19] which could account for the decreased number of pDC in the bone marrow of most CMML patients. The contrasting amplification of pDC detected in 20% of these patients suggests that pDC development escapes the inhibitory effect of GM-CSF, which may be related to additional genetic alterations of signaling pathways, including Ras pathway alterations and FLT3-ITD, promoting pDC development through enhanced progenitor sensitivity to FLT3-L. This is in contrast with a significantly decreased level of FLT-3L in the bone marrow environment (this paper) and the peripheral blood of CMML patients,[57] which appears to be unique among myeloid malignancies.[58]

High risk MDS clones expand in a tolerant and immunosuppressive environment that involves $CD4^+$ Treg expansion and myeloid-derived suppressive cells.[59-61] Similarly, IFN-α-deficient pDC that accumulate in aggressive human tumors promote the expansion of disease-associated Tregs, which contribute to tumor immune tolerance and poor clinical outcome.[62] In CMML, the correlated expansion of pDs and

$CD4^+$ Tregs may contribute to the higher risk of progression into acute leukemia. Whatever their biological effects, therapeutic targeting of pDC, *e.g.* through the use of an IL-3R□-targeted monoclonal antibody,[63] could deserve to be tested in CMML patients with clonal pDC expansion.

Acknowledgements: This work was supported by grants from the Ligue Nationale Contre le Cancer (Equipe Labellisée), the National Cancer Institute (INCa PL-BIO and PRT-K calls), the Molecular Medicine in Oncology program supported by the Agence Nationale de la Recherche, and the SIRIC SOCRATE program. NL was supported by a grant from the Ligue Nationale Contre le Cancer, MD by the ITMO Cancer (Plan cancer 2014-2019). Part of high-throughput sequencing was performed by the genomic platform of the Institut Curie, which is supported by grants ANR-10-EQPX-03 and ANR10-INBS-09-08 from the Agence Nationale de la Recherche (Investissements d'Avenir) and by Cancéropole Ile de France. We are grateful to Sylvain Baulande and Patricia Legoix-Ne from the genomic platform of Curie Institute and Karine Bailly from the Cochin Institute cytometry and immunobiology facility for their technical support, and to Abdelkrim Achibet from the orthopedic surgery department from the hospital of Le Mans for providing us with bone marrow controls.

Authorship contribution: NL and MD collected the samples and performed the experiments, PR set up and performed flow analyses, FN and PM analyzed RNA sequencing data, VS and OK performed conventional microscopy, GP the electron microcopy analysis, MEFZ, MTH and RLK the immunohistochemistry, SN and EP measured FLT-3L in bone marrow plasma, MKD analyzed whole exome sequencing data, PF, RI, CW, VR and MF provided patient samples, ND supervised genomic analyses, ES wrote the manuscript, MF, VS, MMP corrected the manuscript, MMP and ES supervised the whole project.

Disclosure of Conflicts of Interest : None

References

1. Waskow, C., Liu, K., Darrasse-Jèze, G., et al. FMS-like tyrosine kinase 3 is required for dendritic cell development in peripheral lymphoid tissues. *Nat Immunol.* 2008;9(6):676-683.

2. Cisse B, Caton ML, Lehner M, et al. Transcription Factor E2-2 Is an Essential and Specific Regulator of Plasmacytoid Dendritic Cell Development.*Cell*. 2008;135(1):37-48.

3. Guilliams M, Ginhoux F, Jakubzick C, et al. Dendritic cells, monocytes and macrophages: a unified nomenclature based on ontogeny. *Nat Rev Immunol*. 2014;14(8):571-8.

4. Siegal FP, Kadowaki N, Shodell M, et al. The nature of the principal type 1 interferon-producing cells in human blood. *Science*. 1999;284(5421):1835-7.

5. Villadangos JA, Young L. Antigen-Presentation Properties of Plasmacytoid Dendritic Cells. I*mmunity*. 2008;29(3):352-61.

6. Kadowaki N, Antonenko S, Lau JY-N, Liu Y-J. Natural Interferon α/β–Producing Cells Link Innate and Adaptive Immunity. *J Exp Med.* 2000;192(2):219-26.

7. Vermi W, Soncini M, Melocchi L, Sozzani S, Facchetti F. Plasmacytoid dendritic cells and cancer. *J Leukoc Biol.* 2011;90(4):681-90.

8. Zou W, Machelon V, Coulomb-L'Hermin A, et al. Stromal-derived factor-1 in human tumors recruits and alters the function of plasmacytoid precursor dendritic cells. *Nat Med*. 2001;7(12):1339-46.

9. Wei S, Kryczek I, Zou L, et al. Plasmacytoid Dendritic Cells Induce CD8+ Regulatory T Cells In Human Ovarian Carcinoma. *Cancer Res*. 2005;65(12):5020-6.

10. Conrad C, Gregorio J, Wang Y-H, et al. Plasmacytoid Dendritic Cells Promote Immunosuppression in Ovarian Cancer via ICOS Costimulation of Foxp3+ T-Regulatory Cells. *Cancer Res.* 2012;72(20):5240-9.

11.Demoulin S, Herfs M, Delvenne P, Hubert P. Tumor microenvironment converts plasmacytoid dendritic cells into immunosuppressive/tolerogenic cells: insight into the molecular mechanisms. *J Leukoc Biol*. 2013;93(3):343-52.

12. Hishizawa M, Imada K, Kitawaki T, Ueda M, Kadowaki N, Uchiyama T. Depletion and impaired interferon-α-producing capacity of blood plasmacytoid dendritic cells in human T-cell leukaemia virus type I-infected individuals. *Br J Haematol*. 2004;125(5):568-75.

13. Mami NB, Mohty M, Aurran-Schleinitz T, Olive D, Gaugler B. Blood dendritic cells in patients with chronic lymphocytic leukaemia. *Immunobiology*. 2008;213(6):493-8.

14. Deininger MWN, Tyner JW, Solary E. Turning the tide in myelodysplastic / myeloproliferative neoplasms. *Nat Rev Cancer*. 2017;17(7):425-40.

15. Arber DA, Orazi A, Hasserjian R, et al. The 2016 revision to the World Health Organization classification of myeloid neoplasms and acute leukemia. *Blood*. 2016;127(20):2391-405.

16. Itzykson R, Kosmider O, Renneville A, et al. Prognostic score including gene mutations in chronic myelomonocytic leukemia. *J Clin Oncol.* 2013;31(19):2428-36.

17. Merlevede J, Droin N, Qin T, et al. Mutation allele burden remains unchanged in chronic myelomonocytic leukaemia responding to hypomethylating agents. *Nat Commun*. 2016;7:10767. doi:10.1038/ncomms10767.

18. Itzykson R, Kosmider O, Renneville A, et al. Clonal architecture of chronic myelomonocytic leukemias. *Blood.* 2013; 121(12):2186-98.

19. Padron E, Painter JS, Kunigal S, et al. GM-CSF–dependent pSTAT5 sensitivity is a feature with therapeutic potential in chronic myelomonocytic leukemia. *Blood*. 2013;121(25):5068.

20. Patnaik MM, Tefferi A. Chronic myelomonocytic leukemia: 2016 update on diagnosis, risk stratification, and management. *Am J Hematol*. 2016;91(6):631-42.

21. de Witte T, Bowen D, Robin M, et al. Allogeneic hematopoietic stem cell transplantation for MDS and CMML: recommendations from an international expert panel. *Blood*. 2017;129(13):1753-62.

22. Solary E, Itzykson R. How I treat chronic myelomonocytic leukemia. *Blood*. 2017;130(2):126-36.

23. Chen Y-C, Chou J-M, Ketterling RP, Letendre L, Li C-Y. Histologic and Immunohistochemical Study of Bone Marrow Monocytic Nodules in 21 Cases With Myelodysplasia. *Am J Clin Pathol*. 2003;120(6):874-81.

24. Vermi W, Facchetti F, Rosati S, et al. Nodal and extranodal tumor-forming accumulation of plasmacytoid monocytes/interferon-producing cells associated with myeloid disorders. *Am J Surg Pathol*. 2004;28(5):585-95.

25. Orazi A, Chiu R, O'Malley DP, et al. Chronic myelomonocytic leukemia: the role of bone marrow biopsy immunohistology. *Mod Pathol*. 2006;19(12):1536-45.

26. Harris NL, Demirjian Z. Plasmacytoid T-zone cell proliferation in a patient with chronic myelomonocytic leukemia. Histologic and immunohistologic characterization. *Am J Surg Pathol*. 1991;15(1):87-95.

27. Müller-Hermelink HK, Stein H, Steinmann G, Lennert K. Malignant lymphoma of plasmacytoid T-cells. Morphologic and immunologic studies characterizing a special type of T-cell. *Am J Surg Pathol*.7(8):849-62.

28.Facchetti F, de Wolf-Peeters C, Mason DY, Pulford K, Van den Oord JJ, Desmet VJ. Plasmacytoid T cells. Immunohistochemical evidence for their monocyte/macrophage origin. *Am J Pathol*. 1988;133(1):15.

29. Villani A-C, Satija R, Reynolds G, et al. Single-cell RNA-seq reveals new types of human blood dendritic cells, monocytes, and progenitors. *Science*. 2017;356(6335):eaah4573.

30. See P, Dutertre C-A, Chen J, et al. Mapping the human DC lineage through the integration of high-dimensional techniques. *Science*. 2017;356(6342):eaag3009.

31. Such E, Germing U, Malcovati L, et al. Development and validation of a prognostic scoring system for patients with chronic myelomonocytic leukemia. *Blood*. 2013;121(15):3005-15.

32. Patnaik MM, Lasho TL, Vijayvargiya P, et al. Prognostic interaction between ASXL1 and TET2 mutations in chronic myelomonocytic leukemia. *Blood Cancer J*. 2016;6(1):e385.31.

33. Liu Y-J. IPC: Professional Type 1 Interferon-Producing Cells and Plasmacytoid Dendritic Cell Precursors. *Annu Rev Immunol*. 2005;23(1):275-306.

34. Boyle EI, Weng S, Gollub J, et al. GO::TermFinder—open source software for accessing Gene Ontology information and finding significantly enriched Gene Ontology terms associated with a list of genes. *Bioinformatics*. 2004; 20(18), 3710–3715.

35. Yu G, Wang L-G, Han Y, He Q-Y. clusterProfiler: an R Package for Comparing Biological Themes Among Gene Clusters. *OMICS□: a Journal of Integrative Biology*. 2012;16(5):284-287. doi:10.1089/omi.2011.0118.

36. Lee J, Breton G, Oliveira TYK, et al. Restricted dendritic cell and monocyte progenitors in human cord blood and bone marrow. *J Exp Med.* 2015;212(3):385-99.

37. Lee J, Breton G, Aljoufi A, et al. Clonal analysis of human dendritic cell progenitor using a stromal cell culture. *J Immunol Methods*. 2015;425:21.

38. Chen W, Antonenko S, Sederstrom JM, et al. Thrombopoietin cooperates with FLT3-ligand in the generation of plasmacytoid dendritic cell precursors from human hematopoietic progenitors. *Blood*. 2004;103(7):2547-53.

39. Demoulin S, Roncarati P, Delvenne P, Hubert P. Production of large numbers of plasmacytoid dendritic cells with functional activities from CD34+ hematopoietic progenitor cells: Use of interleukin-3. *Exp Hematol*. 2012;40(4):268-78.

40. Pardanani A, Reichard KK, Zblewski D, et al. CD123 immunostaining patterns in systemic mastocytosis: differential expression in disease subgroups and potential prognostic value. *Leukemia.* 2016;30(4):914-8.

41. Tzankov A, Hebeda K, Kremer M, et al. Plasmacytoid dendritic cell proliferations and neoplasms involving the bone marrow: Summary of the workshop cases submitted to the 18th Meeting of the European Association for Haematopathology (EAHP) organized by the European Bone Marrow Working Group, Basel 2016. *Ann Hematol.* 2017;96(5):765-77.

42. Matsui T, Connolly JE, Michnevitz M, et al. CD2 Distinguishes Two Subsets of Human Plasmacytoid Dendritic Cells with Distinct Phenotype and Functions. *J Immunol*. 2009;182(11):6815-23.

43. Zitvogel L, Galluzzi L, Kepp O, Smyth MJ, Kroemer G. Type I interferons in anticancer immunity. *Nat Rev Immunol*. 2015 ; 15:405-414.

44. Touzot M, Grandclaudon M, Cappuccio A, et al. Combinatorial flexibility of cytokine function during human T helper cell differentiation. *Nat Commun.* 2014; 5:3987.

45. Kiladjian J-J, Giraudier S, Cassinat B. Interferon-alpha for the therapy of myeloproliferative neoplasms: targeting the malignant clone. *Leukemia*. 2016;30(4):776-81.

46. Chauhan D, Singh AV, Brahmandam M, et al. Functional Interaction of Plasmacytoid Dendritic Cells with Multiple Myeloma Cells: A Therapeutic Target. *Cancer Cell.* 2009;16(4):309-23.

47. Alculumbre SG, Saint-André V, Di Domizio J, et al. Diversification of human plasmacytoid predendritic cells in response to a single stimulus. *Nat Immunol*. 2018;19(1):63-75.

48. Reynaud D, Pietras E, Barry-Holson K, et al. IL-6 controls leukemic multipotent progenitor cell fate and contributes to chronic myelogenous leukemia development. *Cancer Cell*. 2011;20(5):661.

49. Welner RS, Amabile G, Bararia D, et al. Treatment of chronic myelogenous leukemia by blocking cytokine alterations found in normal stem and progenitor cells. *Cancer Cell*. 2015;27(5):671.

50. Alfaro C, Sanmamed MF, Rodríguez-Ruiz ME, et al. Interleukin-8 in cancer pathogenesis, treatment and follow-up. *Cancer Treat Rev.* 2017;60(Supplement C):24-31.

51. Sinclair A, Park L, Shah M, et al. CXCR2 and CXCL4 regulate survival and self-renewal of hematopoietic stem/progenitor cells. *Blood*. 2016;128(3):371.

52. Tobler A, Moser B, Dewald B, et al. Constitutive expression of interleukin-8 and its receptor in human myeloid and lymphoid leukemia. *Blood*. 1993;82(8):2517-25.

53. Abdul-Aziz AM, Shafat MS, Mehta TK, et al. MIF-Induced Stromal PKCβ/IL8 Is Essential in Human Acute Myeloid Leukemia. *Cancer Res*. 2017;77(2):303-11.

54. Schinke C, Giricz O, Li W, et al. IL8-CXCR2 pathway inhibition as a therapeutic strategy against MDS and AML stem cells. *Blood*. 2015;125(20):3144.

55. Kingston D, Schmid MA, Onai N, Obata-Onai A, Baumjohann D, Manz MG. The concerted action of GM-CSF and Flt3-ligand on in vivo dendritic cell homeostasis. *Blood.* 2009;114(4):835-43.

56. Esashi E, Wang Y-H, Perng O, Qin X-F, Liu Y-J, Watowich SS. The Signal Transducer STAT5 Inhibits Plasmacytoid Dendritic Cell Development by Suppressing Transcription Factor IRF8. *Immunity*. 2008;28(4):509-20.

57. Niyongere S, Lucas N, Zhou JM , et al. Heterogeneous expression of cytokines accounts for clinical diversity and refines prognostication in CMML. *Leukemia*, in press

58. Desterke C, Bilhou-Nabéra C, Guerton B, et al. FLT3-Mediated p38–MAPK Activation Participates in the Control of Megakaryopoiesis in Primary Myelofibrosis. *Cancer Res.* 2011;71(8):2901-15.

59. Kordasti SY, Ingram W, Hayden J, et al. CD4+CD25high Foxp3+ regulatory T cells in myelodysplastic syndrome (MDS). *Blood.* 2007;110(3):847-50.

60. Kotsianidis I, Bouchliou I, Nakou E, et al. Kinetics, function and bone marrow trafficking of CD4+CD25+FOXP3+ regulatory T cells in myelodysplastic syndromes (MDS). *Leukemia.* 2008;23(3):510-8.

61. Kittang AO, Kordasti S, Sand KE, et al. Expansion of myeloid derived suppressor cells correlates with number of T regulatory cells and disease progression in myelodysplastic syndrome. *Oncoimmunology.* 2016;5(2):e1062208.

62. Sisirak V, Faget J, Gobert M, et al. Impaired IFN-α Production by Plasmacytoid Dendritic Cells Favors Regulatory T-cell Expansion That May Contribute to Breast Cancer Progression. *Cancer Res.* 2012;72(20):5188-97.

63. Ray A, Das DS, Song Y, et al. A novel agent SL-401 induces anti-myeloma activity by targeting plasmacytoid dendritic cells, osteoclastogenesis and cancer stem-like cells. *Leukemia.* 2017;31(12):2652-2660.

Table 1. Characteristics of CMML patients whose bone marrow mononucleated cells were prospectively analyzed by flow cytometry (French cohort). pDC defined as Lin- ($CD3^-$, $CD14^-$, $CD15^-$, $CD16^-$, $CD19^-$, $CD24^-$), CD33- and CD11c- mononucleated cells expressing CD45, CD123, HLA-DR, BDCA-2, BDCA-4 and CD4. pDC rich samples defined as pDC > 1.2% of bone marrow mononucleated cells.

Variables	Availabl e	All patients n=159	pDC-rich n=32 (20%)	pDC-poor n=127 (80%)	*P*-value
General characteristics					
Age in years, mean [range]	158	74 [68-81]	78 [73-83]	74 [68-80]	0.04
Male, number (%)	126	81 (64%)	16 (59%)	65 (66%)	NS
Blood cell parameters					
Hemoglobin g/dL, median [IQR]	140	11.1 [9.4-12.9]	11.3 [9.7-12.2]	11.1 [9.2-12.9]	NS
WBC x 10^9/L , median [IQR]	140	11.1 [7.0-18.9]	12.0 [8.4-24.1]	11.1 [6.7-18.6]	NS
ANC x 10^9 /L, median [IQR]	138	5.5 [2.9-10.6]	7.1 [4.1-13.7]	5.4 [2.8-10.4]	NS
ALC x 10^9 /L, median [IQR]	140	2.0 [1.2-2.8]	1.6 [1.0-2.6]	2.0 [1.2-2.8]	NS
AMC x 10^9 /L, median [IQR]	140	2.4 [1.3-4.9]	2.4 [1.8-4.8]	2.4 [1.2-4.9]	NS
Platelets x 10^9/L, median [IQR]	137	102 [54-191]	93 [52-187]	104 [54-197]	NS
BM blast %, median [IQR]	127	6 [3-8]	6 [4-8]	5 [3-8]	NS
WHO 2016 classification					
CMML-0, number (%)		53 (42%)	8 (29%)	45 (46%)	
CMML-1, number (%)	127	52 (41%)	17 (61%)	35 (35%)	NS
CMML-2, number (%)		22 (17%)	3 (11%)	19 (19%)	
Myelodysplastic, number (%)	140	79 (56%)	15 (50%)	64 (58%)	NS
Myeloproliferative, number (%)		61 (44%)	15 (50%)	46 (42%)	
Cytogenetic risk according to CPSS					
Low, number (%)		66 (80%)	14 (82%)	52 (80%)	
Intermediate, number (%)	81	8 (10%)	0	8 (12%)	NS
High, number (%)		8 (10%)	3 (18%)	5 (8%)	
Mutated genes by NGS analysis, number (%)					
ASXL1	126	60 (48%)	12 (46%)	48 (48%)	NS
CBL	126	19 (15%)	6 (23%)	13 (13%)	NS
C-KIT	126	4 (3%)	0	4 (4%)	NS
CSF3R	126	9 (7%)	1 (4%)	8 (8%)	NS
DNMT3A	126	6 (5%)	2 (8%)	4 (4%)	NS
EZH2	126	11 (9%)	2 (8%)	9 (9%)	NS
FLT3-TKD	126	1 (1%)	1 (4%)	0	NS
IDH1	126	2 (2%)	0	2 (2%)	NS
IDH2	126	5 (4%)	2 (8%)	3 (3%)	NS
JAK2	126	9 (7%)	0	9 (9%)	NS
KRAS	126	19 (15%)	5 (19%)	14 (14%)	NS
NF1	126	3 (8%)	2 (25%)	1 (4%)	NS
NRAS	126	24 (19%)	9 (35%)	15 (15%)	0.046
RUNX1	126	23 (18%)	3 (12%)	20 (20%)	NS
SETBP1	126	8 (6%)	3 (12%)	5 (5%)	NS
SF3B1	126	9 (7%)	3 (12%)	6 (6%)	NS
SRSF2	126	53 (42%)	7 (27%)	46 (46%)	NS
TET2	126	87 (69%)	18 (58%)	72 (72%)	NS
Tp53	126	3 (2%)	0	3 (3%)	NS
U2AF1	126	9 (7%)	2 (8%)	7 (7%)	NS
ZRSR2	126	5 (4%)	2 (8%)	3 (3%)	NS
Combined mutations of genes encoding proteins of the Ras pathway, number (%)					
NRAS + KRAS + CBL	126	58 (46%)	18 (69%)	40 (40%)	0.014

WBC, white blood cells ; ANC, Absolute neutrophil count ; ALC, Absolute lymphocyte count ; AMC, absolute monocyte count ; CMML, chronic myelomonocytic leukemia ; BM, bone marrow; CPSS: CMML-specific prognostic scoring system; NS, non significant.

Figures legends

Figure 1. Identification of CD123^{high} cells in bone marrow and peripheral blood of CMML patients. **A**. Histological and immunohistochemical analysis of bone marrow trephine biopsy sections of CMML patients. Two representative cases are shown (magnification x 20). Upper panel: CD123^{+},TCL1^{+} cell-rich CMML; Lower panel: CD123^{+},TCL1^{+} cell-poor CMML. Left column: hematoxylin/eosin staining; middle column: CD123 staining; right column: TCL1 staining. **B**. Multiparameter flow cytometry analysis of putative pDC in bone marrow aspirate and peripheral blood samples collected from CMML patients and age-matched healthy controls. Mononuclear cells were identified among CD45^{+} cells using Side Scatter (SSC) and CD33 staining. Putative pDC were identified among mononucleated cells as HLA-DR^{+} Lineage (CD3, CD14, CD15, CD16, CD19, CD24)$^{-}$, CD33^{-}, CD11c^{-}, CD123^{+}, BDCA-2^{+}, BDCA-4^{+}, CD4^{+} cells. **C,D.** pDC richness was quantified as percentage of pDC among mononuclear cells in bone marrow (BMNC; Controls = 24, CMML = 159) (**C**) and peripheral blood (PBMC; Controls = 34, CMML = 198) (**D**). **E.** Linear regression of pDC in peripheral blood, expressed as the fraction of PBMC, versus pDC in bone marrow, expressed as the fraction of BMNC, in 106 CMML patients with matched samples (R^2 0.75; p<0.0001).

Figure 2. Characteristics of CD123^{high} cells in CMML patients and age-matched controls. A-C. The fraction of pDC in mononuclear cells was determined in bone marrow samples collected from 159 CMML patients and 24 healthy donors (controls) and peripheral blood samples collected from 198 CMML patients and 34 healthy donors (controls). **A.** Fraction of pDC among mononuclear cells in peripheral blood and bone marrow of CMML patients (**** *P*<0.0001, Wilcoxon signed rank test). **B.** Fraction of pDC among bone marrow mononucleated cells collected from healthy donors and CMML patients, separating pDC-poor (<1.2% MNC) from pDC-rich CMML samples, showing a significant decrease in pDC fraction in pDC-poor CMML compared to healthy donors (**** *P*<0.0001, Mann Whitney test). **C.** Fraction of pDC among peripheral blood mononucleated cells collected from healthy donors and CMML patients, separating pDC-poor (<0.6% MNC) from pDC-rich CMML samples, showing a significant decrease in pDC fraction in pDC-poor CMML compared to healthy donors (**P*<0.01, Mann Whitney test)). **D-G.** Staining index of indicated cell surface markers in indicated bone marrow samples. The only detected difference

was a lower expression of BDCA-2 in pDC-poor CMML samples (*P<0.05). **H.** Fraction of CD2 expressing pDC in indicated bone marrow mononucleated cell samples (**P<0.01, ***P<0.001; Mann-Whitney test). **I.** Staining index of CD2 in $CD2^+$pDC in indicated bone marrow samples (*P<0.05, ***P<0.001; Mann-Whitney test). **J, K**. Correlation between pDC in bone marrow, expressed as the fraction of BMNC, and Treg in bone marrow (**J**) or matched peripheral-blood (**K**), expressed as the fraction of T-cells.

Figure 3. Gene expression analysis confirms that $CD123^+$cells are *bona fide* plasmacytoid dendritic cells. A. Heat-map of gene expression measured by RNA sequencing in sorted pDC from healthy donors (n=7), pDC-rich (n = 11) and pDC-poor (n = 5) bone marrow CMML samples, and pDC-rich (n = 3) and pDC-poor (n = 4) peripheral blood CMML samples, distinguishing genes highly expressed in typical pDC from those defining "AS DCs" and other cell lineages. **B**. Principal component analysis of gene expression in pDC sorted from healthy donors (blue), pDC-poor CMML (green) and pDC-rich CMML (red) bone marrow samples (LogCPM gene expression). **C.** Unsupervised hierarchical clustering of bone marrow pDC, based on differentially expressed genes (DEG) as identified by RNA sequencing in pDC sorted from a cohort of 4 healthy donors, 6 pDC-rich CMML and 3 pDC-poor CMML bone marrow samples (DEG between pDC-poor and pDC-rich CMML = 74; DEG between pDC-rich CMML and healthy-donor pDC =13; DEG between pDC-poor CMML and healthy-donor pDC =144).

Figure 4. pDC bone marrow infiltration increases the risk of acute leukemia transformation. A. Relationship between immunohistochemistry analysis of bone marrow $CD123^+$, $TCL1^+$ cells (pDC rich > 5% of bone marrow cells) and flow cytometry measurement of pDC fraction in peripheral blood samples (pDC rich > 0.6% of mononucleated cells) analyzed in 56 patients. P<0.001; Mann Whitney test. Agreement in 92% of cases, Kohen's kappa 0.75. **B**. Cumulative incidence of acute myeloid leukemia transformation in 202 CMML patients according to pDC infiltration, as defined by immunohistochemistry analysis of bone marrow biopsies (pDC-rich > 5% $CD123^+$ $TCL1^+$ cells), considering death as a competing risk (Hazard ratio 2.59 [95% confidence interval (CI) 1.21-5.51]; P=0.014).

Figure 5. Bone marrow infiltrating pDC are observed in Ras-pathway mutated CMML. A. Whole exome sequencing was performed in monocytes, T cells and pDC

sorted from 10 CMML, 1 CMML transformed into AML (#2202) and 1 aCML (#1996) bone marrow samples. Most mutations or loss of heterozygosis were found in both pDC (red left up corner) and monocytes (blue right low corner). In all cases, one or more mutations in genes encoding proteins of the Ras pathway were identified in monocytes. In 11 cases, these mutations were also identified in pDC. The last case (#2202) harbored an internal tandem duplication of Flt3 (Flt3-ITD). Variant categories based on their function and their frequency in sorted monocytes and pDC are indicated on the right **B.** Relationship between variant allele frequencies (VAF) measured in sorted monocytes and sorted pDC from the 12 samples sequenced in A (Linear regression, $r^2 = 0.74$; $p<0.0001$). Ras pathway mutations are in red, other variants in black. **C.** VAF of two *TET2* gene mutations and *NRAS*^{G13D} mutation in sorted pDC and monocytes of patient #2048; **D.** VAF of *PTPN11*^{F285I}, *NRAS*^{A59D} and *KRAS*^{A146T} mutation in sorted pDC and monocytes of patient #1829.

Figure 6. CD34$^+$ cells from pDC-rich CMML are hypersensitive to FLT-3L. A-C. CD34$^+$ cells from pDC-rich CMML, pDC-poor CMML and cord blood were cultured in the presence of SCF, TPO, Flt3-L and IL-3 for indicated times before flow analysis of generated cells. **A,B.** Flow cytometry detection of pDC at day 30 of culture, based on HLA-DR, CD123 and BDCA4 expression; **A**, CD34$^+$ cells from pDC-rich CMML bone marrow; **B**, CD34$^+$ cells from pDC-poor CMML bone marrow. One representative of 10 independent experiments is shown. **C.** Generated pDC were sorted and examined by conventional (upper panel) and electronic (lower panel) microscopy. **D.** Somatic variants were detected by NGS in sorted bone marrow CD34$^+$ cells, sorted bone marrow pDC and pDC generated by ex vivo differentiation of CD34$^+$ cells at day 30. **E.** Time dependent generation of pDC by ex vivo culture of CD34$^+$ cells collected from 5 pDC-rich (in red) and 8 pDC-poor (in green) CMML bone marrow samples (mean +/- SEM; * $P<0.05$, Mann-Whitney test); **F.** Fraction of pDC generated at day 25 by *ex vivo* culture of CD34$^+$ cells sorted from the 5 pDC-rich (red) and 8 pDC-poor (green) CMML bone marrow samples (shown on panel E) compared to 5 cord blood CD34$^+$ cell samples; (mean +/- SEM; * $P<0.05$, Mann-Whitney test); **G.** Fraction of pDC in cells generated by CD34$^+$ cells sorted from 2 pDC-rich CMML bone marrow (in red) and 5 cord blood samples (in blue) and cultured for 30 days as above with indicated concentrations of Flt3-L. **F.** Flt3-L level was measured in bone marrow supernatant of 28 pDC-rich CMML patients (red) and 78 pDC-rich CMML patients

(green) compared to 13 age-matched healthy controls (blue). Boxes: Median, interquartiles and ranges; *** P<0.001; **** P<0.0001 (Mann-Whitney test).

Figure 1.

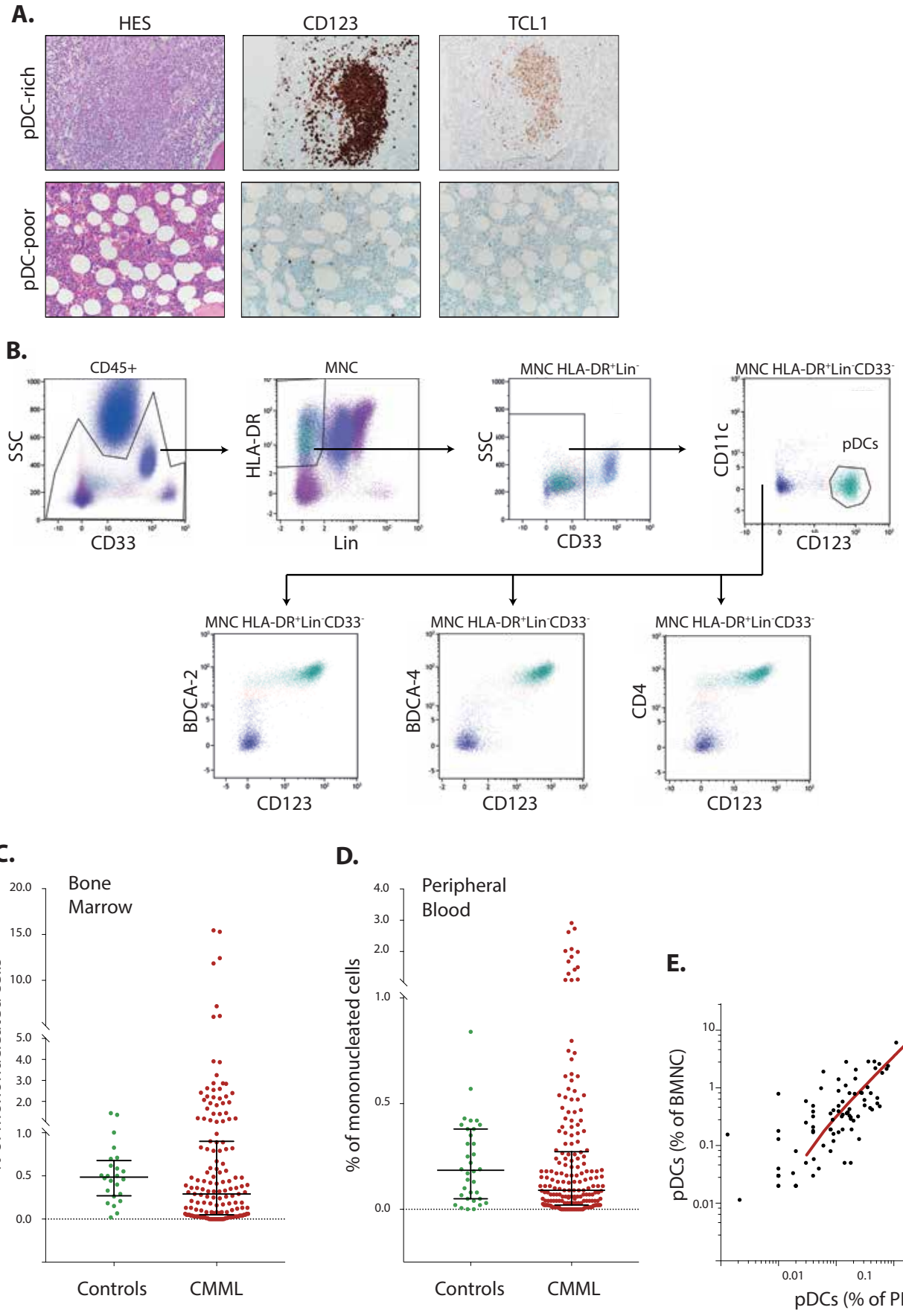
A.
HES
CD123
TCL1
pDC-rich
pDC-poor
B.
CD45+
SSC
CD33
MNC
HLA-DR
Lin
MNC HLA-DR+Lin-
SSC
CD33
MNC HLA-DR+Lin-CD33-
CD11c
pDCs
CD123
MNC HLA-DR+Lin-CD33-
BDCA-2
CD123
MNC HLA-DR+Lin-CD33-
BDCA-4
CD123
MNC HLA-DR+Lin-CD33-
CD4
CD123
C.
Bone Marrow
% of mononucleated cells
20.0
15.0
10.0
5.0
4.0
3.0
2.0
1.0
0.5
0.0
Controls
CMML
D.
Peripheral Blood
% of mononucleated cells
4.0
3.0
2.0
1.0
0.5
0.0
Controls
CMML
E.
pDCs (% of BMNC)
10
1
0.1
0.01
r²=0.75
p <0.0001
0.01
0.1
1
10
pDCs (% of PBMC)

Figure 2.

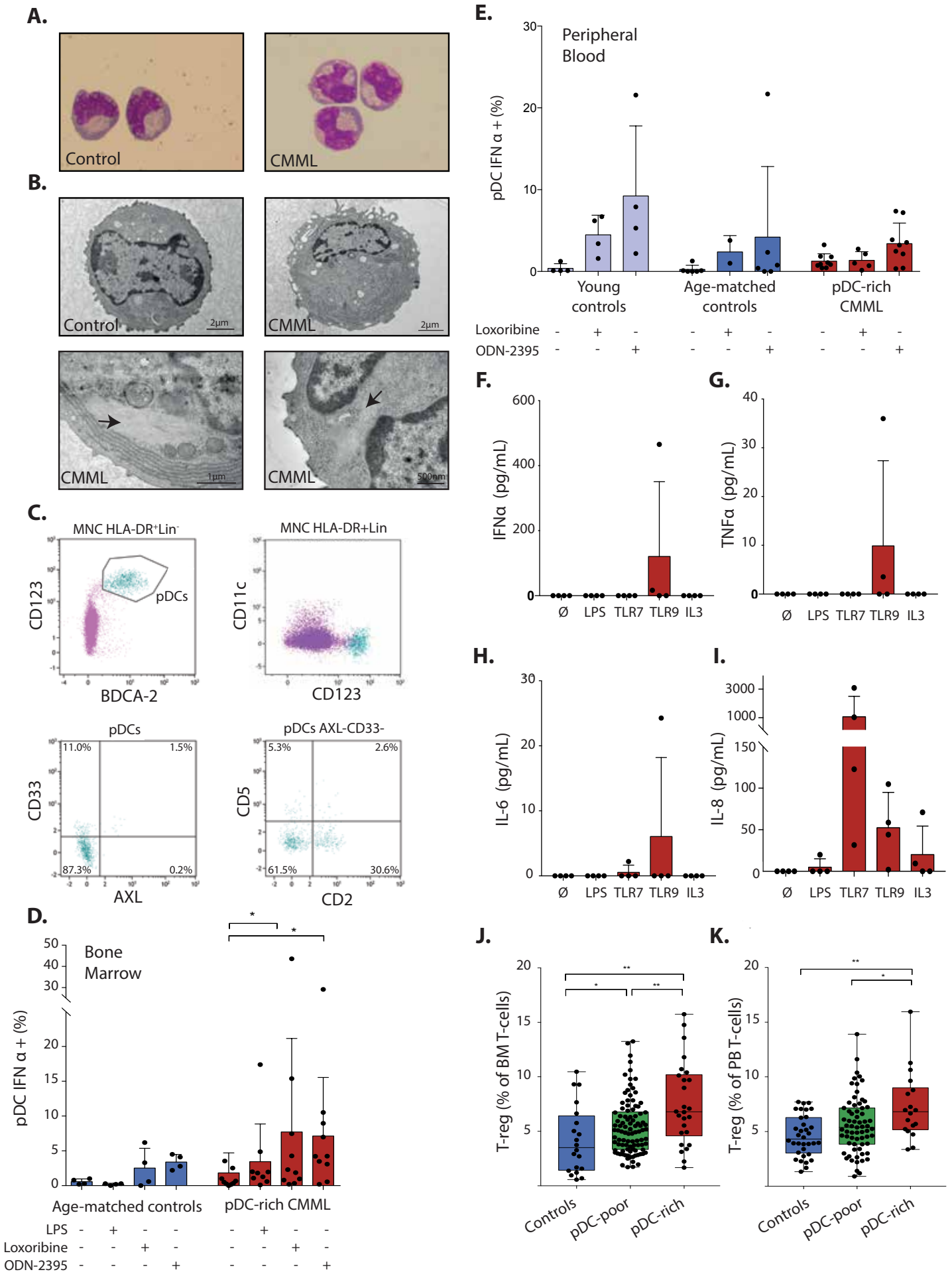
A.
Control
CMML
B.
Control
2µm
CMML
2µm
CMML
1µm
CMML
500nm
C.
MNC HLA-DR+Lin-
CD123
pDCs
BDCA-2
MNC HLA-DR+Lin
CD11c
CD123
pDCs
CD33
11.0%
1.5%
87.3%
0.2%
AXL
pDCs AXL-CD33-
CD5
5.3%
2.6%
61.5%
30.6%
CD2
D.
Bone Marrow
pDC IFN α + (%)
Age-matched controls
pDC-rich CMML
LPS
Loxoribine
ODN-2395
E.
Peripheral Blood
pDC IFN α + (%)
Young controls
Age-matched controls
pDC-rich CMML
Loxoribine
ODN-2395
F.
IFNα (pg/mL)
Ø LPS TLR7 TLR9 IL3
G.
TNFα (pg/mL)
Ø LPS TLR7 TLR9 IL3
H.
IL-6 (pg/mL)
Ø LPS TLR7 TLR9 IL3
I.
IL-8 (pg/mL)
Ø LPS TLR7 TLR9 IL3
J.
T-reg (% of BM T-cells)
Controls
pDC-poor
pDC-rich
K.
T-reg (% of PB T-cells)
Controls
pDC-poor
pDC-rich

Figure 3.

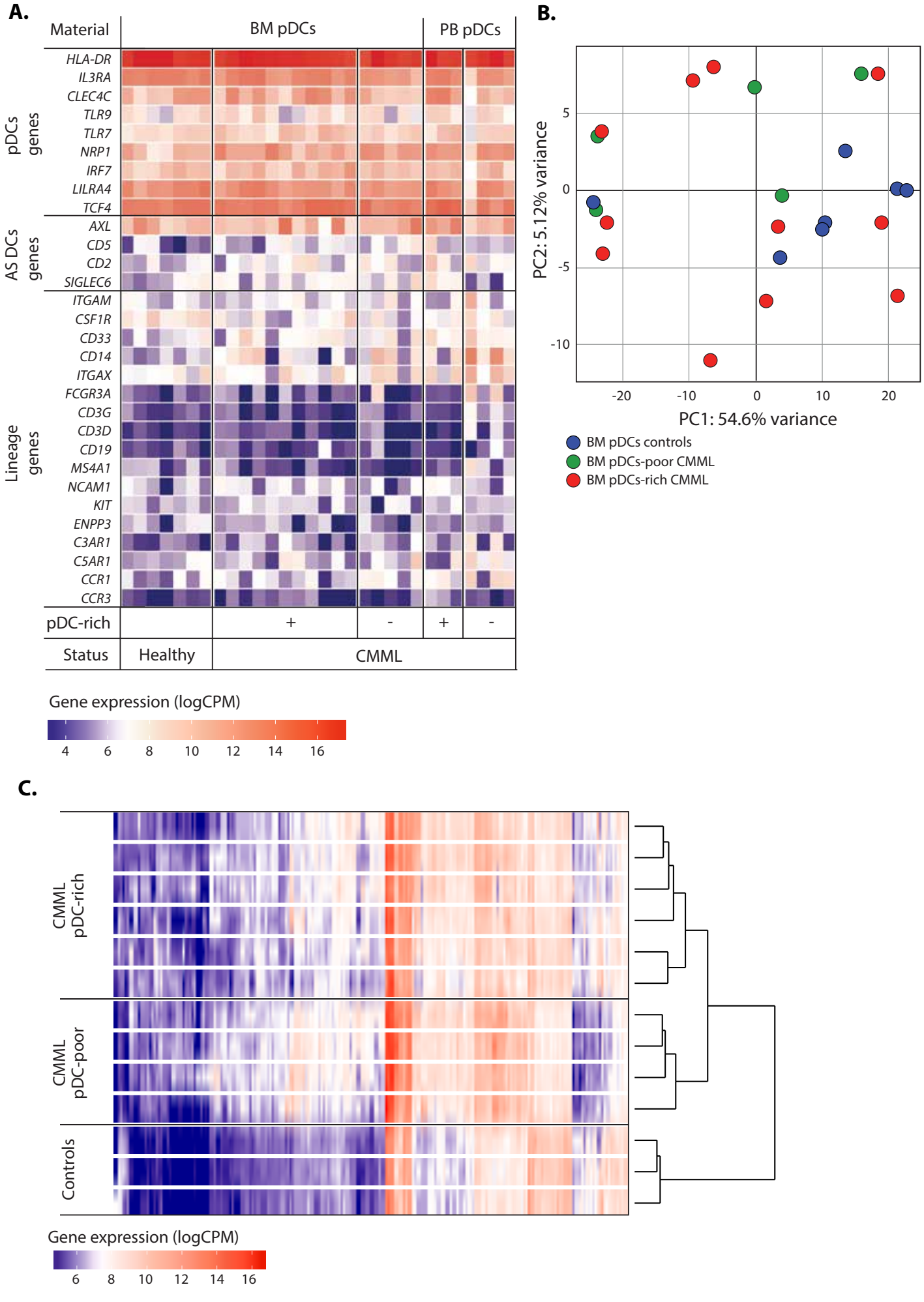
A.
Material
BM pDCs
PB pDCs
pDCs genes
HLA-DR
IL3RA
CLEC4C
TLR9
TLR7
NRP1
IRF7
LILRA4
TCF4
AS DCs genes
AXL
CD5
CD2
SIGLEC6
Lineage genes
ITGAM
CSF1R
CD33
CD14
ITGAX
FCGR3A
CD3G
CD3D
CD19
MS4A1
NCAM1
KIT
ENPP3
C3AR1
C5AR1
CCR1
CCR3
pDC-rich
+
-
+
-
Status
Healthy
CMML
Gene expression (logCPM)
4
6
8
10
12
14
16
B.
PC2: 5.12% variance
PC1: 54.6% variance
5
0
-5
-10
-20
-10
0
10
20
BM pDCs controls
BM pDCs-poor CMML
BM pDCs-rich CMML
C.
CMML pDC-rich
CMML pDC-poor
Controls
Gene expression (logCPM)
6
8
10
12
14
16

Figure 4.

A.

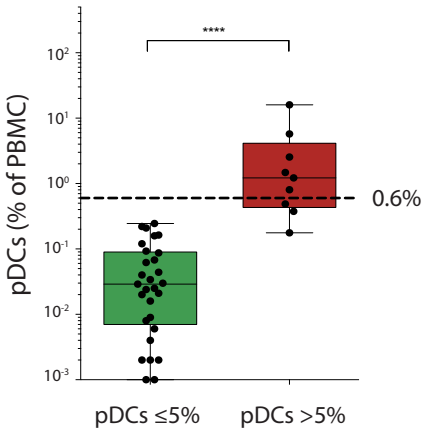
****
pDCs (% of PBMC)
10^2
10^1
10^0
10^{-1}
10^{-2}
10^{-3}
0.6%
pDCs ≤5%
pDCs >5%

B.

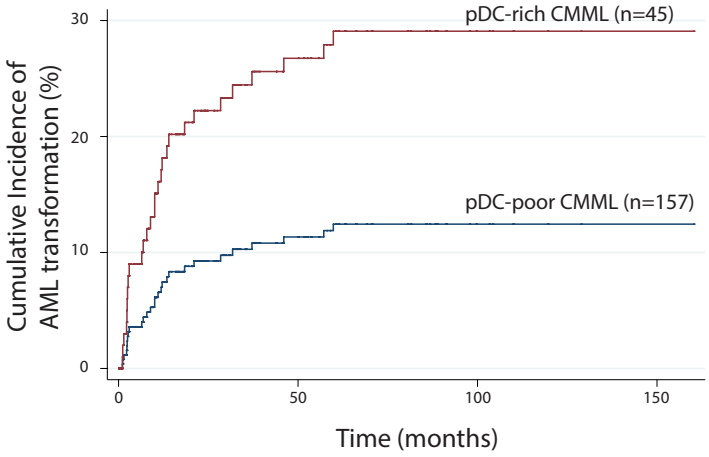
pDC-rich CMML (n=45)
pDC-poor CMML (n=157)
Cumulative Incidence of AML transformation (%)
30
20
10
0
0
50
100
150
Time (months)

Figure 5.

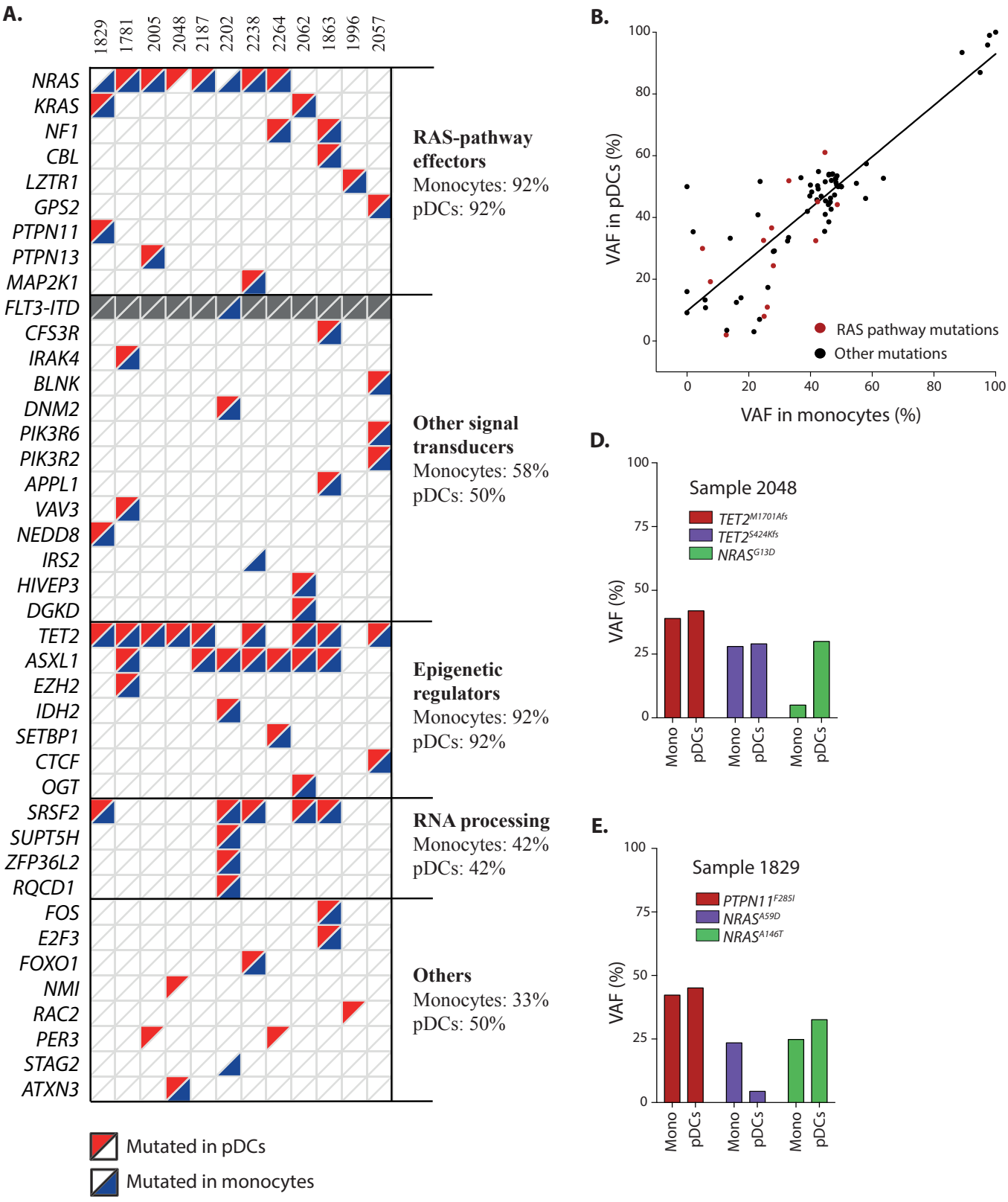
A.
1829
1781
2005
2048
2187
2202
2238
2264
2062
1863
1996
2057
NRAS
KRAS
NF1
CBL
LZTR1
GPS2
PTPN11
PTPN13
MAP2K1
FLT3-ITD
CFS3R
IRAK4
BLNK
DNM2
PIK3R6
PIK3R2
APPL1
VAV3
NEDD8
IRS2
HIVEP3
DGKD
TET2
ASXL1
EZH2
IDH2
SETBP1
CTCF
OGT
SRSF2
SUPT5H
ZFP36L2
RQCD1
FOS
E2F3
FOXO1
NMI
RAC2
PER3
STAG2
ATXN3
RAS-pathway effectors
Monocytes: 92%
pDCs: 92%
Other signal transducers
Monocytes: 58%
pDCs: 50%
Epigenetic regulators
Monocytes: 92%
pDCs: 92%
RNA processing
Monocytes: 42%
pDCs: 42%
Others
Monocytes: 33%
pDCs: 50%
Mutated in pDCs
Mutated in monocytes
B.
VAF in pDCs (%)
VAF in monocytes (%)
RAS pathway mutations
Other mutations
D.
Sample 2048
TET2M1701Afs
TET2S424Kfs
NRASG13D
VAF (%)
Mono
pDCs
E.
Sample 1829
PTPN11F285I
NRASA59D
NRASA146T

Figure 6.

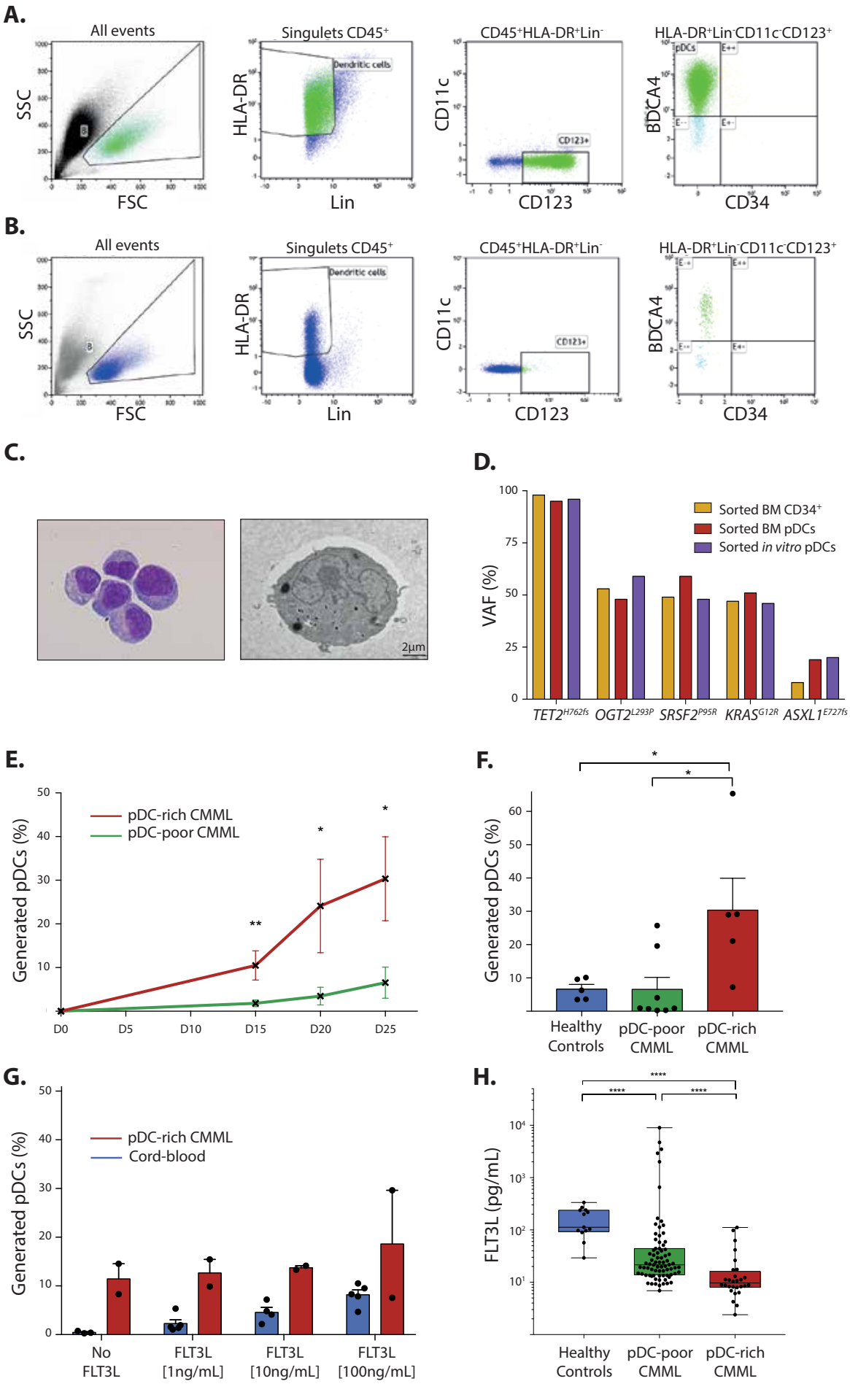
A.
All events
SSC
FSC
Singulets CD45+
HLA-DR
Lin
Dendritic cells
CD45+HLA-DR+Lin-
CD11c
CD123
CD123+
HLA-DR+Lin-CD11c-CD123+
BDCA4
CD34
pDCs
B.
All events
SSC
FSC
Singulets CD45+
HLA-DR
Lin
Dendritic cells
CD45+HLA-DR+Lin-
CD11c
CD123
CD123+
HLA-DR+Lin-CD11c-CD123+
BDCA4
CD34
C.
2µm
D.
VAF (%)
Sorted BM CD34+
Sorted BM pDCs
Sorted in vitro pDCs
TET2H762fs
OGT2L293P
SRSF2P95R
KRASG12R
ASXL1E727fs
E.
Generated pDCs (%)
pDC-rich CMML
pDC-poor CMML
D0
D5
D10
D15
D20
D25
F.
Generated pDCs (%)
Healthy Controls
pDC-poor CMML
pDC-rich CMML
G.
Generated pDCs (%)
pDC-rich CMML
Cord-blood
No FLT3L
FLT3L [1ng/mL]
FLT3L [10ng/mL]
FLT3L [100ng/mL]
H.
FLT3L (pg/mL)
Healthy Controls
pDC-poor CMML
pDC-rich CMML

B Article 2: collaborative work

Alongside PD-1^{+} T cells within tumors, CD8^{+}PD-1^{-}ILT2^{+} T cells are a major intratumor cytotoxic population selectively inhibited by the immune checkpoint HLA-G

Clement Dumont[1,2,3], Alix Jacquier[1,2], Jerome Verine[1,2,5], Floriane Noel [7], Annabelle Goujon[1,2,4], Ching-Lien Wu[1,2], Tzu-Min Hung[1,6], François Desgrandchamps[1,2,4], Stephane Culine[1,2,3], Edgardo D. Carosella[1,2], Nathalie Rouas-Freiss[1,2]* and Joel LeMaoult[1,2]*

* These two authors contributed equally to this work

[1] Hemato-Immunology Research Department, CEA-DRF, Saint-Louis Hospital, Paris, France

[2] Paris-Diderot University, Sorbonne-Paris-Cité Paris, France

[3] Department of Medical Oncology, Saint-Louis Hospital, Assistance Publique-Hôpitaux de Paris, France

[4] Department of Urology, Saint-Louis Hospital, Assistance Publique-Hôpitaux de Paris, Paris, France

[5] Department of Pathology, Saint-Louis Hospital, Assistance Publique-Hôpitaux de Paris, 1 avenue Claude-Vellefaux, 75010 Paris, France & Paris-Diderot University, Paris, France

[6] National Taiwan University Hospital, Taipei City, Taiwan, Republic of China University of Taipei & E-Da Hospital/I-Shou University, Yan-Chau Shiang, Kaohsiung County, Taiwan, Republic of China

[7] Institut Curie, PSL Research University, France & INSERM, UMR 932, Paris, France & Université Paris Sud, Université Paris-Saclay, Orsay, France

Running Title: Intratumor cytotoxic $CD8^+PD1^-ILT2^+$ T cells

Keywords: Immune checkpoints, HLA-G, ILT2, PD-1, infiltrating T cells

Author informations:

Address correspondence to: Joel LeMaoult

Email: joel.lemaoult@cea.fr

Address: CEA-SRHI, IUH-Hopital St Louis, 1 Avenue Claude Vellefaux, 75010 Paris, France

Tel: +33 (0)1 57 27 68 02

Conflict of interest statement: the authors declare no potential conflicts of interest.

Research Article, word count: 4182 words

Total number of figures: 7

Total number of supplementary figures: 1

Total number of tables: 1

Total number of supplementary tables: 1

Abstract

Current immune checkpoint inhibitors yield clinical responses in only some cancer patients, and other therapeutic target are currently researched. Here, we investigated the HLA-G:ILT2 checkpoint in clear-cell renal-cell carcinoma (ccRCC) patients, and focused on tumor-infiltrating $CD8^+$ lymphocytes (TILs) expressing HLA-G receptor ILT2, a population that quantitatively matches $CD8^+PD1^+$ TILs.

Using transcriptomics and flow cytometry, we characterized both peripheral blood and tumor-infiltrating $CD8^+ILT2^+$ T cells from cancer patients as late-differentiated $CD27^-CD28^-CD57^+$ cytotoxic effectors. We observed a clear dichotomy between $CD8^+ILT2^+$ and $CD8^+PD\text{-}1^+$ TIL subsets. These two quantitatively matched populations barely overlapped phenotypically and were easily distinguished by their exclusive expression of sets of surface molecules that included checkpoint molecules, and activatory and inhibitory receptors. Furthermore, $CD8^+ILT2^+$ TILs displayed a more mature phenotype and higher expression of cytotoxic molecules. In *ex vivo* functional experiments with both peripheral blood T cells and TILs, $CD8^+ILT2^+$ T cells displayed significantly higher cytotoxicity and IFNγ production than their $ILT2^{neg}$ (PBMC) and $PD\text{-}1^+$ (TILs) counterparts. HLA-G expression by target cells specifically inhibited $CD8^+ILT2^+$ T cell cytotoxicity but not that of their $CD8^+ILT2^{neg}$ (PBMC) or $CD8^+PD\text{-}1^+$ (TILs) counterparts, an effect counteracted by blocking the HLA-G:ILT2 interaction.

$CD8^+ILT2^+$ TILs may therefore constitute an untapped reservoir of fully differentiated cytotoxic T cells within the tumor microenvironment, independent of the $PD1^+$ TILs targeted by current immune therapies, and specifically inhibited by HLA-G. These results emphasize

the interest of therapeutic targeting of the HLA-G:ILT2 checkpoint in HLA-G-positive tumors, either concomitantly to anti-PD1/PD-L1, or in case of non-responsiveness to anti-PD1/PD-L1.

INTRODUCTION

Mechanisms allowing for the evasion of cancer cells from immune surveillance can be targeted in order to restore the host's antitumor immune response. In recent years, this has been universally accepted in light of the therapeutic efficacy of immune checkpoint inhibitors. Those currently most advanced in their development target exhausted tumor-infiltrating lymphocytes (TILs), which are chronically stimulated T cells fallen into a state of anergy maintained by the engagement of inhibitory receptors, such as PD-1 or CTLA-4. Anti-PD-1 antibodies are active in multiple cancer types albeit only in a subset of patients, as exemplified by metastatic renal-cell-carcinoma (mRCC): the anti-PD-1 antibody Nivolumab (1) is effective in about one-fourth of patients with pretreated mRCC, and the combination of Nivolumab with the anti-CTLA-4 antibody Ipilimumab in about half of the patients with treatment-naive intermediate- or high-risk mRCC (2). Although this illustrates the interest of targeting multiple checkpoints, still, not all patients benefit from immunotherapy. One explanation is that several checkpoints are active in a single tumor, as we recently showed in localized clear-cell renal cell carcinoma (ccRCC) (3): in a series of 19 tumors, we observed that expression of PD-L1 was heterogeneous and could coexist with expression of the immune checkpoint HLA-G.

HLA-G is a non-classical MHC class I molecule primarily found at the maternal-fetal interface (4) which exerts direct inhibitory functions on B, T and NK cells through its receptor ILT2 (Immunoglobulin-like transcript 2, product of the gene *LILRB1*) and on monocytes/macrophages through receptors ILT2 and ILT4 (5), as well as indirect

immunosuppressive effects through induction of regulatory T cells (6) or myeloid-derived suppressor cells (MDSCs) (7). HLA-G is frequently neo-expressed in immunotherapy-sensitive cancer types such as ccRCC (3,8-10), melanoma (11-13) or non-small cell lung cancer (14,15), especially in advanced-stage disease, and is associated with impaired prognosis (13-15). These elements strongly suggest a role in tumor escape from immune surveillance, which was confirmed by animal studies (7,16). We recently showed that TILs expressing ILT2 were present in the tumor microenvironment (TME) of ccRCC (3).

ILT2 is an inhibitory receptor with high affinity for HLA-G and lower affinity for classical MHC class I ligands (17). In the peripheral blood, ILT2 is expressed by a subset of $CD8^+$ T cells: from about 20% in younger healthy subjects (18-21), the proportion of ILT2-positive $CD8^+$ T cells may rise to over 50% with age and chronic viral infections (22,23). Previous reports have associated ILT2 expression by peripheral blood $CD8^+$ T cells with a differentiated phenotype ($CD28^-CD27^-CD57^+$, $CCR7^-CD45RA^+$) (21-25) and perforin expression (21,25). No characterization of $CD8^+ILT2^+$ TILs has ever been published. Furthermore, the impact of ILT2 on effector T cell functions remains unclear (21,23,26).

Here, using transcriptomics and flow cytometry, we characterize peripheral blood and tumor-infiltrating $ILT2^+CD8^+$ T cells as a differentiated cytotoxic population distinct from PD-1 expressing, exhausted T cells. Using *ex vivo* assays, we demonstrate that their effector functions are directly inhibited by target-expressed HLA-G through ILT2. Finally, we discuss HLA-G tumor expression as a mechanism of resistance to current cancer immunotherapy.

METHODS

Patients

T cells used for our experiments were isolated from cancer patients as well as control patients. Cancer patients were either patients who underwent transurethral resection for non-muscle-invasive bladder cancer (NMIBC patients) or patients who underwent nephrectomy for localized ccRCC (ccRCC patients) at our center (Urology Department, Saint-Louis Hospital, Paris, France); control patients were patients aged over 40 with no personal history of cancer, and admitted for planned, non-carcinologic, surgery. Patients provided written informed consent before sampling.

Peripheral blood cells

Blood sampling was performed upon admission to the Urology department prior to surgery. After sampling, peripheral blood mononuclear cells (PBMCs) were isolated using Ficoll gradient (Ficoll-Paque, LifeSciences) as per the manufacturer's instructions and stored at -150°C.

Cell sorting and transcriptomics analysis of peripheral blood $CD8^+$ T cells

For the sorting of $CD8^+ILT2^-$ and $CD8^+ILT2^+$ subpopulations, PBMC were labelled with antibodies specific for CD3, CD4, CD8, CD19 and ILT2. The CD8 subpopulations were then sorted according to ILT2 expression on a BD FacsAria II cell sorter, then immediately lyzed in RNA WIZ reagent (Ambion) and total RNA was extracted using the RNeasy micro kit (Qiagen). Samples were amplified and labelled according to the manufacturer's protocol for

hybridization to Affymetrix Human Gene 2.0 ST arrays. Sample preparation, hybridization, washing, staining, scanning and quality control were performed by the Institut Curie Genomics core facility, Paris, France.

Regulatory network and functional inference

We extracted the expression matrix of the differentially expressed genes between $ILT2^{+}CD8^{+}$ and $ILT2^{-}CD8^{+}$ T cells. We then imported the matrix on Cytoscape software version 3.5.1. Analysis was performed in parallel for the $ILT2^{+}$ and the $ILT2^{-}$ up-regulated genes expression matrix. Network inference was performed using ARACNe application. After selecting genes of the output network from ARACNe, we utilized the ClueGO and CluePedia Applications to determine pathway enrichment. Public datasets of Gene Ontology (GO) – Biological process-GOA, - ImmuneSystemProcess-GOA, - Molecular Function-GOA, KEGG, Reactome, and WikiPathways were used. Only pathways with a “Bonferroni step down” corrected p-value below 0.05 were kept.

Tumor-infiltrating lymphocytes

Tumor-infiltrating lymphocytes (TILs) were extracted from ccRCC specimens. Fresh tumor samples were selected on nephrectomy specimens by a pathologist, rinsed with phosphate-buffered saline (PBS) and placed in RPMI culture medium for 30 minutes before being manually dissociated. Extemporaneous counting and phenotyping of TILs was performed using a MACSQuant 10 flow cytometer (Miltenyi biotec) and cells were then stored at -150°C

for further phenotyping and functional assays. To rule out contamination with peripheral blood cells, a simultaneous flow cytometry analysis of PBMCs was performed.

Immunohistochemistry

Formalin-fixed paraffin-embedded (FFPE) samples from the same ccRCC specimens were analyzed by immunohistochemistry for tumor expression of HLA-G (clone 4H84) and PD-L1 (clone E1L3N) as previously described (3). Percentages of PD-L1 positivity in tumor cells and tumor-infiltrating cells were reported and HLA-G expression was estimated by the percentage of tumor cells positive for membrane staining.

Flow cytometry analysis

The following antibodies were used for cell surface staining and analysis: from Miltenyi Biotec: CD3-PerCP, CD3-VioBlue, CD4-PE-Vio770, CD4-VioBright-FITC, CD4-APC-Vio770, CD45RA-VioGreen, CD8-APC-Vio770, CD8-PerCP-Vio770, CD8-VioGreen, CD11b-FITC, CD38-PE-Vio770, CD45RA-VioGreen, CD57-VioBlue, CD127-PE-Vio770, CCR7-APC, IFNγ-FITC, KLRG1-FITC, NKp80-APC, Perforin-VioBlue, Granzyme B-PE, PD-1 PE-Vio770; from Beckman Coulter: CD27-PE, CD62L-FITC, CD69-PE, CD127-PE; from BD Pharmingen: CD28-FITC, CD137-PE; from eBioscience: ILT2-PE or ILT2-APC (Clone HP-F1), Tim-3-FITC; from Biolegend: PD-1-BV421.

Intracellular staining was performed using the Inside Stain kit (Miltenyi biotec), according to the manufacturer's instructions. Acquisition was made on a MACSQuant 10 flow cytometer

(Miltenyi biotec); analysis was performed using the MACSQuantify software (Miltenyi biotec) and Flowjo software.

Cell lines

For functional studies, the monocytic cell line THP-1 (ATCC) transduced or not to express membrane-bound HLA-G1 (THP1-HLA-G1) was used as target cells. Cell-surface expression of HLA-G on THP-1-HLA-G1 cells was confirmed by flow cytometry, using a PE-conjugated anti-HLA-G mAb (clone MEM-G9, Exbio).

Peripheral blood T cell degranulation and IFNγ secretion assays

THP1 or THP1-HLA-G1 cells were placed in a 96-well culture plate in RPMI culture medium (Sigma) supplemented with 10% fetal calf serum (Sigma), L-glutamine, gentamicine and amphothericin B (Gibco), and containing 50ng/mL phorbol 12-myristate 13-acetate (PMA, Sigma). Cells were cultured with PMA for 72h in order to obtain a confluent macrophage layer (mTHP1/mTHP1-HLA-G1). Then, cells were coated for 15 minutes with αCD3 mAb (clone OKT3, Orthoclone). Coating concentrations of OKT3 for CD107a and interferon-gamma (IFNγ) secretion assays were 20 and 10ng/mL, respectively. PBMCs from NMIBC patients were incubated for 20 minutes at 37°C with 20µg/mL of a blocking anti-ILT2 antibody (clone GHI/75, BioLegend) or a control antibody. PBMCs were then added to the OKT3-coated mTHP1/mTHP1-HLA-G1 target cells in culture medium supplemented with monensin and brefeldin A (Protein Transport Inhibitor Cocktail, eBioscience) in the presence of PE-conjugated anti-CD107a antibody (clone H4A3, BioLegend) or isotype control.

After 4h of co-incubation at 37°C, cells were washed and stained for flow cytometry analysis. For IFNγ secretion assays intracellular staining was then performed using the Inside Stain kit (Miltenyi biotec) according to the manufacturer's instructions.

The cytolytic degranulation and IFNγ secretion of $CD3^+CD8^+$ T cell subsets were evaluated using the percentage of CD107a- and IFNγ-positive cells respectively. $CD8^+$ T cell subsets were defined by the expression of ILT2 and CD57. Because of interference between the anti-ILT2 mAb GHI/75 used for blocking and the anti-ILT2 mAb HP-F1 used for staining we used the $CD57^{high}$ subset, which was constantly made up of more than 75% ILT2-positive T cells in selected patients as opposed to the $CD57^-$ subset, as a surrogate population for ILT2-positive T cells in blocking experiments.

TIL effector functions assays

THP1 or THP1-HLA-G1 cells were differentiated into macrophage target cells as described above. TILs were incubated with the anti-ILT2 mAb or isotype control and added to the target cells in culture medium supplemented with monensin and brefeldin A (Protein Transport Inhibitor Cocktail, eBioscience) and PE-conjugated anti-CD107a mAb or control isotype as described above. TILs stimulated by PMA and ionomycin (Cell stimulation cocktail, eBioscience) served as positive controls and TILs incubated with non-OKT3-coated target cells served as negative controls. After a 4-hour co-incubation, cells were washed and stained for flow cytometry analysis as described above. Results from a preliminary phenotypical characterization of TILs served to select the best surrogate markers for the $CD8^+ILT2^+$ TIL population in each sample (either $CD57^{high}$ or $CD45RA^+$ TILs).

Statistical analyses

For transcriptomic experiments, gene expression data were normalized using RMA algorithm on custom Brainarray CDF. We selected the 500 most variant genes by IQR (27) to perform unsupervised analyses. Differential subgroups were identified by hierarchical clustering using Pearson correlation metric and Ward distance. Differentially expressed genes between two groups were defined using limma R-package ($p \leq 0.05$ adjusted with Benjamini & Hochberg and $|\log \text{fold-change}| > 1.5$). All these analyses were performed with R software environment.

For flow cytometry phenotyping, comparisons between T cell subsets were made using t-tests paired by sample.

For functional studies, differences in terms of cytolytic degranulation or IFNγ production between different T cell subsets from the same PBMC or TIL samples were evaluated with t-tests paired by sample. The impact of HLA-G expression by the target cells and of ILT2 blocking on a specific T cell subset was evaluated using unpaired t-tests.

RESULTS

Transcriptomic profiling of the $CD8^+ILT2^+$ T cell subpopulation

First, we performed transcriptomic analysis to identify key features of ILT2 positive subpopulation. Peripheral blood $CD8^+$ T cells from 4 NMIBC patients were sorted with respect to ILT2 cell-surface expression and transcriptome analysis was performed on the $CD8^+ILT2^+$ vs $CD8^+ILT2^-$ T cell subpopulations. Hierarchical clustering demonstrated that these two cell populations could easily be distinguished (Figure 1A). 71 genes were specifically upregulated in the $CD8^+ILT2^+$ T cell population while 113 upregulated genes characterized their $CD8^+ILT2^-$ counterparts (Figure 1B). A list of these genes is provided in Supplementary Table 1. Functional network inference revealed that the genes upregulated in the $CD8^+ILT2^+$ population belonged to effector function- and effector function regulation-related categories (Figure 1C), centered around NK cell-type categories (natural killer cell-mediated cytotoxicity / natural killer cell-mediated immunity) and immune regulation (immune response-inhibiting cell surface receptor signaling pathways / regulation of alpha-beta T cell activation / immunoregulation interactions between a lymphoid and a non-lymphoid cell). Comparatively, the functional network inference of down-regulated genes in ILT2-positive vs ILT2-negative $CD8^+$ T cell populations was less restricted, but nevertheless centered around function-related categories (e.g. Cytokine-cytokine receptor interaction / regulation of cell-cell adhesion, positive regulation of chemotaxis), and differentiation (T cell differentiation / myeloid leukocyte differentiation, binding of TCF/LEF:CTNNB1 to target gene promoters). The aim of this analysis was originally to characterize the $CD8^+ILT2^+$ T cell subpopulation

using phenotyping in the context of an anti-tumor function. Thus, we next focused on cell-surface-expressed markers and function or differentiation-related genes. Out of the 184 genes found to be differently expressed between $CD8^+ILT2^+$ and $CD8^+ILT2^-$ subsets, 46 matched these criteria, including 19 upregulated and 27 down-regulated in $CD8^+ILT2^+$ T cells (Figure 1D). As suggested by the functional inference network data, upregulated genes in the $CD8^+ILT2^+$ population were mostly involved in NK and/or cytotoxic T cell functions. Cytotoxic T/NK-related genes were *TBX21* (T-bet), *GNLY* (granulysin), *GZMB* and *GZMH* (granzymes B and H), *ITGAM* (CD11b), and *FCRL6*. Genes usually associated with NK cells were *NCAM1* (CD56), cytotoxicity-triggering receptors *NCR1* (NKp46), *KLRF1* (NKp80) and *CD244*, lectin-like receptors *KLRK1*, *KLRC3* and *KLRC4* (NKG2D, NKG2E and NKG2F), and immunoglobulin-like receptors *KIR2DL1*, *KIR2DL3*, *KIR3DL2*.

Downregulated genes in the $CD8^+ILT2^+$ population were more diverse, but two categories stood out: genes involved in T cell stimulation/costimulation (*CD28*, CD28H (*TMIGD2)*, *CD27*, *TNFRSF8*, *CD40LG*, *TESPA1*), and genes associated with T-cell differentiation (*CD28*, *CD27*, *CCR7*, *CCR4*, *SELL*, *IL7R*, *TCF7*).

These data clearly indicated that ILT2-positive CD8+ T cells were likely to be antigen-experienced T cells with a high cytotoxic function, and expressing NK surface molecules (activating and inhibitory).

ILT2 cell-surface expression is a feature of differentiated cytotoxic CD8$^+$ T cells

Frozen PBMCs from 4 NMIBC patients, 4 ccRCC patients and 2 control patients were used for phenotypical validation of transcriptomics findings using flow cytometry. No differences were observed across these various clinical settings regarding the phenotype of CD8$^+$ILT2$^+$ T cells.

In accordance with transcriptomics findings, flow cytometry showed significantly lower expression of surface markers CD28, CD27 and CD127 on ILT2-positive CD8$^+$ T cells (Figure 2A-B). These cells also frequently expressed CD57 and virtually all ILT2-positive cells expressed KLRG1.

Conversely, the proportion of ILT2-positive cells was significantly higher in CD28-negative, CD57-positive or KLRG1-positive subpopulations (Figure 3A). Most NKp80-positive and perforin-positive CD8+ T cells also expressed ILT2 . Progressive acquisition of ILT2 during CD8$^+$ T cell differentiation was apparent through the rising proportion of ILT2-positive cells between the CD27-high, CD27-low and CD27-negative subpopulations, in that order. ILT2-positive cells were constantly CCR7-negative (Figure 3B-C), consistent with antigen-experienced effector-memory CD8$^+$ T cells (28); ILT2 expression was most frequent in the CCR7$^-$CD45RA$^+$ subset of CD8$^+$ T cells (TEMRA or effector T cells).

$CD8^+ILT2^+$ T cells display enhanced cytotoxic functions selectively impaired by target-expressed HLA-G

After having characterized their phenotype, we studied the cytotoxicity of $CD8^+ILT2^+$ T cells through the assessment of IFNγ secretion and cytolytic degranulation of peripheral blood T cells after *ex vivo* co-incubation with αCD3-coated target cells.

As the previous results let figure, ILT2-positive $CD8^+$ T cells constantly showed higher degranulation levels than their ILT2-negative counterparts (Figure 4A-B). Expression of HLA-G1 by the target cells significantly reduced degranulation levels of $CD8^+ILT2^+$ T cells by a mean 33% (range 18% to 47%) whereas $CD8^+ILT2^-$ cells were unaffected (Figure 4B). In restoration experiments, when ILT2 staining was impossible because of previous ILT2 blocking, this could also be observed in surrogate T cell subpopulations defined by CD57 expression: expression of HLA-G1 by the target cells reduced degranulation levels in the ILT2-enriched $CD8^+CD57^{high}$ subpopulation by a mean 34% (range 21% to 43%), whereas ILT2-negative $CD8^+CD57^-$ T cell subpopulation was unaffected (Figure 4C). ILT2 blocking significantly increased the degranulation levels of $CD8^+CD57^{high}$ T cells in the presence of HLA-G1, reversing HLA-G1-associated inhibition by a mean 86% (range 63% to 112%) whereas $CD8^+CD57^-$ T cells were unaffected.

Similarly, $CD8^+ILT2^+$ T cells showed higher IFNγ secretion than their ILT2-negative counterparts (Figure 4D-E), which was reduced by a mean 30% (range 13% to 56%) in the presence of HLA-G1 whereas $CD8^+ILT2^-$ cells were unaffected (Figure 4E). Expression of HLA-G1 by the target cells reduced IFNγ secretion by $CD8^+CD57^{high}$ T cells by a mean 40%

(range 24% to 56%), $CD8^+CD57^-$ T cells were typically unaffected (Figure 4F). ILT2 blocking significantly restored IFNγ secretion by $CD8^+CD57^{high}$ T cells in the presence of HLA-G1 by a mean 113% (range 57% to 177%) whereas $CD8^+CD57^-$ T cells were unaffected.

ILT2 is expressed by tumor-infiltrating $CD8^+$ cytotoxic effectors in ccRCC

After studying the peripheral blood T cells of patients, tumor-infiltrating cells from 8 ccRCC specimens were investigated. Expression of immune checkpoint ligands HLA-G and PD-L1 in these tumors as well as the distribution of PD-1^+ and $ILT2^+$ TILs are summarized in Table 1 and Figure 5. Blood contamination was deemed minimal in all TIL samples, as shown by clear-cut phenotypical discrepancies between PBMCs and TILs such as the absence of specific subpopulations in the tumor, eg. $CD8^+CCR7^+$ T cells (Supplementary Figure 1).

As we previously reported (3), the proportions of $CD8^+$PD-1^+ and $CD8^+ILT2^+$ TILs varied among specimens. Most strikingly, we observed that PD-1 expression and ILT2 expression by tumor-infiltrating $CD8^+$ T cells defined two subpopulations that were mutually exclusive (Figure 6A). $CD8^+ILT2^+$ TILs harbored a phenotype similar to that of their peripheral blood counterparts, expressing high levels of CD57 and being strictly $KLRG1^+CD28^-$ $CD27^-$ (Figure 6B) and most of them displayed an effector phenotype ($CCR7^-CD45RA^+$; Figure 6C). Perforin expression was again a specific feature of ILT2-positive cells (Figure 6B). Conversely, $CD8^+$PD-1^+ TILs displayed a less mature phenotype with negative-to-low expression of CD57, CD28 and CD27 and no expression of KLRG1 or perforin (Figure 6B); they typically pertained of the effector-memory phenotype ($CCR7^-CD45RA^-$; Figure 6C). In accordance with previous large-scale studies (29), expression of exhaustion-associated markers Tim-3,

CD38, CD69 and 4-1BB/CD137 was only seen on PD-1-positive cells and never on ILT2-positive cells (Figure 6B). Conversely, most cells expressing CD11b were ILT2-positive (Figure 6B).

HLA-G specifically inhibits the effector functions of tumor-infiltrating CD8$^+$ effectors through ILT2

Finally, to compare with the results obtained on PBMCs, the effector functions of tumor-infiltrating CD8$^+$ T cells were investigated. Again, cytolytic degranulation levels after *ex vivo* co-incubation with αCD3-coated target cells were higher in CD8$^+$ILT2$^+$ TILs than in CD8$^+$PD-1$^+$ TILs (Figure 7A). HLA-G1 expression by the target cells reduced the degranulation levels of CD8$^+$ILT2$^+$ TILs by a mean 32% (range 17% to 44%), whereas no such effect was observed with CD8$^+$PD-1$^+$ TILs. When considering ILT2-enriched surrogate TIL subsets selected for each individual sample (namely CD8$^+$PD-1$^-$CD45RA$^+$ or CD8$^+$PD-1$^-$CD57^{high} cells), expression of HLA-G1 by the target cells reduced degranulation levels by a mean 27% (range 25% to 28%). Interestingly, while this was not apparent in our preliminary assays with PBMCs, ILT2 blocking in the *absence* of HLA-G1 resulted in an increase in the degranulation of these surrogate ILT2$^+$ TILs, consistent with the removal of a HLA-G-independent lower-level inhibition due to the engagement of ILT2 by target-expressed classical MHC class I molecules. In any case, ILT2 blocking fully counteracted HLA-G1-mediated inhibition, as shown by a mean 197% reversion (range 127% to 318%).

As with cytolytic degranulation, IFNγ secretion by CD8$^+$ILT2$^+$ TILs was higher than that of CD8$^+$PD-1$^+$ TILs (Figure 7B). HLA-G1 expression by the target cells reduced the

degranulation levels of $CD8^+ILT2^+$ TILs by a mean 34% (range 28% to 42%) and of surrogate $ILT2^+$ populations by a mean 34% (range 19% to 46%). Again, ILT2 blocking resulted in an increase in IFNγ secretion by surrogate $ILT2^+$ TIL subsets in the absence of HLA-G1 as well as in full reversion of HLA-G1-mediated inhibition (mean 243% reversion, range 222% to 256%).

DISCUSSION

Since we recently described for the first time the presence of $CD8^+ILT2^+$ TILs in the stroma of ccRCC (3), their functional nature was a crucial question. The phenotypical and functional studies described here definitely associate $ILT2^+$ TILs and their peripheral-blood counterparts with late differentiation and strong cytotoxic capacity. A most striking finding was the clear dichotomy between $ILT2^+$ and $PD\text{-}1^+$ TILs in the tumor microenvironment, which was especially relevant considering that the latter are the prime target of current cancer immunotherapy despite being less cytotoxic and sometimes less numerous than the former.

Our transcriptomics and flow cytometry analyses provide a definitive characterization of both peripheral blood and tumor-infiltrating $CD8^+ILT2^+$ T cells as late-differentiated ($CD28^-CD27^-CD57^+$) T cells in accordance with previous reports (19-22), ILT2 expression being a specific feature of effector-memory ($CCR7^-$) cells, even more prevalent in terminally differentiated ($CCR7^-CD45RA^+$) TEMRA/effector T cells (30). The $CD8^+ILT2^+$ T cell subpopulation overlaps with those defined by trans-lineage cell-surface markers of cytotoxicity KLRG1 (31) and NKp80 (32) and indeed these cells display high expression of perforin and granzyme B at the transcript and protein levels. Consistent with these cytotoxic and innate-like phenotypical traits, $CD8^+ILT2^+$ T cells exhibit the highest degranulation levels upon CD3 engagement, appearing to be “ready-to-kill” effector cells. Interestingly, the cytotoxic functions of $CD8^+$ T cells expressing the costimulatory receptor NKp80 have also been shown to be triggered without engagement of the TCR/CD3 complex (33) through NK-like costimulation. Whether

such T cell-borne antigen-independent cytotoxicity is a component of antitumor immunity, possibly kept in check through ILT2, is of the highest interest.

We chose to characterize $CD8^+ILT2^+$ T cells as a cytotoxic population characterized by its differentiation stage, rather than antigen specificity, by performing CD3-mediated polyclonal activation of uncultured PBMCs or TILs *ex vivo*, since the culture and cloning of T cells strongly alters their properties and phenotype, including ILT2 expression (21). This allowed us to observe the immediate effects of HLA-G on its native T cell targets. Indeed, the historical demonstration that HLA-G could inhibit T cell cytotoxicity was made using a cultured virus-specific cytotoxic T lymphoid (CTL) clone, with no regard to ILT2 expression, leaving doubts as to its relevance *in vivo* (34). Furthermore, previous studies of the impact of ILT2 on T cell functions did not test its engagement by HLA-G (21,23,26), and we believe that in such conditions the blocking of ILT2 could only lift the lower-level inhibition consecutive to its engagement by classical MHC class I molecules (17). Of note, we only inconsistently observed such an effect with uncultured PBMCs, as already reported (23), but we did observe it with TILs here. We hypothesize that TILs within the tumor microenvironment, while having been exposed to prolonged stimulation, had also been rendered more sensitive to classical MHC class I-mediated inhibition. This would reunite our observations with the enhancement of *in vitro* cytotoxicity through ILT2 blocking which was observed in functional assays that used T cells expanded through repeated *in vitro* stimulation (21,25). In any case, our experiments clearly evidenced superior ILT2-mediated inhibition of T cell cytotoxicity when HLA-G was expressed by the target cells.

Apart from a single observation of circulating melanoma-specific $CD8^+ILT2^+$ T cells (19), a possible role for $CD8^+ILT2^+$ T cells in antitumor response has been overlooked. We previously observed that $CD8^+ILT2^+$ T cells were abundant in the microenvironment of ccRCC (3), and we show here that they are effective cytotoxic effectors, functionally and phenotypically distinct from exhausted T cells, and readily inhibited by target-borne HLA-G.

Although HLA-G expression by normal adult tissue is extremely restricted, it is frequently neo-expressed in immunotherapy-sensitive cancer types (35), including ccRCC (3,10). Our findings suggest that tumor-expressed HLA-G, through ILT2, could be a major inhibitory checkpoint for the effector functions of the naturally-occurring $CD8^+ILT2^+$ cytotoxic T cells in the tumor microenvironment. Apart from our own observations, the relevance of this phenomenon may be inferred from a mass cytometry study of 77 ccRCC cases by Chevrier *et al*., who described 22 TIL clusters as well as their frequent associations (29). Based on our flow cytometry data, we postulate that ILT2-positive effector $CD8^+$ TILs may be found in several of their PD-1-negative clusters, namely the T-11 (CD11b-positive), T-14 (CD45RA-positive) and T-4 (PD-1-negative with no other positive discriminatory marker) clusters. Interestingly, these clusters segregate together and may be more represented than PD-1-positive clusters in about one-third of ccRCC cases: it still remains to be clarified whether this constitutes an “effector-infiltrated” subset of ccRCCs in which targeting HLA-G may be of particular interest.

Therapeutic targeting of the PD-1/PD-L1 checkpoint is the backbone of modern cancer immunotherapy. In metastatic renal cell carcinoma, anti-PD-1 monotherapy yields clinical

responses in about one-fourth of patients (1), despite frequent PD-1 expression on TILs. We show here that naturally-occurring $CD8^+PD\text{-}1^+$ TILs display an incompletely differentiated phenotype, less mature than that of $CD8^+ILT2^+$ TILs, and a much lower expression of perforin. We postulate that efficient PD-1 blockade and release from exhaustion may allow $CD8^+PD\text{-}1^+$ TILs to undergo proliferation and full differentiation towards ILT2-positive effectors, as suggested by the study by Choueiri *et al*. (36) in which transcriptomics analyses were performed on ccRCC biopsy specimens from patients before and on treatment with Nivolumab. Their data showed that anti-PD-1 treatment led to higher expression of CD3 and CD8 transcripts, suggestive of $CD8^+$ T cell proliferation, as well as higher expression of *PRF1*, *GZMB* or *IFNG*, suggestive of full cytotoxic differentiation. Among other genes overexpressed under PD-1 blockade were *KLRG1* and *LILRB1*, the ILT2 gene. Regarding *KLRG1*, Choueiri et al. suggested that PD-1 blockade may lead to NK cell proliferation since KLRG1 is primarily known to be expressed by NK cells; *LILRB1*, which they classify as a myeloid cell gene, is not discussed. When completed by our present observations, this can be interpreted as revealing the expansion on PD-1 blockade of differentiated cytotoxic $CD8^+KLRG1^+ILT2^+$ TILS such as one can also observe in untreated patients. In this perspective, we hypothesize that HLA-G expression by cancer cells could be a mechanism of resistance to PD-1/PD-L1 blockade in ccRCC patients, since these newly-generated effectors would eventually be inhibited by tumor-borne HLA-G. Studies are ongoing at our center to confirm this hypothesis and may plead in favor of combined PD-1/PD-L1 and HLA-G/ILT2 blockade in selected patients.

In conclusion, ILT2 expression is a key feature of differentiated cytotoxic $CD8^+$ T cells, rendering them susceptible to HLA-G-mediated inhibition. ILT2-positive, HLA-G-sensitive, effector T cells are present in the tumor microenvironment of ccRCC, a solid cancer type in which HLA-G is frequently neo-expressed. This suggests that direct effector inhibition through the HLA-G/ILT2 checkpoint could be a mechanism of tumor escape from immune surveillance as well as of resistance to current checkpoint blockade therapy. This strengthens the rationale for targeting HLA-G concomitantly with other immune checkpoints in selected cancer patients.

REFERENCES

1. Motzer RJ, Escudier B, McDermott DF, George S, Hammers HJ, Srinivas S*, et al.* Nivolumab versus Everolimus in Advanced Renal-Cell Carcinoma. New Engl J Med 2015;373:1803-13
2. Motzer RJ, Tannir NM, McDermott DF, Frontera OA, Melichar B, Choueiri TK*, et al.* Nivolumab plus Ipilimumab versus Sunitinib in Advanced Renal-Cell Carcinoma. New Engl J Med 2018;378:1277-90
3. Rouas-Freiss N, LeMaoult J, Verine J, Tronik-Le Roux D, Culine S, Hennequin C*, et al.* Intratumor heterogeneity of immune checkpoints in primary renal cell cancer: Focus on HLA-G/ILT2/ILT4. Oncoimmunology 2017;6
4. Carosella ED, Favier B, Rouas-Freiss N, Moreau P, Lemaoult J. Beyond the increasing complexity of the immunomodulatory HLA-G molecule. Blood 2008;111:4862-70
5. Carosella ED, Rouas-Freiss N, Roux DT, Moreau P, LeMaoult J. HLA-G: An Immune Checkpoint Molecule. Advances in immunology 2015;127:33-144
6. Naji A, Le Rond S, Durrbach A, Krawice-Radanne I, Creput C, Daouya M*, et al.* CD3+CD4low and CD3+CD8low are induced by HLA-G: novel human peripheral blood suppressor T-cell subsets involved in transplant acceptance. Blood 2007;110:3936-48
7. Agaugue S, Carosella ED, Rouas-Freiss N. Role of HLA-G in tumor escape through expansion of myeloid-derived suppressor cells and cytokinic balance in favor of Th2 versus Th1/Th17. Blood 2011;117:7021-31
8. Ibrahim EC, Guerra N, Lacombe MJ, Angevin E, Chouaib S, Carosella ED*, et al.* Tumor-specific up-regulation of the nonclassical class I HLA-G antigen expression in renal carcinoma. Cancer research 2001;61:6838-45
9. Ibrahim EC, Allory Y, Commo F, Gattegno B, Callard P, Paul P. Altered pattern of major histocompatibility complex expression in renal carcinoma: tumor-specific expression of the nonclassical human leukocyte antigen-G molecule is restricted to clear cell carcinoma while up-regulation of other major histocompatibility complex antigens is primarily distributed in all subtypes of renal carcinoma. The American journal of pathology 2003;162:501-8
10. Li BL, Lin A, Zhang XJ, Zhang X, Zhang JG, Wang Q*, et al.* Characterization of HLA-G expression in renal cell carcinoma. Tissue antigens 2009;74:213-21
11. Chang CC, Murphy SP, Ferrone S. Differential in vivo and in vitro HLA-G expression in melanoma cells: potential mechanisms. Human immunology 2003;64:1057-63
12. Rebmann V, Wagner S, Grosse-Wilde H. HLA-G expression in malignant melanoma. Seminars in cancer biology 2007;17:422-9
13. Melsted WN, Johansen LL, Lock-Andersen J, Behrendt N, Eriksen JO, Bzorek M*, et al.* HLA class Ia and Ib molecules and FOXP3+TILs in relation to the prognosis of malignant melanoma patients. Clinical Immunology 2017;183:191-7
14. Lin A, Zhu CC, Chen HX, Chen BF, Zhang X, Zhang JG*, et al.* Clinical relevance and functional implications for human leucocyte antigen-g expression in non-small-cell lung cancer. Journal of cellular and molecular medicine 2010;14:2318-29
15. Yie SM, Yang H, Ye SR, Li K, Dong DD, Lin XM. Expression of human leucocyte antigen G (HLA-G) is associated with prognosis in non-small cell lung cancer. Lung Cancer 2007;58:267-74
16. Loumagne L, Baudhuin J, Favier B, Montespan F, Carosella ED, Rouas-Freiss N. In vivo evidence that secretion of HLA-G by immunogenic tumor cells allows their evasion from immunosurveillance. International journal of cancer Journal international du cancer 2014;135:2107-17
17. Colonna M, Navarro F, Bellon T, Llano M, Garcia P, Samaridis J*, et al.* A common inhibitory receptor for major histocompatibility complex class I molecules on human lymphoid and myelomonocytic cells. The Journal of experimental medicine 1997;186:1809-18

18. Saverino D, Fabbi M, Ghiotto F, Merlo A, Bruno S, Zarcone D*, et al.* The CD85/LIR-1/ILT2 inhibitory receptor is expressed by all human T lymphocytes and down-regulates their functions. Journal of Immunology 2000;165:3742-55
19. Speiser DE, Valmori D, Rimoldi D, Pittet MJ, Lienard D, Cerundolo V*, et al.* CD28-negative cytolytic effector T cells frequently express NK receptors and are present at variable proportions in circulating lymphocytes from healthy donors and melanoma patients. European journal of immunology 1999;29:1990-9
20. Young NT, Uhrberg M, Phillips JH, Lanier LL, Parham P. Differential expression of leukocyte receptor complex-encoded Ig-like receptors correlates with the transition from effector to memory CTL. Journal of Immunology 2001;166:3933-41
21. Ince MN, Harnisch B, Xu Z, Lee SK, Lange C, Moretta L*, et al.* Increased expression of the natural killer cell inhibitory receptor CD85j/ILT2 on antigen-specific effector CD8 T cells and its impact on CD8 T-cell function. Immunology 2004;112:531-42
22. Northfield J, Lucas M, Jones H, Young NT, Klenerman P. Does memory improve with age? CD85j (ILT-2/LIR-1) expression on CD81 T cells correlates with 'memory inflation' in human cytomegalovirus infection. Immunology and cell biology 2005;83:182-8
23. Gustafson CE, Qi Q, Hutter-Saunders J, Gupta S, Jadhav R, Newell E*, et al.* Immune Checkpoint Function of CD85j in CD8 T Cell Differentiation and Aging. Frontiers in immunology 2017;8
24. Rothe K, Quandt D, Schubert K, Rossol M, Klingner M, Jasinski-Bergner S*, et al.* Latent Cytomegalovirus Infection in Rheumatoid Arthritis and Increased Frequencies of Cytolytic LIR-1+CD8+T Cells. Arthritis & Rheumatology 2016;68:337-46
25. Anfossi N, Doisne JM, Peyrat MA, Ugolini S, Bonnaud O, Bossy D*, et al.* Coordinated expression of ig-like inhibitory MHC class I receptors and acquisition of cytotoxic function in human CD8(+) T cells. Journal of Immunology 2004;173:7223-9
26. Costa P, Rusconi S, Mavilio D, Fogli M, Murdaca G, Pende D*, et al.* Differential disappearance of inhibitory natural killer cell receptors during HAART and possible impairment of HIV-1-specific CD8 cytotoxic T lymphocytes. AIDS 2001;15:965-74
27. Servant N, Gravier E, Gestraud P, Laurent C, Paccard C, Biton A*, et al.* EMA - A R package for Easy Microarray data analysis. BMC research notes 2010;3:277
28. Sallusto F, Lenig D, Forster R, Lipp M, Lanzavecchia A. Two subsets of memory T lymphocytes with distinct homing potentials and effector functions. Nature 1999;401:708-12
29. Chevrier S, Levine JH, Zanotelli VRT, Silina K, Schulz D, Bacac M*, et al.* An Immune Atlas of Clear Cell Renal Cell Carcinoma. Cell 2017;169:736-49.e18
30. Mahnke YD, Brodie TM, Sallusto F, Roederer M, Lugli E. The who's who of T-cell differentiation: human memory T-cell subsets. European journal of immunology 2013;43:2797-809
31. Strioga M, Pasukoniene V, Characiejus D. CD8+ CD28- and CD8+ CD57+ T cells and their role in health and disease. Immunology 2011;134:17-32
32. Kuttruff S, Koch S, Kelp A, Pawelec G, Rammensee H-G, Steinle A. NKp80 defines and stimulates a reactive subset of CD8 T cells. Blood 2009;113:358-69
33. Simoni Y, Becht E, Fehlings M, Loh CY, Koo S-L, Teng KWW*, et al.* Bystander CD8+ T cells are abundant and phenotypically distinct in human tumour infiltrates. Nature 2018;557:575-9
34. Le Gal FA, Riteau B, Sedlik C, Khalil-Daher I, Menier C, Dausset J*, et al.* HLA-G-mediated inhibition of antigen-specific cytotoxic T lymphocytes. International immunology 1999;11:1351-6
35. Curigliano G, Criscitiello C, Gelao L, Goldhirsch A. Molecular pathways: human leukocyte antigen G (HLA-G). Clinical cancer research : an official journal of the American Association for Cancer Research 2013;19:5564-71
36. Choueiri TK, Fishman MN, Escudier B, McDermott DF, Drake CG, Kluger H*, et al.* Immunomodulatory Activity of Nivolumab in Metastatic Renal Cell Carcinoma. Clinical Cancer Research 2016;22:5461-71

Table 1. Immune checkpoint expression in ccRCC

Expression of immune checkpoint molecules in ccRCC samples used for this study. Expression of immune checkpoint ligands PD-L1 and HLA-G were determined using immunohistochemistry. Distribution of TIL subsets expressing immune checkpoint receptors PD-1 and ILT2 were determined using flow cytometry. A range of values denotes spatial heterogeneity when several tumor zones were studied.

Sample	PD-L1 expression (tumor cells)	PD-L1 expression (infiltrating cells)	HLA-G expression (tumor cells)	% CD8+PD-1+ TILs	% CD8+ILT2+ TILs
23	0%	0%	10-50%	17-56%	26-56%
24	>50%	20%	100%	85-91%	9-14%
25	0%	5%	1%	92%	2-4%
26	0%	<10%	80%	64%	22-31%
0	0%	0%	<5%	43%	32%
27	0%	0%	5%	42%	30%
28	0%	0%	0%	38%	13%
29	0%	0%	1%	59%	45-55%

FIGURE LEGENDS

Figure 1. Characterization of peripheral blood ILT2-positive CD8$^+$ T cells using transcriptomic data analysis

(A) mRNA expression profiles of ILT2-positive and ILT2-negative CD8$^+$ T cells. Heatmap generated using the 500 most variant genes accross all samples. Red indicates an increase of mRNA expression and green indicates a decrease. Hierachical clustering was performed on genes (rows) and samples (columns) using Pearson correlation method and Ward distance. **(B)** Volcano plot of genes comparing ILT2-positive versus ILT2-negative. Down-regulated genes in ILT2-positive compared to ILT2-negative (Log2 Fold Change <1.5 and FDR < 0.05) are colored in grey, up-regulated genes in ILT2-positive compared to ILT2-negative (Log2 Fold Change >1.5 and FDR < 0.05) are colored in black. The number of DEG (Down-expressed Genes) for each condition is described. **(C)** Functional network inference allows distinguishing the most significantly overrepresented biological pathways for ILT2-positive networks on top panel and ILT2-negative networks on bottom panel. Different colors represent distinct pathways. Only pathways with Bonferroni corrected pvalue < 0.05 are shown. **(D)** Barplot of the moderated t-statistics of selected differentially expressed genes between ILT2-positive and ILT2-negative CD8$^+$ T cells. Genes up regulated in ILT2-positiveCD8$^+$ T cells are colored in black, genes downregulated in ILT2-positive CD8$^+$ T cells are in grey. Adjusted p-values are shown on the plot (* p<0.05, ** p<0.01, *** p<0.001).

Figure 2. Phenotypical characterization of peripheral blood ILT2-positive $CD8^+$ T cells.

(A) Flow cytometry plots from a representative NMIBC patient showing expression of ILT2 (vertical axis) and selected markers (horizontal axis) on peripheral blood $CD3^+CD8^+$ lymphocytes. **(B)** Positivity of ILT2-negative (white boxes) and ILT2-positive (grey boxes) peripheral blood $CD3^+CD8^+$ lymphocytes for selected cell-surface and intracytosolic markers. Data is pooled from 4 NIMBC patients and 2 control patients. GzmB: Granzyme B; ** p<0,01 and *** p<0,001 by t-test paired by sample. Error bars represent minimal and maximal values, + represent mean values.

Figure 3. ILT2 cell-surface expression is a feature of differentiated cytotoxic $CD8^+$ T cells.

(A) Percentage of ILT2-positive cells on peripheral blood CD3+CD8+ lymphocytes subsets defined by expression of selected single markers. Data is pooled from 4 NIMBC patients and 2 control patients. GzmB: Granzyme B; ** p<0,01 and *** p<0,001 by t-test paired by sample. Error bars represent minimal and maximal values, + represent mean values. **(B)** Representative flow cytometry plots from a NMIBC patient showing the repartition of ILT2-negative (left) and ILT2-positive (right) $CD3^+CD8^+$ lymphocytes among memory subtypes defined by expression of CCR7 and CD45RA. **(C)** Percentage of ILT2-positive cells among memory subtypes of peripheral blood $CD3^+CD8^+$ lymphocytes defined as follows: naïve T cells (TN) $CCR7^+CD45RA^+$, central memory T cells (TCM) $CCR7^+CD45RA^-$, effector memory T cells (TEM) $CCR7^-CD45RA^-$, effector T cells/effector memory T cells reexpressing

CD45RA (TEMRA) $CCR7^{-}CD45RA^{+}$. Data is pooled from 3 NMIBC patients and 2 control patients. GzmB: Granzyme B; * p<0,05 ** p<0,01 and *** p<0,001 by t-test paired by sample. Error bars represent minimal and maximal values, + represent mean values.

Figure 4. HLA-G1 inhibits the CD3-mediated cytolytic degranulation of $CD8^{+}$ T cells through ILT2

(A) Representative flow cytometry analysis of staining with an PE-conjugated anti-CD107a) mAb on $CD8^{+}$ T cells after a 4-hour co-incubation of PBMCs with target cells (mTHP1, left) and target cells coated with an agonist anti-CD3 antibody (αCD3 right). **(B)** Percentage of CD107a-positive cells on ILT2-negative (left) and ILT2-positive (right) $CD8^{+}$ T cells after a 4-hour co-incubation with αCD3-coated parental (mTHP1, white) or HLA-G1-expressing (mTHP1-HLA-G1, grey) target cells. **(C)** Percentage of CD107a-positive cells on $CD57^{-}$ (left) and $CD57^{high}$ (right) $CD8^{+}$ T cells after a 4-hour co-incubation with αCD3-coated parental (mTHP1, white) or HLA-G1-expressing (mTHP1-HLAG1, grey) target cells in the presence of a control IgG2b (Ctrl, plain) or the anti-ILT2 mAb GHI/75 (αILT2, striped). For (B) and (C) conditions were reproduced in sextuplicates using PBMCs from a NMIBC patient with 20% and 71% ILT2-positive cells in the $CD57^{-}$ and $CD57^{high}$ subpopulations, respectively. Wells with the highest and lowest global degranulation levels (appreciated using the percentage of CD107a-positive cells on the total $CD3^{+}CD8^{+}$ cells) were exluded from the analysis for all T cell subsets. Representative of 3 independent experiments with samples from 3 different NMIBC patients. * p<0,05 ** p<0,01 and *** p<0,001. **(D)** Representative flow cytometry analysis of staining with an FITC-conjugated anti-IFNg mAb on $CD8^{+}$ T cells after a 3-hour co-incubation of PBMCs with target cells (mTHP1, left) and target cells coated with an

agonist anti-CD3 antibody (αCD3 right) **(E)** Percentage of IFNγ-positive cells on ILT2-negative (left) and ILT2-positive (right) $CD8^+$ T cells after a 3-hour co-incubation with αCD3-coated parental (mTHP1, white) or HLA-G1-expressing (mTHP1-HLA-G1, grey) target cells. **(F)** Percentage of IFNγ-positive cells on $CD57^-$ (left) and $CD57^{high}$ (right) $CD8^+$ T cells after a 3-hour co-incubation with αCD3-coated parental (mTHP1, white) or HLA-G1-expressing (mTHP1-HLAG1, grey) target cells in the presence of a control IgG2b (Ctrl, plain) or the anti-ILT2 mAb GHI/75 (αILT2, striped). For (D) and (E) conditions were reproduced in sextuplicates using PBMCs from a ccRCC patient with 13% and 93% ILT2-positive cells in the $CD57^-$ and $CD57^{high}$ subpopulations respectively. Figure representative of 3 independent experiments with samples from 3 (D) or 4 (E) different ccRCC patients. * p<0,05 ** p<0,01 and *** p<0,001.

Figure 5: Representative examples of HLA-G staining in tumor tissue specimens from two ccRCC patients.

(A) and **(C)**: H&E staining is shown with the cytoplasm in pink and the nuclei in purple. **(B)** and **(D)** HLA-G expression in tumor cells is detected with the 4H84 mAb. Brown labeling indicates HLA-G positivity. Original magnification x 200.

Figure 6. ILT2-positive tumor-infiltrating T cells are differentiated cytolytic effectors that do not present an exhausted phenotype.

(A) Flow cytometry plot of tumor-infiltrating $CD8^+$ T cells from 1 representative ccRCC patient showing ILT2-positive and PD-1-positive cells as distinct subpopulations. Figure representative of 8 ccRCC patients. **(B)** Flow cytometry plots of tumor-infiltrating $CD8^+$ T cells

from 1 representative ccRCC showing the expression of perforin and selected cell-surface markers according to PD-1 (upper) or ILT2 (lower) expression on tumor-infiltrating CD8+ T cells. Figures representative of 3 ccRCC patients except for CD57 (6 patients) and CD11b (2 patients). **(C)** Flow cytometry plots of expression of memory markers CCR7 and CD45RA on PD-1-positive (left) and ILT2-positive (right) $CD8^+$ T cells from 1 representative ccRCC patient. Representative of 5 ccRCC patients.

Figure 7. Target-borne HLA-G1 inhibits the effector functions of ILT2-positive tumor-infiltrating $CD8^+$ T cells

(A) Percentage of CD107a-positive cells on the PD-1-positive, ILT2-positive and ILT2-enriched surrogate subsets of $CD8^+$ TILs ($CD45RA^+PD1^-$) after a 4-hour co-incubation with αCD3-coated parental target cells (white bars) or HLA-G1-expressing (mTHP1-HLA-G1) target cells (grey bars) in the absence (Ctrl: plain bars) or in the presence of the anti-ILT2 mAb GHI/75 (αILT2: striped bars). Conditions were reproduced in triplicate using TILs from a ccRCC sample. Representative of 3 independent experiments performed on TIL samples from 2 patients. * $p<0,05$ ** $p<0,01$ and *** $p<0,001$.

(B) Percentage of IFNγ-positive cells on the PD-1-positive, ILT2-positive and ILT2-enriched surrogate subsets of $CD8^+$ TILs ($CD57^+PD1^-$) after a 3-hour co-incubation with αCD3-coated parental target cells (white bars) or HLA-G1-expressing (mTHP1-HLA-G1) target cells (grey bars) in the absence (Ctrl: plain bars) or in the presence of the anti-ILT2 mAb GHI/75 (αILT2: striped bars). Conditions were reproduced in sextuplicate using TILs from a ccRCC sample.

Representative of 2 independent experiments performed on TIL samples from 2 patients. * $p<0,05$ ** $p<0,01$ and *** $p<0,001$.

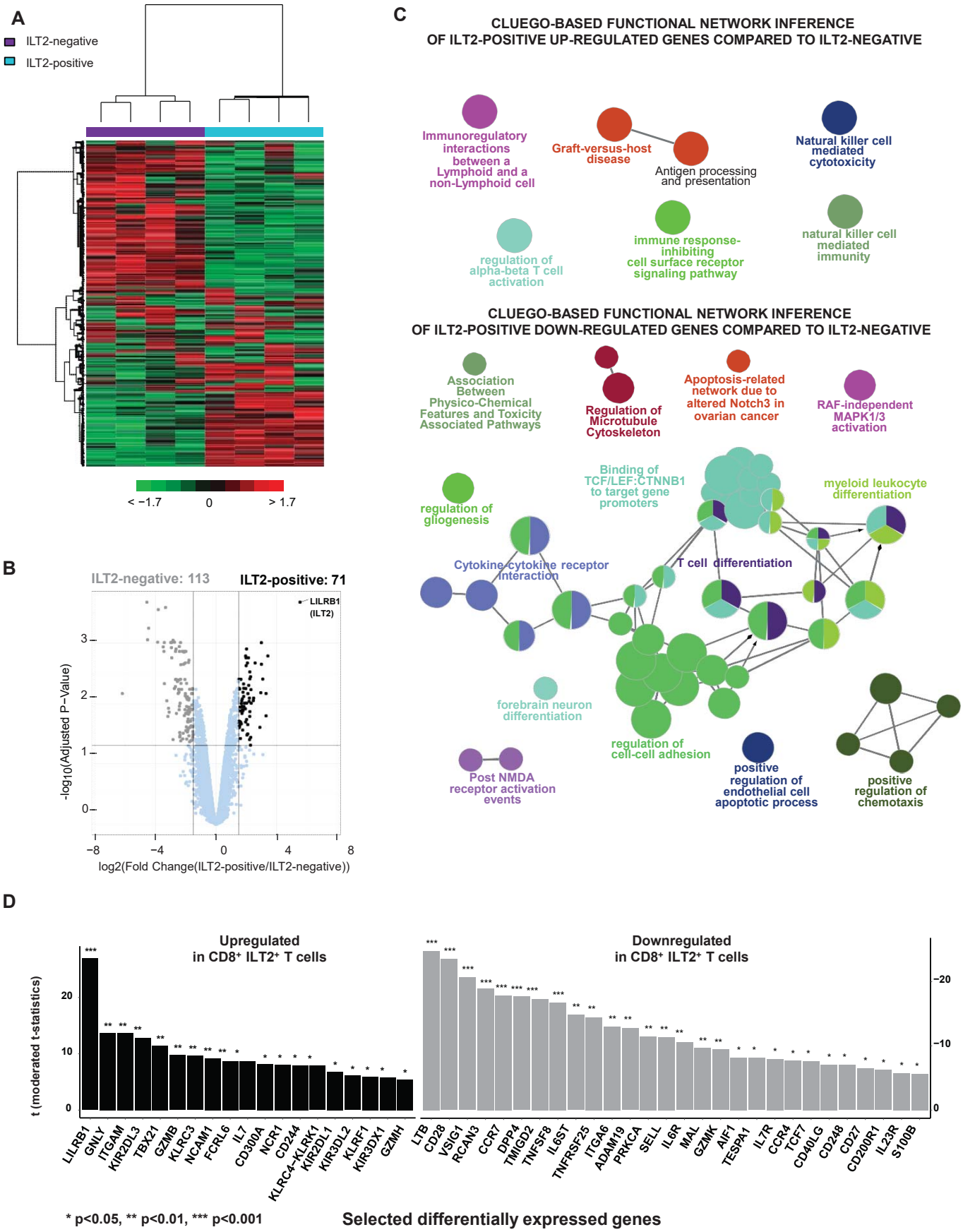
A
ILT2-negative
ILT2-positive
< −1.7
0
> 1.7
B
ILT2-negative: 113
ILT2-positive: 71
LILRB1 (ILT2)
-log10(Adjusted P−Value)
log2(Fold Change(ILT2-positive/ILT2-negative))
C
CLUEGO-BASED FUNCTIONAL NETWORK INFERENCE OF ILT2-POSITIVE UP-REGULATED GENES COMPARED TO ILT2-NEGATIVE
Immunoregulatory interactions between a Lymphoid and a non-Lymphoid cell
Graft-versus-host disease
Antigen processing and presentation
Natural killer cell mediated cytotoxicity
regulation of alpha-beta T cell activation
immune response-inhibiting cell surface receptor signaling pathway
natural killer cell mediated immunity
CLUEGO-BASED FUNCTIONAL NETWORK INFERENCE OF ILT2-POSITIVE DOWN-REGULATED GENES COMPARED TO ILT2-NEGATIVE
Association Between Physico-Chemical Features and Toxicity Associated Pathways
Regulation of Microtubule Cytoskeleton
Apoptosis-related network due to altered Notch3 in ovarian cancer
RAF-independent MAPK1/3 activation
Binding of TCF/LEF:CTNNB1 to target gene promoters
myeloid leukocyte differentiation
regulation of gliogenesis
Cytokine-cytokine receptor interaction
T cell differentiation
forebrain neuron differentiation
regulation of cell-cell adhesion
Post NMDA receptor activation events
positive regulation of endothelial cell apoptotic process
positive regulation of chemotaxis
D
Upregulated in CD8+ ILT2+ T cells
Downregulated in CD8+ ILT2+ T cells
t (moderated t-statistics)
LILRB1 GNLY ITGAM KIR2DL3 TBX21 GZMB KLRC3 NCAM1 FCRL6 IL7 CD300A NCR1 CD244 KLRC4-KLRK1 KIR2DL1 KIR3DL2 KLRF1 KIR3DX1 GZMH
LTB CD28 VSIG1 RCAN3 CCR7 DPP4 TMIGD2 TNFSF8 IL6ST TNFRSF25 ITGA6 ADAM19 PRKCA SELL IL6R MAL GZMK AIF1 TESPA1 IL7R CCR4 TCF7 CD40LG CD248 CD27 CD200R1 IL23R S100B
* p<0.05, ** p<0.01, *** p<0.001
Selected differentially expressed genes

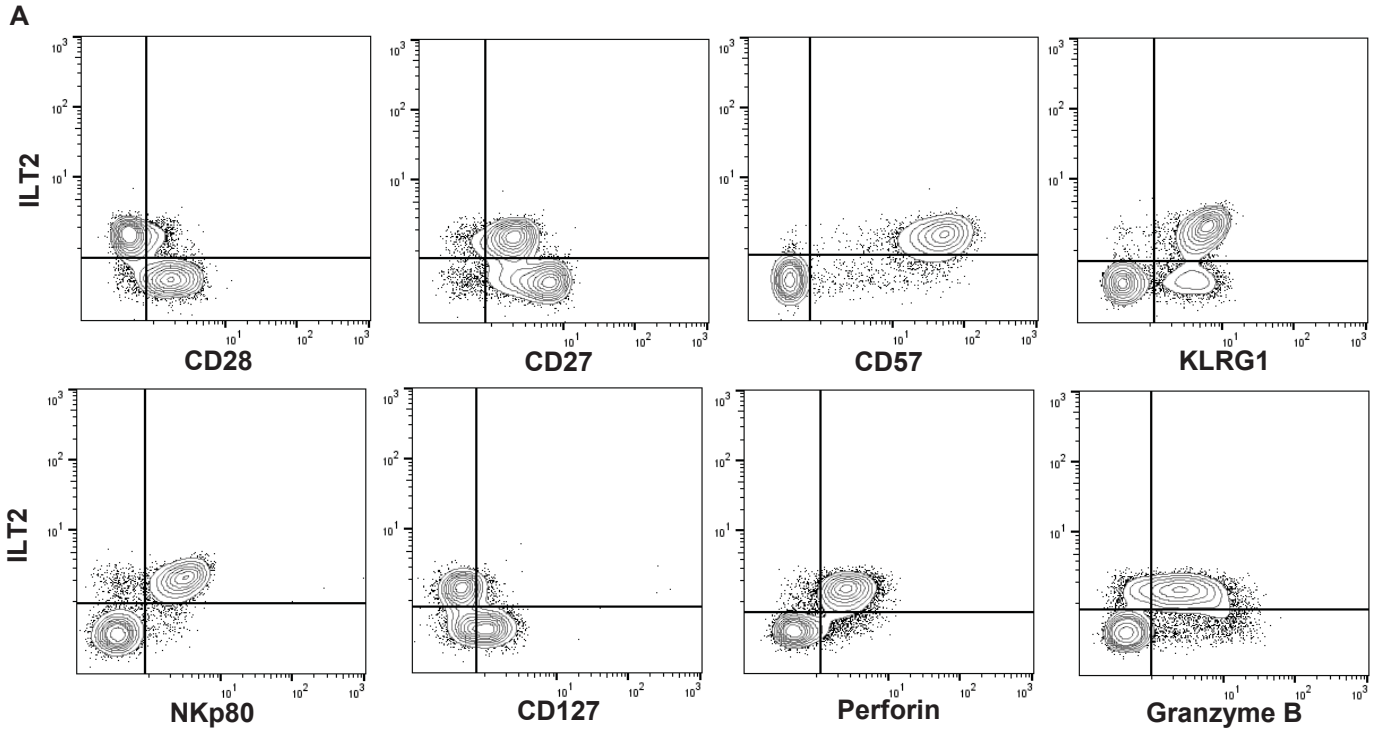
A
ILT2
CD28
CD27
CD57
KLRG1
ILT2
NKp80
CD127
Perforin
Granzyme B

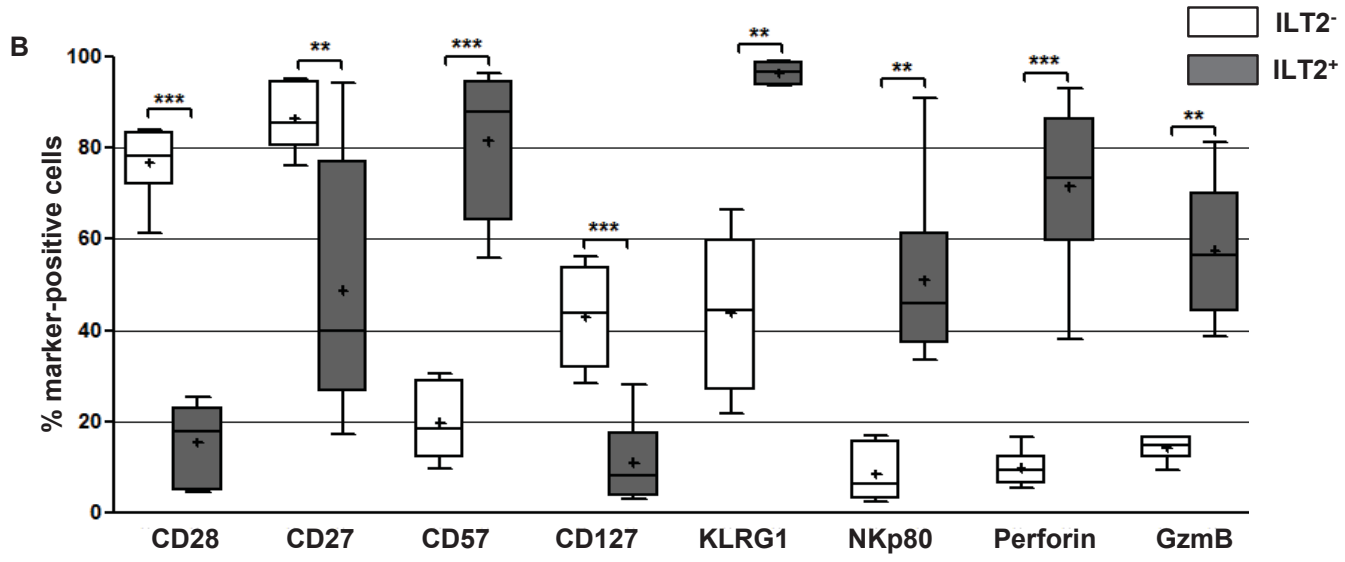
B
ILT2-
ILT2+
% marker-positive cells
100
80
60
40
20
0
CD28
CD27
CD57
CD127
KLRG1
NKp80
Perforin
GzmB

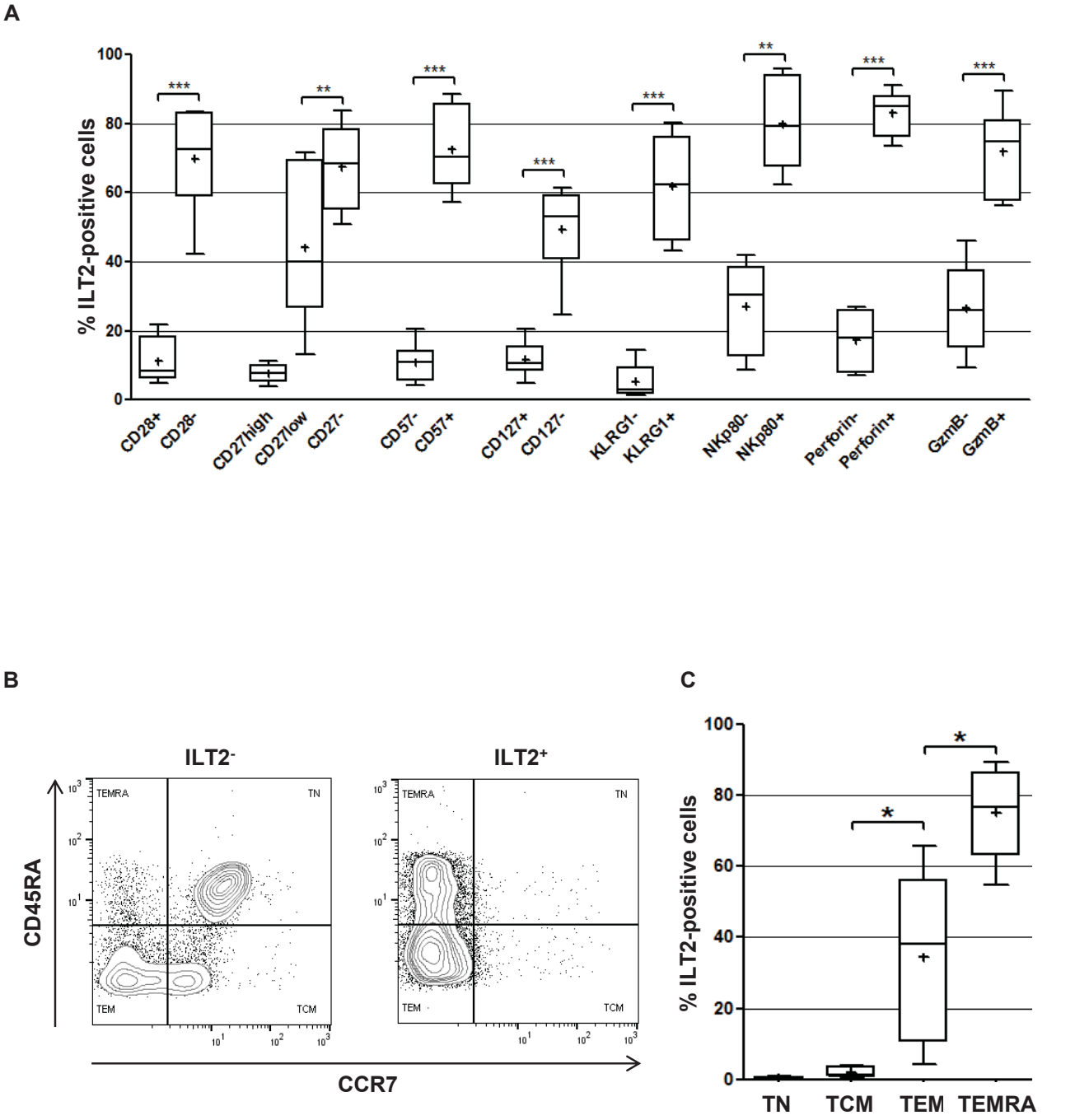
A
% ILT2-positive cells
100
80
60
40
20
0
***
**
***
***
***
**
***
***
CD28+
CD28-
CD27high
CD27low
CD27-
CD57-
CD57+
CD127+
CD127-
KLRG1-
KLRG1+
NKp80-
NKp80+
Perforin-
Perforin+
GzmB-
GzmB+
B
ILT2-
ILT2+
CD45RA
CCR7
TEMRA
TN
TEM
TCM
C
% ILT2-positive cells
100
80
60
40
20
0
*
*
TN
TCM
TEM
TEMRA

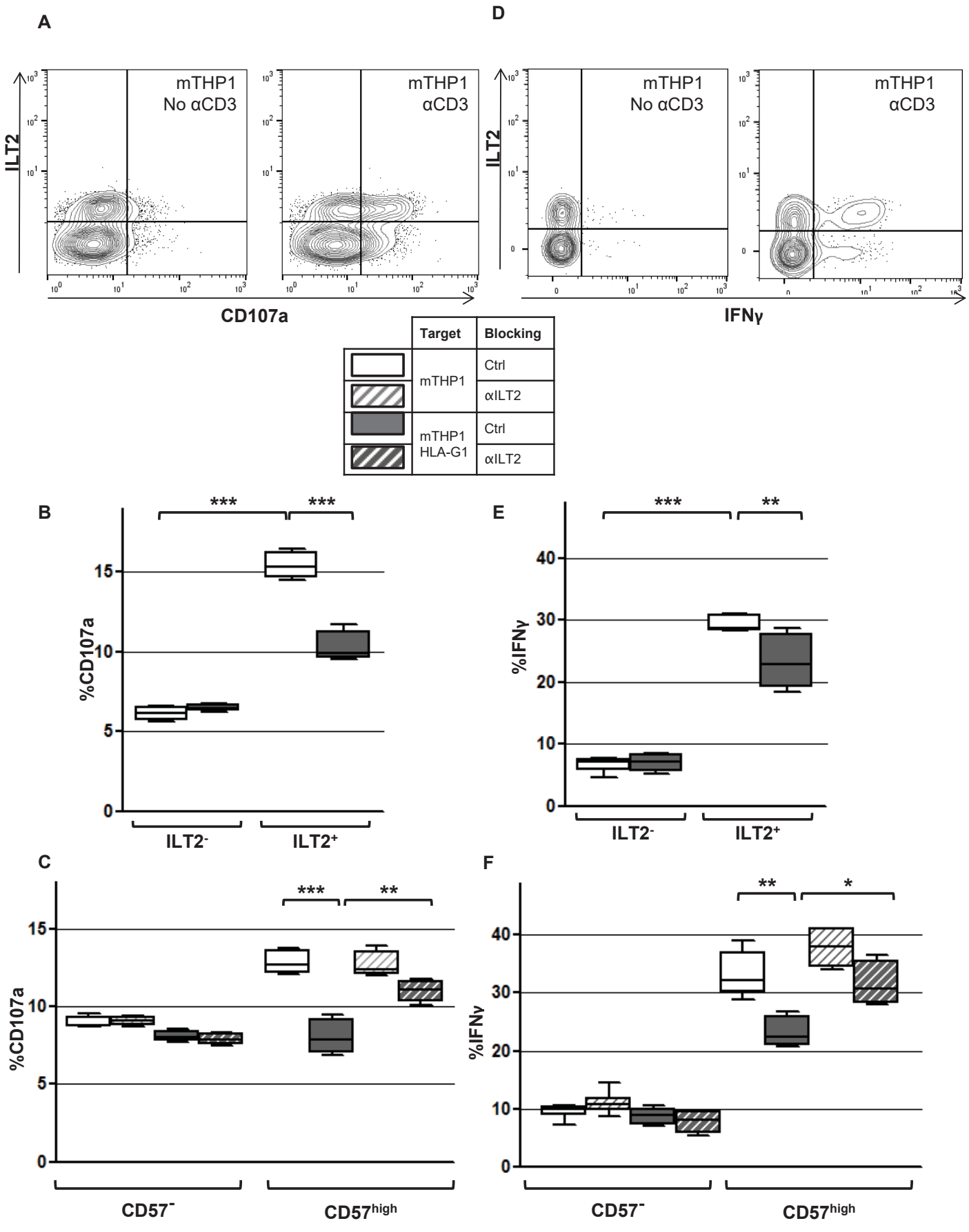
A
D
mTHP1
No αCD3
mTHP1
αCD3
ILT2
CD107a
IFNγ
Target
Blocking
mTHP1
Ctrl
αILT2
mTHP1 HLA-G1
Ctrl
αILT2
B
E
%CD107a
%IFNγ
ILT2-
ILT2+
C
F
%CD107a
%IFNγ
CD57-
CD57high

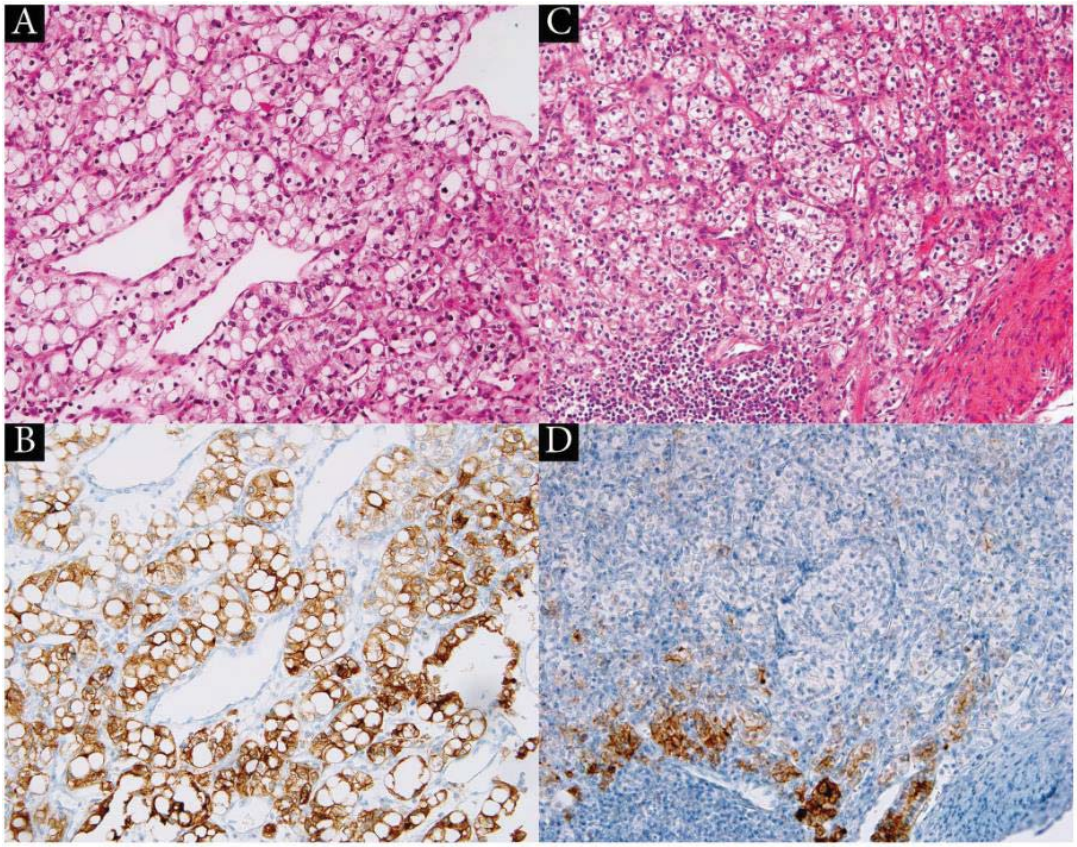
A
C
B
D

Figure 6

Dumont *et al.*

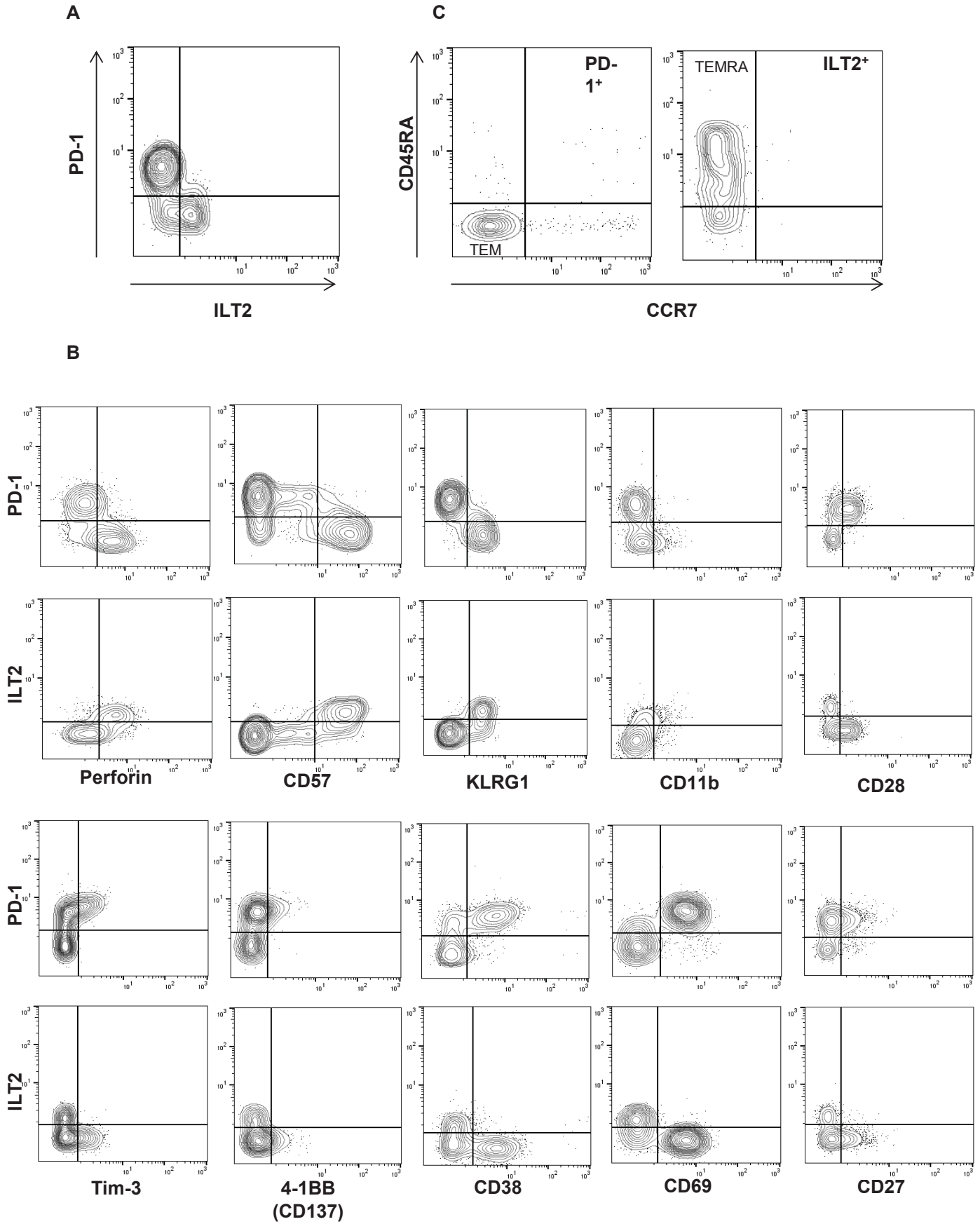

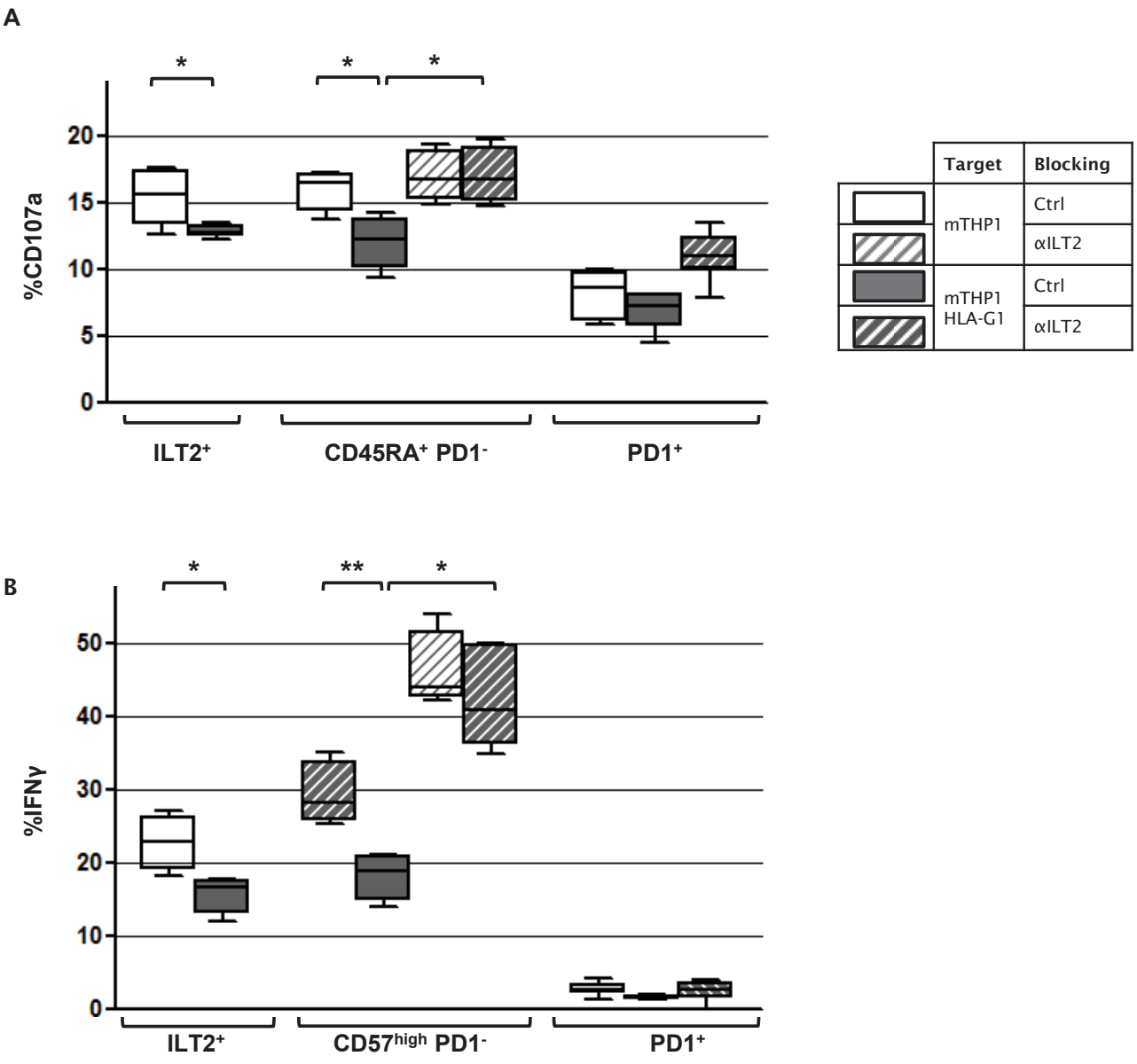
A
%CD107a
0
5
10
15
20
*
*
*
ILT2+
CD45RA+ PD1-
PD1+
Target
Blocking
mTHP1
Ctrl
αILT2
mTHP1 HLA-G1
Ctrl
αILT2
B
%IFNγ
0
10
20
30
40
50
*
**
*
ILT2+
CD57high PD1-
PD1+

Supplementary Figures

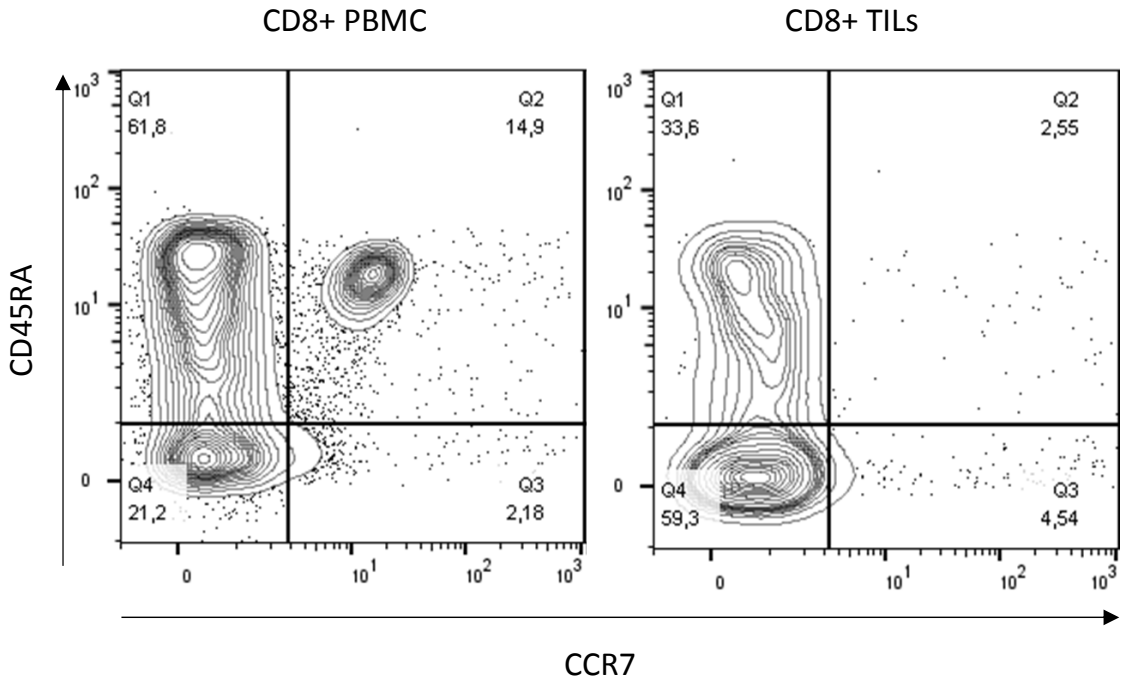

Figure S1. Control of non-presence of peripheral subpopulations among the tumor infiltrate

Flow cytometry plots from a representative ccRCC patient showing expression of CD45RA (vertical axis) and CCR7 (horizontal axis) on peripheral blood $CD3^+CD8^+$ cells (PBMC, left panel) and intratumoral $CD3^+CD8^+$ lymphocytes (TILs, right panel). The absence of $CD45RA^+CCR7^+$ subpopulation in TILS indicates minimal blood contamination

Supplementary Table I. Specifically upregulated and downregulated genes in CD8+ILT2+ T cells vs CD8+ILT2- T cells

	Probeset	adjusted P Value	Fold difference	SYMBOL	GENENAME
Upregulated in CD8+ILT2+ T cells	10859_at	2.09E-04	8.81	LILRB1	leukocyte immunoglobulin like receptor B1
	353345_at	9.81E-04	6.69	GPR141	G protein-coupled receptor 141
	162966_at	1.25E-03	6.29	ZNF600	zinc finger protein 600
	353189_at	1.63E-03	5.79	SLCO4C1	solute carrier organic anion transporter family member 4C1
	59084_at	1.63E-03	5.76	ENPP5	ectonucleotide pyrophosphatase/phosphodiesterase 5 (putative)
	10578_at	1.75E-03	5.64	GNLY	granulysin
	3684_at	1.75E-03	5.64	ITGAM	integrin subunit alpha M
	64097_at	2.13E-03	5.33	EPB41L4A	erythrocyte membrane protein band 4.1 like 4A
	81553_at	2.13E-03	5.35	FAM49A	family with sequence similarity 49 member A
	3804_at	2.24E-03	5.24	KIR2DL3	killer cell immunoglobulin like receptor, two Ig domains and long cytoplasmic tail 3
	9788_at	2.36E-03	5.15	MTSS1	MTSS1, I-BAR domain containing
	81563_at	2.99E-03	4.93	C1orf21	chromosome 1 open reading frame 21
	102724104_at	3.61E-03	4.74	LOC102724104	uncharacterized LOC102724104
	10875_at	3.91E-03	4.65	FGL2	fibrinogen like 2
	284367_at	3.94E-03	4.60	SIGLEC17P	sialic acid binding Ig like lectin 17, pseudogene
	30009_at	3.97E-03	4.57	TBX21	T-box 21
	23314_at	4.01E-03	4.48	SATB2	SATB homeobox 2
	53637_at	4.01E-03	4.45	S1PR5	sphingosine-1-phosphate receptor 5
	5874_at	4.01E-03	4.46	RAB27B	RAB27B, member RAS oncogene family
	4646_at	4.75E-03	4.16	MYO6	myosin VI
	445347_at	5.02E-03	4.09	TARP	TCR gamma alternate reading frame protein
	11098_at	5.62E-03	3.95	PRSS23	protease, serine 23
	79899_at	5.62E-03	3.94	PRR5L	proline rich 5 like
	105370660_at	5.67E-03	3.91	LOC105370660	uncharacterized LOC105370660
	79180_at	5.78E-03	3.85	EFHD2	EF-hand domain family member D2
	4067_at	5.91E-03	3.73	LYN	LYN proto-oncogene, Src family tyrosine kinase
	124221_at	6.52E-03	3.59	PRSS30P	protease, serine, 30 pseudogene
	3002_at	6.64E-03	3.55	GZMB	granzyme B
	51314_at	6.85E-03	3.49	NME8	NME/NM23 family member 8
	3823_at	6.87E-03	3.46	KLRC3	killer cell lectin like receptor C3
	5782_at	7.66E-03	3.29	PTPN12	protein tyrosine phosphatase, non-receptor type 12
	105376387_at	8.15E-03	3.17	LOC105376387	uncharacterized LOC105376387
	4684_at	8.15E-03	3.16	NCAM1	neural cell adhesion molecule 1
	9832_at	8.41E-03	3.08	JAKMIP2	janus kinase and microtubule interacting protein 2
	105369656_at	8.98E-03	2.99	LOC105369656	uncharacterized LOC105369656
	59352_at	9.05E-03	2.93	LGR6	leucine rich repeat containing G protein-coupled receptor 6
	9839_at	9.26E-03	2.90	ZEB2	zinc finger E-box binding homeobox 2
	343413_at	9.91E-03	2.78	FCRL6	Fc receptor like 6
	57458_at	9.91E-03	2.77	TMCC3	transmembrane and coiled-coil domain family 3
	100507195_at	9.93E-03	2.75	LINC02384	long intergenic non-protein coding RNA 2384
	3574_at	1.00E-02	2.73	IL7	interleukin 7
	114879_at	1.12E-02	2.54	OSBPL5	oxysterol binding protein like 5
	401124_at	1.12E-02	2.53	DTHD1	death domain containing 1
	10417_at	1.16E-02	2.49	SPON2	spondin 2
	11314_at	1.23E-02	2.37	CD300A	CD300a molecule
	9437_at	1.27E-02	2.30	NCR1	natural cytotoxicity triggering receptor 1
	51744_at	1.31E-02	2.22	CD244	CD244 molecule
	100528032_at	1.33E-02	2.15	KLRC4-KLRK1	KLRC4-KLRK1 readthrough
	313_at	1.33E-02	2.17	AOAH	acyloxyacyl hydrolase
	692229_at	1.33E-02	2.16	SNORD105	small nucleolar RNA, C/D box 105
	9331_at	1.37E-02	2.11	B4GALT6	beta-1,4-galactosyltransferase 6
	5911_at	1.47E-02	1.99	RAP2A	RAP2A, member of RAS oncogene family
	3904_at	1.61E-02	1.83	LAIR2	leukocyte associated immunoglobulin like receptor 2
	5351_at	1.64E-02	1.78	PLOD1	procollagen-lysine,2-oxoglutarate 5-dioxygenase 1
	5341_at	1.85E-02	1.57	PLEK	pleckstrin
	80310_at	1.97E-02	1.42	PDGFD	platelet derived growth factor D
	117157_at	2.03E-02	1.34	SH2D1B	SH2 domain containing 1B
	79815_at	2.04E-02	1.33	NIPAL2	NIPA like domain containing 2
	55026_at	2.18E-02	1.22	TMEM255A	transmembrane protein 255A
	221895_at	2.20E-02	1.21	JAZF1	JAZF zinc finger 1
	3802_at	2.25E-02	1.18	KIR2DL1	killer cell immunoglobulin like receptor, two Ig domains and long cytoplasmic tail 1
	23209_at	2.36E-02	1.05	MLC1	megalencephalic leukoencephalopathy with subcortical cysts 1
	9289_at	2.50E-02	0.93	ADGRG1	adhesion G protein-coupled receptor G1
	387895_at	2.53E-02	0.89	LINC00944	long intergenic non-protein coding RNA 944
	84131_at	2.77E-02	0.77	CEP78	centrosomal protein 78
	3812_at	3.20E-02	0.50	KIR3DL2	killer cell immunoglobulin like receptor, three Ig domains and long cytoplasmic tail 2
	107984889_at	3.34E-02	0.43	LOC107984889	uncharacterized LOC107984889
	51348_at	3.66E-02	0.29	KLRF1	killer cell lectin like receptor F1
	23603_at	3.83E-02	0.22	CORO1C	coronin 1C
	90011_at	3.98E-02	0.13	KIR3DX1	killer cell immunoglobulin like receptor, three Ig domains X1
	2999_at	4.93E-02	-0.27	GZMH	granzyme H
	105373204_at	2.09E-04	8.95	LOC105373204	uncharacterized LOC105373204
	4050_at	2.56E-04	8.51	LTB	lymphotoxin beta
	940_at	2.77E-04	8.31	CD28	CD28 molecule

Downregulated in CD8+ILT2+ T cells	340547_at	5.65E-04	7.77	VSIG1	V-set and immunoglobulin domain containing 1
	11123_at	8.78E-04	7.37	RCAN3	RCAN family member 3
	360_at	8.94E-04	7.25	AQP3	aquaporin 3 (Gill blood group)
	1236_at	9.63E-04	7.08	CCR7	C-C motif chemokine receptor 7
	1803_at	9.63E-04	7.02	DPP4	dipeptidyl peptidase 4
	126259_at	9.77E-04	6.92	TMIGD2	transmembrane and immunoglobulin domain containing 2
	145864_at	9.77E-04	6.75	HAPLN3	hyaluronan and proteoglycan link protein 3
	4609_at	9.77E-04	6.82	MYC	MYC proto-oncogene, bHLH transcription factor
	944_at	9.77E-04	6.76	TNFSF8	TNF superfamily member 8
	399665_at	1.14E-03	6.53	FAM102A	family with sequence similarity 102 member A
	5820_at	1.15E-03	6.47	PVT1	Pvt1 oncogene (non-protein coding)
	105370652_at	1.19E-03	6.40	LINC02295	long intergenic non-protein coding RNA 2295
	256987_at	1.25E-03	6.28	SERINC5	serine incorporator 5
	114804_at	1.37E-03	6.05	RNF157	ring finger protein 157
	120425_at	1.37E-03	6.10	JAML	junction adhesion molecule like
	3572_at	1.37E-03	6.10	IL6ST	interleukin 6 signal transducer
	4753_at	1.37E-03	5.99	NELL2	neural EGFL like 2
	60468_at	1.37E-03	6.02	BACH2	BTB domain and CNC homolog 2
	9057_at	1.37E-03	6.05	SLC7A6	solute carrier family 7 member 6
	8718_at	1.41E-03	5.94	TNFRSF25	TNF receptor superfamily member 25
	6920_at	1.75E-03	5.62	TCEA3	transcription elongation factor A3
	196_at	1.92E-03	5.52	AHR	aryl hydrocarbon receptor
	7294_at	2.09E-03	5.42	TXK	TXK tyrosine kinase
	3655_at	2.13E-03	5.34	ITGA6	integrin subunit alpha 6
	100750325_at	2.24E-03	5.26	RCAN3AS	RCAN3 antisense
	8728_at	2.27E-03	5.21	ADAM19	ADAM metallopeptidase domain 19
	5578_at	3.97E-03	4.55	PRKCA	protein kinase C alpha
	1880_at	4.01E-03	4.44	GPR183	G protein-coupled receptor 183
	6402_at	4.01E-03	4.51	SELL	selectin L
	9805_at	4.01E-03	4.46	SCRN1	secernin 1
	28567_at	4.06E-03	4.41	TRBV20-1	T cell receptor beta variable 20-1
	51176_at	4.33E-03	4.32	LEF1	lymphoid enhancer binding factor 1
	10207_at	4.65E-03	4.21	PATJ	PATJ, crumbs cell polarity complex component
	55061_at	4.65E-03	4.21	SUSD4	sushi domain containing 4
	90139_at	4.69E-03	4.18	TSPAN18	tetraspanin 18
	3570_at	5.25E-03	4.03	IL6R	interleukin 6 receptor
	100506915_at	5.67E-03	3.88	CHRM3-AS2	CHRM3 antisense RNA 2
	2053_at	5.67E-03	3.90	EPHX2	epoxide hydrolase 2
	51301_at	5.81E-03	3.83	GCNT4	glucosaminyl (N-acetyl) transferase 4, core 2
	101929623_at	5.84E-03	3.77	LINC01215	long intergenic non-protein coding RNA 1215
	28685_at	5.84E-03	3.79	TRAV8-1	T cell receptor alpha variable 8-1
	5924_at	5.84E-03	3.78	RASGRF2	Ras protein specific guanine nucleotide releasing factor 2
	104326191_at	5.89E-03	3.74	LINC01336	long intergenic non-protein coding RNA 1336
	4747_at	6.52E-03	3.60	NEFL	neurofilament light
	105377225_at	6.85E-03	3.49	LOC105377225	uncharacterized LOC105377225
	4118_at	6.85E-03	3.48	MAL	mal, T-cell differentiation protein
	101927777_at	6.87E-03	3.41	SATB1-AS1	SATB1 antisense RNA 1
	130367_at	6.87E-03	3.44	SGPP2	sphingosine-1-phosphate phosphatase 2
	80824_at	6.87E-03	3.43	DUSP16	dual specificity phosphatase 16
	3003_at	7.49E-03	3.32	GZMK	granzyme K
	55824_at	7.73E-03	3.26	PAG1	phosphoprotein membrane anchor with glycosphingolipid microdomains 1
	203328_at	7.98E-03	3.21	SUSD3	sushi domain containing 3
	23406_at	8.26E-03	3.13	COTL1	coactosin like F-actin binding protein 1
	22866_at	8.57E-03	3.05	CNKSR2	connector enhancer of kinase suppressor of Ras 2
	101954266_at	8.80E-03	3.02	RNVU1-14	RNA, variant U1 small nuclear 14
	28674_at	9.05E-03	2.94	TRAV12-1	T cell receptor alpha variable 12-1
	6322_at	9.91E-03	2.78	SCML1	sex comb on midleg like 1 (Drosophila)
	1606_at	1.07E-02	2.65	DGKA	diacylglycerol kinase alpha
	129293_at	1.11E-02	2.59	TRABD2A	TraB domain containing 2A
	351_at	1.12E-02	2.54	APP	amyloid beta precursor protein
	51522_at	1.16E-02	2.49	TMEM14C	transmembrane protein 14C
	55423_at	1.20E-02	2.42	SIRPG	signal regulatory protein gamma
	199_at	1.23E-02	2.38	AIF1	allograft inflammatory factor 1
	9840_at	1.23E-02	2.36	TESPA1	thymocyte expressed, positive selection associated 1
	5217_at	1.25E-02	2.33	PFN2	profilin 2
	6812_at	1.27E-02	2.30	STXBP1	syntaxin binding protein 1
	7074_at	1.27E-02	2.29	TIAM1	T-cell lymphoma invasion and metastasis 1
	28594_at	1.27E-02	2.27	TRBV7-4	T cell receptor beta variable 7-4 (gene/pseudogene)
	3575_at	1.33E-02	2.19	IL7R	interleukin 7 receptor
	101927596_at	1.39E-02	2.07	LOC101927596	uncharacterized LOC101927596
	54674_at	1.39E-02	2.08	LRRN3	leucine rich repeat neuronal 3
	101927613_at	1.46E-02	2.01	LOC101927613	uncharacterized LOC101927613
	28692_at	1.46E-02	2.01	TRAV1-2	T cell receptor alpha variable 1-2
	1233_at	1.47E-02	1.98	CCR4	C-C motif chemokine receptor 4
	6932_at	1.51E-02	1.94	TCF7	transcription factor 7 (T-cell specific, HMG-box)
	23508_at	1.59E-02	1.86	TTC9	tetratricopeptide repeat domain 9
	106481624_at	1.64E-02	1.78	RNU1-106P	RNA, U1 small nuclear 106, pseudogene

	105379362_at	1.82E-02	1.63	LOC105379362	uncharacterized LOC105379362
	196264_at	1.83E-02	1.59	MPZL3	myelin protein zero like 3
	7273_at	1.84E-02	1.58	TTN	titin
	6959_at	1.97E-02	1.41	TRBV21OR9-2	T cell receptor beta variable 21/OR9-2 (pseudogene)
	959_at	1.97E-02	1.41	CD40LG	CD40 ligand
	57124_at	1.99E-02	1.40	CD248	CD248 molecule
	9934_at	1.99E-02	1.38	P2RY14	purinergic receptor P2Y14
	8821_at	2.03E-02	1.34	INPP4B	inositol polyphosphate-4-phosphatase type II B
	641518_at	2.36E-02	1.05	LEF1-AS1	LEF1 antisense RNA 1
	1263_at	2.39E-02	1.03	PLK3	polo like kinase 3
	220158_at	2.44E-02	0.97	GTSCR1	Gilles de la Tourette syndrome chromosome region, candidate 1
	28715_at	2.44E-02	0.97	TRAJ40	T cell receptor alpha joining 40
	28751_at	2.45E-02	0.96	TRAJ4	T cell receptor alpha joining 4
	28738_at	2.51E-02	0.92	TRAJ17	T cell receptor alpha joining 17
	939_at	2.60E-02	0.85	CD27	CD27 molecule
	8609_at	2.77E-02	0.76	KLF7	Kruppel like factor 7
	387748_at	2.83E-02	0.73	OR56B1	olfactory receptor family 56 subfamily B member 1
	5324_at	2.94E-02	0.65	PLAG1	PLAG1 zinc finger
	131450_at	2.98E-02	0.62	CD200R1	CD200 receptor 1
	57282_at	3.04E-02	0.59	SLC4A10	solute carrier family 4 member 10
	107986485_at	3.13E-02	0.55	LOC107986485	uncharacterized LOC107986485
	27018_at	3.30E-02	0.44	BEX3	brain expressed X-linked 3
	28680_at	3.41E-02	0.39	TRAV8-6	T cell receptor alpha variable 8-6
	105375547_at	3.45E-02	0.37	LOC105375547	uncharacterized LOC105375547
	105376892_at	3.60E-02	0.32	LOC105376892	uncharacterized LOC105376892
	28659_at	3.64E-02	0.30	TRAV24	T cell receptor alpha variable 24
	107984947_at	3.88E-02	0.20	LOC107984947	uncharacterized LOC107984947
	2776_at	3.90E-02	0.19	GNAQ	G protein subunit alpha q
	149233_at	3.98E-02	0.13	IL23R	interleukin 23 receptor
	28984_at	4.07E-02	0.07	RGCC	regulator of cell cycle
	6285_at	4.18E-02	0.02	S100B	S100 calcium binding protein B
	814_at	4.18E-02	0.02	CAMK4	calcium/calmodulin dependent protein kinase IV
	28595_at	4.33E-02	-0.05	TRBV7-3	T cell receptor beta variable 7-3

université PARIS-SACLAY | ÉCOLE DOCTORALE Cancérologie, biologie, médecine, santé (CBMS)

Titre : Analyse systémique des sous-populations immunitaires et réseaux de communication intercellulaires dans les tumeurs du sein humaines

Mots clés : Biologie des systèmes, immunologie, transcriptome, immunité antitumorale, cellules dendritiques

Résumé : La communication intercellulaire est à la base de l'organisation d'ordre supérieur observée dans les tissus, les organes et l'organisme. Comprendre la communication intercellulaire et ses mécanismes sous-jacents qui sont impliqués dans le cancer est essentiel. Le microenvironnement des tumeurs du sein est composé d'une grande diversité cellulaire, telle que les cellules endothéliales, stromales ou immunitaires, qui peuvent influencer la progression tumorale ainsi que la réponse au traitement. Parmi les différentes populations de cellules immunitaires, les sous-populations de cellules dendritiques (DCs) intègrent les signaux du microenvironnement puis joue un rôle critique en orchestrant le développement d'une réponse immunitaire spécifique par activation des lymphocytes T. Cependant, les différentes fonctions de ces sous-populations et leurs interactions au sein du microenvironnement tumoral restent mal décrites.

L'objectif principal de ma thèse a été de comprendre l'impact du microenvironnement tumoral du sein sur les sous-populations de DCs par analyse systémique. Nous avons utilisé le séquençage de l'ARN pour analyser systématiquement les transcriptomes des pré-DC plasmacytoïdes infiltrant les tumeurs, les populations cellulaires enrichies pour les DC classiques de type 1, les DC classiques de type 2, les DC CD14+ et les monocytes-macrophages chez des patientes atteintes de cancer primitif du sein luminal et cancer du sein triple négatif. Nous avons constaté que la reprogrammation transcriptionnelle des cellules présentatrices d'antigène infiltrant la tumeur est spécifique à un sous-ensemble. Ces résultats suggèrent une interaction complexe entre l'ontogenèse et l'empreinte tissulaire dans le conditionnement de la diversité des DCs et de leur fonction dans le cancer. En second lieu, j'ai cherché à étudier les communications intercellulaires afin de comprendre comment les cellules intègrent les signaux de leur environnement. Nous avons développé ICELLNET, un outil pour reconstruire les réseaux de communication intercellulaires. Cette méthode quantitative originale, intégrant les interactions ligand-récepteur et l'expression génique spécifique à un type cellulaire, peut être appliquée automatiquement à tous profils transcriptomiques de population cellulaire, que ce soit dans divers contextes pathologiques ou d'autres domaines de la biologie.

Title: Systems level analysis of immune cell subsets and intercellular communication networks in human breast cancer

Keywords: Systems biology, immunology, transcriptome, anti-tumor immunity, dendritic cells

Abstract: Cell-to-cell communication is at the basis of the higher order organization observed in tissues, organs, and organism. Understanding cell-to-cell communication, and its underlying mechanisms that drive the development of cancer is essential. Breast tumor microenvironment (TME) is composed of a great cellular diversity, such as endothelial, stromal or immune cells that can influence tumor progression as well as its response to treatment. Among the different immune cell populations, dendritic cells (DCs) subsets integrate signals from their microenvironment and are subsequently essential in orchestrating specific immune response through T cell activation. However, the differential function of these subsets, and their interactions within the TME remain poorly described.

My main objective was to understand the impact of the breast TME on DC subsets using systems-level analysis. We used RNA sequencing to systematically analyze the transcriptomes of tumor-infiltrating plasmacytoid pre-DCs, cell populations enriched for type 1 classical DCs, type 2 classical DCs, CD14+DCs, and monocytes-macrophages from human primary luminal breast cancer and triple-negative breast cancer. We found that transcriptional reprogramming of tumor-infiltrating antigen-presenting cells is subset-specific. These results suggest a complex interplay between ontogeny and tissue imprinting in conditioning DC diversity and function in cancer.

As a second objective, I aimed at studying the cellular communications in order to understand how cells integrate signals from their environment. I developed ICELLNET, a tool to reconstruct intercellular communication networks. This original quantitative method, integrating ligand-receptor interactions and cell type specific gene expression, can be automatically applied to any cell population level transcriptomic profile opening perspectives of application in several disease contexts and biology fields.

Université Paris-Saclay
Espace Technologique / Immeuble Discovery
Route de l'Orme aux Merisiers RD 128 / 91190 Saint-Aubin, France